BULK ELECTRIC SYSTEM RELIABILITY SIMULATION AND APPLICATION

A Thesis
Submitted to the College of Graduate Studies and Research
in Partial Fulfillment of the Requirements
for the Degree of

Doctor of Philosophy

in the
Department of Electrical Engineering
University of Saskatchewan
Saskatoon

By

Wijarn Wangdee

PERMISSION TO USE

The author has agreed that the Library, University of Saskatchewan, may make this thesis freely available for inspection. Moreover, the author has agreed that permission for extensive copying of this thesis for scholarly purpose may be granted the professor or professors who supervised the thesis work recorded herein or, in their absence, by the Head of the Department or the Dean of the College in which the thesis work was done. It is understood that due recognition will be given to the author of this thesis and to the University of Saskatchewan in any use of the material in this thesis. Copying or publication or any other use of this thesis for financial gain without approval by the University of Saskatchewan and the author's written permission is prohibited.

Request for permission to copy or to make any other use of the material in this thesis in whole or part should be addressed to:

Head of the Department of Electrical Engineering
57 Campus Drive
University of Saskatchewan
Saskatoon, Saskatchewan
Canada S7N 5A9

… สัมมาทิฐิ …

" Just as when a sugar cane seed, a rice grain, or a grape seed is placed in moist soil, whatever nutriment it takes from the soil and the water, all conduce to its sweetness, tastiness and unalloyed delectability. Why is that? Because the seed is auspicious. In the same way, when a person has right view... right release, whatever bodily deeds he undertakes in line with that view, whatever verbal deeds... whatever mental deeds he undertakes in line with that view, whatever intentions, whatever vows, whatever determinations, whatever fabrications, all lead to what is agreeable, pleasing, charming, profitable and easeful. Why is that? Because the view is auspicious."

The Buddha

(Translated by Thanissaro Bhikkhu)

Dedicated To My Beloved Parents

PRATEEP & KWANJAI WANGDEE

who taught me the value of education,

and have always blessed and encouraged me in all my endeavors.

And in memory of my grandmother, SARAI RUAMPRASERT.

ACKNOWLEDGEMENTS

The author would like to express his gratitude and appreciation to his supervisor, Dr. Roy Billinton, for his invaluable guidance, discussions, criticisms, support and encouragement throughout the course of this research work. His kindly advice and assistance in the preparation of this thesis are thankfully acknowledged. These simple words are however incapable of entirely conveying the author's sincere appreciation for all the help and opportunities that have been given by Professor Billinton to the author. The author will always remain deeply indebted towards him.

The author would like to thank the Advisory Committee members Professor R. Karki, Professor S.O. Faried, Professor G. Wacker, Professor D. Klymyshyn and Professor I. Oguocha for their guidance and encouragement throughout this research work. The author would like to thank Professor W. Xu from the University of Alberta for acting as his external examiner. The author would also like to thank J.E. Billinton from Alberta Electric System Operator (AESO) for his suggestions and guidance in regard to wind power issues.

The author expresses his indebtedness to his parents, sisters Kwanruthai and Jomkwan, brother Wijit, and friends for their encouragement and moral support during the course of study. The author is sincerely grateful to his homestay family, the Eidsness family, for their enduring support and encouragement since the first day the author arrived in Canada.

Financial assistance provided in part by the Natural Sciences and Engineering Research Council of Canada and in part by the University of Saskatchewan in the form of a Graduate Scholarship is gratefully acknowledged.

BULK ELECTRIC SYSTEM RELIABILITY SIMULATION AND APPLICATION

Candidate: Wijarn Wangdee Supervisor: Dr. Roy Billinton

Doctor of Philosophy Thesis
Submitted to the College of Graduate Studies and Research
University of Saskatchewan, December 2005

ABSTRACT

Bulk electric system reliability analysis is an important activity in both vertically integrated and unbundled electric power utilities. Competition and uncertainty in the new deregulated electric utility industry are serious concerns. New planning criteria with broader engineering consideration of transmission access and consistent risk assessment must be explicitly addressed. Modern developments in high speed computation facilities now permit the realistic utilization of sequential Monte Carlo simulation technique in practical bulk electric system reliability assessment resulting in a more complete understanding of bulk electric system risks and associated uncertainties. Two significant advantages when utilizing sequential simulation are the ability to obtain accurate frequency and duration indices, and the opportunity to synthesize reliability index probability distributions which describe the annual index variability.

This research work introduces the concept of applying reliability index probability distributions to assess bulk electric system risk. Bulk electric system reliability performance index probability distributions are used as integral elements in a performance based regulation (PBR) mechanism. An appreciation of the annual variability of the reliability performance indices can assist power engineers and risk

managers to manage and control future potential risks under a PBR reward/penalty structure. There is growing interest in combining deterministic considerations with probabilistic assessment in order to evaluate the "system well-being" of bulk electric systems and to evaluate the likelihood, not only of entering a complete failure state, but also the likelihood of being very close to trouble. The system well-being concept presented in this thesis is a probabilistic framework that incorporates the accepted deterministic N-1 security criterion, and provides valuable information on what the degree of the system vulnerability might be under a particular system condition using a quantitative interpretation of the degree of system security and insecurity. An overall reliability analysis framework considering both adequacy and security perspectives is proposed using system well-being analysis and traditional adequacy assessment. The system planning process using combined adequacy and security considerations offers an additional reliability-based dimension. Sequential Monte Carlo simulation is also ideally suited to the analysis of intermittent generating resources such as wind energy conversion systems (WECS) as its framework can incorporate the chronological characteristics of wind. The reliability impacts of wind power in a bulk electric system are examined in this thesis. Transmission reinforcement planning associated with large-scale WECS and the utilization of reliability cost/worth analysis in the examination of reinforcement alternatives are also illustrated.

TABLE OF CONTENTS

LIST OF TABLES

LIST OF FIGURES

LIST OF ABBREVIATIONS

AC	Alternating Current
ACP	Annual Capital Payment ($/year)
ARMA	Auto-Regressive and Moving Average
Avg.	Average
BES	Bulk Electric System
CCDF	Composite Customer Damage Function
CDF	Customer Damage Function
CEA	Canadian Electricity Association
CRF	Capital Recovery Factor
CTU	Combustion Turbine Unit
DC	Direct Current
Discos	Distribution companies
DP	Delivery Point
DPUI	Delivery Point Unavailability Index (system·minutes)
Dur{H}	Average residence duration in the healthy state (hours/occurrence)
Dur{M}	Average residence duration in the marginal state (hours/occurrence)
Dur{R}	Average residence duration in the at risk state (hours/occurrence)
EBCost	Event-Based Customer Interruption Cost
ECOST	Expected Customer Interruption Cost ($/year)
EDLC	Expected Duration of Load Curtailment (hours/year)
EDNS	Expected Demand Not Supplied (MW)
EENS	Expected Energy Not Supplied (MWh/year)
EFLC	Expected Frequency of Load Curtailment (occurrences/year)
ELCC	Effective Load Carrying Capability
ENLC	Expected Number of Load Curtailment (occurrences/year)
EORC	Expected Overall Reliability Cost ($/year)

EPIC	Expected Potential Insecurity Cost ($/year)
ERD	Expected Restoration Duration (hours/occurrence)
ERP	Expected Reward/Penalty Payments
FACTS	Flexible AC Transmission System
FOR	Forced Outage Rate
Freq{H}	Frequency of the healthy state (occurrences/year)
Freq{M}	Frequency of the marginal state (occurrences/year)
Freq{R}	Frequency of the at risk state (occurrences/year)
Gencos	Generation companies
GWh	Gigawatt-hours
HL	Hierarchical Level
HL-I	Hierarchical Level-I
HL-II	Hierarchical Level-II
HL-III	Hierarchical Level-III
hrs	Hours
IEAR	Interrupted Energy Assessment Rate ($/kWh)
IEEE-RTS	IEEE-Reliability Test System
ISO	Independent System Operator
km	Kilometers
kV	Kilovolts
kW	Kilowatt
kWh	Kilowatt-hours
LDC	Load Duration Curve
L.F.	Load Factor
LOEE	Loss of Energy Expectation (MWh/year)
LOLE	Loss of Load Expectation (hours/year)
LOLF	Loss of Load Frequency (occurrences/year)
MC	Multi-Circuit Supplied Delivery Point
MECORE	Monte carlo and Enumeration COmposite Reliability Evaluation
MR-RBTS	Modified Reinforced Roy Billinton Test System
MTTF	Mean Time To Failure (hours)

MTTR	Mean Time To Repair (hours)
MVA	MegaVolt-Amperes
MVAr	Megavar
MW	Megawatt
MWh	Megawatt-hours
NID	Normally Independent Distributed
No.	Number
OPF	Optimal Power Flow
PBR	Performance Based Regulation
PI	Performance Index (for security contingency ranking)
PLC	Probability of Load Curtailment (/year)
Prob{H}	Probability of the healthy state (/year)
Prob{M}	Probability of the marginal state (/year)
Prob{R}	Probability of the at risk state (/year)
p.u.	Per Unit
PX	Power Exchange
RapHL-II	Reliablity analysis program for HL-II
RBTS	Roy Billinton Test System
R-RBTS	Reinforced Roy Billinton Test System
SAIDI	System Average Interruption Duration Index (hours/year)
SAIFI	System Average Interruption Frequency Index (occurrences/year)
SARI	System Average Restoration Index (hours/occurrence)
SC	Single Circuit Supplied Delivery Point
SCDF	Sector Customer Damage Function
S.D.	Standard Deviation
SECOREL	SEquential COmposite system RELiability evaluation software
SIC	Standard Industrial Classifications
sys.mins	system·minutes
Transcos	Transmission companies
TTF	Time To Failure (hours)
TTR	Time To Repair (hours)

TOC	Total Cost ($)
VoLL	Value of Lost Load ($/kWh)
WECS	Wind Energy Conversion System
WTG	Wind Turbine Generator
yr	Year
$	Dollars

CHAPTER 1
INTRODUCTION

Electric power systems throughout the world are undergoing considerable change in regard to structure, operation and regulation. Technological developments and evolving customer expectations are among the driving factors in the new electricity paradigm. Competition and uncertainty in the new deregulated electric utility industry are serious concerns. Electric power utilities also face increasing uncertainty regarding the political, economic, societal and environmental constraints under which they have to operate existing systems and plan future systems. All these conditions have created new electric utility environments that require extensive justification of new facilities, optimization of system configurations, improvements in system reliability and decreases in construction and operating costs. New planning criteria with broader engineering considerations of transmission access and consistent risk assessment must be explicitly addressed. The likelihood of the occurrence of worst possible scenarios must also be recognized in the criteria and acceptable risk levels incorporated in the decision making process [1].

The development of modern society has significantly increased the dependency on electric supply availability. The basic function of an electric power system is to supply its customers with electrical energy as economically as possible and with a reasonable degree of continuity and quality [2]. It is not economical and technically feasible to attempt to design a power system with one hundred percent reliability. Power system engineers, therefore, attempt to achieve an acceptable level of system reliability in their planning, design and operation within the existing economic constraints. In order to resolve the conflict between the economic and reliability constraints, a wide range of techniques and criteria has been developed and used in the system design, planning and

operating phases. It is believed that the application of reliability concepts in electric power system planning and operation will continue to increase in the future in both regulated and deregulated utility environments.

1.1 Restructured Electric Power Industry

Electric power systems have traditionally been organized and operated as vertically integrated utilities in which generation, transmission and distribution facilities are owned by one company. In this structure, the company controls all aspects of system planning, design and operation. It also manages all functions of producing, delivering and selling electric power to the end users. One of the advantages that this traditionally regulated electricity industry has is in the coordination of all the functions required to provide a highly reliable electrical supply. One of the important disadvantages of the traditionally regulated industry is the lack of competition in the created monopoly, which leads to losses in efficiency and economic incentives. This traditionally regulated electricity industry structure has existed for a long time and continues to exist in some locations.

In recent years, social, economic, political and technical changes have forced the regulated electric power industry to adapt. The power industry is now undergoing considerable changes due to restructuring. Competition has become the key factor driving the restructuring or deregulation process in the electric power industry, and should benefit both the customers and the participating companies. The key concept behind deregulation in many countries is that no one company should have a monopoly on either the production, the wholesale or retail sale of electricity and electricity-based services. The delivery function associated with transmission and distribution is still a regulated, monopoly business due to its natural characteristics [3]. One of the advantages in the newly deregulated electricity industry is the resulting competition and the benefits that it brings to the customers, utility companies and therefore society. One of the biggest problems associated with the deregulation process, however, is the resulting financial risk caused by the uncertainty existing in the market. Figure 1.1

illustrates some of the general differences between the traditionally regulated (vertically integrated) electric power structure and the new deregulated industry.

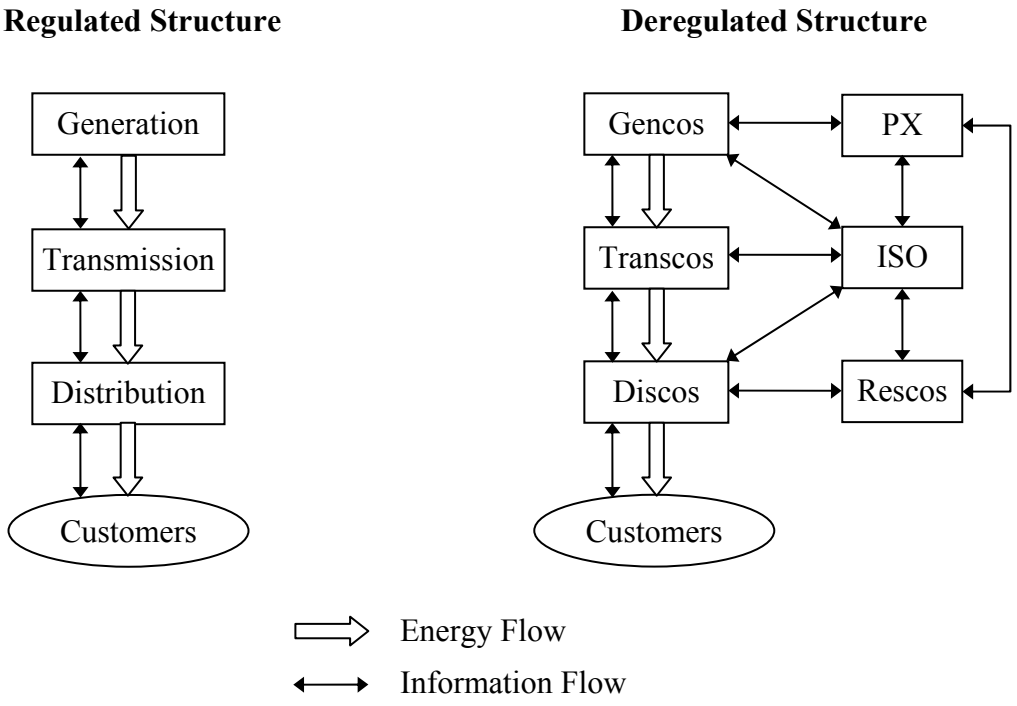

Figure 1.1: The regulated and deregulated power industry structures.

In Figure 1.1, the vertically integrated utility structure represents the traditional regulated power industry. In the new deregulated industry structure, generation companies (Gencos) are separately owned and compete to sell energy to customers, and are no longer controlled by the same entities that control the transmission system. Transmission companies (Transcos) own high voltage transmission lines and move power in bulk quantities from where it is produced to where it is needed. Distribution companies (Discos) are the monopoly-franchise owner-operators who locally deliver power at the retail level to end-use customers. A Power Exchange (PX) is an organization somewhat like a stock exchange where the buyers and sellers of wholesale electricity are allowed to buy and sell electric energy as a commodity. Retail energy services companies (Rescos) are retailers of electric power who buy power from a power market and sell it directly to consumers [3]. These entities must work cooperatively to provide cost effective and reliable electric power supply. In order to do so, independent

entities designated as Independent System Operators (ISO) are established to coordinate the activities among these energy-related entities to achieve the overall goal of serving the customers.

The ISO is an entity entrusted with the responsibility of ensuring the reliability and security of the bulk electric system consisting of the generation and transmission facilities. It is an independent authority who does not participate in the electricity market trades nor own generation facilities for business (except for owning some capacity for emergency use) [4]. In general, the ISO is a neutral operator who has the objective to guarantee comparable and non-discriminatory access by power suppliers and users to the regional electric transmission system. The ISO performs its function by controlling the dispatch of generation and gives orders to adjust or curtail load to ensure that loads match the available generating resources in the system. It has the operational control of the transmission grid components, administers system wide transmission tariffs, maintains and ensures system reliability, coordinates maintenance scheduling, and has a role in coordinating long-term planning. Consequently, the ISO's activities have significant impacts on all the energy-related participants.

In the new deregulated industry structure Gencos produce electric power, which Transcos and Discos deliver to the end-use customers, under the control of the ISO. In this process, the PX and Rescos coordinate the market information and transfer the knowledge to the other entities to facilitate their decision making and operating strategies. The new power industry is facing many problems such as how to operate the new power structure economically and reliably, how to minimize production costs, how to attract the new investment required to construct the required generation and transmission facilities under the uncertainty of market competition, etc. Power system reliability evaluation is an important activity in vertically integrated utilities, and is at least equally important in the unbundled electric power utility environment. As noted earlier, the requirements of low cost electrical energy and high levels of reliability are in conflict. Balancing these two aspects is a big challenge for power system managers, planners and operators. The research in this thesis is focused on reliability analysis of

bulk electric systems. This is an important activity in both the traditional and more recent power system structures, and is a primary responsibility of the ISO in a deregulated system.

1.2 Power System Reliability and Related Concepts

Reliability is an inherent characteristic and a specific measure of any component, device or system, which describes its ability to perform its intended function. In the context of power systems, reliability in general terms is related to the ability of the system to supply electric power to its customers under both static and dynamic conditions, with a mutually acceptable assurance of continuity and quality [5]. The term "system reliability" can be subdivided into the two fundamental aspects of system adequacy and system security [2] shown in Figure 1.2.

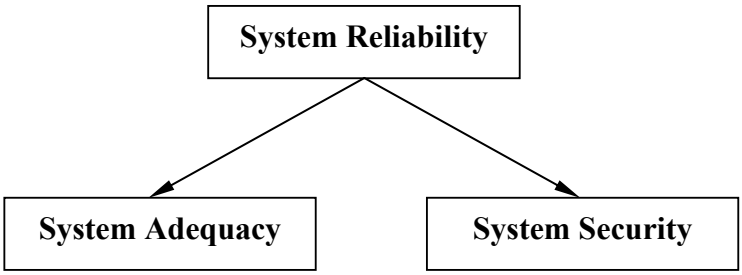

Figure 1.2: Subdivision of system reliability.

System adequacy relates to the existence of sufficient facilities within the system to satisfy the consumer load demand or system operational constraints. These include the facilities necessary to generate sufficient energy and the associated transmission and distribution facilities required to transport the energy to the actual consumer load points. Adequacy is therefore associated with static conditions, which do not include system disturbances. On the other hand, system security relates to the ability of the system to respond to disturbances arising within that system. Security is therefore associated with the response of the system to whatever perturbations arise. These include the conditions associated with both local and widespread disturbances and the loss of major generation and transmission facilities [2]. In system security considerations, the analysis can be

further classified into two types designated as transient (dynamic) and steady-state (static). Transient stability assessment consists of determining if the system oscillations following an outage or a fault will cause loss of synchronism between generators. The objective of steady-state security analysis is to determine whether, following the occurrence of a contingency, there exists a new steady-state secure operating point where the perturbed power system will settle after the dynamic oscillations have damped out. The focus of this thesis is on the adequacy domain and on extended adequacy assessment incorporating the steady-state security perspective. The research work does not incorporate dynamic phenomena, i.e. oscillations and system faults, in the overall security constraints.

An overall power system can be divided into the three basic functional zones of generation, transmission and distribution. Power system adequacy assessment can be conducted in each functional zone and at each hierarchical level [2]. Figure 1.3 shows the three hierarchical levels.

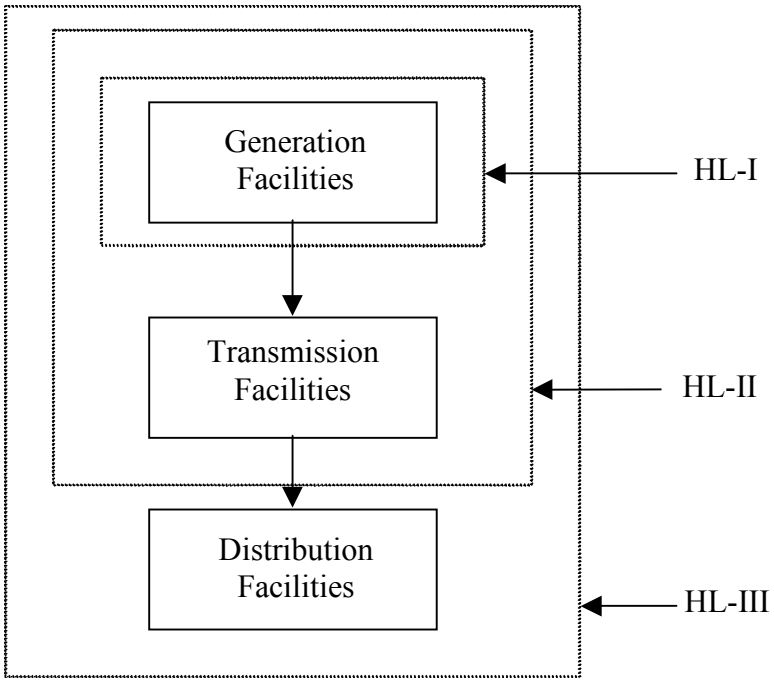

Figure 1.3: Hierarchical levels.

Reliability assessment at hierarchical level-I (HL-I) involves the ability of the generation facilities to meet the system demand. In hierarchical level-II (HL-II) reliability assessment, the generation and transmission facilities are considered as a composite system or bulk electric system that is responsible for delivering the required energy to the bulk supply points (delivery points). Reliability assessment at hierarchical level-III (HL-III) pertains to the complete system consisting of the three functional zones of generation, transmission and distribution. HL-III assessment is difficult to do in a large system because of the computational complexity and scale of the problem. Detailed analysis is usually conducted at HL-I, HL-II and in the distribution functional zone. The focus of this thesis is on reliability assessment at hierarchical level-II (HL-II).

The need to evaluate system reliability has resulted in a wide range of deterministic and probabilistic criteria for subsystem and system assessment. Deterministic techniques provide a reliability analyst with information on how a system failure can happen or how system success can be achieved. The most common deterministic criterion dictates that specific credible outages will not result in system failure. The traditional deterministic criterion used particularly in bulk electric systems (BES) is known as the N-1 security criterion [6, 7] under which the loss of any BES component will not result in system failure. Deterministic techniques, which are also often referred to as engineering judgment, do not include an assessment of the actual system reliability as they do not incorporate the probabilistic or stochastic nature of system behavior and component failures. These approaches, therefore, are inconsistent and cannot be used for comparing alternative equipment configurations, and performing economic analyses. Probabilistic methods, however, can respond to the significant factors that affect the reliability of a system. These techniques provide quantitative indices, which can be used to decide if system performance is acceptable or if changes need to be made. Most of the published papers on reliability assessment of engineering systems are based on probabilistic approaches rather than deterministic concepts [8]. There is, however, considerable reluctance to using probabilistic techniques in many areas due to the difficulty in interpreting the resulting numerical indices. Although deterministic criteria do not consider the stochastic behavior of system components, they

are easier for system planners, designers and operators to understand than a numerical risk index determined using probabilistic techniques. This difficulty can be alleviated by incorporating the accepted N-1 deterministic consideration, which is a hard criterion, in a probabilistic assessment to provide a resulting soft criterion. This concept is designated as system well-being analysis [9, 10] and is one of the main research tasks illustrated in this thesis.

1.3 Concept of Bulk Electric System Reliability Analysis

The term "bulk electric system" used in this thesis is equivalent to the term "composite generation and transmission system" introduced in [11], which falls into hierarchical level-II (HL-II) noted earlier. The reliability assessment of composite generation and transmission systems or bulk electric systems is extremely complicated as it is necessary to include detailed modeling of both the generation and transmission facilities to consider multiple levels of component failure. Composite power system reliability evaluation provides an assessment of the ability of an electric power system to satisfy the load and energy requirements at the major load points and for the overall system. The most significant quantitative indices in composite power system reliability evaluation are those that relate to load curtailment. Reliability assessment at HL-II can be performed using analytical methods or Monte Carlo simulation techniques [2].

Analytical methods such as contingency enumeration [12] represent the system by a mathematical model and evaluate the reliability indices from the model using direct numerical solutions. An analytical method will always give the same numerical result for the same system, same model and same set of input data. The methods, therefore, tend to give more confidence to reliability evaluation results obtained by an exact solution from an accepted system model. Assumptions, however, are frequently required in order to simplify the problem and to produce an analytical model of the system. This is particularly the case when complex operating procedures have to be modeled. The resulting analysis can therefore sometimes lose some or much of its significance. This difficulty can be reduced or eliminated by using a simulation approach. Monte Carlo

simulation methods estimate the reliability indices by simulating the actual process and random behavior of the system. The method therefore treats the problem as a series of experiments. There are merits and demerits in both methods. Generally, Monte Carlo simulation requires a large amount of computing time compared to analytical methods. Monte Carlo simulation techniques, however, can theoretically take into account virtually all aspects and contingencies inherent in the planning, design and operation of a power system [2, 13]. These include random events such as outages and repairs of elements represented by general probability distributions and different types of operating policies. On the other hand, numerous assumptions and approximations may be required in an analytical approach to handle complex operations and inherent characteristics. References 14 – 17 show 145 published papers during the last two decades on the subject of composite generation and transmission system reliability evaluation using analytical or Monte Carlo simulation techniques, or a hybrid of both methods. There has been a growing interest and an increasing trend in applying Monte Carlo simulation approaches to bulk electric system reliability analysis during the last decade due to the development and availability of high speed computation facilities.

There are two basic techniques when applying Monte Carlo simulation methods to bulk power system reliability evaluation. These methods are designated as the sequential and non-sequential approaches. Sequential simulation can fully take into account the chronological behavior of the system, while the non-sequential method involves non-chronological system state considerations. The sequential technique, therefore, provides more accurate frequency and duration assessments than the non-sequential method. The significant merit when utilizing the sequential simulation approach is the ability to provide information on the mean or average values and on the probability distributions of the indices. Both sequential and non-sequential simulation techniques, however, have advantages and disadvantages. These issues are addressed in detail in Chapter 2 in conjunction with the simulation procedures used in the different Monte Carlo methods.

1.4 Scope and Objectives of the Thesis

This research work is focused on the utilization of sequential Monte Carlo simulation in bulk electric system reliability analysis and the application of these concepts in system planning and decision making. A fundamental objective of this research work is to take advantage of the sequential simulation technique to create reliability index probability distributions, which indicate the annual variability of reliability indices and the likelihood of specific values being exceeded from both the adequacy and steady-state security perspectives. An inherent benefit of the chronological representation used in sequential simulation is the opportunity to investigate the impact on bulk electric system reliability of intermittent energy resources such as wind power. The following list of conducted tasks indicates the specific objectives of the research described in this thesis.

1. A detailed investigation of the possible utilization of sequential Monte Carlo simulation in composite system reliability evaluation including reliability worth considerations.
2. An examination of the ability to develop and utilize probability distribution analysis in composite system evaluation.
3. An examination of the ability to predict performance based adequacy indices including their probability distributions.
4. An investigation of the ability to develop both system and load point indices in the steady-state security domain based on system well-being analysis including probability distribution considerations.
5. The development of combined reliability indices obtained using adequacy assessment and steady-state security evaluation.
6. An investigation of the impact of large-scale wind power on bulk electric system reliability.

The basic concepts and different types of Monte Carlo simulation are described in Chapter 2 and the advantages and disadvantages of the different Monte Carlo

simulation approaches are addressed. Sequential Monte Carlo simulation is discussed in detail. Chapter 3 presents an overall procedure for bulk electric system reliability analysis using sequential Monte Carlo simulation. Network solution techniques using DC and Fast Decoupled AC load flow are presented. Linear programming techniques for corrective actions due to system operating limits such as generation, transmission capacity, and bus voltage constraints are presented. These corrective actions include overload alleviation, generation rescheduling, bus voltages adjustment, and a minimization model for load curtailment. Approximation techniques required due to network ill-condition problems and network separation problems are discussed. Different load curtailment philosophies used in the analyses are also addressed. The two test systems used throughout this thesis are also described in this chapter.

The impacts of utilizing sequential and non-sequential simulation techniques in bulk electric system reliability evaluation is presented in Chapter 4. Reliability indices obtained using both techniques are compared and discussed in terms of annualized and annual reliability indices. A discussion of the frequency index calculation and the pertinent factors affecting the frequency indices are provided. Chapter 5 presents reliability worth assessment methodologies for bulk electric systems. An event-based customer interruption cost evaluation technique is incorporated in a composite system reliability evaluation framework using sequential Monte Carlo simulation. This method provides a realistic and accurate incorporation of the temporal variations in the customer outage costs in a reliability worth analysis. Approximate methods for customer interruption cost evaluation are also presented and compared with the customer interruption costs obtained using the more accurate procedure.

Reliability index probability distribution analysis of bulk electric systems is presented in Chapter 6. Two basic types of reliability indices designated as predictive and performance indices are demonstrated. Delivery point and overall system reliability indices obtained using different system operating policies are examined. Some factors that influence the reliability index probability distributions such as load curtailment philosophies and the probability distributions of component repair times are illustrated.

Chapter 7 presents the utilization of reliability index probability distributions in a performance based regulation (PBR) framework. This provides an opportunity to extend the existing models for performance based regulation (PBR) used in the deregulated utility environment from a bulk electric system perspective. Selected performance based indices associated with a PBR structure for bulk electric systems are illustrated. Sensitivity analyses such as changing system operating policies are also demonstrated in order to examine these impacts on reward and penalty payments under a PBR structure. The potential utilization of the PBR mechanism associated with reliability index probability distributions for an overall bulk electric system and for a transmission system are also discussed.

The inclusion of security constraints in adequacy evaluation can overcome some of the difficulties associated with the more traditional methods. Chapter 8 extends the adequacy assessment process described in Chapter 3 by incorporating steady-state security considerations. This extended adequacy assessment is designated as security constrained adequacy analysis and is focused on the overall operation of the power system. In this analysis, the system is classified into different operating states defined in terms of adequacy and security. The system well-being concept presented in Chapter 8 is a probabilistic framework that incorporates a practical simplification of the traditional operating states associated with the accepted deterministic N-1 security criterion. The procedure used to extend traditional adequacy assessment to incorporate steady-state security considerations in system well-being analysis is addressed. System well-being index probability distributions of bulk electric systems are also investigated. Chapter 9 presents the combined reliability framework using adequacy assessment and steady-state security evaluation. This is achieved using a combination of reliability indices obtained using adequacy assessment and system well-being analysis. Selected reliability indices from both adequacy and security domains are proposed in order to create a compact combination in an overall reliability framework. An expected potential insecurity cost due to system security concerns is proposed. The combined reliability indices are utilized in a system reinforcement process using various study cases. The utilization of a combined reliability framework considering both adequacy and static security

perspectives provide complementary information insight to identify potential system adequacy and security problems.

Wind power integration in bulk electric system reliability evaluation is presented in Chapter 10. One advantage of utilizing sequential Monte Carlo simulation in bulk electric system reliability evaluation is that the framework already exists to incorporate the chronological characteristics of wind (diurnal and season wind speeds), load profiles and chronological transition states of all the components within a system. A wind energy conversion system (WECS) model involving wind turbine and wind speed characteristics is illustrated and a technique to simulate single and multiple wind farms is presented. The effect of wind speed correlation between wind farms from a system reliability perspective is quantitatively demonstrated. The effective load carrying capability (ELCC) associated with a wind energy conversion system (WECS) is also discussed. The impact on overall system reliability due to connecting WECS to different locations in a bulk electric system is examined and transmission planning for large-scale wind farms using cost-benefit analysis is illustrated.

Chapter 11 summarizes the thesis and presents the conclusions.

CHAPTER 2
BASIC CONCEPTS OF SEQUENTIAL MONTE CARLO SIMULATION

2.1 Introduction

The application of quantitative reliability evaluation in electric power systems has now evolved to the point at which most utilities use these techniques in one or more areas of their planning, design, and operation [13]. As noted in Chapter 1, the two main procedures for power system reliability evaluation are designated as analytical and Monte Carlo simulation methods. Analytical methods have been in use for a long time to assess expected indices because of their relatively short computing times and fewer computing resource constraints compared to the utilization of simulation methods. Improvements in and increased availability of high-speed digital computer facilities have created opportunities to analyze many problems using stochastic simulation methods. Over the last decade, there has been increased interest in utilizing Monte Carlo simulation in quantitative power system reliability analysis. Although Monte Carlo simulation is not a new concept, as its application has existed for at least 50 years, the availability of high speed computation facilities has now made Monte Carlo simulation an available and sometimes preferable option for many power system reliability applications. Simulation can be also used to experiment with new situations where there is little or no available information. In addition, simulation can sometimes be valuable in breaking down a complicated system into subsystems, each of which can then be modeled and analyzed separately.

2.2 Monte Carlo Simulation Techniques

Monte Carlo simulation for power system reliability analysis can be classified into two general types designated as non-sequential and sequential methods. The basic principles of three simulation techniques used in power system reliability evaluation are described in the following sections. These three techniques are designated as the state sampling, state transition sampling and state duration sampling approaches [13]. The state sampling and state transition sampling approaches fall into the non-sequential simulation category and the state duration sampling approach is a sequential simulation procedure.

2.2.1 State Sampling Approach

The state sampling approach [18, 19] is a non-sequential simulation procedure. In this approach, the states of all components are sampled and a non-chronological system state is obtained by combining all the component states. The basic sampling procedure is conducted by generating pseudo-random numbers and assuming that the behavior of each component can be described by a uniform distribution between [0,1]. Each consecutive sample of system states is randomly selected independently from previous and subsequent samples. The advantage of the state sampling approach is that it is a relatively simple process involving the utilization of uniformly distributed random numbers, and has a relatively short computation time with small memory requirements. The major disadvantage of the state sampling approach when applied to power systems is that it cannot be used by itself to calculate an actual frequency index, as this approach cannot recognize the impact of failure state transitions and transitions associated with a chronological load model. These factors directly affect a frequency index calculation and are addressed in detail in Chapter 4.

2.2.2 State Transition Sampling Approach

The state transition sampling approach [20, 21] is focused on state transitions of the whole system rather than individual component state transitions. A long system state transition sequence can be obtained by a number of samples and the probability of each system state can be evaluated. The major advantage of this approach is that it can be used to calculate an actual frequency index by creating a system state transition chain. The state transition sampling approach in general does not involve sampling component state duration distribution functions nor the storage of chronological information as required in the sequential approach. The disadvantage of the state transition sampling approach is that it only applies to components with exponentially distributed state residence duration characteristics, which may not always be the case.

2.2.3 State Duration Sampling Approach (Sequential Simulation)

The state duration sampling approach [13] is a sequential simulation process, and is utilized in this research. The state duration sampling approach is based on sampling the probability distribution of the component state duration. In this approach, chronological component state transition processes for all components are first simulated. The chronological system state transition process is then created by combining the individual chronological component state transition processes. The term "sequential simulation" is often used in engineering literature [22] to designate the technique in which the history of a system is simulated in fixed discrete time steps. This thesis uses the term sequential simulation in the engineering sense [23], in which any event occurring within a particular time step is considered to occur at the end of the time step, and the system states are updated accordingly. A time step of one hour is considered to be adequate for power system reliability assessment since the number of changes within that period is generally small.

In sequential simulation, each subsequent system state sample is related to the previous set of system states (historically dependent). A sequential time evolution of

system behavior is created which enables a wide range of reliability indices to be assessed. The random factors affecting the capacity and energy states of history dependent systems and the required operating scenarios can be incorporated using sequential Monte Carlo simulation. The sequential simulation approach is very useful when the system to be analyzed is past-dependent, i.e. the state of the system at any given time is partially determined by the historical time evolution of the system. Sequential simulation is particularly useful when the operating system is history-dependent or time correlated. This often applies to hydro generation systems in which the reservoir storage capacity is relatively small and the use of water has to be carefully controlled [24]. In such situations, the available power at any moment is dependent on, among other factors, the past water inflows, past operating policies and the historical behavior of the system load. Sequential simulation can incorporate realistic and sophisticated load models that incorporate the chronological characteristics inherent within each customer sector and the customer mix at each bulk system supply point. If the operating life of the system is simulated over a long period of time, it is possible to study the behavior of the system and to obtain a clear picture of possible deficiencies that the system may suffer. The recorded information can be used to calculate the expected values of selected reliability indices together with an appreciation of the dispersion of these indices. There is frequently a need to know the likely range of reliability indices, the likelihood of certain values being exceeded, and similar parameters. These can be assessed from a knowledge of the probability distribution associated with the expected value. At the present time, sequential simulation is the only realistic option available to investigate the distributional aspects associated with system index mean values.

In conclusion, the sequential simulation approach can be used to represent most of the contingencies and operating characteristics inherent in a bulk electric system and provide a comprehensive range of reliability indices. This comprehensive information provides a detailed description, and hence understanding, of the system reliability. The major disadvantage of the sequential simulation method is that it requires more computation time and storage than non-sequential methods because it is necessary to

generate a random variate following a given distribution for each component and store information on the chronological component state transition processes of all the components in a long time span. This disadvantage is now becoming less significant due to the availability of high speed computation facilities.

2.3 Basic Methodology of Sequential Simulation

2.3.1 Sequential Simulation Procedure

The sequential simulation approach is based on sampling the probability distributions of the system component state durations. This approach uses the component state duration distribution functions. In a two state component representation, these are the operating and repair state duration distribution functions and are usually assumed to be exponential. Other distributions can also be easily utilized and this is discussed in Chapter 6. The sequential simulation method can be summarized in the following steps:

Step 1: The initial state of each component is specified. Generally, it is assumed that all components are initially in the success or up state (operating state).

Step 2: The duration of each component residing in its present state is sampled from its probability distribution. For example, an exponentially distributed random variate T has the probability distribution function [22],

$$f_T(t) = \lambda e^{-\lambda t} \tag{2.1}$$

where λ is the mean value of the distribution. Its cumulative probability distribution function is:

$$F(t) = 1 - e^{-\lambda t} \tag{2.2}$$

Using the inverse transform method the random variate T is given by [22]:

$$T = -\frac{1}{\lambda} ln(1-U) \tag{2.3}$$

where U is a uniformly distributed random number obtained from a multiplicative congruential pseudo-random number generator [22]. The procedure used to generate the pseudo-random number is described in Appendix A. Since the term *1-U* distributes uniformly in the same way as *U* in the interval [0,1],

$$T = -\frac{1}{\lambda} ln(U) \tag{2.4}$$

If the present state is the up state (success state), λ is the failure rate of the component. If the present state is the down state (failure state), λ is the repair rate of the component.

Step 3: Step 2 is repeated in the given time span, i.e. normally a year, and sampling values of each state duration for all components are recorded. The chronological component state transition processes in the given time span of all components are then combined to create the chronological system state transition process.

Step 4: System analysis is conducted for each different system state to obtain the reliability index function $\Phi(S)$. The expected value of the index $\Phi(S)$ is designated as $E(\Phi)$. The mathematical expectation of the index or test function $E(\Phi)$ of all system states is given by:

$$E(\Phi) = \sum_{S \in G} \Phi(S) P(S) \tag{2.5}$$

where S is the system state and G is the set of system states. Assuming that each system state has the probability $P(S)$.

Substituting the sampling frequency of the system state S for its probability $P(S)$ results in:

$$E(\Phi) = \sum_{S \in G} \Phi(S) \frac{n(S)}{N} \tag{2.6}$$

where N is the total number of samples and $n(S)$ is the number of occurrences of system state S. $\Phi(S)$ can be obtained by appropriate system analysis. For

example, to determine the system probability of load curtailment, the index $\Phi(S)$ is given as [25]:

$$\Phi(S) = \begin{cases} 1 & \text{if there is a load curtailment associated with system state } S \\ 0 & \text{if there is no load curtailment} \end{cases} \quad (2.7)$$

Equations 2.5 and 2.6 are associated with the random state sampling approach (non-sequential simulation). When the sequential simulation technique is used, the concept used to estimate the expected value of the index can be extended as follows:

$$E(\Phi) = \frac{\sum_{i=1}^{NS}\left(\sum_{j=1}^{n_i(S)}\Phi(S_{j,i})\right)}{NS} \quad (2.8)$$

where: $n_i(S)$ = Number of occurrences of system state S in year i,

$\Phi(S_{j,i})$ = Index function corresponding to j^{th} occurrence in year i,

NS = Number of simulation years.

Sequential Simulation Illustration:

The sequential simulation process described above is briefly illustrated using the simple system composed of two parallel redundant components shown in Figure 2.1. This system is in the failed state when both components are in the failed state at the same time.

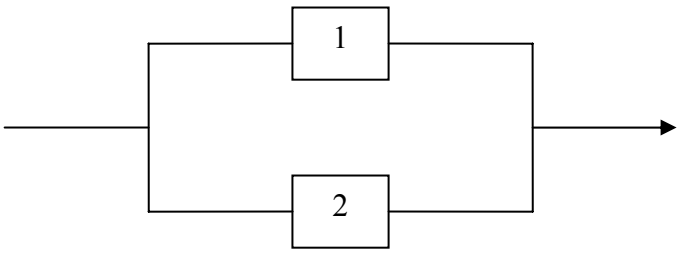

Figure 2.1: A simple parallel system.

The chronological component state transition processes of the two components obtained using Steps 1-3 for the first three simulation years are illustrated in Figure 2.2. The chronological system state transition process is obtained by combining the

chronological component state transition processes as shown in the bottom of Figure 2.2. There is no system failure in the first simulation year and there are one and two failures in the second and third simulation years respectively. If the desired reliability index $\Phi(S)$ is the system failure frequency index, the expected value $E(\Phi)$ based on the three simulation years can be calculated as follows using Equation 2.8.

$$E(\Phi) = \frac{\Phi(S_{fail,\,1}) + \Phi(S_{fail,\,2}) + \Phi(S_{fail,\,3})}{3}$$

$$E(\Phi) = \frac{(0) + (1) + (1+1)}{3} = 1.0 \text{ occurrence/year}$$

It is important to note that a large number of simulation years is required in order to obtain a reasonable result when utilizing Monte Carlo simulation. The following section addresses the stopping criterion used to terminate the simulation process.

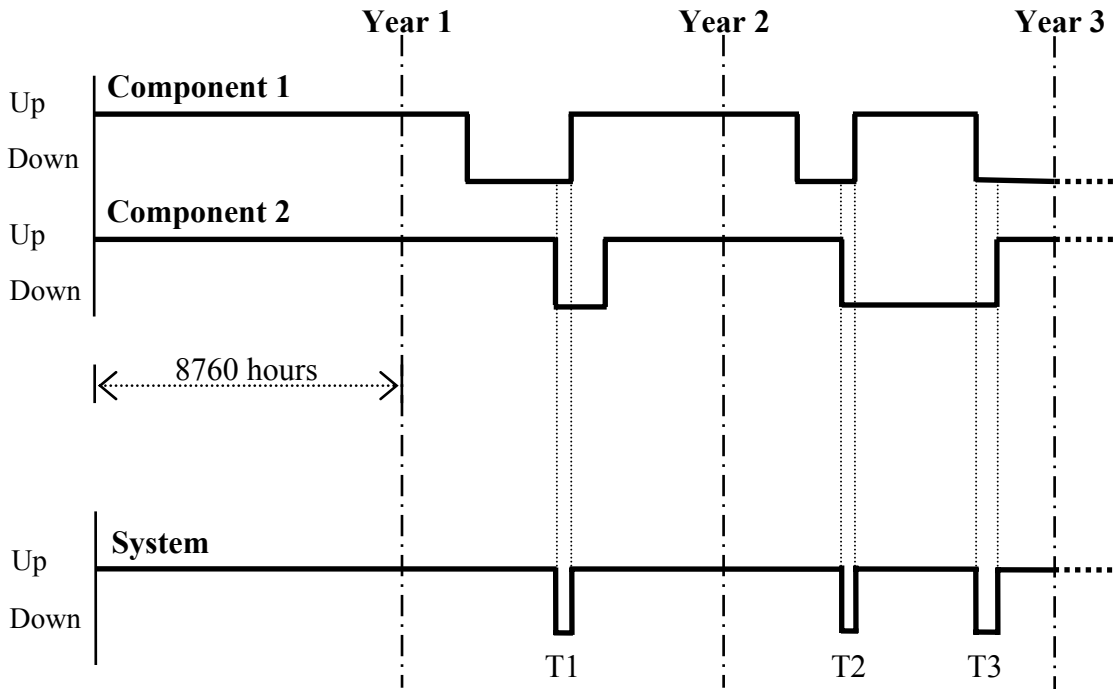

Figure 2.2: Chronological component and system state transition process of a simple parallel redundant system during the first three simulation years.

2.3.2 Simulation Convergence and Stopping Criterion

Monte Carlo simulation creates a fluctuating convergence process and there is no guarantee that a few more samples will definitely lead to a smaller error. It is true, however, that the error bound or the confidence range decreases as the number of samples increase. It is, however, not practical to run the simulation for an extremely large number of samples requiring an extensive computation time. A compromise, therefore, must be made between the required accuracy and the computing time. The purpose of a stopping rule is to allow the simulation to run until the reliability index achieves a specified degree of accuracy. The basic parameter used in the stopping criterion is the coefficient of variation and is derived as follows:

A fundamental parameter in reliability evaluation is the mathematical expectation of a given reliability index. Salient features of Monte Carlo simulation for reliability analysis therefore can be discussed from an expectation point of view [13]. Let X be the reliability index to be estimated. In sequential simulation, the number of samples is the number of simulation years. The expect value of the reliability index (X) is given by

$$E(X) = \frac{1}{N}\sum_{i=1}^{N} x_i \tag{2.9}$$

where: x_i = The observed value of X in year i,

N = The total number of simulation years.

The unbiased variance of the reliability index (X) is

$$V(X) = \frac{1}{N-1}\sum_{i=1}^{N}(x_i - E(X))^2 \tag{2.10}$$

It is important to note that Equation (2.9) provides only the expected value of the reliability index (X). The uncertainty around the estimate can be measured by the variance of the expectation estimate:

$$V(E(X)) = \frac{V(X)}{N} \tag{2.11}$$

The standard deviation of the expectation estimate is given by

$$\sigma(E(X)) = \sqrt{V(E(X))} = \sqrt{\frac{V(X)}{N}} \tag{2.12}$$

The accuracy level of a sequential Monte Carlo simulation can be expressed by the coefficient of variation (β) which is defined as follows:

$$\beta = \frac{\sigma(E(X))}{E(X)} \tag{2.13}$$

The coefficient of variation (β) shown in Equation (2.13) can be rewritten using Equation (2.12) as:

$$\beta = \frac{1}{E(X)}\sqrt{\frac{V(X)}{N}} = \frac{\sigma(X)}{E(X)\times\sqrt{N}} \tag{2.14}$$

where $\sigma(X) = \sqrt{V(X)}$. The simulation can be terminated when a specified coefficient of variation has been achieved. The selected stopping criterion is designated as the acceptable tolerance error (ε) in the simulation as shown in Equation (2.15).

$$\frac{\sigma(X)}{E(X)\times\sqrt{N}} < \varepsilon \tag{2.15}$$

where ε is the maximum (tolerance) error allowed, i.e. 5% or 0.05.

As shown in Equations (2.14) and (2.15), the value of β will decrease as the number of simulation years increase and the simulation process can be terminated when β is less than ε. It is important to note that the specified accuracy level of a Monte Carlo simulation is directly related to the number of simulation samples and is not dependent on the size of the system. Monte Carlo simulation techniques are therefore quite suitable for handling large systems with complex features. It is also important to note that the computation effort is affected by the value being estimated, i.e. the more reliable the system is, the harder it is to estimate the value. In power system reliability analysis, different reliability indices have different convergence speeds. It has been found that the coefficient of variation of the expected energy not supplied (EENS) index has the lowest rate of convergence. This coefficient of variation is therefore utilized as the convergence criterion in order to guarantee reasonable accuracy in a multi-index study [13].

The sequential simulation approach briefly described in this chapter is utilized to conduct bulk electric system reliability analysis in the research work described in this thesis. The advantages and disadvantages of this approach are summarized in the following.

Advantages:

- Accurate frequency-related indices in reliability assessment can be obtained when utilizing the sequential simulation approach.
- Any state duration distribution function related to component reliability characteristics can be easily incorporated in the sequential simulation approach.
- The probability distributions of the reliability indices can be obtained in addition to the expected values.
- Detailed system operating conditions and historical system behavior can be incorporated in the simulation process.

Disadvantages:

- The sequential simulation approach requires considerably more computation time and memory storage than non-sequential simulation methods because it is necessary to generate a random variate following a given distribution function for each component and to store information on the chronological component state transition processes of all the components in a long time span. This technique can now, however, be realistically used in bulk electric system reliability evaluation due to the developments in high speed computation facilities.
- The sequential simulation approach requires detailed input data such as chronological load curves, which some utilities may not have. Such detailed data, however, are becoming more important especially in the competitive electricity environment. It is expected that such detailed data will become more routinely available in the future.

2.4 Conclusions

Non-sequential Monte Carlo simulation techniques are briefly introduced in this chapter. The basic concept and methodology of the sequential Monte Carlo simulation approach are discussed and illustrated. The advantages and disadvantages when applying sequential simulation to bulk electric system reliability analysis are briefly addressed.

CHAPTER 3
BULK ELECTRIC SYSTEM RELIABILITY ANALYSIS USING SEQUENTIAL SIMULATION

3.1 Introduction

A bulk electric system contains both generation and transmission facilities and is sometimes designated as a composite generation and transmission system (or composite system) [11]. Bulk electric system reliability analysis is concerned with the total problem of assessing the ability of the generation and transmission system to supply reliable electrical energy to the major system load points. These load points are known as bulk supply points, points of delivery or delivery points. This form of study can also be designated as hierarchical level II (HL-II) reliability analysis [2]. In a bulk electric system, the transmission configuration which links the generating units to the major load buses is usually relatively complicated and it is rarely possible to model the transmission configuration using simple series/parallel reduction techniques. The reliability analysis of a bulk electric system, therefore, normally involves the solution of the network configuration under random outage situations. Network solution and related techniques for bulk electric system reliability evaluation are described in this chapter. As noted earlier, system reliability can be divided into the two domains designated as system adequacy and system security. This chapter deals with reliability modeling from a system adequacy perspective. Extended adequacy assessment incorporating system security considerations is addressed in Chapter 8.

There is a wide range of adequacy indices which can be calculated at the individual delivery points and for the overall bulk electric system. Individual delivery point indices are useful in identifying weak points in the system and in establishing

appropriate system reinforcements. They are also useful as input indices in the reliability analysis of electric distribution systems fed from the relevant bulk supply points. The overall system indices provide an appreciation of the global system adequacy in regard to the ability of the system to satisfy its overall load and energy requirements. These indices are useful for overall system adequacy management. They can also be used in a comparison of one system with another. The delivery point and system indices, therefore, do not replace each other, but complement each other [2].

3.2 Adequacy Indices

Adequacy indices are computed using the fundamental parameters of frequency, duration and magnitude of power outage events. The magnitude of an outage event depends on the components on outage (contingencies), their relative importance and their location in the network. An outage event may affect a wide area of the system or it may affect only a small group of buses or perhaps a single bus. Different outage events (contingencies) can affect different sets of delivery points, and create different individual delivery point indices. Overall system indices cannot, however, offer this information. It is therefore not reasonable to draw conclusions regarding the adequacy of a particular delivery point from the overall system indices.

3.2.1 Delivery Point Indices

Expected Duration of Load Curtailment (EDLC) at Bus k:

$$EDLC_k = \frac{\sum_{i=1}^{NS}\left(\sum_{j=1}^{N_{i,k}} d_{j,i,k}\right)}{NS} \quad \text{(hours/year)} \tag{3.1}$$

where: $N_{i,k}$ = Number of interruptions occurring in year i, at Bus k,

$d_{j,i,k}$ = Duration of the j^{th} interruption (hours) in year i at Bus k,

NS = Number of simulation years.

Probability of Load Curtailment (PLC) at Bus *k*:

$$PLC_k = \frac{EDLC_k}{8760} \quad \text{(/year)} \tag{3.2}$$

Expected Frequency of Load Curtailment (EFLC) at Bus *k*:

$$EFLC_k = \frac{\sum_{i=1}^{NS} N_{i,k}}{NS} \quad \text{(occurrences/year)} \tag{3.3}$$

Expected Energy Not Supplied (EENS) at Bus k:

$$EENS_k = \frac{\sum_{i=1}^{NS}\left(\sum_{j=1}^{N_{i,k}} BusENS_{j,i,k}\right)}{NS} \quad \text{(MWh/year)} \tag{3.4}$$

where: $BusENS_{j,i,k}$ = Energy not supplied in MWh for the j^{th} interruption, in year *i* at Bus *k*.

3.2.2 System Indices

Expected Duration of Load Curtailment (EDLC) of the overall system:

$$EDLC = \frac{\sum_{i=1}^{NS}\left(\sum_{j=1}^{N_i} d_{j,i}\right)}{NS} \quad \text{(hours/year)} \tag{3.5}$$

Where: N_i = Number of system interruptions in year i,

$d_{j,i}$ = Duration of the j^{th} system interruption (hours), in year i.

Probability of Load Curtailment (PLC) of the overall system:

$$PLC = \frac{EDLC}{8760} \quad \text{(/year)} \tag{3.6}$$

Expected Frequency of Load Curtailments (EFLC) of the overall system:

$$EFLC = \frac{\sum_{i=1}^{NS} N_i}{NS} \qquad \text{(occurrences/year)} \qquad (3.7)$$

Expected Energy Not Supplied (EENS) of the overall system:

$$EENS = \frac{\sum_{i=1}^{NS}\left(\sum_{j=1}^{N_i} SysENS_{j,i}\right)}{NS} \qquad \text{(MWh/year)} \qquad (3.8)$$

where: $SysENS_{j,i}$ = System energy not supplied in MWh for the j^{th} interruption, in year i.

These adequacy indices when calculated for a single load level (constant load) over a period of one year are referred to as "annualized indices". In practical systems, the load demand does not remain constant throughout the period and the chronological load model (time varying load) can be used to produce more representative "annual indices". The basic annual indices are different from the annualized indices obtained using peak load levels. All the adequacy indices described by Equations (3.1) – (3.8) are utilized in the research described in this thesis and are obtained using the sequential Monte Carlo simulation technique.

3.3 Network Solution Techniques

Adequacy assessment of a bulk electric system generally involves the solution of the network configuration under random outage situations (contingencies). Various techniques, depending upon the adequacy criteria used and the intent behind these studies, are used in analyzing the adequacy of a power system. The three basic techniques used in network solutions are as follows [12, 26]:

- A network flow method [27, 28]
- DC load flow method [29, 30]
- AC load flow method [30, 31, 32]

The selection of an appropriate technique is of prime importance and is an engineering decision. The key point is that the selected technique should be capable of satisfying the intent behind the studies from a management, planning and design perspective. One of the simplest techniques is to treat the system as a transportation model (network flow model) [27]. This method is based on the movement of a particular commodity from a number of sources to a number of demand centers. The network flow model preserves the power balance at each node of the network and does not satisfy Kirchhoff's law which may not be appropriate for practical power system operation. Approximate load flow techniques such as DC load flow are quite simple and fast but only provide estimates of the line power flows, without including any estimate of the bus voltages and the generating unit reactive power limits. When both continuity and quality of the power supply are of concern, then it is necessary to examine the voltage levels at each major load center and the reactive power (MVAr) limit of each generating unit while considering the effect of component outages i.e. generating units, transmission line and transformers [33]. Considering a power network as a transportation model or using DC load flow does not provide an estimate of the quality of the power supply. If the quality of power supply including acceptable voltage levels and appropriate generating unit MVAr limits is an important adequacy requirement, more accurate AC load flow methods [30, 32] such as Newton-Raphson, Gauss-Seidel techniques must be utilized to calculate the adequacy indices. These techniques however require large computer storage and are computational expensive. A fast AC load flow technique such as the "fast decoupled load flow" [31] method, which is a modification of the Newton-Raphson load flow approach, can be employed. The following is a brief description of the two network solution techniques used in this research work.

3.3.1 DC Load Flow Method

One of the simplest network solution techniques applied in contingencies studies is the DC load flow method. Reference [34] presents work on composite generation and transmission system reliability evaluation utilizing the DC load flow technique. This approach uses the following linear model:

$$[P] = [B'][\delta] \tag{3.9}$$

where: $[P]$ = Vector of bus power injection,
$[B']$ = System susceptance matrix,
$[\delta]$ = Vector of phase angle (in radian).

The dimensions of $[P]$ and $[B']$ are $(n-1)\times 1$ and $(n-1)\times(n-1)$ respectively, where n is the total number of buses in the system, and one bus is specified as the slack or swing bus (reference bus).

The vector of bus phase angles $[\delta]$ can be calculated by solving Equation (3.9) using $[B']$ and $[P]$. The computed bus phase angles are then used to determine the individual branch flows (power flow on a line or transformer) as given in Equation (3.10).

$$P_{ij} = \frac{\delta_i - \delta_j}{X_{ij}} \tag{3.10}$$

Where: P_{ij} = Real power flow from Bus i to Bus j,
δ_i = Phase angle at Bus i,
δ_j = Phase angle at Bus j,
X_{ij} = Reactance of the line between Bus i and Bus j.

Voltage and reactive power constraints and transmission line losses cannot be evaluated using this simple method. The solution is, however, fast and free of convergence problems. The DC load flow method described in this section is not the main network solution technique used in this research work. The fast decoupled AC load flow method described in the following section is used as the basic network solution technique. The DC load flow method is, however, employed if the fast decoupled AC load flow cannot find a solution due to divergence when dealing with an infrequent

system ill-conditioned network situation. This issue is addressed later in the corrective actions section.

3.3.2 Fast Decoupled AC Load Flow Method

The fast decoupled load flow technique [31] is a good compromise between the basic AC and DC load flow approaches in regard to storage requirements and solution speed. It can be used to check the continuity as well as the quality of a power system thus meeting the two important adequacy requirements involving reactive power and voltage constraints. Reactive power and voltage constraints are becoming serious concerns in current bulk electric systems in the deregulated electricity environment where the transmission open access paradigm has created heavy utilization of the transmission network. Reactive power problems were a significant factor in the August 14/2003 outage affected the Northeastern U.S. and parts of Canada [35]. The fast decoupled load flow method is therefore used to conduct bulk electric system reliability analysis in this research. A brief description of the fast decoupled load flow technique is given below.

The general equations for the power system mismatch at all system buses except the swing bus (reference bus) can be obtained using the Newton-Raphson load flow technique [36]. The fast decoupled load flow method neglects the weak coupling between the changes in real power and voltage magnitude, and the changes in reactive power and phase angle. The mismatches of active power and reactive power are expressed in Equations (3.11) and (3.12) respectively.

$$[\Delta P] = [J_\delta][\Delta\delta] \tag{3.11}$$

$$[\Delta Q] = [J_v][\Delta V/V] \tag{3.12}$$

where: ΔP_i = Active power mismatch at Bus i,

ΔQ_i = Reactive power mismatch at Bus i,

$\Delta\delta_i$ = Increment in phase angle of the voltage at Bus i,

ΔV_i = Increment in magnitude of the voltage at Bus *i*,

J_δ, J_v = Submatrices of the Jacobian matrix [36],

δ_i = Phase angle of the voltage at Bus *i*,

V_i = Magnitude of the voltage at Bus *i*.

Equations (3.11) and (3.12) can be further simplified by making the following assumptions, which are usually valid in a practical power system:

$$\cos(\delta_i - \delta_j) \approx 1.0 ,$$

$$g_{ij}.\sin(\delta_i - \delta_j) << b_{ij} ,$$

$$Q_i << b_{ij}.V_i^2$$

where: $(g_{ij} - jb_{ij})$ = Series admittance of the line connecting Buses *i* and *j*,

Q_i = Reactive power at Bus *i*.

The final equations used in the fast decoupled load flow technique are given by Equations (3.13) and (3.14) using the simplifications [31] noted above.

$$[\Delta P/V] = [B'][\Delta\delta] \quad (3.13)$$

$$[\Delta Q/V] = [B''][\Delta V] \quad (3.14)$$

Both matrices *[B']* and *[B'']* are real, sparse and contain only network admittances. Since *[B']* and *[B'']* are constant, they need to be inverted or factorized only once at the beginning of iterative process. The voltage magnitude at each load bus and the phase angle at each bus except the swing bus are modified in each iteration as shown in Equations (3.15) and (3.16).

$$[\delta]_{new} = [\delta]_{old} + [\Delta\delta] \quad (3.15)$$

$$[V]_{new} = [V]_{old} + [\Delta V] \quad (3.16)$$

The power mismatches *[ΔP]* and *[ΔQ]* are calculated for each new value of bus angle and bus voltage. Equations (3.13) and (3.14) are iterated in some defined manner towards an exact solution, i.e. when power mismatches are less than the tolerance. In the case of transmission line or transformer outages, the Sherman-Morrison correction formula [26, 37] can be used to reflect the outages without rebuilding and refactorizing the system matrices *[B']* and *[B"]*.

3.4 Corrective Actions

In normal operation, all the operating limits are satisfied. The operating constraints are described as follows [13]:

1. Voltage magnitude constraints: Operating limits are imposed on the voltage magnitude of buses, i.e.,

$$V^{min} \leq V \leq V^{max} \tag{3.17}$$

where: V^{min} and V^{max} represent the minimum and maximum voltage limits respectively.

2. Branch flow constraints: These are the thermal capacity limits on transmission lines and transformers. In some cases, the steady state stability limits on transmission lines expressed by angle differences can also be transformed into branch flow constraints.

$$|T| \leq T^{max} \tag{3.18}$$

where: T = Power flow on a branch,

T^{max} = Maximum capacity limit of a line or transformer.

3. Real power (MW) generation constraints: The real power generation constraints at the swing bus and generator buses are

$$P^{min} \leq P \leq P^{max} \tag{3.19}$$

where: P^{min} and P^{max} represent the minimum and the maximum power generation at each generator bus respectively.

4. Reactive power (MVAr) generation constraints: The reactive power generation constraints at the swing bus and generator buses are

$$Q^{min} \leq Q \leq Q^{max} \tag{3.20}$$

where: Q^{min} and Q^{max} represent the minimum and the maximum reactive power generation at each generator bus respectively.

All the operating constraints described above must be satisfied for normal operation of a bulk electric system. When any operating constraint is violated, corrective action(s) is required in order to alleviate the operating constraint problem and to restore the system to normal operation. The occurrence of a system problem may by itself be recorded as a failure event. In many cases, however, it may be possible to eliminate a system problem by taking appropriate corrective action. It is, therefore, of interest to determine whether it is possible to eliminate a system problem by employing proper corrective action. There is no consensus among power utilities and related organizations regarding uniform failure criteria and therefore all organizations do not use the same fundamental solution technique to calculate the adequacy of their systems [38]. The broad categories of corrective action [26, 31, 39, 40] that can be employed are as follows:

1. Generation rescheduling in the case of a capacity deficiency in the system.
2. Alleviation of transmission line overloads.
3. Correction of generating unit MVAr limits violations.
4. Correction of a voltage problem at a bus and the solution of ill-conditioned network situations when using AC load flow techniques.
5. Bus isolation and system splitting under transmission line or transformer outages.
6. Load curtailment in the event of a system problem.

Corrective action to alleviate operating constraint violations can be conducted using an optimal power flow (OPF) approach. Nonlinear OPF requires a large amount of CPU time and can encounter convergence problems in some multi-component failure situations. The ability to include a high degree of accuracy in corrective calculations will

never override the inherent uncertainties in the forecast data including load, failure rates, repair rates and in the Monte Carlo simulation. It is therefore reasonable to use a linear optimization model for corrective action analysis [13] in bulk electric system reliability assessment.

3.4.1 Linear Programming Model for Load Curtailment and Generation Rescheduling

In the event of constraint violation(s), the system encounters an emergency situation in which load may or may not be curtailed after corrective action has been taken to eliminate the operating constraint violations. The initial activity is normally to alleviate the problem by rescheduling generation without requiring load curtailments. If it is not possible to overcome this difficulty by rescheduling the generation, then load will be curtailed at different buses while minimizing the total load curtailment. A linear programming method designated as a dual simplex algorithm [41, 42], which is described in detail in Appendix B, is used for generation rescheduling and load curtailment minimization. The objective of the minimization model is to minimize the total load curtailed at each bus while simultaneously satisfying the power balance. This minimization model is as follows [13]:

Objective function:
$$\min \sum_{i \in ND} W_i . C_i \tag{3.21}$$

Subject to:
$$T(S^k) = A(S^k)(PG + C - PD) \tag{3.22}$$
$$\sum_{i \in NG} PG_i + \sum_{i \in ND} C_i = \sum_{i \in ND} PD_i \tag{3.23}$$
$$PG^{min} \leq PG \leq PG^{max} \tag{3.24}$$
$$0 \leq C \leq PD \tag{3.25}$$
$$| T(S^k) | \leq T^{max} \tag{3.26}$$

where: $T(S^k)$ = Line flow vector under system state S^k,

T^{max} = Maximum capacity limit vector for the line flows $T(S^k)$,

$A(S^k)$ = Relation matrix between line flows and power injections under state S^k,

PG = Generation vector with minimum (PG^{min}) and maximum (PG^{max}) limits,

PD = Load vector,

NG = Set of generator buses,

ND = Set of load buses,

C = Load curtailment vector,

W = Weighting factor vector related to a specified load shedding policy

Equation (3.21) incorporates the system load curtailment philosophy using the variable W_i which is designated as the bus weighting factor. Different load shedding policies can be incorporated by assigning a different W_i value at each load bus (delivery point). There is a wide range of possible load curtailment philosophies. Three possible policies are used in this research. These three possible schemes are implemented by assigning different sets of weighting factors (W_i). Load curtailment philosophy considerations are addressed later in this chapter.

3.4.2 Linear Programming Model for Voltage Adjustment and Reactive Load (MVAr) Curtailment

Bus voltage violations can be alleviated by adjusting the generator bus voltages and/or by reactive power injections from reactive sources. If it is not possible to eliminate all the bus voltage violations by these adjustments, then reactive load curtailments at some buses are unavoidable. Reactive load curtailments should be minimized in this case. The linear programming model designated as a primal simplex algorithm [41, 43] and described in detail in Appendix B is used for this purpose [13, 44].

Objective function: $$min\left(\sum_{i \in NG} \alpha_i \mid \Delta V_i^0 \mid + \sum_{j \in ND} \beta_j \Delta Q_j \right) \tag{3.27}$$

Subject to: $$[B][\Delta V] + [B^0][\Delta V^0] = [\Delta Q] \tag{3.28}$$

$$\Delta V_i^{min} \leq \Delta V_i \leq \Delta V_i^{max} \qquad (i \in NG \cup NR) \tag{3.29}$$

$$\Delta V_j \geq \Delta V_j^* \qquad (j \in ND) \tag{3.30}$$

$$\Delta Q_i^{min} \leq \Delta Q_i \leq \Delta Q_i^{max} \qquad (i \in NG \cup NR) \qquad (3.31)$$

$$0 \leq \Delta Q_j \leq \Delta Q_j^{max} \qquad (j \in ND) \qquad (3.32)$$

where:

ΔV^0 = Bus voltage change vector associated with generation buses, and static reactive source buses with lower limit ΔV^{min} and upper limit ΔV^{max},

ΔV = Bus voltage change vector associated with load buses with lower limit ΔV^{min} and upper limit ΔV^{max},

ΔV^* = Voltage violations at load buses,

ΔQ = Reactive power change vector with lower limit ΔQ^{min} and upper limit ΔQ^{max},

$[B^0]$ = Elements of the admittance matrix associated with generation buses, and static reactive source buses,

$[B]$ = Elements of the $[B'']$ matrix in Equation (3.14) associated with load buses,

NG = Set of generator buses,

ND = Set of load buses,

NR = Set of static reactive source buses,

α = Weighting factor vector associated with generation buses, and static reactive source buses,

β = Weighting factor vector associated with load buses.

The main objective of the optimization model is to minimize the total reactive load (MVAr) curtailment. The β_j weighting factors therefore have to be larger than the α_i weighting factors. This means that the voltage constraint violations are initially corrected by generator bus and/or reactive source bus voltage adjustments without reactive load curtailment. If it is not possible to overcome the difficulty by generator bus voltage adjustments, then reactive load will be curtailed. The first term in the objective function provides the possibility that when there is no need for reactive load curtailment, the generator bus voltage adjustments will be minimized. Equation (3.29) indicates that the generator and reactive source bus voltage adjustments should be within the permissible changes, which are the differences between the bus voltage limits and their actual values in the contingency state. Equation (3.30) indicates that load bus voltage

changes should be larger than their violations, which are the differences between the actual load bus voltages in the contingency state and their limits. Equation (3.31) indicates that reactive power adjustments at generator and reactive source buses should be within the permissible changes, which are the differences between the bus reactive power limits and their actual values in the contingency state. Equation (3.32) indicates that when load bus reactive power curtailments are unavoidable, these curtailments cannot exceed the actual reactive loads. Therefore ΔQ_j^{max} are basically the bus reactive loads. It is important to note that reactive load (MVAr) curtailment cannot be done alone without curtailing a portion of real power load (MW). The load power factor is assumed to be fixed at each load bus, and is used to calculate the resulting real power load (MW) that must be shed corresponding to the required curtailed reactive load (MVAr). This optimization model is also used as a corrective action for generating unit reactive power (MVAr) limit violations.

3.4.3 Split Network Solution

Changes in the network configuration due to the outages of line(s) and/or transformer(s) may result in splitting a network into two or more than two smaller networks. Each network may consist of load buses and generator buses. Under steady-state conditions, they can be treated as separate independent networks. The most appropriate technique for this purpose is to recompute the system matrices *[B']* and *[B"]* for each of subnetworks and then use AC load flow to determine the system problem(s). This technique requires a large computation time to recompute and factorize the system matrices for each network. This method also needs additional memory to store the matrices for each of the networks. In a practical bulk electric system, a split network situation usually has a low probability of occurrence, and therefore occurs infrequently. An approximate method for split network solution can be used to reduce the computation time. The following approximate method has been used in this research work to solve split network situations [26].

Figure 3.1 is used to illustrate the approximate method used to solve split network situations. Lines on outage can be ideally represented as lines in service having infinite impedances. It can, therefore, be assumed that networks A and B in Figure 3.1 are connected by two lines with very high impedances. The power flow through these lines will be very small due to the high impedances and essentially these lines therefore do not connect the networks. The change to high impedance values in the network matrix *[B']* can be easily incorporated using Woodbury's formula [45]. In order to further limit the power flows, the capacity of these lines can be assumed to be close to zero in the linear programming model, i.e. in Equation (3.26). The Woodbury formula has been used to update the $[B']^{-1}$ matrix using high impedances for the line(s) which cause the split network. The linear programming model is developed with the updated matrix using normal line power capacities for the lines not on outage. The lines on outage which cause a split network are considered to be in service with very low power flow capacities and high impedance.

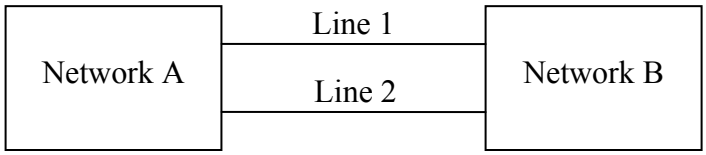

Figure: 3.1 Split network situation

3.4.4 Solution of Ill-Conditioned Network Situations

A drawback when utilizing the AC load flow technique is the possibility of non-convergent situations in the network. These non-convergent situations are frequently encountered while considering the outages of transmission lines/transformers. Most of the non-convergent situations result due to high values of mismatch in the reactive power beyond the permissible tolerance limit. Very few situations result due to high values of mismatch in the active power. Another possibility is that a load flow may not converge although a solution, in fact, does exist. This non-convergence could occur due to numerical problems with the fast decoupled algorithm and/or the characteristics of the

numerical formulations used [46]. In order to avoid these non-convergent situations when a solution does exist, an additional algorithm is required in the load flow algorithm. Reference [47] suggests that the convergence property of the Newton-Raphson load flow can be improved by scaling the solution projection calculated by the load flow algorithm without changing the direction of the projection. A heuristic technique that is adaptable to the fast decoupled AC load flow was suggested [29, 46] to adjust the scaling factor by monitoring the sum of the squares of the power mismatches before and after each voltage magnitude and phase angle correction. Under normal load flow situations, the scaling factor is taken as 1.0, but in the case when the sum of the squares of the power mismatches for the new iteration exceeds the value calculated from the previous iteration, the scaling factor is decreased from its initial value of 1.0 by a factor. The value of the factor is arbitrary and could lie between 0.0 and 1.0. During one complete load flow cycle, the value of the scaling factor is decreased whenever the sum of the squares of the power mismatches exceeds its previous value [46]. This heuristic technique is incorporated in the fast decoupled AC load flow algorithm used in this research work when non-convergent situations occur.

Although the heuristic technique for non-convergence described above is able to eliminate the non-convergent situations when a load flow solution does exist, a non-convergent situation may still persist due to the fact that the AC load flow equations may have no real solution under a given operating condition. This kind of problem, which can be designated as power flow unsolvability, could happen when a heavily stressed system is subjected to a severe contingency situation leading to voltage collapse in the system. In the case of a power flow unsolvability situation, the network solution technique switches to the DC load flow method described in Section 3.3.1. The DC load flow approach is used in this research work as an approximate method to solve a problem when there is no AC load flow solution under some severe outage contingencies. In the DC load flow approach, reactive power and voltage constraints are relaxed. Operating constraints are therefore only focused on generating unit real power constraints and branch flow constraints. The linear programming model for load

curtailments and generation rescheduling expressed in Equations (3.21) – (3.26) is applied to solve operating constraints under power flow unsolvability circumstances.

3.4.5 Load Curtailment Philosophies

During extreme emergency situations, system operators are required to make load shedding decisions based on system security concerns, i.e. voltage, current, power and frequency constraints, to alleviate system constraints and maintain system stability. Load shedding policies can differ from one system to another. These differences are basically dependent on the individual utility philosophies and objectives under extreme emergency situations. Three load curtailment philosophies designated as the priority order, pass-1 and pass-2 policies are utilized in this research work. In these three policies, loads are classified according to their importance and divided into the categories of firm and interruptible load. Interruptible load is initially curtailed followed by firm load, if necessary. The mathematical formulation and algorithms for load shedding are described in [13]. The basic concept utilizes an optimization technique using linear programming for the minimization model of bus load curtailment described by Equations (3.21) – (3.26). A weighting factor (W_i) expressed in Equation (3.21) is assigned to each load bus i (delivery point i). Incorporating different load shedding policies can be done by quantifying the W_i value of each load bus. When adopting the pass-1 policy, the load buses closest to the elements on outage(s) are assigned with a relatively small W_i and those far from the outage(s) are assigned with a relatively large W_i. The pass-2 policy is an extension of the pass-1 policy to include load buses further removed from the contingency area. When the priority order policy is used as the load curtailment philosophy, the most important load bus is assigned with the largest W_i while the least important load bus has the smallest W_i. The optimization process is then conducted in order to provide the optimum solution by assigning a W_i to each load bus as input to the linear programming technique. The three load curtailment philosophies are used to illustrate the importance of individual delivery points under system emergency situations, and are described further in the following.

A. Priority Order Policy

This philosophy is based on ranking all the bulk delivery points using a reliability worth index such as the interrupted energy assessment rate (IEAR) in $/kWh [2, 48, 49]. This parameter is similar to the value of lost load (VoLL) used in the UK [50]. The bulk delivery point that has the highest IEAR will have the highest priority, and the delivery point that has the lowest IEAR will have the lowest priority. When the bulk power system encounters a severe contingency that requires load curtailments, the delivery point that has the lowest priority will be initially curtailed. This policy minimizes customer interruption costs due to load curtailments. There are two basic test systems used in this research work. These systems are designated as the RBTS [51] and the IEEE-RTS [52] and are described in detail later. The priority order for the RBTS and IEEE-RTS are shown in Tables 3.1 and 3.2 respectively.

Table 3.1: IEAR values and priority order for each delivery point in the RBTS.

Delivery Point (DP)	IEAR ($/kWh)	Priority order	Delivery Point (DP)	IEAR ($/kWh)	Priority order
Bus 2	9.6325	1	Bus 5	8.6323	2
Bus 3	4.3769	5	Bus 6	5.5132	4
Bus 4	8.0267	3			

Table 3.2: IEAR values and priority order for each delivery point in the IEEE-RTS.

Delivery Point (DP)	IEAR ($/kWh)	Priority order	Delivery Point (DP)	IEAR ($/kWh)	Priority order
Bus 1	8.9815	3	Bus 10	5.1940	14
Bus 2	7.3606	5	Bus 13	7.2813	6
Bus 3	5.8990	11	Bus 14	4.3717	16
Bus 4	9.5992	1	Bus 15	5.9744	10
Bus 5	9.2323	2	Bus 16	7.2305	7
Bus 6	6.5238	9	Bus 18	5.6149	13
Bus 7	7.0291	8	Bus 19	4.5430	15
Bus 8	7.7742	4	Bus 20	5.6836	12
Bus 9	3.6623	17			

B. Pass-1 Policy

In this load shedding policy, loads are curtailed at the delivery points that are closest to (or one line away from) the element(s) on outage. This load shedding policy tends to localize the severity of an event within the area in which the element outage(s) occur. This policy minimizes the number of delivery points affected by a specific event.

C. Pass-2 Policy

This load shedding policy extends the concept of the pass-1 policy. Loads are curtailed at the delivery points that surround the outaged element. Delivery points which are one line away and two lines away from the outaged element are considered for load curtailment. Interruptible loads at delivery points that are one line away from the outaged element are initially curtailed followed by interruptible loads at delivery points that are two lines away from the outaged element. It is important to note that firm load curtailments at delivery points that are one line away from the outaged element are not initially applied unless interruptible load curtailments at delivery points that are two lines away from the outaged element are not sufficient to eliminate the system operating constraints.

There is a wide range of possible load curtailment policies. The three policies used in this research work are three possible schemes, and are used to illustrate the impact on the delivery point indices of an adopted load curtailment policy.

3.5 Sequential Simulation Process for Bulk Electric System Reliability Analysis

The sequential Monte Carlo simulation approach can be used to realistically represent most contingencies and the complex operating characteristics inherent in a bulk electric system and provide a comprehensive range of reliability indices. Sequential Monte Carlo simulation can be used to estimate the indices by simulating the actual chronological process and random behavior of the system in fixed discrete time steps.

Any event that occurs within a particular time step is considered to occur at the end of the time step [23]. Research on the application of the sequential simulation technique to bulk electric system reliability evaluation has been published [13, 23, 53, 54]. The overall procedure for composite generation and transmission system reliability evaluation using a sequential Monte Carlo simulation approach is briefly summed up in the following steps:

Step 1: Specify the initial state of each component (all generating units and transmission links). Normally, it is assumed that all components are initially in the normal state (up state).

Step 2: Simulate the duration of each component residing in its present state using the inverse transform method [22] and the distribution functions of the component failure and repair rates. For example, given an exponential distribution function, i.e. $f(t) = \lambda e^{-\lambda t}$, then the sampled value of the state duration (T) is: $T_i = -ln(U_i)/\lambda_i$, where U_i is a uniformly distributed random number [0,1] corresponding to the i^{th} component. λ_i is a failure rate or repair rate depending on the current state of the i^{th} component.

Step 3: Repeat step 2 in a given time span, normally a year. A chronological transition process (up and down state) for each component is then constructed in a given time span. Chronological hourly load models for individual delivery points are constructed and incorporated in the analysis.

Step 4: The simulated operation (fast decoupled AC load flow analysis) is assessed for each hour during a given time span. If operating constraints occur, corrective actions described in Section 3.4 are required to alleviate the constraints and load curtailed if necessary.

Step 5: At the end of each simulated year, the delivery point and system adequacy indices described in Section 3.2 are calculated and updated. Steps 2-4 are

repeated until the coefficient of variation is less than the specified tolerance error.

Bulk electric system reliability analysis software using sequential simulation has been developed to incorporate all the considerations described in this chapter. Some fundamental algorithms have been taken from the SECOREL program [34] which uses a DC-based load flow analysis. The developed computer software includes many features to deal with reactive power and bus voltage constraint considerations using the fast decoupled AC load flow approach. The software was extended to include a more accurate method to calculate reliability worth indices (Chapter 5), and to create reliability index probability distributions for both delivery points and the overall system (Chapter 6). In addition, the extended adequacy analysis to incorporate security considerations in the form of system well-being analysis is integrated into the software (Chapter 8). Another significant feature of the developed software is the ability to integrate an intermittent energy resource such as wind power generation into bulk electric system reliability analysis (Chapter 10). The developed computer software for bulk electric system (HL-II) reliability analysis with the above features is designated as "**RapHL-II**" which stands for "**R**eliability **a**nalysis **p**rogram for **HL-II**".

3.6 Study Systems

The two basic test systems used in this research work are the RBTS [51] and IEEE-RTS [52]. Both the original and modified versions of these two study systems are utilized in this research work. The original versions of the RBTS and IEEE-RTS are briefly described in the following. The basic data for the two test systems are given in Appendix C.

3.6.1 Roy Billinton Test System (RBTS)

The RBTS [51] is an educational test system developed by the Power System Research Group at the University of Saskatchewan. The RBTS is a 6 bus system

composed of 2 generator buses, 5 load buses, 9 transmission lines and 11 generating units. The system peak load is 185 MW and the total generation is 240 MW. A single line diagram of the RBTS is shown in Figure 3.2.

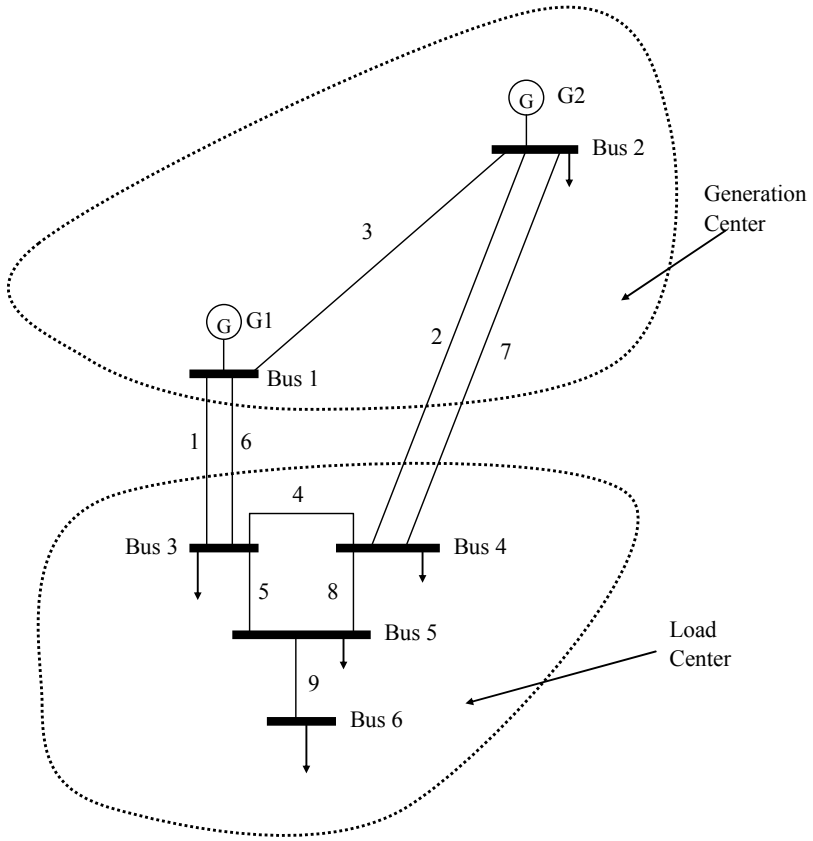

Figure 3.2: The single line diagram of the RBTS.

3.6.2 IEEE-Reliability Test System (IEEE-RTS)

The IEEE-RTS [52] is a 24 bus system with 10 generator buses, 17 load buses, 33 transmission lines, 5 transformers and 32 generating units. The system peak load is 2,850 MW and the total generation is 3,405 MW. The single line diagram is shown in Figure 3.3.

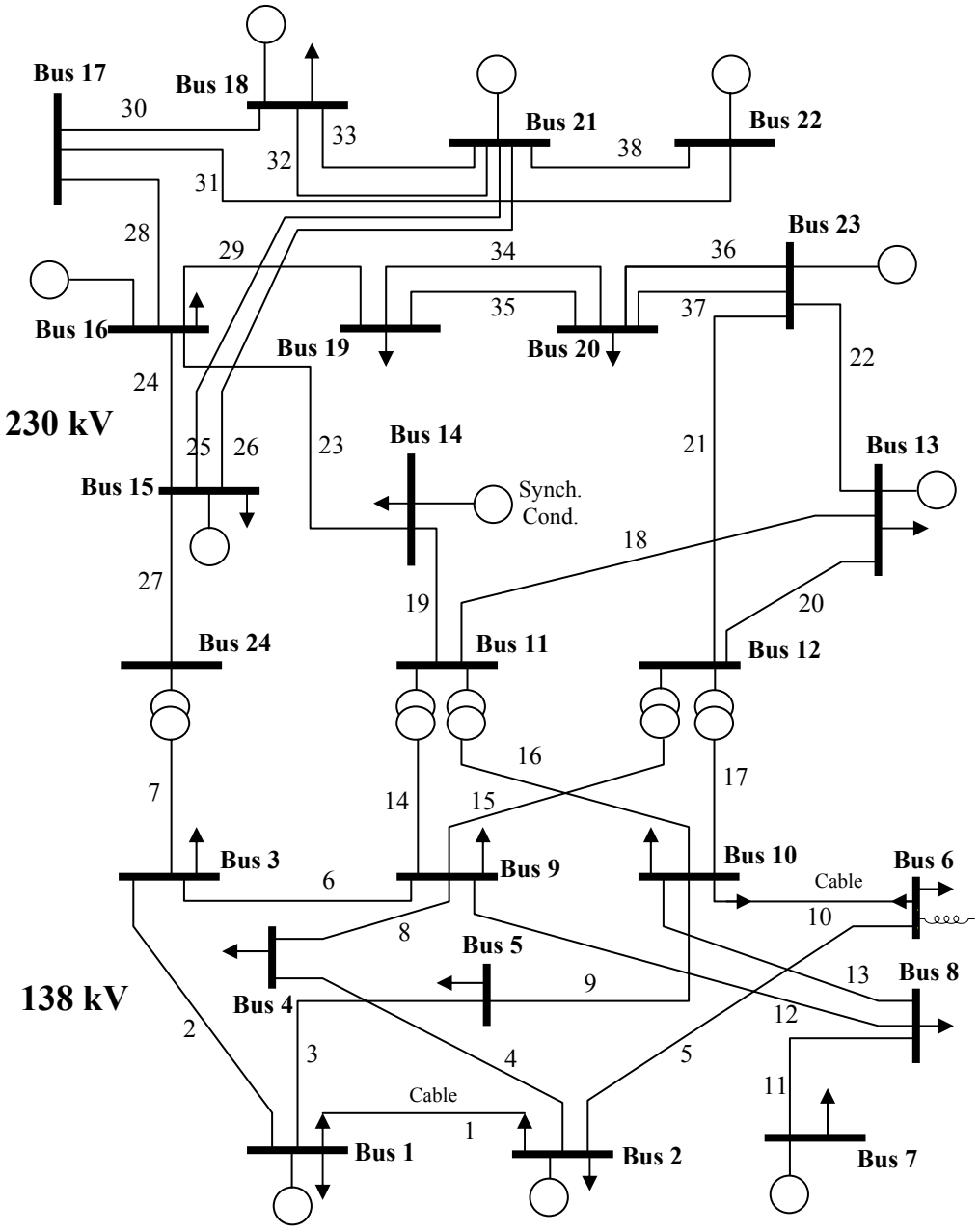

Figure 3.3: The single line diagram of the IEEE-RTS.

3.7 Chronological Load Model

The chronological or time varying load curves used in this thesis were created using a bottom-up approach [34, 54]. This approach was used to develop annual

customer sector load profiles. Seven types of customer sectors designated as agricultural, industrial, commercial, large users, residential, government and institutions, office and building were identified and the chronological load characteristics of these customer sectors are presented in Appendix D. The peak load and load factor (L.F.) can be calculated from the annual load profile of each sector. The equation and the calculation of the sector load factors are shown in Appendix D. Customer sector allocations at different load buses for the RBTS and IEEE-RTS are also shown in Appendix D.

3.8 Conclusions

This chapter presents the basic elements in bulk electric system reliability analysis using sequential Monte Carlo simulation. The equations used to obtain the delivery point and system reliability indices are presented. The network solution techniques and the methods used for corrective action due to system operating constraints violations are presented and approximate methods for split network and ill-conditioned network solutions are addressed. The concept of different load curtailment philosophies and their implementation in the linear programming technique is also discussed in this chapter. The overall sequential simulation procedure used for bulk electric system reliability analysis is demonstrated. The computer software developed in this research work is designated as RapHL-II (Reliability analysis program for HL-II) and the two test systems used in this research work are briefly illustrated.

CHAPTER 4
IMPACT OF UTILIZING SEQUENTIAL AND NON-SEQUENTIAL SIMULATION TECHNIQUES IN BULK ELECTRIC SYSTEM RELIABILITY ANALYSIS

4.1 Introduction

The two basic Monte Carlo approaches are designated as the sequential and non-sequential simulation techniques. In the non-sequential approach, the states of all components are sampled and a non-chronological system state is determined. An approximate frequency index is obtained using this method. In the sequential approach, the chronological up and down cycles of all the components are simulated and the system operating cycle is determined by combining all the component cycles. The sequential simulation technique provides an opportunity to incorporate chronological factors, and reliability index probability distributions can be calculated using this method. This approach normally requires considerably more computation time and effort than the non-sequential method. This chapter demonstrates the effects of using the non-sequential and the sequential Monte Carlo simulation techniques in bulk power system reliability evaluation. The focus is primarily on frequency-related index calculations as this index is largely affected by factors associated with failure state transitions and chronology. These two factors are discussed and investigated in this chapter. The sequential (state duration sampling) and non-sequential (state sampling) techniques are applied to the RBTS and the IEEE-RTS. Two computer software packages were used in the studies described in this chapter. The first is a commercial software known as MECORE [55] which utilizes the state sampling (non-sequential) method. The second computer program is known as SECOREL [34] and uses the sequential technique. Both software packages utilize a DC-based load flow approach and therefore can be used for

comparison purposes. The developed computer software RapHL-II was not employed in the studies described in this chapter. The RapHL-II software is illustrated in the following chapters.

4.2 Sequential and Non-Sequential Monte Carlo Simulation Procedures

As noted earlier, this chapter utilizes the two basic Monte Carlo simulation techniques designated as the non-sequential (state sampling) and sequential methods. A brief outline of the two techniques is given in the following:

4.2.1 Non-Sequential Technique

The state sampling method is used to simulate a non-sequential approach in this chapter. In the state sampling technique, the states of all components are sampled and a non-chronological system state is obtained. The basic sampling process is conducted using the random behavior of each component categorized by uniform distributions [0,1]. The probability of each component outage is given by its forced outage rate (FOR). All components are sampled using a random number generator. If a sampled random number of component *i* is less than FOR_i, this component is assumed to be in an outage state, otherwise it is in the normal state. When all components are sampled, the states of all components are combined, and the system state can be determined. The simulation procedure in this approach can be briefly summarized as follows.

Step 1: A system state is simulated.

Step 2: If the system is in a normal state, then there is no load curtailment. Go back to step 1 for the next sampling. If the sampled state is a contingency state, load curtailment may be required. Load flow analysis is conducted in this case.

Step 3: If constraints occur such as line overload, corrective actions, i.e. generation rescheduling, load curtailment, may be needed to alleviate the constraints.

Step 4: Reliability indices are calculated and updated. Steps 1-3 are repeated until the coefficient of variation is less than the specified tolerance error.

This state sampling technique is relatively simple. Distribution functions of the component failure and repair rates are not required. This method, however, cannot be used by itself to calculate the actual frequency index. It provides only an approximate estimate of the frequency index.

4.2.2 Sequential Technique

The sequential or state duration sampling approach is based on sampling the probability distributions of the component state durations. This technique can be used to model all the contingencies and operating characteristics inherent in the system. Chronological load models can also be easily incorporated. The overall process used in the sequential approach for bulk electric system reliability analysis is given in Section 3.5.

4.3 Simulation Results

There are two basic types of reliability indices. They are designated as annualized indices when derived using a constant peak load, and annual indices when calculated using a load duration curve or a chronological load model. In the non-sequential (state sampling) approach, the expected number of load curtailments (ENLC) is the sum of the occurrences of the load curtailment states. The ENLC is a surrogate for the more accurate frequency index designated as the expected frequency of load curtailment (EFLC) [13]. The sequential and non-sequential techniques are applied to two test systems designated as the RBTS and the IEEE-RTS. The results obtained using the two computer programs are given in the following subsections.

4.3.1 Annualized Indices

Tables 4.1 and 4.2 present the annualized system indices for the RBTS and the IEEE-RTS respectively. Similar indices can be obtained for each individual load point in the composite generation and transmission systems. The load point and system indices complement each other in providing an overall assessment of system adequacy. The system indices are used in this chapter to illustrate the variability of the frequency related index due to the technique and factors used in the calculation.

Table 4.1: Annualized system indices for the RBTS.

Annualized Indices	Non-Sequential	Sequential
Expected Number of Load Curtailments (occ/yr), ENLC	5.40	--
Expected Frequency of Load Curtailments (occ/yr), EFLC	--	3.70
Probability of Load Curtailments, PLC	0.01024	0.00914
Expected Energy Not Supplied (MWh/yr), EENS	1110.8	998.7
Computation time (seconds)	0.14	19.10

Table 4.2: Annualized system indices for the IEEE-RTS.

Annualized Indices	Non-Sequential	Sequential
Expected Number of Load Curtailments (occ/yr), ENLC	54.72	--
Expected Frequency of Load Curtailments (occ/yr), EFLC	--	18.57
Probability of Load Curtailments, PLC	0.07980	0.08451
Expected Energy Not Supplied (MWh/yr), EENS	122192.5	134590.6
Computation time (seconds)	0.24	75.04

An accurate frequency index (EFLC) cannot be obtained using the non-sequential technique. The ENLC shown in Tables 4.1 and 4.2 is a surrogate or approximate value for the more accurate frequency index obtained using the sequential method. When a constant load is used, the annualized ENLC obtained using the non-sequential method is a high estimate of the annualized EFLC obtained using the sequential approach. It is important to note, however, that both techniques provide quite similar estimates for other reliability indices such as the PLC and EENS, which are not frequency-related indices. The EENS index is used in a wide range of power system reliability studies and is often extended to estimate the expected customer outage costs

using an interrupted energy assessment rate in $/kWh [2]. The computation times are also shown in Tables 4.1 and 4.2 in order to illustrate the computational effort required in the two cases.

4.3.2 Annual Indices

Annual indices are normally calculated using a chronological load model or a load duration curve (LDC) on an annual basis (8760 hours). A segment of the chronological load model used for the overall RBTS is shown in Figure 4.1. Chronological load models for the individual customer types were developed using a bottom-up approach [34, 54]. The complete time-varying load model in the form shown in Figure 4.1 was transformed to an annual load duration curve (LDC) and is shown in Figure 4.2.

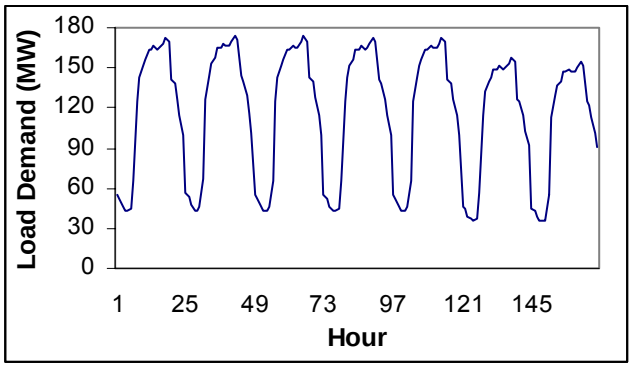

Figure 4.1: Chronological load model of the RBTS (1st week of the annual model).

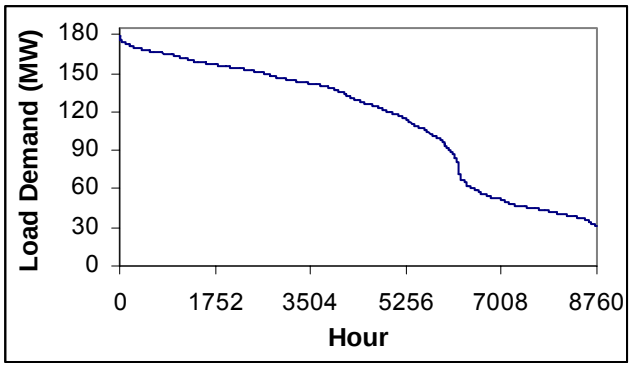

Figure 4.2: Annual load duration curve of the RBTS.

The cumulative chronological load model shown in Figure 4.2 has a peak load of 179.28 MW. This peak value is different from the peak demand in [51] which is 185 MW. The reason is that individual delivery points have different chronological load characteristics dominated by the customer types, i.e. industrial, commercial or residential, embedded in each delivery point. The peak demands occurring at each individual delivery point may not be coincident. The system peak demand, therefore, is lower than that of a load model in which all the delivery points reach their peak loads at the same time. In a similar manner, the peak load of the IEEE-RTS derived from the chronological loads is 2754.75 MW instead of 2850 MW.

The results shown in Tables 4.3 and 4.4, obtained using the sequential technique, utilize the chronological load model shown in Figure 4.1. The results obtained using the non-sequential technique utilize a multi-step model derived from the load duration curve (LDC) shown in Figure 4.2. The LDC is divided into 40 non-uniform load steps.

Table 4.3: Annual system indices for the RBTS.

Annual Indices	Non-Sequential (40-step LDC)	Sequential (Chronological)
Expected Number of Load Curtailments (occ/yr), ENLC	1.44	--
Expected Frequency of Load Curtailments (occ/yr), EFLC	--	1.66
Probability of Load Curtailments, PLC	0.00171	0.00152
Expected Energy Not Supplied (MWh/yr), EENS	180.3	140.0
Computation time (seconds)	3.89	110.44

Table 4.4: Annual system indices for the IEEE-RTS.

Annual Indices	Non-Sequential (40-step LDC)	Sequential (Chronological)
Expected Number of Load Curtailments (occ/yr), ENLC	3.00	--
Expected Frequency of Load Curtailments (occ/yr), EFLC	--	8.20
Probability of Load Curtailments, PLC	0.00422	0.00357
Expected Energy Not Supplied (MWh/yr), EENS	4387.0	3911.4
Computation time (seconds)	11.25	955.88

Tables 4.1 and 4.2 indicate that the ENLC provides a high estimate of the EFLC when calculating annualized indices using a constant peak load model. This conclusion,

however, cannot be drawn for annual indices obtained by utilizing a load duration curve or a chronological load model. The ENLC obtained using the non-sequential method and a load duration curve is a low estimate of the EFLC determined using the sequential approach and a chronological load model, as shown in Tables 4.3 and 4.4. An explanation of this variance in the frequency index calculation is given in the following section.

4.4 Discussion on the Frequency Index Calculation

The non-sequential (state sampling) technique can be used to provide reasonably accurate probability and energy-related indices. It cannot, however, be used to directly calculate accurate frequency-related indices [13]. Consequently, this method calculates the expected number of load curtailments (ENLC) as an approximation to the actual frequency index. There are two major factors involved in accurate frequency index calculations. They are failure state transitions and chronological load considerations. A detailed investigation of the impact of these two factors is presented in the following:

4.4.1 Impact of the Failure State Transitions

The frequency concept is based on transitions between the system states. It is a difficult task in composite system reliability evaluation to calculate the actual frequency index particularly when the system is composed of a large number of components. For each load curtailment state *i*, it is necessary to identify all the non-load curtailment states that can be reached from state *i* in one transition [56]. This state transition condition is illustrated in Figure 4.3. Figure 4.3 shows that if the system is in state B which is a failure state, the transition to state C will not bring the system across a boundary wall to a system success state. A system failure event should not be counted in this case as the state transition does not cross the boundary wall. This state transition, which does not cross the boundary wall, is designated in this thesis as a failure state transition. The basic state sampling (non-sequential) technique is not able to recognize this state transition problem. Consequently, the state transition from state B to state C or vice versa is seen

as an additional system failure event (a failure state transition), and is included in the ENLC index. This leads to overestimation of the frequency index. Methods to correct this state transition problem in a frequency index calculation are described in [20, 56]. The chronology of load demand is another major factor in the frequency index calculation and cannot be taken into account using the techniques proposed in [20, 56].

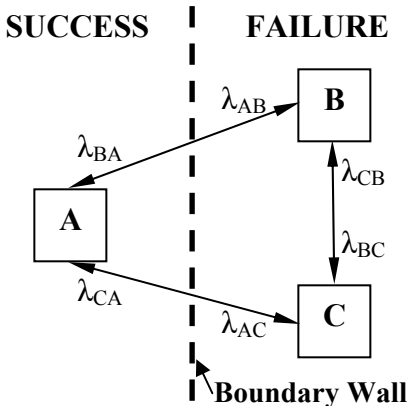

Figure 4.3: Simple system with three states.

4.4.2 Impact of the Chronology of Load Demand

The load duration curve (LDC) shown in Figure 4.2 is used in this section. The load duration curve is divided into 10 constant load steps. The accumulated results are derived by weighting each load step by its step probability. The results obtained using the sequential and non-sequential methods incorporating 10 non-uniform load steps are shown in Table 4.5. The sequential and non-sequential results shown in Table 4.5 were obtained in a similar manner to that used to calculate the annualized indices shown in Tables 4.1 and 4.2. The difference is that there are now 10 constant load levels. Each constant load level is utilized one at a time, and the accumulated results are obtained using the appropriate weighting probabilities. As shown in Table 4.5, the ENLC is a high estimate of the EFLC at every load step. The accumulated ENLC is also higher than the accumulated EFLC. The reason is that the impact of failure state transitions still exists. The load duration curve does not convey the impact of chronology in the

calculation as each load step represents a constant load level throughout the year of simulation.

Table 4.5: Annual indices for the RBTS obtained using 10 non-uniform load steps.

Step No.	Load (p.u.)	Probability of step	Non-sequential			Sequential		
			ENLC	PLC	EENS	EFLC	PLC	EENS
1	0.97	0.00320	2.899	0.00410	675.1	1.792	0.00354	625.8
2	0.95	0.07158	2.656	0.00388	587.1	1.792	0.00353	547.8
3	0.90	0.12135	2.510	0.00366	373.5	1.694	0.00331	353.9
4	0.85	0.14384	1.384	0.00154	226.7	1.016	0.00144	213.4
5	0.80	0.10799	1.273	0.00138	196.2	0.972	0.00136	182.0
6	0.75	0.05023	1.227	0.00130	173.4	0.892	0.00118	155.3
7	0.70	0.12774	1.227	0.00130	156.3	0.886	0.00117	141.7
8	0.60	0.08242	1.177	0.00122	128.2	0.870	0.00113	118.5
9	0.40	0.06084	1.177	0.00122	85.5	0.868	0.00113	78.9
10	0.30	0.23082	1.177	0.00122	64.1	0.868	0.00113	59.2
Total	--	1.00000	**1.499**	0.00179	202.5	**1.074**	0.00165	188.6
Note: System peak load for RBTS = 179.28 MW (179.28/185.00 = 0.9691 p.u.)								

The accumulated frequency indices obtained in Table 4.5 can be used to determine the impact of failure state transitions. Since both techniques utilize the same load curve and the same load step probability, the difference between the accumulated ENLC and EFLC is directly influenced by the failure state transition impact, as the sequential method recognizes the failure state transitions while the basic non-sequential method cannot detect them. The error due to the failure state transition impact, therefore, can be approximately expressed as (1.499-1.074)/1.074 = 0.3957 or 39.57%.

The total EFLC shown in Table 4.5 does not include the impact of chronology but does incorporate the failure state transition impact. This result can be compared with that obtained using the sequential method and a chronological load, as shown in Table 4.3. In the annual index analysis of the RBTS, the EFLC is equal to 1.66. This value includes both the failure state transition and chronology impacts. The chronology impact, therefore, can be approximately calculated as (1.660-1.074)/1.074 = 0.5456 or 54.56%. As shown above, the chronology impact percentage is higher than that of the failure state transition impact. Although both impacts amplify the EFLC value, the

chronology impact seems to dominate. The IEEE-RTS was also studied in the same manner, and the results are shown in Table 4.6.

Table 4.6: Annual indices of the IEEE-RTS obtained using 10 non-uniform load steps.

Step No.	Load (p.u.)	Probability of step	Non-sequential			Sequential		
			ENLC	PLC	EENS	EFLC	PLC	EENS
1	0.97	0.00263	33.649	0.04890	73119	11.320	0.04938	73843
2	0.95	0.06530	28.118	0.04210	54984	8.730	0.04216	54817
3	0.90	0.12877	11.787	0.01585	17532	4.675	0.01553	18660
4	0.85	0.15080	4.169	0.00555	4934	1.930	0.00547	5876
5	0.80	0.10046	1.397	0.00185	1303	0.665	0.00191	1780
6	0.75	0.04658	0.228	0.00030	319	0.225	0.00051	533
7	0.70	0.12934	0.049	0.00016	65	0.070	0.00019	157
8	0.60	0.08447	0.000	0.00000	0	0.015	0.00003	23
9	0.40	0.05571	0.000	0.00000	0	0.010	0.00002	13
10	0.30	0.23596	0.000	0.00000	0	0.010	0.00002	10
Total	--	1.00000	**4.228**	0.00596	6938	**1.583**	0.00596	7291
Note: System peak load for IEEE-RTS = 2754.75 MW (2754.75/2850 = 0.9666 p.u.)								

In Table 4.6, the failure state transition impact percentage is approximately (4.228-1.583)/1.583 = 1.6709 or 167.09%. The EFLC obtained in Table 4.4 is 8.20, the percentage of chronology impact is, therefore, approximately (8.200-1.583)/1.583 = 4.180 or 418.00%. These results confirm that the impact of chronology in a frequency index calculation dominates the impact of the failure state transitions (it is approximately 250% different for the IEEE-RTS). It is interesting to note that the impacts of failure state transitions and chronology on the IEEE-RTS are much higher than those for the RBTS. This implies that there may be a wide range of impacts due to failure state transitions and chronology considerations for each individual system depending on system topology, size, load patterns, operating strategies, etc.

As noted earlier, the frequency concept is based on the transitions between the system states. The chronological load model has a significant effect by changing the system state transition conditions. These transitions are not due to component state changes as shown in Figure 4.3, but are generated by the changes in the chronological

load curve across a boundary wall in which either an increased load leads to load curtailments or a decreased load results in no load curtailments.

The impact of chronology is clearly represented when incorporating a chronological load model as shown in Figure 4.1. As shown in Tables 4.3 and 4.4, the ENLC tends to become a low estimate of the EFLC when a chronological load model is applied. The accumulated EFLC of the IEEE-RTS shown in Table 4.6 is significantly lower than that shown in Table 4.4 even though both studies utilize the same load data but represent it in different forms. The impact of the chronology dominates the impact of the failure state transitions in the frequency index calculation, as noted earlier. A pictorial appreciation of the impact of the chronology on the interruption frequency index calculation is demonstrated in Figure 4.4.

Severe load curtailments can occur in bulk electric power systems due to outages of main transmission lines, transformers or generators. Potential load interruptions are more likely to occur during heavy load periods rather than light load ones. In some situations, load curtailments can exist for relatively long periods under these contingencies, as shown in Figure 4.4. The sequential technique utilizes a chronological load model as shown in Figure 4.4(a). The non-sequential technique uses a constant step load model as shown in Figure 4.4(b). Assume that load curtailment is required for this contingency situation if the system load is higher than 0.8 p.u. Under the same contingency, all the load steps in Figure 4.4(b) which are higher than 0.8 p.u. will also have load curtailments. Figure 4.4(a) will have a load curtailment frequency contribution of three, while there is only a single load curtailment event in Figure 4.4(b) in which a step load is used. Consequently, the EFLC obtained using the chronological load model in the sequential technique tends to be higher than that obtained using the constant step load model in the non-sequential technique. In the other words, the EFLC obtained using a load duration curve tends to be a low estimate of the EFLC obtained using a chronological load model.

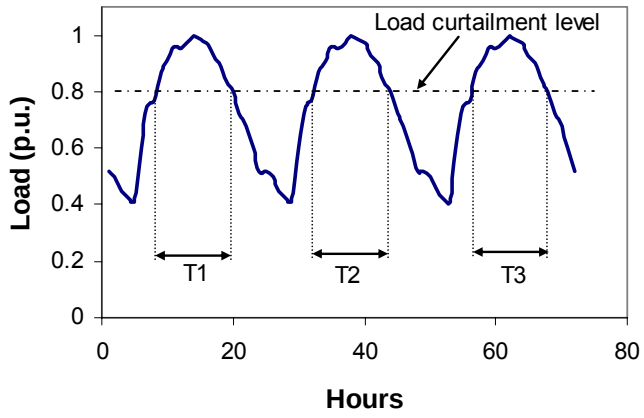

(a) Chronological load model

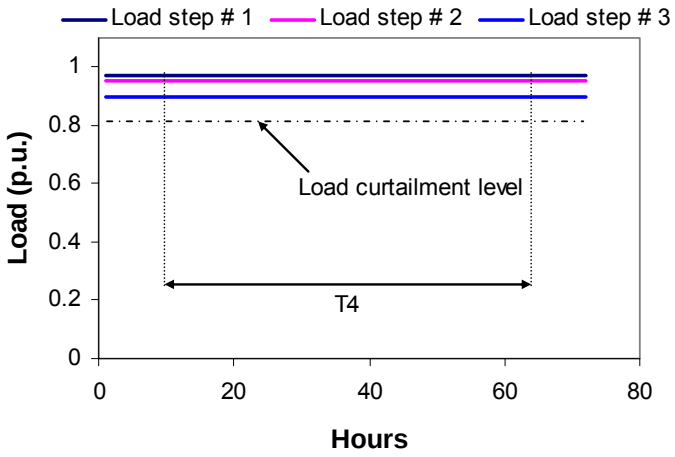

(b) Multi-step load model

Figure 4.4: Comparison of using different load models in load curtailments.

Another possibility that results in an increased interruption frequency when utilizing a chronological load model is shown in Figure 4.5. In this case, the delivery point load profiles have two significant peak loads in a normal day, i.e. at noon and in the evening. If the load curtailment level is 0.83, as shown in Figure 4.5, there could be two possible interruptions during a single day when incorporating a chronological load model in the sequential approach.

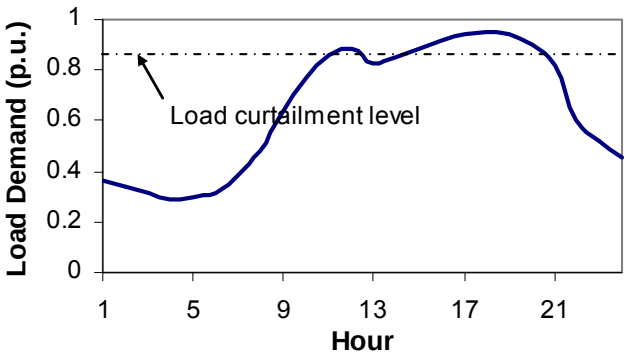

Figure 4.5: Load demand with two peaks in a normal day.

4.5 Conclusions

The application of sequential and non-sequential Monte Carlo simulation techniques can have significant impacts on the calculated interruption frequency indices in a bulk electric power system. Two major factors that influence the frequency index calculation are failure state transitions and load chronology. These two factors are discussed and examined in this chapter. The impact of chronology is not presented in an annualized index calculation and the impact of failure state transitions is not considered in the non-sequential method but is incorporated in the sequential approach. Ignoring failure state transitions in the non-sequential method will result in overestimation of the frequency indices. In an annual index calculation, the impacts of chronology and failure state transitions are not incorporated in the non-sequential method while both impacts are included in the sequential technique. Ignoring both the chronology and failure state transitions will usually result in underestimating the frequency. The impacts of these two factors are illustrated in this chapter. The results show that the impact of chronology is highly significant, and can exceed the impact of failure state transitions. The results shown in the chapter are based on the RBTS and the IEEE-RTS. The systems are relatively different and provide a reasonable indication of the results that would be obtained for a wide range of systems.

The non-sequential Monte Carlo simulation technique requires considerably less computation time than the sequential technique, particularly in large bulk system

reliability studies. The sequential technique can, however, provide more accurate reliability indices, particularly in regard to the frequency of load point and system failures, but also requires considerable additional data in the form of individual bus chronological load profiles. Both techniques therefore have advantages and disadvantages in the reliability evaluation of large practical bulk electric power systems. Both techniques can, however, be used to provide reasonable estimates of system adequacy given that the underlying differences and approximations are understood.

CHAPTER 5
RELIABILITY WORTH ASSESSMENT METHODOLOGIES FOR BULK ELECTRIC SYSTEMS

5.1 Introduction

The basic function of an electric power system is to supply its customers with electrical energy as economically as possible and with a reasonable degree of continuity and quality [2]. The two aspects of relatively low cost electrical energy at a high level of reliability are often in direct conflict. Balancing these two aspects is a big challenge to power system managers, planners and operators. Electric power utilities are also facing increasing uncertainty regarding the economic, political, societal and environmental constraints under which they operate and plan their future systems. This has created increasing requirements for extensive justification of new facilities and increased emphasis on the justification of system costs and reliability. An integral element in the overall problem of allocating capital and operating resources is the assessment of reliability cost and reliability worth. The ability to assess the costs associated with providing reliable service is reasonably well established and accepted. On the other hand, the ability to assess the worth of service reliability is a difficult and subjective task. A practical alternative, which is being widely used, is to evaluate the impacts and monetary losses incurred by customers due to electric supply failures. Customer interruption costs provide a valuable surrogate for the actual worth of electric power supply reliability [57 – 60]. Reliability worth evaluation, therefore, provides the opportunity to incorporate cost analysis and quantitative assessment in a common framework [61].

Utility planners consider important factors such as, capital investment, operating and maintenance costs in reliability cost/worth analysis. They also incorporate customer interruption costs in the overall cost minimization process. The reliability of a system can be improved by installing additional components or better equipment. The customer interruption costs in these cases will decrease as the capital and operating costs increase. The main objective is to balance the benefits realized from providing higher reliability and the cost of providing it. A major objective of reliability cost/worth assessment is to determine the optimum level of service reliability. The basic concept is illustrated in Figure 5.1.

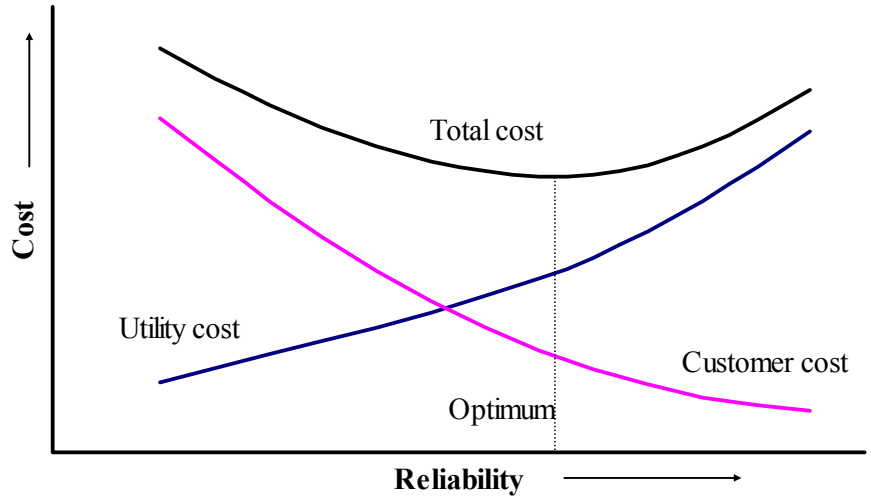

Figure 5.1: Reliability cost components.

As shown in Figure 5.1, the utility cost, i.e. investment cost, maintenance cost and operating cost, increases while the socio-economic customer interruption cost decreases with increase in the level of service reliability. The total cost is the sum of the two curves. The optimum level of reliability occurs at the point of lowest total cost. In a reliability cost/worth analysis, the annual expected customer interruption costs are added to the predicted annual capital and operating costs to obtain a total cost evaluation. Possible alternative configurations are examined to minimize the total cost and to identify the most appropriate configuration. The application of reliability cost/worth analysis in system reinforcement planning is illustrated in Chapters 9 and 10.

5.2 Customer Interruption Cost

When an electricity supply interruption occurs, its result normally has both monetary and social customer impacts. The direct monetary impacts include interruptions of production processes, idle but paid labor, raw material damages, equipment damages, and loss of income etc. The direct social impacts include inconvenience in various activities, discomfort and loss of leisure time. In addition, indirect social and economic impacts may arise as consequences of the interruption, i.e. increases in crime, or decreases in safety at work or leisure etc. The indirect impacts depend on many factors and are very difficult to quantify. Most interruption cost evaluation methods are therefore focused on direct impact evaluation [57 – 61].

The electric utility industry is moving towards an environment of competition and customer choices. Reliability is a key factor influencing customer loyalty. Utilities must understand and meet their customers' expectations [1]. Customer satisfaction regarding reliable electric supply is becoming increasingly important in the new deregulated electric utility environment. Customer outage costs due to electric supply failures are of concern to both utilities and customers. Customer outage cost assessments have been conducted in many countries [62] and the results applied using both analytical and simulation techniques [2, 13] to assess reliability worth. A CIGRE report [62] provides a brief summary of survey work conducted in Australia, Canada, Denmark, Great Britain, Greece, Iran, Nepal, New Zealand, Norway, Portugal, Saudi Arabia, Sweden and the United States of America. Reference [62] also includes a bibliography of over 150 publications on the subject of interruption cost assessment and application in power systems. The most recent North American survey on customer interruption costs was conducted by the MidAmerican Energy Company and is described in [63]. The CIGRE report [62] also illustrates the use of these data in determining capacity payments, expansion planning, network design, determination of security standards and reliability cost/worth assessment in generation, transmission and distribution systems. There is also increasing interest in the utilization of interruption cost data in the determination of appropriate service disruption payment schemes and a number of such

schemes are in place [62]. As noted in [64], it is mandatory for all power companies in Norway from 2001 to calculate the energy not supplied and the interruption costs for all their delivery points. Customer interruption cost surveys [48, 49] conducted by the Power System Research Group at the University of Saskatchewan illustrate that customer interruption costs vary with customer type and as a function of outage duration. Customer damage functions (CDF) can be used to describe the cost ($/kW peak load) associated with a power supply interruption as a function of the outage duration. The CDF representing a group of customers belonging to particular standard industrial classifications (SIC) [65] can be broadly categorized into seven customer sectors designated as agricultural, residential, large users, industrial, commercial, government and institutions, office and building. The CDF of these seven customer types are designated as sector customer damage functions (SCDF). The SCDF used in this chapter were obtained from [48, 49] and are presented in Table 5.1.

Table 5.1: Sector customer damage functions (SCDF) in $/kW.

Customer Sector	Interruption Duration		
	1 hour	4 hours	8 hours
Agricultural	1.3398	2.3341	3.9229
Residential	0.1626	1.8126	4.0006
Large users	3.1900	6.8900	10.4700
Industrial	9.5600	29.1476	52.0955
Commercial	32.1991	106.3483	185.9804
Government and institutions	7.2297	21.3650	40.2121
Office and building	7.2053	26.8283	52.9923

The SCDF shown in Table 5.1 depict the sector customer interruption cost as a function of the interruption duration. The cost of interruption in $/kW was obtained for interruption durations of 1, 4 and 8 hours. The cost of interruption for any duration in between the existing data points can be determined by interpolation and the cost of interruption for a longer duration than 8 hours can be calculated using a linear extrapolation. The customer costs associated with an outage of any delivery point in the system involves the combination of costs associated with all customer types affected by the system outage [66]. Conceptually, the composite customer damage function (CCDF)

for a particular load bus represents the total costs for that delivery point as a function of the interruption duration. The customer load composition has to be known in order to proportionally weight the SCDF. In this chapter, the annual energy consumption percentage of each customer sector is used (in an approximate method) as a weighting factor, and the SCDF can be aggregated to create the composite customer damage function (CCDF), which measures the cost associated with power supply interruptions as a function of the interruption duration for the customer mix at a load bus.

5.3 Event-Based Customer Interruption Cost Evaluation

A wide range of customer cost evaluations has been done using both analytical and Monte Carlo simulation techniques [2, 13]. Relatively little work has been published, however, on estimating the cost associated with specific failure events. Customer interruption costs due to failure in electrical energy supply depend on many factors such as the customer types interrupted, the actual load demand at the time of the outage, the duration of the outage, the time of day and the day in which the outage occurs. An event-based customer interruption cost evaluation (EBCost) approach was developed as a part of the author's M.Sc. research work [67 – 69], and is incorporated in the bulk electric system reliability worth analysis demonstrated in this chapter. The EBCost approach provides a realistic and accurate incorporation of the temporal variations in customer outage costs in reliability worth analysis.

5.3.1 Calculation Model

Three basic indices are applied in reliability worth analysis. They are the expected energy not supplied (EENS), the expected customer interruption cost (ECOST), and the interrupted energy assessment rate (IEAR). The basic equations for these indices using the EBCost approach are as follows:

$$EENS_i = L_1 + L_2 + L_3 + \ldots + L_n \tag{5.1}$$

$$ECOST_i = WF_1 \times C(d_1) \times L_1 + WF_2 \times \{C(d_2) - C(d_1)\} \times L_2 + WF_3 \times \{C(d_3) - C(d_2)\} \times L_3 + \ldots + WF_n \times \{C(d_n) - C(d_{n-1})\} \times L_n \quad (5.2)$$

$$IEAR_i = \frac{ECOST_i}{EENS_i} \quad (5.3)$$

where: i = Load bus i (delivery point i),

n = Duration of an interruption (n hours),

L_n = Average load demand interrupted during hour n (MW),

$C(d_n)$ = Interruption cost at hour n from the CCDF of Bus i (\$/kW),

WF_n = Cost weight factor at hour n.

It is important to note that the composite customer damage function (CCDF) of each load bus used in the EBCost approach is not a fixed function. This implies that the CCDF of each load bus is created using the sector customer damage functions (SCDF) of the customer mix at that load bus weighted with the percentages of expected unserved energy during a particular interruption. The CCDF is therefore created only when a specified interruption occurs. The CCDF created in this way has therefore a time varying characteristic (time varying CCDF). This is a significant difference from the fixed set of CCDF created by weighting with the annual energy consumptions. The fixed CCDF is used in an approximate method and is addressed later in this chapter.

It is important to note that the customer interruption cost evaluation process for a specific outage event and that used for reliability worth simulation are quite different. Reliability worth analysis models used in the simulation approach can be quite variable and may be different from the actual situation when assessing the consequences of specific outage events. Detailed knowledge of each individual outage, i.e. a number of customers affected, outage duration of individual customers, feeder outage rotation procedures etc., are not specifically known in a simulation approach. This is not the case when attempting to assess a monetary loss due to a specific outage event in real life where the number of customers affected, customer types affected, individual customer

outage durations and load shedding rotation procedures are known. There is therefore a prerequisite to determine the appropriate reliability worth analysis model to be used in the simulation process. Generally, reliability worth analysis models can be broadly categorized by two perspectives designated as a single event-based or multiple event-based models. These two concepts are explained using Figure 5.2.

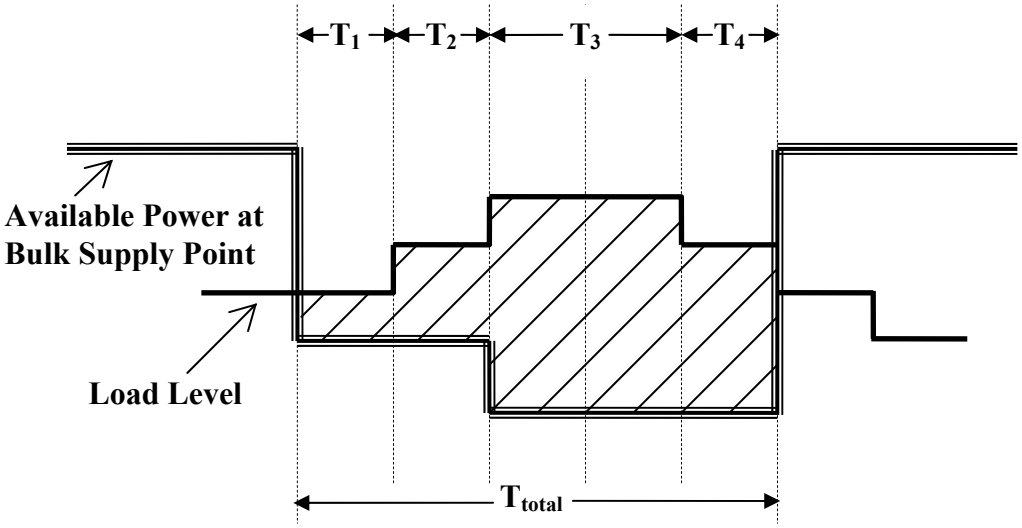

Figure 5.2: A bulk supply point interruption scenario.

The assumed interruption scenario at a bulk supply point shown in Figure 5.2 is used to illustrate the two concepts of reliability worth assessment. This interruption scenario describes two coincident or overlapping contingencies that result in two levels of power deficiency at the bulk supply point. The first contingency results in a power deficiency at one level (during T_1+T_2) followed by the second contingency which gives rise to another level of power deficiency (during T_3+T_4). The shaded area in Figure 5.2 indicates the amount of load that must be curtailed to maintain system integrity. A fixed time step of one hour is used to describe the chronological load profile. As noted earlier, the two concepts are designated as the single event-based and multiple event-based models. The basic concept in the single event-based model is that the total interruption duration (T_{total}) is used in the reliability worth calculation resulting in a single long outage duration. On the other hand, the total interruption duration (T_{total}) is divided into multiple sub-events with short outage durations in the multiple event-based model. The

division is based on the amount of load curtailment. In other words, if the amount of load curtailment changes, a new outage event is considered. As shown in Figure 5.2, the interruption scenario can be divided into four outage events with outage durations of T_1, T_2, T_3 and T_4 respectively. This model can be thought of as a rotating blackout or a load shedding rotation which affects a higher number of customers with shorter outage durations. Monetary loss predictions [70] indicate that rotating outages with short durations will basically result in higher IEAR and ECOST than single outage events with long durations. The multiple event-based model can therefore be considered as an upper bound of the monetary loss. In bulk electric system reliability simulation, there may be hundreds of random outage events occurring in a long simulation sequence in which detailed outage knowledge such as the actual customers interrupted, the outage durations of the individual customers and the load shedding rotation procedures applied to the individual outage events are not clearly known. It is therefore more appropriate to assess the reliability worth of a bulk electric system using a single event-based model which is more likely to provide a base or a lower bound of the monetary loss rather than an upper bound using the multiple event-based model. The single event-based concept is therefore adopted in this chapter as the reliability worth analysis model for bulk electric system simulation.

5.3.2 Simulation Results

This section presents reliability worth indices (ECOST and IEAR) obtained using the event-based customer interruption cost evaluation (EBCost) approach for the original RBTS and IEEE-RTS. The computer software RapHL-II is utilized in this chapter. The simulation years used for the RBTS and IEEE-RTS are 8,000 and 6,000 years respectively and provide a coefficient of variation of the expected energy not supplied (EENS) less than 2%.

Tables 5.2 and 5.3 present the reliability worth indices obtained using the EBCost approach for the RBTS and IEEE-RTS respectively. The results shown in Tables 5.2 and 5.3 are obtained using the pass-1 load curtailment philosophy described

in Section 3.4.5. The ECOST with and without incorporating time varying cost weight factors are also compared. Cost weight factors represent the impact of the time that the interruption occurred and have a maximum value of 1.0 per unit. The interrupted energy assessment rates (IEAR) are also provided.

Table 5.2: Reliability worth indices for the RBTS using the pass-1 policy.

Bus No.	With Cost Weight Factors		Without Cost Weight Factors	
	ECOST (k$/yr)	IEAR ($/kWh)	ECOST (k$/yr)	IEAR ($/kWh)
2	12.01	7.3201	12.93	7.8858
3	75.69	2.5566	79.62	2.6891
4	105.65	6.0126	110.40	6.2824
5	9.35	6.6889	10.41	7.4456
6	373.21	3.6326	395.44	3.8490
System	**575.92**	**3.7662**	**608.80**	**3.9812**

Table 5.3: Reliability worth indices for the IEEE-RTS using the pass-1 policy.

Bus No.	With Cost Weight Factors		Without Cost Weight Factors	
	ECOST (k$/yr)	IEAR ($/kWh)	ECOST (k$/yr)	IEAR ($/kWh)
1	161.38	6.9957	170.04	7.3710
2	315.51	5.8339	344.18	6.3640
3	418.65	4.9022	435.47	5.0992
4	287.29	7.4202	313.04	8.0853
5	420.38	7.6271	441.67	8.0134
6	595.49	5.3744	623.01	5.6227
7	378.62	5.7350	394.99	5.9829
8	820.91	5.6719	870.04	6.0113
9	12.10	2.8831	12.78	3.0469
10	22.50	4.7159	23.46	4.9167
13	3265.41	5.1488	3460.67	5.4567
14	20.58	3.4993	21.20	3.6054
15	873.79	3.6598	926.66	3.8813
16	857.19	4.9473	920.06	5.3102
18	8527.98	3.3528	8992.46	3.5354
19	718.53	2.8259	757.84	2.9805
20	237.97	4.4010	254.17	4.7005
System	**17934.29**	**3.9938**	**18961.73**	**4.2226**

Tables 5.2 and 5.3 show that the ECOST incorporating time varying cost weight factors are slightly less than those obtained without time varying cost weight factor consideration. The cost weight factors are used to incorporate the effect of different days

and seasons on outage costs. As noted earlier, the single event-based concept used in this research establishes a lower bound for customer interruption cost estimates. Incorporating cost weight factors will further lower the ECOST values and has not been applied in the following analyses. The results obtained without incorporating cost weight factors shown in Tables 5.2 and 5.3 are used as the base case results in a comparison with the approximate methods developed later in this chapter.

In a bulk system reliability simulation, the ECOST results are not only based on pertinent factors such as customer types and time of outages, but are also dependent on the system operating policies employed, i.e. different load curtailment philosophies. As noted in Section 3.4.5, the priority order policy tends to minimize customer interruption costs due to load curtailments while the pass-1 policy minimizes the number of delivery points affected by a given load curtailment without considering customer outage cost minimization. Tables 5.4 and 5.5 respectively show the reliability worth indices for the RBTS and IEEE-RTS without cost weight factor considerations using the priority order philosophy.

Table 5.4: Reliability worth indices for the RBTS using the priority order policy.

Bus No.	Without Cost Weight Factors	
	ECOST (k$/yr)	IEAR ($/kWh)
2	2.38	7.6920
3	120.71	2.7048
4	12.10	6.2932
5	9.09	7.3879
6	404.33	3.8552
System	**548.61**	**3.5873**

Tables 5.4 and 5.5 show that the ECOST and IEAR obtained using the priority order policy for both RBTS and IEEE-RTS are considerably lower than those obtained using the pass-1 policy shown in Tables 5.2 and 5.3. This indicates that considerable differences in customer interruption cost estimates can occur due to how the bulk power system is operated.

Table 5.5: Reliability worth indices for the IEEE-RTS using the priority order policy.

Bus No.	Without Cost Weight Factors	
	ECOST (k$/yr)	IEAR ($/kWh)
1	10.40	9.1286
2	8.78	7.7393
3	209.71	5.0819
4	9.64	9.0172
5	9.62	9.2743
6	38.06	6.0012
7	23.51	6.6536
8	17.97	7.2838
9	4247.02	2.4314
10	1572.18	4.0522
13	29.18	6.8261
14	3666.89	2.9932
15	134.04	4.0239
16	14.81	5.9988
18	1168.99	3.6629
19	1975.44	2.9754
20	224.77	4.4610
System	**13360.99**	**2.9752**

5.4 Approximate Methods for Customer Interruption Cost Evaluation

The ECOST results shown in the previous section are obtained using the event-based customer interruption cost evaluation (EBCost) technique. This method provides accurate results when dealing with a specific outage event and the results therefore can serve as benchmarks in the development of more approximate methods required due to the absence of detailed information in most real life situations. In this section, a series of approximate method are developed and compared with the results obtained using the EBCost approach shown in the previous section. The chronological load profile for each customer sector in a bulk electric system may be quite difficult for most power utilities to assess. The data available may be only the annual or monthly energy consumption of the customer load mix at the bulk supply point monitored. The approximate methods are aimed at reducing the detailed information required and the computation process involved while maintaining reasonable customer interruption cost estimates in bulk electric systems.

5.4.1 Average Demand Interrupted Approach

This approximate method relies on the single event-based concept. The average load curtailment (average demand interrupted) can be calculated as the ratio of the unserved energy during an interruption to the duration of the interruption. This approximate method is similar to the process designated as Method A1 in [71]. The composite customer damage function (CCDF) of each load bus is formed using the sector customer damage functions (SCDF) allocated at that bus weighted by their sector annual energy consumptions. The CCDF formed for each load bus is therefore a fixed function, and is calculated at the beginning as input data before starting the simulation. This is the major difference between the EBCost and average demand interrupted approaches where the CCDF used in the EBCost method is formed during the simulation when the specific outage event occurs and it is a time varying CCDF. The CCDF used in the average demand interrupted approach is a fixed function. Equation (5.2) used in the EBCost approach is therefore reduced to Equation (5.4) when the cost weight factor (WF_i) is neglected and the load curtailment is presented as the average demand interrupted (L_{avg}).

$$ECOST_i = C(d_n) \times L_{avg} \tag{5.4}$$

where: n = Duration of an interruption (n hours),

L_{avg} = Average demand interrupted (MW) as the ratio of the total unserved energy divided by the duration of the outage ($EENS/n$),

$C(d_n)$ = Interruption cost at duration n from the CCDF of Bus i (\$/kW).

The fixed CCDF for all the load buses (delivery points) in the RBTS and the IEEE-RTS are shown in Tables 5.6 and 5.7 respectively. These CCDF were formed and weighted using the annual energy consumptions.

Table 5.6: Composite customer damage functions (CCDF) for all the delivery points and the overall RBTS.

Bus No.	CCDF formed using annual energy percentages ($/kW)		
	$C(d_1)$ at 1 hr.	$C(d_4)$ at 4 hrs.	$C(d_8)$ at 8 hrs.
2	9.6299	31.0063	55.5004
3	4.3536	12.1565	20.5634
4	7.9887	25.6599	45.7731
5	8.5667	28.4677	51.5559
6	5.4781	17.4849	31.1432
System	6.2990	19.4771	34.3165

Table 5.7: Composite customer damage functions (CCDF) for all the delivery points and the overall IEEE-RTS.

Bus No.	CCDF formed using annual energy percentages ($/kW)		
	$C(d_1)$ at 1 hr.	$C(d_4)$ at 4 hrs.	$C(d_8)$ at 8 hrs.
1	8.9893	28.5880	51.1420
2	7.2643	23.7361	42.9401
3	6.4470	20.7470	37.1455
4	9.4700	30.5485	55.0380
5	9.1513	29.9145	53.1093
6	6.9738	22.6030	40.4540
7	7.6155	24.3085	43.2714
8	7.1922	23.8749	42.4934
9	3.7364	10.4673	17.8266
10	5.5961	17.3417	30.5833
13	7.4685	23.5102	41.9196
14	4.7307	13.7685	23.9277
15	5.7062	16.6311	28.3838
16	6.9168	21.0724	36.7938
18	5.6002	16.4487	28.5402
19	4.3816	12.4892	21.0616
20	5.5013	17.0328	29.9137
System	6.2575	19.3452	34.0628

Table 5.6 shows that Bus 2 has the highest interruption cost function while Bus 3 has the lowest interruption cost function in the RBTS. In the IEEE-RTS, Bus 4 has the highest interruption cost function and Bus 9 has the lowest interruption cost function, as shown in Table 5.7. The CCDF shown in Tables 5.6 and 5.7 are used as fixed functions

to estimate the customer interruption costs using the average demand interrupted approach.

Tables 5.8 and 5.9 show the reliability worth indices obtained using the average demand interrupted approach for the RBTS and the IEEE-RTS respectively. The results obtained using the pass-1 and priority order load curtailment policies are shown. It is important to note that cost weight factors cannot be applied in the approximate method due to the constant CCDF utilization. The results obtained using the approximate method can be compared with the base case results (EBCost approach without cost weight factors) shown in Tables 5.2 – 5.5.

Table 5.8: Reliability worth indices obtained using the average demand interrupted approach for the RBTS with two different load curtailment policies.

Bus No.	Pass-1 Policy		Priority Order Policy	
	ECOST (k$/yr)	IEAR ($/kWh)	ECOST (k$/yr)	IEAR ($/kWh)
2	11.99	7.3079	2.09	6.7407
3	80.14	2.7069	120.32	2.6959
4	104.15	5.9272	11.69	6.0796
5	9.34	6.6815	8.15	6.6253
6	361.57	3.5193	370.55	3.5331
System	**567.19**	**3.7091**	**512.79**	**3.3530**

The results shown in Table 5.8 for the RBTS can be directly compared to those shown in Table 5.2 for the pass-1 policy and those shown in Table 5.4 for the priority order policy without considering cost weight factors. The differences in the ECOST obtained using the EBCost and the average demand interrupted approaches are approximately 7% for both the pass-1 and priority order cases.

The results shown in Table 5.9 for the IEEE-RTS can be directly compared to those shown in Table 5.3 for the pass-1 policy and those shown in Table 5.5 for the priority order policy without considering cost weight factors. The differences in the ECOST obtained using the EBCost and the average demand interrupted approaches are approximately 0.02% for the pass-1 case and 0.7% for the priority order case. These

small differences indicate that the average demand interrupted approach can provide reasonable results when compared to the base case results obtained using the EBCost method.

Table 5.9: Reliability worth indices obtained using the average demand interrupted approach for the IEEE-RTS with two different load curtailment policies.

Bus No.	Pass-1 Policy		Priority Order Policy	
	ECOST (k$/yr)	IEAR ($/kWh)	ECOST (k$/yr)	IEAR ($/kWh)
1	160.46	6.9559	9.10	7.9919
2	314.00	5.8059	7.27	6.4090
3	429.02	5.0237	205.01	4.9681
4	291.87	7.5384	8.39	7.8479
5	402.97	7.3112	7.90	7.6221
6	606.25	5.4714	35.42	5.5851
7	388.70	5.8877	21.95	6.2128
8	816.79	5.6434	14.77	5.9899
9	12.02	2.8659	4201.35	2.4053
10	22.18	4.6478	1581.07	4.0751
13	3442.52	5.4281	27.14	6.3485
14	21.37	3.6340	3895.88	3.1801
15	908.78	3.8064	131.39	3.9444
16	866.06	4.9986	13.81	5.5932
18	9313.86	3.6618	1202.18	3.7669
19	723.55	2.8457	1888.65	2.8447
20	237.20	4.3866	207.15	4.1113
System	**18957.60**	**4.2217**	**13458.43**	**2.9969**

The percentage differences introduced by the average demand interrupted approach for the RBTS (approximately 7%) are considerably larger than those for the IEEE-RTS. The reason for this comes from the RBTS topology and customer mix at Bus 6. Bus 6 is a single circuit delivery point at which most of customers are agricultural and residential (approximately 75% altogether). Their annual energy consumptions are quite seasonally dependent. The sector customer damage functions for these two sectors are relatively low. The fixed set of CCDF formed using annual energy consumption percentages is, therefore, quite different than the time varying CCDF (formed at a particular time of the outage) used in the EBCost approach. The total system customer interruption cost is considerably influenced by the loss of load at Bus 6 (approximately

65%). The customer interruption cost differences at this delivery point when using the EBCost approach (utilizing the time varying CCDF) and the average demand interrupted approach (utilizing the fixed CCDF) are therefore larger due to the major contribution of this load point to the total system cost. If the customer interruption cost at Bus 6 is excluded, the percentage differences between the two methods reduce to approximately 3% and 1% for the pass-1 and priority order cases respectively.

In conclusion, the average demand interrupted approach generally provides a reasonable estimate of the customer interruption cost. The magnitude of error is relatively low and it is system dependent. As noted above, if the fixed set of CCDF for a load bus is quite different from the time varying CCDF of the bus, this will introduce more error in the approximation. This error, however, may not be significant if the contribution of this load bus to the total system cost is relatively small.

5.4.2 Average Delivery Point Restoration Duration Approach

This approximate approach is generally much simpler than the average demand interrupted method introduced in the previous section. The customer interruption cost in this case is not calculated during the simulation process, but it is estimated using the outcome of the simulation results. This approximate method is focused on the utilization of delivery point indices to estimate the customer interruption costs of the individual load points. The total system customer interruption cost can be aggregated from all the delivery point customer outage costs. The basic delivery point reliability indices used in the approximate method are described in Section 3.2.1 and are the expected duration of load curtailment (EDLC), the expected frequency of load curtailment (EFLC) and the expected energy not supplied (EENS). Two additional indices can be directly derived using the three basic reliability indices and are designated as the expected restoration duration (ERD) and the expected demand not supplied (EDNS). The ERD is approximately obtained as the ratio of EDLC to EFLC. The EDNS is calculated as the ratio of EENS to ERD. The concept in this approximate method is to use the delivery point ERD as the outage duration (*n* hours) to estimate the value ($/kW) from the fixed

cost function (CCDF), which is equivalent to the element $C(d_n)$ shown in Equation (5.4). The EDNS is equivalent to the average demand interrupted (L_{avg}) shown in Equation (5.4). The delivery point customer interruption cost (ECOST) can be calculated by multiplying the $C(d_{ERD})$ by the EDNS.

Tables 5.10 and 5.11 show the reliability indices and cost functions for the RBTS obtained using the pass-1 and priority order load curtailment policies respectively. The interruption cost value $C(d_{ERD})$ shown in the last column of Tables 5.10 and 5.11 are interpolated from the delivery point CCDF shown in Table 5.6 using the ERD as the outage duration. Similarly, Tables 5.12 and 5.13 show reliability indices and cost functions for the IEEE-RTS obtained using the pass-1 and priority order load curtailment policies respectively. The interruption cost values $C(d_{ERD})$ shown in the last column of Tables 5.12 and 5.13 are interpolated from the delivery point CCDF shown in Table 5.7. The delivery point ECOST can be obtained by multiplying the values in the last and second last columns. The delivery point IEAR can be calculated using the resulting ECOST divided by the delivery point EENS. The delivery point ECOST and IEAR obtained using the average delivery point restoration duration approach are shown in Tables 5.14 and 5.15 for the RBTS and the IEEE-RTS respectively. It is important to note that the system indices presented in the last row of Tables 5.10 – 5.13 are not used in this approximate method (the system indices are used in the next approximate method addressed later). The delivery point ECOST are summed to produce the system ECOST in the average delivery point restoration duration approach.

Table 5.10: Reliability indices and cost functions for the RBTS obtained using the pass-1 policy.

Bus No.	EDLC hrs/yr	EFLC occ/yr	EENS MWh/yr	ERD hrs/occ	EDNS MW	$C(d_{ERD})$ \$/kW
2	0.56	0.21	1.64	2.63	0.62	21.7695
3	3.27	0.76	29.61	4.29	6.90	12.8192
4	2.54	0.58	17.57	4.34	4.05	27.4687
5	0.27	0.10	1.40	2.68	0.52	20.1228
6	9.70	0.92	102.74	10.49	9.80	39.6455
System	13.32	1.72	152.96	7.73	19.79	33.3672

Table 5.11: Reliability indices and cost functions for the RBTS obtained using the priority order policy.

Bus No.	EDLC hrs/yr	EFLC occ/yr	EENS MWh/yr	ERD hrs/occ	EDNS MW	$C(d_{ERD})$ $/kW
2	0.10	0.07	0.31	1.45	0.21	13.1745
3	3.83	0.88	44.63	4.35	10.27	12.9549
4	0.29	0.11	1.92	2.58	0.75	17.7400
5	0.24	0.09	1.23	2.68	0.46	20.1228
6	10.49	1.19	104.88	8.79	11.93	33.8407
System	13.32	1.72	152.97	7.73	19.79	33.3672

Table 5.12: Reliability indices and cost functions for the IEEE-RTS obtained using the pass-1 policy.

Bus No.	EDLC hrs/yr	EFLC occ/yr	EENS MWh/yr	ERD hrs/occ	EDNS MW	$C(d_{ERD})$ $/kW
1	0.70	0.22	23.07	3.23	7.13	23.9160
2	1.91	0.62	54.08	3.08	17.56	18.9872
3	1.82	0.60	85.40	3.03	28.15	16.4158
4	1.65	0.55	38.72	2.98	13.01	23.8223
5	2.44	0.80	55.12	3.05	18.09	23.7284
6	2.77	0.89	110.80	3.13	35.45	18.3575
7	1.88	0.61	66.02	3.11	21.25	19.6902
8	2.97	0.85	144.73	3.51	41.20	21.3217
9	0.05	0.02	4.20	2.52	1.67	7.4255
10	0.06	0.03	4.77	2.22	2.15	10.7267
13	8.10	2.02	634.21	4.01	158.16	23.5592
14	0.08	0.03	5.88	2.69	2.19	10.1415
15	3.04	0.86	238.75	3.54	67.38	15.1349
16	5.21	1.48	173.26	3.53	49.14	19.0586
18	25.97	6.20	2543.54	4.19	607.35	17.0669
19	4.38	1.24	254.26	3.52	72.18	11.3393
20	1.54	0.64	54.07	2.40	22.53	11.2312
System	35.26	9.02	4490.88	3.91	1148.56	18.9901

Table 5.14 shows that the delivery point and system ECOST for the RBTS obtained using the average delivery point restoration duration approach are reasonable estimates when compared to the base case results shown in Tables 5.2 (pass-1) and 5.4 (priority order). The results obtained using this approach are slightly higher than the

base case values. The percentage differences in the results with respect to the base case values are approximately less than 2.5%. In a similar manner, Table 5.15 demonstrates that the system ECOST for the IEEE-RTS obtained using this approximate approach are slightly higher than the base case results shown in Tables 5.3 (pass-1) and 5.5 (priority order) with percentage differences of approximately 10% for both cases.

Table 5.13: Reliability indices and cost functions for the IEEE-RTS obtained using the priority order policy.

Bus No.	EDLC hrs/yr	EFLC occ/yr	EENS MWh/yr	ERD hrs/occ	EDNS MW	$C(d_{ERD})$ $/kW
1	0.02	0.01	1.14	1.92	0.59	15.4938
2	0.03	0.01	1.13	2.17	0.52	14.0787
3	0.87	0.26	41.27	3.28	12.58	17.5506
4	0.04	0.01	1.07	2.62	0.41	21.3670
5	0.03	0.01	1.04	2.61	0.40	20.7711
6	0.15	0.05	6.34	2.88	2.21	17.1060
7	0.18	0.07	3.53	2.52	1.40	16.5105
8	0.03	0.01	2.47	2.27	1.09	14.6218
9	35.14	8.98	1746.71	3.91	446.46	10.2918
10	7.48	2.10	387.98	3.57	108.75	15.8050
13	0.04	0.02	4.27	2.24	1.91	14.5532
14	22.29	5.90	1225.07	3.78	324.48	13.1812
15	0.46	0.14	33.31	3.29	10.11	14.3033
16	0.06	0.02	2.47	2.59	0.95	14.8603
18	4.24	1.17	319.14	3.61	88.46	15.1881
19	12.85	3.38	663.93	3.81	174.45	12.0383
20	1.35	0.42	50.39	3.20	15.74	14.1998
System	35.26	9.03	4491.26	3.91	1148.66	18.9901

The average delivery point restoration duration approach provides a slightly better system and delivery point ECOST estimate than that obtained using the average demand interrupted approach in the case of the RBTS. This is, however, not the case for the IEEE-RTS where the average demand interrupted approach provides a better ECOST estimation. This implies that the factors that affect the degree of error in the approximation do not only come from the methods used, but also depend on the system itself.

Table 5.14: Reliability worth indices for the RBTS obtained using the average delivery point restoration duration approach with the two load curtailment policies.

Bus No.	Pass-1 Policy		Priority Order Policy	
	ECOST (k$/yr)	IEAR ($/kWh)	ECOST (k$/yr)	IEAR ($/kWh)
2	13.56	8.2711	2.82	9.0862
3	88.48	2.9883	133.02	2.9806
4	111.26	6.3323	13.23	6.8927
5	10.50	7.5029	9.24	7.5092
6	388.46	3.7809	403.64	3.8486
System	**612.27**	**4.0038**	**561.95**	**3.6746**

Table 5.15: Reliability worth indices for the IEEE-RTS obtained using the average delivery point restoration duration approach with the two load curtailment policies.

Bus No.	Pass-1 Policy		Priority Order Policy	
	ECOST (k$/yr)	IEAR ($/kWh)	ECOST (k$/yr)	IEAR ($/kWh)
1	170.59	7.3946	9.20	8.0717
2	333.50	6.1667	7.37	6.5198
3	462.16	5.4117	220.72	5.3481
4	309.90	8.0037	8.71	8.1414
5	429.17	7.7861	8.26	7.9429
6	650.75	5.8732	37.73	5.9509
7	418.32	6.3362	23.15	6.5570
8	878.40	6.0692	15.91	6.4395
9	12.38	2.9488	4594.86	2.6306
10	23.07	4.8374	1718.87	4.4303
13	3726.13	5.8752	27.76	6.5009
14	22.19	3.7736	4277.04	3.4913
15	1019.73	4.2711	144.62	4.3417
16	936.58	5.4056	14.16	5.7311
18	10365.52	4.0752	1343.48	4.2097
19	818.46	3.2190	2100.09	3.1631
20	253.04	4.6798	223.57	4.4367
System	**20829.88**	**4.6387**	**14775.49**	**3.2901**

5.4.3 Average System Restoration Duration Approach

This approximate method uses a similar process to the average delivery point restoration duration approach described in the previous section. The difference is that

this approximate method utilizes the system reliability indices rather than delivery point reliability indices. The system reliability indices presented in the last row of Tables 5.10 – 5.13 shown in the previous section are used in the system customer interruption cost evaluation. This approximate method can be used to provide a quick estimate of the overall system monetary loss. Tables 5.16 and 5.17 show the system customer interruption cost obtained using the average system restoration duration approach for the RBTS and the IEEE-RTS respectively.

Table 5.16: Reliability worth indices for the RBTS obtained using the average system restoration duration approach with the two load curtailment policies.

Overall System	Pass-1 Policy		Priority Order Policy	
	ECOST (k$/yr)	IEAR ($/kWh)	ECOST (k$/yr)	IEAR ($/kWh)
	660.26	4.3166	660.31	4.3166

Table 5.17: Reliability worth indices for the IEEE-RTS obtained using the average system restoration duration approach with the two load curtailment policies.

Overall System	Pass-1 Policy		Priority Order Policy	
	ECOST (k$/yr)	IEAR ($/kWh)	ECOST (k$/yr)	IEAR ($/kWh)
	21811.32	4.8568	21813.16	4.8568

Tables 5.16 and 5.17 show that the reliability worth indices obtained using the average system restoration duration approach are insensitive to the load curtailment strategies used. This is due to the fact that there is no insight on delivery point index contributions to the overall system indices. The degrees of error when utilizing this approximate method are considerably larger than those obtained using the other two approximate methods described in the previous sections. This method could, however, be useful in system customer interruption cost estimates in the absence of detailed information on the individual delivery points.

Three approximate methods for reliability worth analysis in a bulk electric system are described in this section. The degree of error associated with each

approximate method is obtained by comparing the results with those obtained from the base case using the EBCost approach. The average demand interrupted approach appears to provide reasonable results and offers the closest approximation, following by the average delivery point restoration duration and the average system restoration duration approaches respectively. The average demand interrupted method, however, requires the implementation of an additional algorithm in the simulation software. The average delivery point restoration duration and the average system restoration duration approaches do not require an embedded algorithm in the simulation process. The methods utilize the outcome from the simulation to estimate the customer interruption costs. This may be more flexible for some power utilities who already have the software to estimate the basic reliability indices without performing the reliability worth assessment function. The reliability worth assessment can be done by hand using the basic outcomes from the software.

5.5 Conclusions

This chapter presents four reliability worth assessment methodologies for bulk electric systems. Two reliability worth assessment procedures designated as the single and multiple event-based models are discussed. The event-based customer interruption cost evaluation (EBCost) technique has been implemented in the simulation software (RapHL-II). The EBCost approach provides realistic and accurate incorporation of the temporal variations in customer outage costs, and its results are used as benchmarks in the development of more approximate methods. Three approximate methods are presented and the results obtained using these methods are compared with those obtained using the EBCost approach. The three methods are designated as the average demand interrupted, the average delivery point restoration duration and the average system restoration duration approaches. The approximate methods described in this chapter provide power utilities with the ability to perform meaningful reliability worth analysis in the absence of detailed customer information or sophisticated reliability software functions to evaluate customer monetary losses. A summary of the data requirements for the four reliability worth assessment methodologies presented in this chapter is shown in Table 5.18.

Table 5.18: A summary of the data requirements for the reliability worth assessment methodologies.

Approach	Requirements
EBCost	- Sector customer damage functions (SCDF) are used directly in the calculation process to form a "time varying" composite customer damage function (CCDF) for each load point when interruption occurs. - Chronological load curve of each customer sector is required. - Cost weight factors can be incorporated if required. - Computer is required in order to implement the calculation algorithms.
Average Demand Interrupted	- A "fixed" CCDF for each load point is calculated prior to the simulation process. This fixed CCDF is formed by using the annual energy consumption percentages. - Computer is required in order to implement the calculation algorithms.
Average Delivery Point Restoration Duration	- Computer is *not* required for ECOST calculation (no algorithm is implemented). - This approach is conducted after the simulation results are obtained. The delivery point reliability indices (EDLC, EFLC, EENS) are, used to incorporate the "fixed" CCDF for each delivery point in the ECOST calculation.
Average System Restoration Duration	- Computer is *not* required for ECOST calculation (no algorithm is implemented). - This approach is conducted after the simulation results are obtained. The delivery point reliability indices (EDLC, EFLC, EENS) are *not* required. The system reliability indices are used to incorporate the "fixed" system CCDF in the ECOST calculation. - This approach cannot be used to estimate delivery point ECOST.

It is important to note that the customer interruption cost evaluation process applied to a specific outage event and that used for reliability worth simulation are quite different. The objective in the first case is to estimate the consequences of specified outage events and therefore the EBCost approach is directly applicable. The focus in the second case is on reliability worth analysis in a simulation process. The EBCost approach used in this case may not be significantly better when compared with the other approximate methods as there may be hundreds of outage events occurring in the simulation and a detailed knowledge of the individual outages in terms of the number of

customers affected, actual customer types and outage rotation procedures is unknown. The customer interruption cost obtained in the simulation is, therefore, an average of all the random outage consequences. The customer interruption cost estimates obtained from a simulation are, however, extremely valuable and can be used in reliability cost/worth analysis in system planning.

CHAPTER 6
RELIABILITY INDEX PROBABILITY DISTRIBUTION ANALYSIS OF BULK ELECTRIC SYSTEMS

6.1 Introduction

A significant advantage when utilizing sequential Monte Carlo simulation in bulk electric system reliability analysis is the ability to provide reliability index probability distributions in addition to the expected values of these indices. Reliability index probability distributions provide a pictorial representation of the annual variability of the parameters around their mean values. At the present time, sequential Monte Carlo simulation is the only realistic option available to investigate the distributional aspects associated with system index mean values. There is an interest in applying reliability index probability distributions to manage bulk electricity system risks. Reliability index probability distribution analysis and its utilization are relatively new concepts in composite power system reliability analysis and decision making. There is frequently a need to know the range of a predictive reliability index and the likelihood of a certain value being exceeded. These factors can be assessed using the probability distribution associated with the expected value. System reliability index probability distributions provide additional valuable information and a more complete understanding of composite power system behavior. In certain situations, the system can be determined to be "very" reliable but the probability distribution is highly skewed [2]. In these cases, the average value is very close to the ordinate axis (zero). An appreciation of the very important distribution tail values, which although they may occur very infrequently, is important as these events can have serious system consequences. The average values, in these cases, may not be valid indicators of satisfactory system performance. Reliability index probability distributions can provide valuable additional system insight. Research

on the application of the sequential simulation technique to bulk electric system reliability evaluation has been published [13, 23, 53, 54]. These publications are valuable references in the evolution of composite power system reliability evaluation using sequential simulation. References [13, 23, 53, 54], however, do not focus on the development of reliability index probability distributions. Reference [72] illustrates the use of sequential simulation to obtain system reliability index distributions. These concepts are extended in this chapter to examine the delivery point index probability distributions in a composite generation and transmission system.

Bulk electric system reliability indices can be classified into two basic types designated as predictive indices [73] and past performance indices [74, 75]. Predictive indices provide relevant information associated with future system reliability and are normally associated with system planning. Past performance indices reflect the actual system reliability and are therefore related to the actual operation of the system. Virtually all the major utilities in Canada are actively engaged in reporting past performance indices, using the Canadian Electricity Association (CEA), Electric Power System Reliability Assessment protocols [76 – 78]. The reliability performance of a bulk electricity system can be predicted using probability techniques. The predicted indices can be directly linked to past performance using the indices presently compiled and used by the participating Canadian utilities. The performance data for successive years presented in References [76 – 78] show that the indices vary from year to year and that the annual performance indices can be considered as random variables. The historical data can be used to create reliability performance index probability distributions. In order to compare the predicted future performance with past performance, it is important to link the predictive and past performance indices. When planning additions to an existing bulk system, the predicted reliability can be directly compared with the past performance indices if the future performance indices and the past performance indices are in a similar form. Sequential Monte Carlo simulation can be used to estimate the reliability indices more accurately than those provided by other traditional methods. Delivery point reliability indices obtained using the sequential technique can, therefore, be realistically used to forecast future system reliability performance. This chapter

presents the development of probability distributions for delivery point and system predictive indices, and presents a technique to create performance index probability distributions for bulk electric systems.

6.2 Predictive Reliability Indices

The descriptions of the basic predictive delivery point and system reliability indices for bulk electric systems are presented in Section 3.2. Selected predictive reliability indices are presented in this section in the form of expected values and their associated probability distributions.

6.2.1 Mean or Expected Predictive Indices

The mean or expected predictive delivery point and system reliability indices utilized in this section are as follows:

EDLC – Expected Duration of Load Curtailment (hours/year)
EFLC – Expected Frequency of Load Curtailment (occurrences/year)
EENS – Expected Energy Not Supplied (MWh/year)
ECOST – Expected Customer Interruption Cost (M$/year)

The delivery point and system EDLC, EFLC and EENS for the RBTS are presented in Tables 5.10 and 5.11 using the pass-1 and priority order load curtailment policies respectively. The delivery point and system ECOST are also shown in Tables 5.2 and 5.4 using the pass-1 and priority order load curtailment policies respectively. These ECOST were obtained using the event-based customer interruption cost evaluation (EBCost) technique. This reliability worth analysis approach is utilized in subsequent studies in this thesis. The results presented in the tables noted above are summarized and shown in Table 6.1 together with results obtained using the pass-2 load curtailment policy described in Section 3.4.5. Similarly, Table 6.2 summarizes the four selected predictive indices for the IEEE-RTS obtained using the pass-1 and priority

order policies (EDLC, EFLC and EENS presented in Tables 5.12 and 5.13, and the ECOST shown in Tables 5.3 and 5.5) together with the indices obtained using the pass-2 load curtailment policy. The simulation years used for the RBTS and IEEE-RTS are 8,000 and 6,000 years respectively and provide a coefficient of variation of the EENS less than 2%. The computation time is approximately 6 and 68 minutes on a PC Pentium IV, 2.66GHz for the RBTS and IEEE-RTS respectively.

Table 6.1: Delivery point and system predictive reliability indices for the RBTS using the three different load shedding policies.

Bus No.	Priority Order Policy				Pass-1 Policy				Pass-2 Policy			
	EDLC hrs/yr	EFLC occ/yr	EENS MWh/yr	ECOST k$/yr	EDLC hrs/yr	EFLC occ/yr	EENS MWh/yr	ECOST k$/yr	EDLC hrs/yr	EFLC occ/yr	EENS MWh/yr	ECOST k$/yr
2	0.10	0.07	0.31	2.38	0.56	0.21	1.64	12.93	0.56	0.21	1.64	12.93
3	3.83	0.88	44.63	120.71	3.27	0.76	29.61	79.62	3.27	0.76	29.61	79.62
4	0.29	0.11	1.92	12.10	2.54	0.58	17.57	110.40	2.54	0.58	17.57	110.40
5	0.24	0.09	1.23	9.09	0.27	0.10	1.40	10.41	0.27	0.10	1.40	10.41
6	10.49	1.19	104.88	404.33	9.70	0.92	102.74	395.44	9.70	0.92	102.74	395.44
Sys.	**13.32**	**1.72**	**152.97**	**548.61**	**13.32**	**1.72**	**152.96**	**608.80**	**13.32**	**1.72**	**152.96**	**608.80**

Table 6.1 shows that the load shedding policy selected has a significant impact on the delivery point indices for the RBTS. Delivery points that have lower economic priority have a higher number of interruptions (lower reliability) with the priority order policy. These delivery points may or may not experience a high number of interruptions when the pass-1 or pass-2 policies are used. Delivery point No. 6 (DP6) has the lowest reliability for all the load shedding policies even though it does not have the lowest economic priority. The reason is that DP6 is a single circuit delivery point connected by a radial line. The loss of this radial line will result in total load curtailment at DP6. It is important to note that the pass-1 and pass-2 policies provide identical results (both delivery point and system) for the RBTS. The reason is that the RBTS is a relatively small system and the pass-2 policy is not really effective in this case. Table 6.1 clearly shows that the system reliability indices are, in general, basically the same with the different load curtailment policies. The EDLC, EFLC and EENS are basically unchanged. The ECOST, however, are quite different depending on the load shedding policy employed. As noted earlier, the priority order policy tends to minimize the overall

customer interruption costs by heavily curtailing loads at lower priority load points, while the pass-1 policy does not involve any customer outage cost considerations. The system ECOST obtained using the pass-1 and pass-2 policies are, therefore, higher than those obtained using the priority order policy.

Table 6.2: Delivery point and system predictive reliability indices for the IEEE-RTS using the three different load shedding policies.

Bus No.	Priority Order Policy				Pass-1 Policy				Pass-2 Policy			
	EDLC hrs/yr	EFLC occ/yr	EENS MWh/yr	ECOST M$/yr	EDLC hrs/yr	EFLC occ/yr	EENS MWh/yr	ECOST M$/yr	EDLC hrs/yr	EFLC occ/yr	EENS MWh/yr	ECOST M$/yr
1	0.02	0.01	1.14	0.010	0.70	0.22	23.07	0.170	0.88	0.27	28.74	0.211
2	0.03	0.01	1.13	0.009	1.91	0.62	54.08	0.344	1.91	0.62	53.30	0.340
3	0.87	0.26	41.27	0.210	1.82	0.60	85.40	0.435	1.82	0.60	84.72	0.433
4	0.04	0.01	1.07	0.010	1.65	0.55	38.72	0.313	1.70	0.57	38.64	0.314
5	0.03	0.01	1.04	0.010	2.44	0.80	55.12	0.442	2.44	0.80	53.89	0.434
6	0.15	0.05	6.34	0.038	2.77	0.89	110.80	0.623	2.86	0.92	108.00	0.612
7	0.18	0.07	3.53	0.024	1.88	0.61	66.02	0.395	1.88	0.61	63.47	0.382
8	0.03	0.01	2.47	0.018	2.97	0.85	144.73	0.870	2.98	0.85	135.45	0.821
9	35.14	8.98	1746.71	4.247	0.05	0.02	4.20	0.013	0.86	0.26	41.28	0.105
10	7.48	2.10	387.98	1.572	0.06	0.03	4.77	0.023	1.65	0.52	83.02	0.343
13	0.04	0.02	4.27	0.029	8.10	2.02	634.21	3.461	8.09	2.02	615.39	3.367
14	22.29	5.90	1225.07	3.667	0.08	0.03	5.88	0.021	0.37	0.12	20.85	0.067
15	0.46	0.14	33.31	0.134	3.04	0.86	238.75	0.927	3.26	0.93	249.70	0.973
16	0.06	0.02	2.47	0.015	5.21	1.48	173.26	0.920	5.22	1.48	165.84	0.888
18	4.24	1.17	319.14	1.169	25.97	6.20	2543.54	8.992	25.96	6.20	2430.96	8.646
19	12.85	3.38	663.93	1.975	4.38	1.24	254.26	0.758	4.76	1.35	250.34	0.758
20	1.35	0.42	50.39	0.225	1.54	0.64	54.07	0.254	1.89	0.75	67.16	0.313
Sys.	**35.26**	**9.03**	**4491.26**	**13.361**	**35.26**	**9.02**	**4490.88**	**18.962**	**35.26**	**9.02**	**4490.77**	**19.008**

In Table 6.2, DP9 has the lowest reliability when using the priority order policy as this load point has the lowest priority in the list. DP18 has the lowest reliability when using the pass-1 and pass-2 policies, as this load point is connected to several critical components, i.e. two major generating units. The loss of these components coincident with other contingencies can create an extreme emergency situation. There are also no other load points around DP18. If load curtailments are required due to contingencies occurring in this area, DP18 will suffer load curtailment. The pass-2 policy is quite effective for the IEEE-RTS. The use of the pass-2 policy tends to reduce the severity at DP18 by curtailing interruptible loads from other delivery points in its proximity. The pass-2 policy, therefore, tends to share wellbeing and risk among all the delivery points

within the system rather than heavily curtailing the load at one particular bus and leaving some buses relatively untouched. In a similar manner to that shown for the RBTS, Table 6.2 clearly illustrates that the system reliability indices are, in general, basically identical for the different load curtailment policies. The EDLC, EFLC and EENS are relatively unchanged. The ECOST, however, are considerably different. The system ECOST obtained using the pass-1 and pass-2 policies are relatively similar, and are higher than that obtained using the priority order policy.

6.2.2 Predictive Reliability Index Probability Distributions

The results shown in the previous section are based on the average or expected values of the predictive reliability indices. One advantage when utilizing sequential Monte Carlo simulation in bulk electric system reliability analysis is the ability to provide reliability index probability distributions associated with their expected values. The reliability index probability distributions for the delivery points and the overall system provide a pictorial representation of the annual variability of the indices, and are illustrated in this section. The probability distributions associated with the system reliability indices shown in Tables 6.1 and 6.2 are illustrated in Figures 6.1 and 6.2 for the RBTS and IEEE-RTS respectively, using the priority order and pass-1 policies. The annual values for each simulated year are designated as the frequency of load curtailment (FLC), the duration of load curtailment (DLC), the energy not supplied (ENS) and the customer interruption cost (COST). The mean values given in Figures 6.1 and 6.2 are the EFLC, EDLC, EENS and the ECOST respectively.

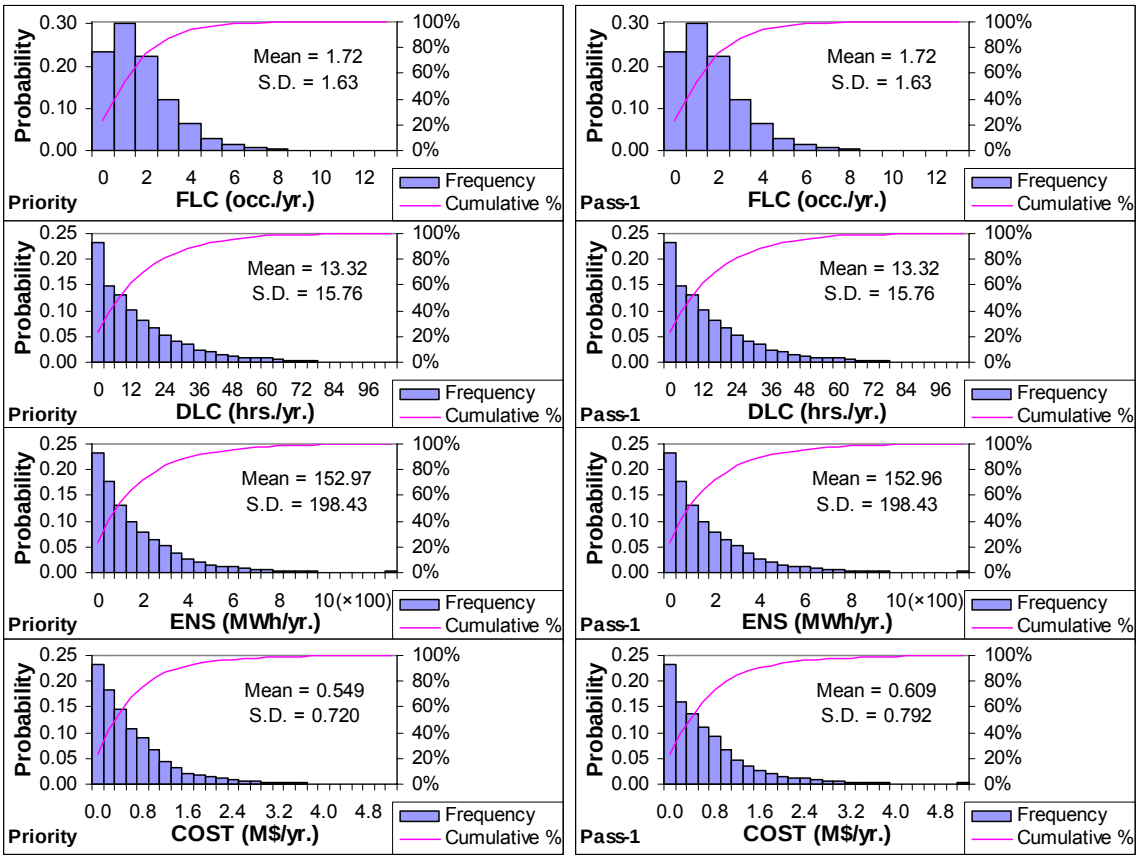

Figure 6.1: Probability distributions of the system reliability indices of the RBTS for the priority order and pass-1 load curtailment policies.

Figures 6.1 and 6.2 show that the probability distributions of the DLC, FLC and ENS for the two load curtailment policies are basically the same. The probability distributions of the COST for the two load shedding policies are, however, slightly different for both study systems. The pass-1 philosophy results in higher COST than those of the priority order policy with more dispersion in the COST shape as this load curtailment policy is not focused on minimizing the customer outage cost. In summary, the different load curtailment policies have relatively little impact on the probability distributions of the DLC, FLC and ENS while the probability distribution of COST is dependent on the load shedding philosophy used.

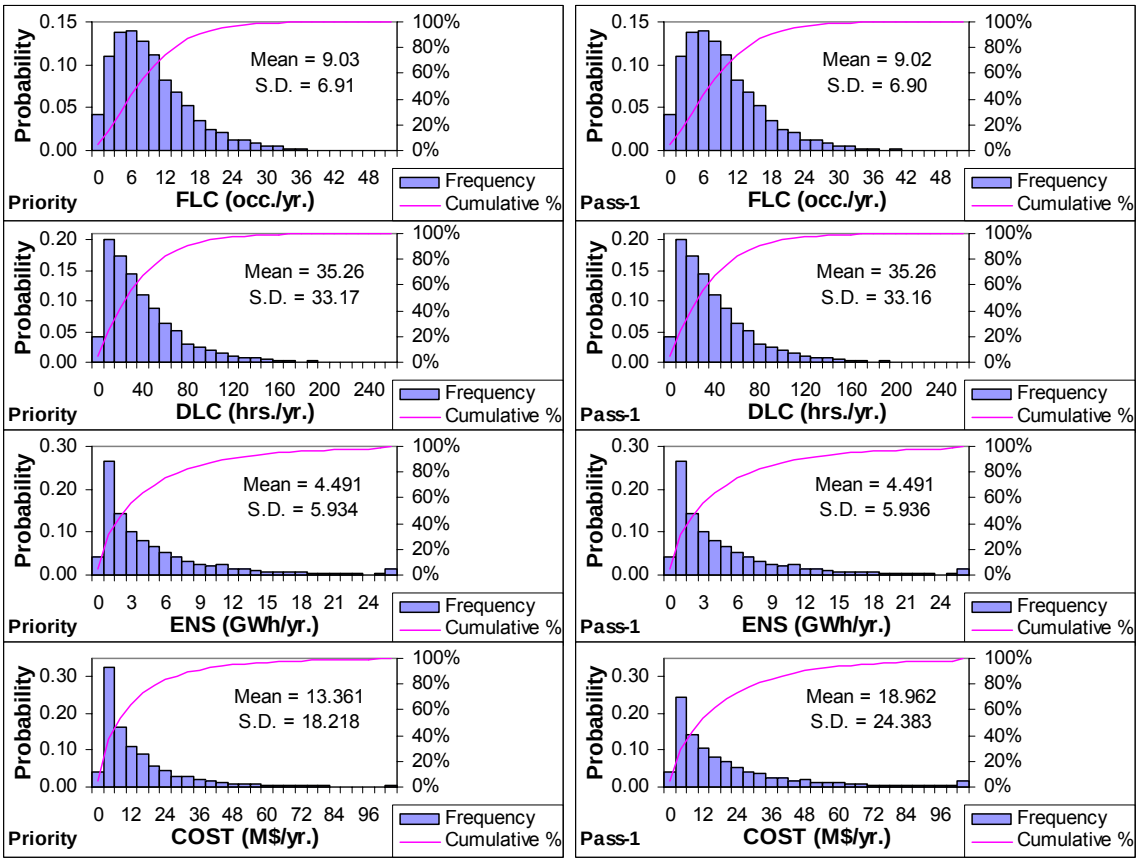

Figure 6.2: Probability distributions of the system reliability indices of the IEEE-RTS for the priority order and pass-1 load curtailment policies.

The computer software RapHL-II can also produce the annual variations in the reliability indices for all the delivery points. The index probability distributions at several selected delivery points in the two test systems are illustrated in this section. Delivery points No. 3, 4 and 6 (DP3, DP5 and DP6) were selected in the RBTS. Figures 6.3 – 6.5 respectively demonstrate the FLC, DLC and ENS for the selected delivery points using the two different load curtailment policies. The mean values, standard deviations (S.D.) and the probability distributions are shown. The mean values of the delivery point FLC, DLC and ENS given in Figures 6.3 – 6.5 are the EFLC, EDLC and EENS shown in Table 6.1 respectively.

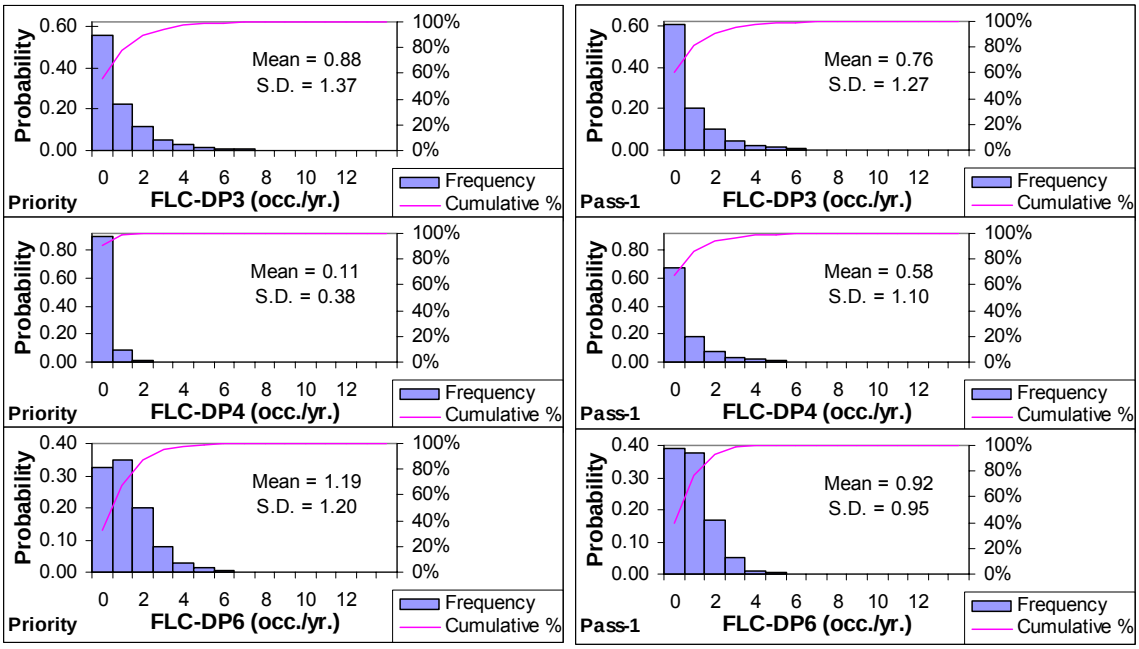

Figure 6.3: Probability distributions of the frequency of load curtailment (FLC) for the selected delivery points in the RBTS based on the priority order and pass-1 load curtailment policies.

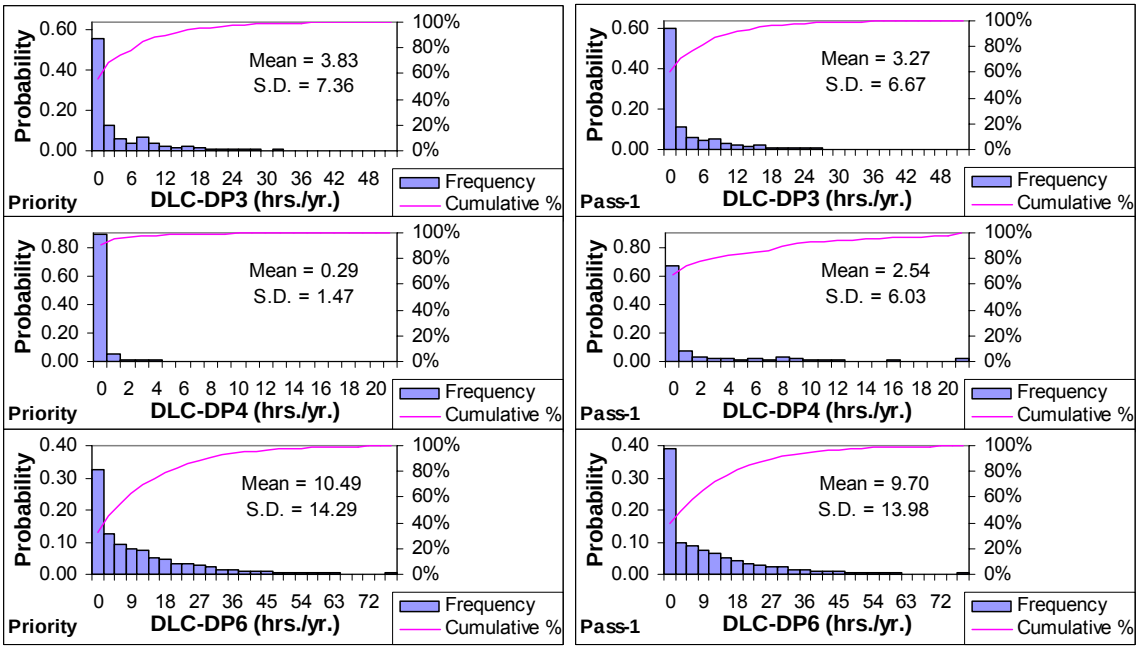

Figure 6.4: Probability distributions of the duration of load curtailment (DLC) for the selected delivery points in the RBTS based on the priority order and pass-1 load curtailment policies.

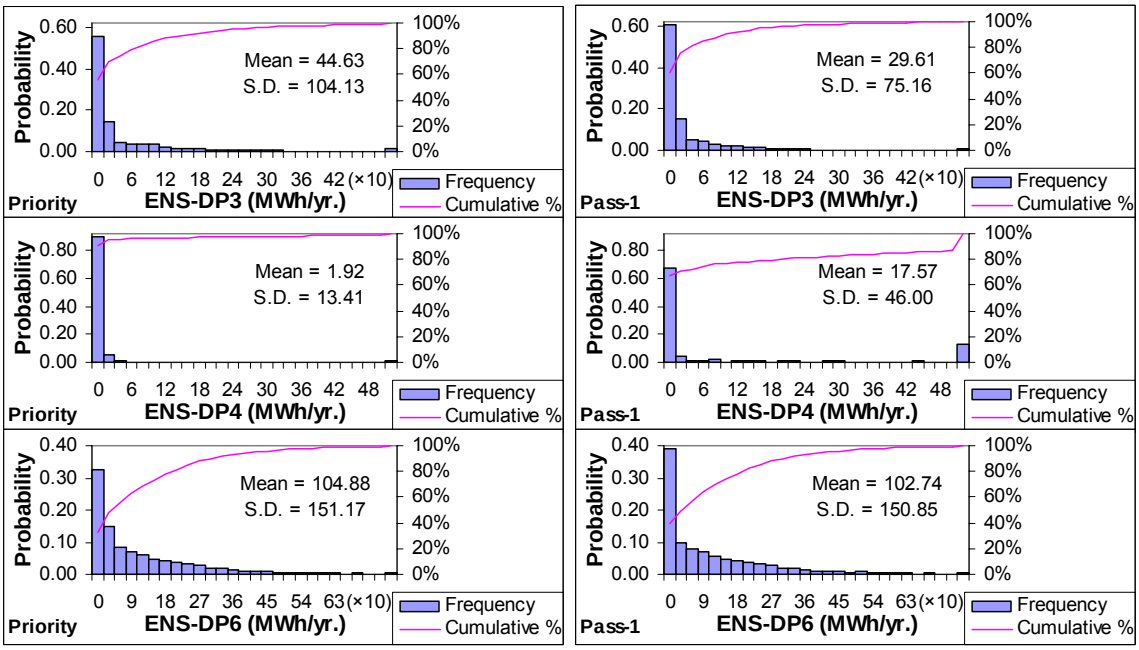

Figure 6.5: Probability distributions of the energy not supplied (ENS) for the selected delivery points in the RBTS based on the priority order and pass-1 load curtailment policies.

The probability distributions of FLC, DLC and ENS for each delivery point shown in Figures 6.3 – 6.5 have their own unique characteristics. The FLC distribution shape for DP6 tends to deviate from the basic exponential form. It is worth noting that the degree of difference between the two load curtailment policies may not be significant for the RBTS. There are two obvious reasons for this. First, the delivery points in the RBTS are dependent on the system topology and DP6 is a single circuit delivery point connected to the system through a radial line. This is not the case for DP3 and DP4 which are multi-circuit delivery points connected to several lines. DP6 is adversely affected by the system topology, but not significantly affected by different load curtailment philosophies. The second reason is that the RBTS is a small system with five delivery points. The different load shedding policies are more likely to have less impact on the small system than on a larger system.

The delivery point reliability index probability distributions are further examined using the IEEE-RTS. Delivery points No. 4, 9, 18 and 19 (DP4, DP9, DP18 and DP19)

were selected for illustration. DP4 has the highest priority order and DP9 has the lowest priority order, as shown in Table 3.2. DP18 is a load bus connected to many elements, and with no other load buses in close proximity. In contrast, DP19 is a delivery point that is directly connected to other two load buses. Figures 6.6 – 6.8 respectively show the FLC, DLC and ENS for the four selected delivery points using the two different load curtailment policies. The mean values of the delivery point FLC, DLC and ENS given in Figures 6.6 – 6.8 are the EFLC, EDLC and EENS shown in Table 6.2 respectively.

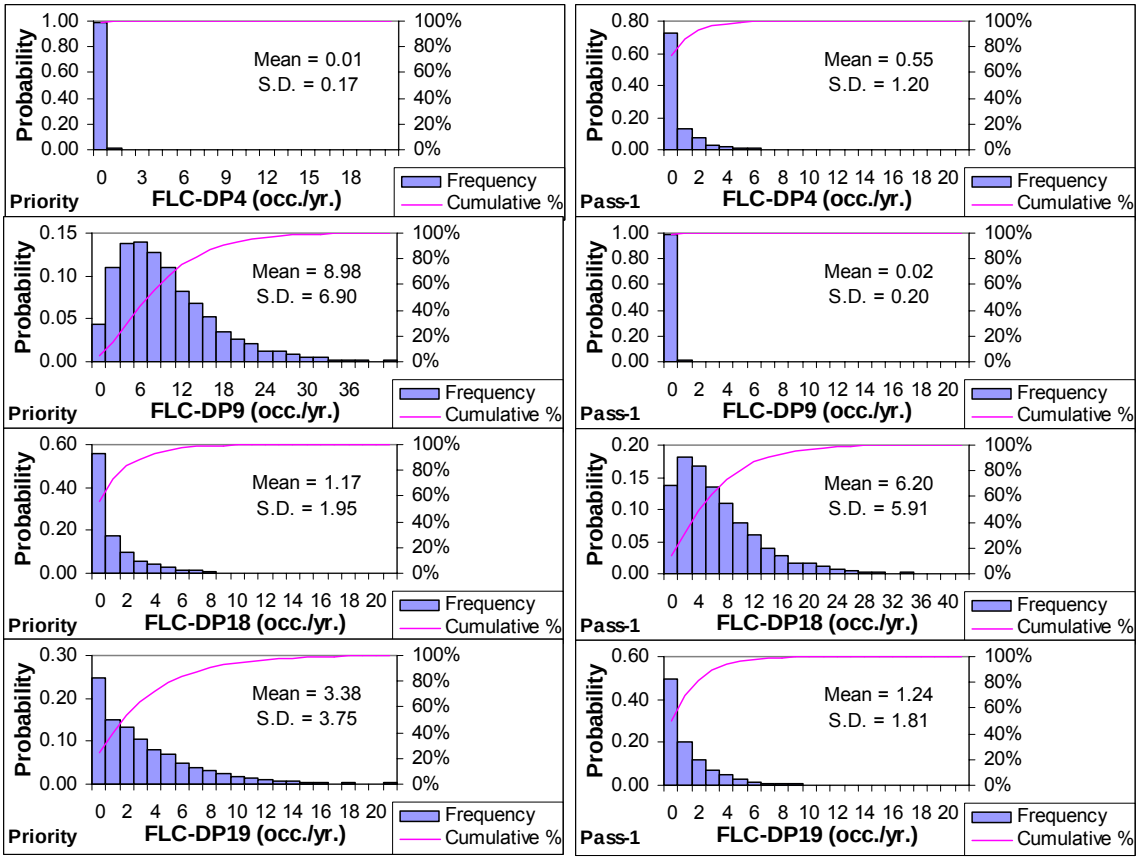

Figure 6.6: Probability distributions of the frequency of load curtailment (FLC) for the selected delivery points in the IEEE-RTS based on the priority order and pass-1 load curtailment policies.

Figure 6.6 shows that the FLC for all four delivery points have quite different probability distributions for both load shedding philosophies. In the priority order policy scenario, the most reliable delivery point (lowest FLC) is DP4, as this load point has the

highest priority whereas DP9 tends to encounter more interruptions due to its lower priority. Figure 6.6 indicates that the FLC for each delivery point based on the pass-1 policy is significantly different from those obtained using the priority order policy. In the pass-1 policy scenario, DP9 is a very reliable load point as it has a number of connected transmission lines and neighboring load buses. DP18 has the lowest reliability (highest FLC). The reason for this is that DP18 is attached to many elements, and there are no other load buses in close proximity. Any system constraints that occur in this area and result in load curtailments will create interruptions at this load bus. An important related factor is that the biggest generating unit (400 MW) is connected to this load point, and another 400 MW generating unit is connected to the neighboring bus. Losing either one of these generating units coincident with other element outages will bring the system to an emergency state. This will increase the interruption frequency at this point.

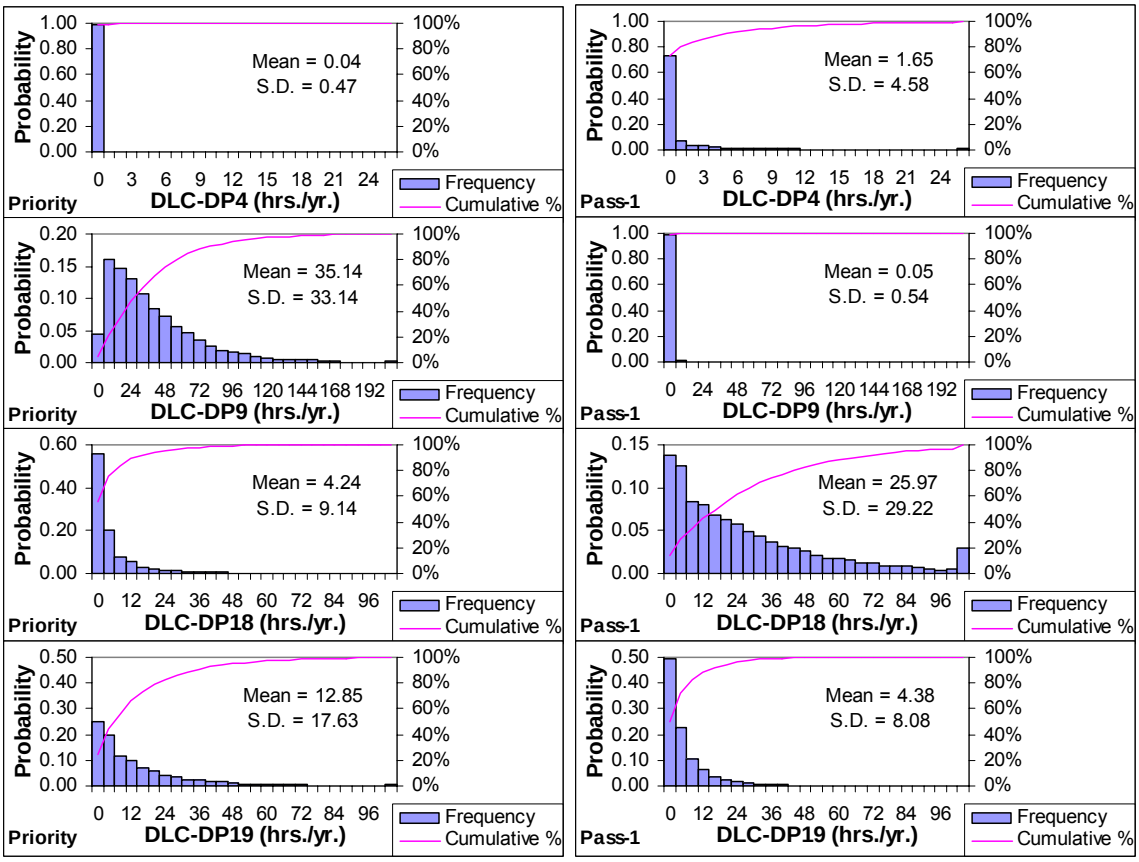

Figure 6.7: Probability distributions of the duration of load curtailment (DLC) for the selected delivery points in the IEEE-RTS based on the priority order and pass-1 load curtailment policies.

The probability distributions of the DLC and ENS for the selected delivery points in the IEEE-RTS are shown in Figures 6.7 and 6.8. In general, they tend to have exponential characteristics, and are relatively more dispersed than the probability distributions of FLC shown in Figure 6.6. The probability of ENS for DP18 exceeding 12 GWh/yr is 0.011. As noted earlier, DP18 is closely connected to two critical generating units and there are no other load buses in the immediate area. DP18 will, therefore, experience significant load curtailments under the pass-1 policy. In general, the dispersions of the DLC and ENS probability distributions are related to the dispersion characteristics of the FLC probability distributions.

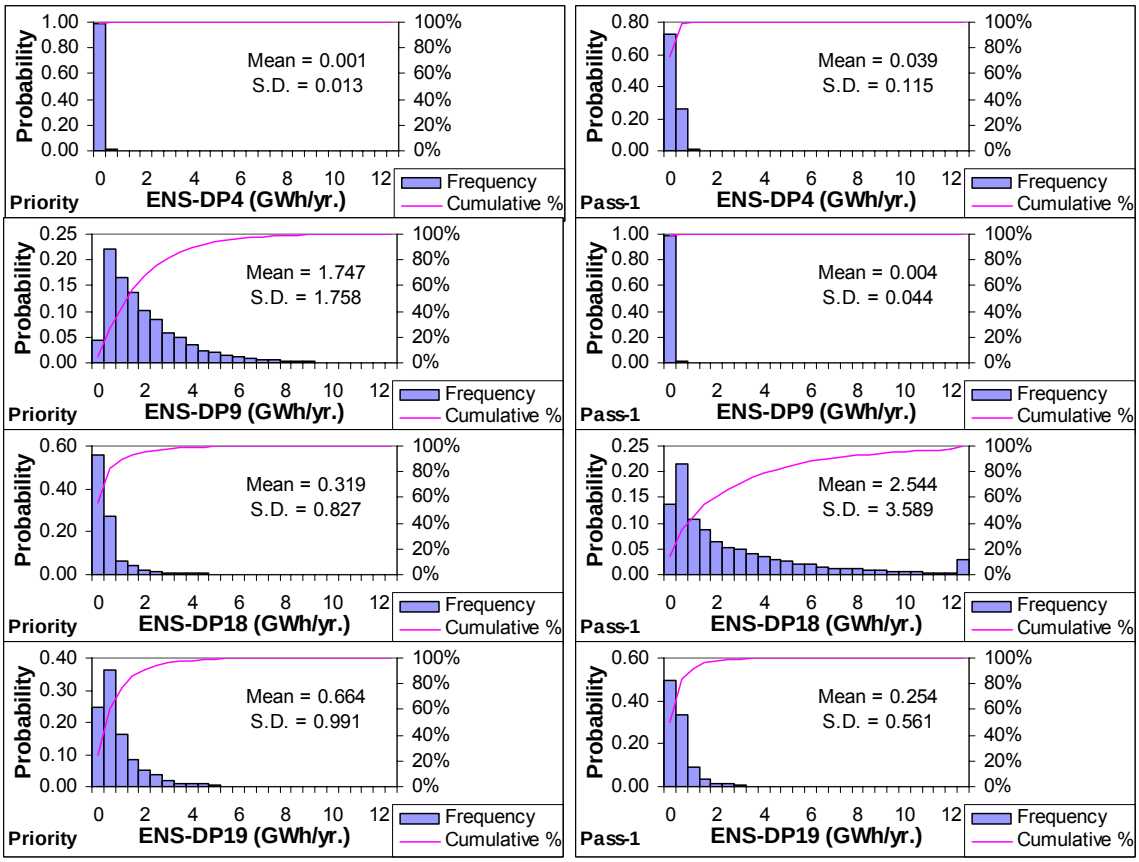

Figure 6.8: Probability distributions of the energy not supplied (ENS) for the selected delivery points in the IEEE-RTS based on the priority order and pass-1 load curtailment policies.

In conclusion, the probability distributions of the predictive delivery point reliability indices shown in Figures 6.3 – 6.8 provide a pictorial representation of the

manner in which the parameters vary around their mean values. Reliability index probability distribution analysis shows that the reliability indices of the individual delivery points have unique characteristics. These unique characteristics are basically dependent on the system topology and system load shedding philosophy. The distributions of very reliable delivery points have mean values close to the ordinate axis and have exponential characteristics. Delivery points which have low reliability have their mean values further away from the ordinate axis and can have quite different distribution characteristics. The distributions can be identified by Weibull characteristics with different shape factors. The exponential, Rayleigh and normal distributions are Weibull distributions with shape factors of 1, 2 and 3.5 respectively. One benefit of being able to determine the variability in the individual delivery point indices is the ability to provide probabilistic input data to distribution system reliability analysis. HLIII reliability evaluation composed of generation, transmission and distribution elements can be conducted using sequential simulation in which the input data to a distribution system are the reliability index probability distributions at the specific bulk delivery point. The development of system reliability index probability distributions provides additional information and an understanding of composite power system behavior.

6.3 Reliability Performance Indices

As noted earlier, there are two basic types of bulk electric system reliability indices. They are predictive indices and past performance indices. Predictive indices provide relevant information associated with future system reliability and are normally associated with system planning. The predictive indices for the delivery points and for the overall system are presented in the previous section. Past performance indices reflect the actual system reliability and are therefore related to the actual operation of the system. Even though the two types of bulk electric system reliability indices have been proposed and discussed in a number of papers [73 – 75], relatively little attention has been given to developing the linkage between them. In order to compare the predicted future performance with past performance, it is important to link the predictive and past

performance indices. When planning additions to an existing bulk electric system, the predicted reliability can be directly compared with the past performance indices if the future performance indices and the past performance indices are in a similar form. This section is focused on how to forecast the future performance indices and their probability distributions using the predictive indices developed in the previous section.

6.3.1 Bulk Electric System Performance Protocol

Virtually all the major utilities in Canada are actively engaged in reporting past performance indices, using the Canadian Electricity Association (CEA), Electric Power System Reliability Assessment protocols [76, 77]. The performance data for successive years show that the indices vary from year to year and that the annual performance indices can be considered as random variables. The following is a brief summary of some relevant definitions and the basic performance index equations. The detailed definitions in the CEA bulk system reliability performance protocol are given in [76, 77].

Delivery Point (DP)

The delivery point is the point of supply where the energy from the BES is transferred to the Distribution System or the retail customer. This point is generally taken as the low voltage busbar at step-down transformer stations (the voltage is stepped down from a transmission or sub-transmission voltage, which may cover the range of 60-750 kV to a distribution voltage of under 60 kV). For customer-owned stations supplied directly from the transmission system, this point is generally taken as the interface between utility-owned equipment and the customer's equipment.

Single-Circuit Supplied Delivery Point (SC)

A DP supplied from the BES by one circuit whereby the interruption of that will cause an interruption to the delivery point.

Multi-Circuit Supplied Delivery Point (MC)

A DP supplied from the BES by more than one circuit such that the interruption of one circuit does not cause a delivery point interruption.

Delivery Point Primary Supply Voltage

The transmission voltage level before transformation to the delivery point. For the purpose of this reporting system, four Voltage Classes have been identified.

Voltage Class 1: 60 - 99 kV
Voltage Class 2: 100 - 199 kV
Voltage Class 3: 200 - 299 kV
Voltage Class 4: 300 - 750 kV

System Average Interruption Frequency Index – Sustained Interruptions (SAIFI-SI)

A measure of the average number of sustained interruptions that a DP experiences during a given period, usually one year (occurrences/year). In this thesis, SAIFI is used as a short form of SAIFI-SI.

$$SAIFI - SI = \frac{Total\ Number\ of\ Sustained\ Interruptions}{Total\ Number\ of\ Delivery\ Points\ Monitored} \quad (6.1)$$

System Average Interruption Duration Index (SAIDI)

A measure of the average total interruption duration that a DP experiences during a given period, usually one year (hours/year).

$$SAIDI = \frac{Total\ Duration\ of\ all\ Interruptions}{Total\ Number\ of\ Delivery\ Points\ Monitored} \quad (6.2)$$

System Average Restoration Index (SARI)

A measure of the average duration of a delivery point interruption. In essence, it represents the average restoration time for each delivery point interruption (hours/occurrence).

$$SARI = \frac{Total\ Duration\ of\ all\ Interruptions}{Total\ Number\ of\ Interruptions} \tag{6.3}$$

Delivery Point Unavailability Index **(DPUI)**

A measure of overall BES performance in terms of a composite index of unavailability in System Minutes (system·minutes).

$$DPUI = \frac{Total\ Unsupplied\ Energy\ (MW\ -\ Minutes)}{System\ Peak\ Load\ (MW)} \tag{6.4}$$

The system performance indices expressed in Equations (6.1) – (6.4) can be predicted using conventional composite system reliability evaluation [2]. This can be done using a contingency evaluation approach or by Monte Carlo simulation. References [79, 80] presented techniques to predict reliability performance indices using analytical and non-sequential Monte Carlo simulation methods respectively. These two approaches, however, cannot provide performance index probability distributions. The concept of predicting reliability performance indices is extended in this chapter to creating the system performance index probability distributions in bulk electric systems using the sequential simulation approach.

The delivery points in the RBTS and the IEEE-RTS are classified in Tables 6.3 and 6.4 respectively based on the CEA definition.

Table 6.3: Classification of delivery points for the RBTS.

Delivery Point (DP)	Circuit		Voltage Class			
	Single (SC)	Multi (MC)	1	2	3	4
2		✓			✓	
3		✓			✓	
4		✓			✓	
5		✓			✓	
6	✓				✓	

Table 6.4: Classification of delivery points for the IEEE-RTS.

Delivery Point (DP)	Circuit		Voltage Class			
	Single (SC)	Multi (MC)	1	2	3	4
1		✓		✓		
2		✓		✓		
3		✓		✓		
4		✓		✓		
5		✓		✓		
6		✓		✓		
7		✓		✓		
8		✓		✓		
9		✓		✓		
10		✓		✓		
13		✓			✓	
14		✓			✓	
15		✓			✓	
16		✓			✓	
18		✓			✓	
19		✓			✓	
20		✓			✓	

Table 6.3 shows that the RBTS consists of both single-circuit (1 DP) and multi-circuit (4 DPs) at the 230 kV Voltage level (Class 3) based on the CEA definitions. The IEEE-RTS contains only multi-circuit delivery points with the two different voltage classes of 138 kV (Class 2) and 230 kV (Class 3), as shown in Table 6.4. In order to demonstrate how to calculate performance indices, sampled interruption frequencies and durations of the delivery points based on two consecutive simulation years are shown in Table 6.5 for demonstration purposes. Frequencies of load curtailment (FLC) of all the

delivery points are used to calculate SAIFI, while the durations of load curtailment (DLC) of all the delivery points are used to calculate SAIDI as shown in Table 6.5. The DPUI is calculated using the energy not supplied (ENS) divided by the system peak load (185 MW in this example), and then multiplied by 60 minutes. Table 6.5 shows example sequentially simulated results for two consecutive years. The performance indices vary from year to year due to the random behavior of the system.

Table 6.5: Performance index calculations for two consecutive simulation years.

Delivery Point (DP)	**Bus 2**	**Bus 3**	**Bus 4**	**Bus 5**	**Bus 6**
FLC (occ/yr) for year 1	1.0	4.0	1.0	1.0	3.0
FLC (occ/yr) for year 2	0.0	1.0	0.0	0.0	0.0
SAIFI (year 1) = (1+4+1+1+3)/5 = 2.0 SAIFI (year 2) = (0+1+0+0+0)/5 = 0.2					
DLC (hrs/yr) for year 1	1.0	6.0	1.0	1.0	8.0
DLC (hrs/yr) for year 2	0.0	2.0	0.0	0.0	0.0
SAIDI (year 1) = (1+6+1+1+8)/5 = 3.4 SAIDI (year 2) = (0+2+0+0+0)/5 = 0.4					
ENS (MWh/yr) for year 1	2.5	91.3	11.6	15.4	70.8
ENS (MWh/yr) for year 2	0.0	18.2	0.0	0.0	0.0
DPUI ((year 1) = (2.5+91.3+11.6+15.4+70.8)×60/185 = 62.1 DPUI ((year 2) = (0.0+18.2+0.0+0.0+0.0)×60/185 = 5.9					

6.3.2 Mean or Expected Performance Indices

Simulation periods of 8,000 and 6,000 years respectively were used for the RBTS and IEEE-RTS, as noted in Section 6.2, to create the probability distributions of the system reliability performance indices. The mean values of SAIFI, SAIDI and DPUI can therefore be obtained by summing up the individual year results and dividing by the total number of simulation years.

Tables 6.6 – 6.9 show the expected values of the RBTS performance indices obtained using the three different load shedding policies. The results clearly show that the adopted load curtailment policy has a considerable impact on the system reliability performance indices. Table 6.6 shows that the priority order policy results in a higher

SAIFI for the single circuit (SC) and lower SAIFI for the multi-circuit (MC) compared with those obtained using with the pass-1 and pass-2 policies. The priority order policy, however, provides the lowest value for the overall SAIFI (total circuits). Similarly, the overall SAIDI of the RBTS obtained using the priority order policy is the lowest among the three load shedding policies as shown in Table 6.7. This shows that system reliability performance can be improved by selecting appropriate operating strategies. The SARI shown in Table 6.8 is dependent on the SAIFI and SAIDI, as it is the ratio of SAIDI and SAIFI. An approximate SARI can be calculated using the results in Tables 6.6 and 6.7. The SARI shown in Table 6.8 are, however, slightly different from those obtained by dividing SAIDI by SAIFI. The reason for this is that the SARI shown in Table 6.8 are calculated for only the simulation years that have load curtailments. For example, if load curtailments occur for 7,500 of the 8,000 simulation years, the SARI is calculated based on these 7,500 years while SAIFI and SAIDI are still calculated based on 8,000 simulation years. The pass-1 and pass-2 policies create no differences in the SAIFI, SAIDI and SARI. As noted earlier, the RBTS is a relatively small system and the pass-2 policy is not effective in this case. The results obtained using the pass-1 and pass-2 policies are therefore identical. The DPUI is referred to as the Severity Index. The DPUI can be used for reliability comparisons between different size systems, as it is normalized by the system peak load. It can be seen in Table 6.9 that the DPUI obtained using the three different load shedding policies are the same.

Table 6.6: SAIFI (occ/yr) for the RBTS using the three different load shedding policies.

Priority Order Policy				Pass-1 Policy				Pass-2 Policy			
Volt. Class	SC	MC	Total Circuits	Volt. Class	SC	MC	Total Circuits	Volt. Class	SC	MC	Total Circuits
1	-	-	-	1	-	-	-	1	-	-	-
2	-	-	-	2	-	-	-	2	-	-	-
3	1.19	0.29	0.47	3	0.92	0.42	0.52	3	0.92	0.42	0.52
4	-	-	-	4	-	-	-	4	-	-	-
Total	1.19	0.29	0.47	Total	0.92	0.42	0.52	Total	0.92	0.42	0.52

Table 6.7: SAIDI (hrs/yr) for the RBTS using the three different load shedding policies.

Priority Order Policy				Pass-1 Policy				Pass-2 Policy			
Volt. Class	SC	MC	Total Circuits	Volt. Class	SC	MC	Total Circuits	Volt. Class	SC	MC	Total Circuits
1	-	-	-	1	-	-	-	1	-	-	-
2	-	-	-	2	-	-	-	2	-	-	-
3	10.49	1.11	2.99	3	9.70	1.66	3.27	3	9.70	1.66	3.27
4	-	-	-	4	-	-	-	4	-	-	-
Total	10.49	1.11	2.99	Total	9.70	1.66	3.27	Total	9.70	1.66	3.27

Table 6.8: SARI (hrs/occ) for the RBTS using the three different load shedding policies.

Priority Order Policy				Pass-1 Policy				Pass-2 Policy			
Volt. Class	SC	MC	Total Circuits	Volt. Class	SC	MC	Total Circuits	Volt. Class	SC	MC	Total Circuits
1	-	-	-	1	-	-	-	1	-	-	-
2	-	-	-	2	-	-	-	2	-	-	-
3	8.00	2.34	6.94	3	8.32	2.13	6.94	3	8.32	2.13	6.94
4	-	-	-	4	-	-	-	4	-	-	-
Total	8.00	2.34	6.94	Total	8.32	2.13	6.94	Total	8.32	2.13	6.94

Table 6.9: DPUI (sys.mins) for the RBTS using the three different load shedding policies.

Priority Order Policy	Pass-1 Policy	Pass-2 Policy
51.19	51.19	51.19

Tables 6.10 – 6.13 show the system performance indices for the IEEE-RTS obtained using the three different load shedding policies. Table 6.10 shows that the priority order policy results in higher SAIFI for the Voltage Class 2 delivery points and lower SAIFI for the Voltage Class 3 delivery points than those obtained using with the pass-1 and pass-2 policies. The overall SAIFI obtained using the priority order policy is, however, considerably higher than those obtained using the pass-1 and pass-2 policies. The pass-1 policy provides slightly lower SAIFI than the pass-2 policy. Similarly, the overall SAIDI obtained using the priority order policy shown in Table 6.11 results in the highest value followed by the values obtained using the pass-2 and pass-1 policies respectively. This conclusion is opposite to that for the RBTS. This implies that the system performance indices are significantly dependent on the system topology and the

system operation. An operating policy such as the load curtailment philosophy that provides better system performance on one system may not result in better system performance on another system. The technique provided in this chapter could prove useful for system operators attempting to determine the most appropriate load shedding policy for their particular system. The overall SARI obtained using the pass-1 policy shown in Table 6.12 is slightly higher than that obtained using the priority order and pass-2 policies. The pass-2 policy provides the lowest SARI. This implies that the benefit of the pass-2 policy is to reduce the average restoration time of the overall system. Table 6.13 shows that the DPUI obtained using the three load shedding policies are basically the same. As noted earlier for the RBTS, an operating policy such as the load shedding philosophy has basically no impact on the DPUI.

Table 6.10: SAIFI (occ/yr) for the IEEE-RTS using the three different load shedding policies.

Priority Order Policy				Pass-1 Policy				Pass-2 Policy			
Volt. Class	SC	MC	Total Circuits	Volt. Class	SC	MC	Total Circuits	Volt. Class	SC	MC	Total Circuits
1	-	-	-	1	-	-	-	1	-	-	-
2	-	1.15	1.15	2	-	0.52	0.52	2	-	0.60	0.60
3	-	1.58	1.58	3	-	1.78	1.78	3	-	1.84	1.84
4	-	-	-	4	-	-	-	4	-	-	-
Total	-	1.33	1.33	Total	-	1.04	1.04	Total	-	1.11	1.11

Table 6.11: SAIDI (hrs/yr) for the IEEE-RTS using the three different load shedding policies.

Priority Order Policy				Pass-1 Policy				Pass-2 Policy			
Volt. Class	SC	MC	Total Circuits	Volt. Class	SC	MC	Total Circuits	Volt. Class	SC	MC	Total Circuits
1	-	-	-	1	-	-	-	1	-	-	-
2	-	4.40	4.40	2	-	1.63	1.63	2	-	1.90	1.90
3	-	5.90	5.90	3	-	6.90	6.90	3	-	7.08	7.08
4	-	-	-	4	-	-	-	4	-	-	-
Total	-	5.01	5.01	Total	-	3.80	3.80	Total	-	4.03	4.03

Table 6.12: SARI (hrs/occ) for the IEEE-RTS using the three different load shedding policies.

Priority Order Policy				Pass-1 Policy				Pass-2 Policy			
Volt. Class	SC	MC	Total Circuits	Volt. Class	SC	MC	Total Circuits	Volt. Class	SC	MC	Total Circuits
1	-	-	-	1	-	-	-	1	-	-	-
2	-	3.38	3.38	2	-	1.74	1.74	2	-	1.67	1.67
3	-	2.87	2.87	3	-	3.40	3.40	3	-	3.37	3.37
4	-	-	-	4	-	-	-	4	-	-	-
Total	-	3.15	3.15	Total	-	3.16	3.16	Total	-	3.11	3.11

Table 6.13: DPUI (sys.mins) for the IEEE-RTS using the three different load shedding policies.

Priority Order Policy	Pass-1 Policy	Pass-2 Policy
97.82	97.81	97.81

6.3.3 Reliability Performance Index Probability Distributions

The expected values of the performance indices for the RBTS and the IEEE-RTS are presented in the previous section. Performance index probability distributions of the indices shown in the previous section are illustrated in this section. Figures 6.9 – 6.12 provide pictorial representations of the RBTS reliability performance index annual variability with the two different load curtailment policies.

Figure 6.9 shows that the two different load shedding policies provide relatively different SAIFI distributions. The SAIFI distributions for the subsystems and the overall system are also different. The distributions of the more reliable multi-circuit DP have mean values close to the ordinate axis and have exponential characteristics. On the other hand, the single-circuit DP has a lower reliability. The mean values are further from the ordinate axis and the probability distributions have different characteristics.

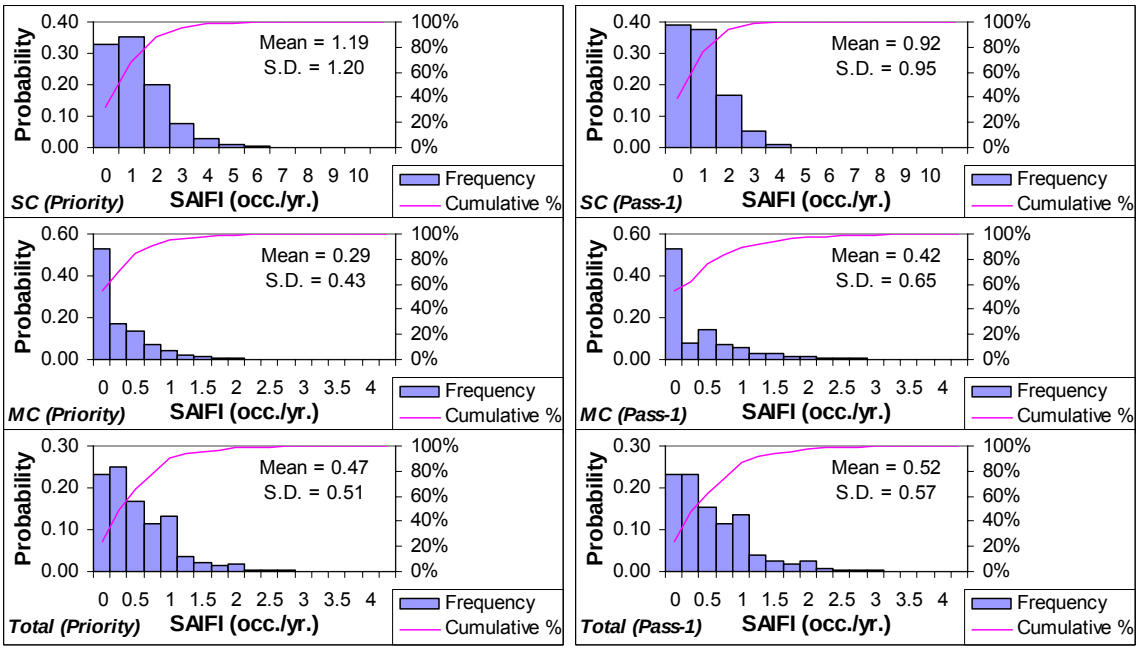

Figure 6.9: Single-circuit, multi-circuit and overall SAIFI of the RBTS using the priority order and pass-1 load curtailment policies.

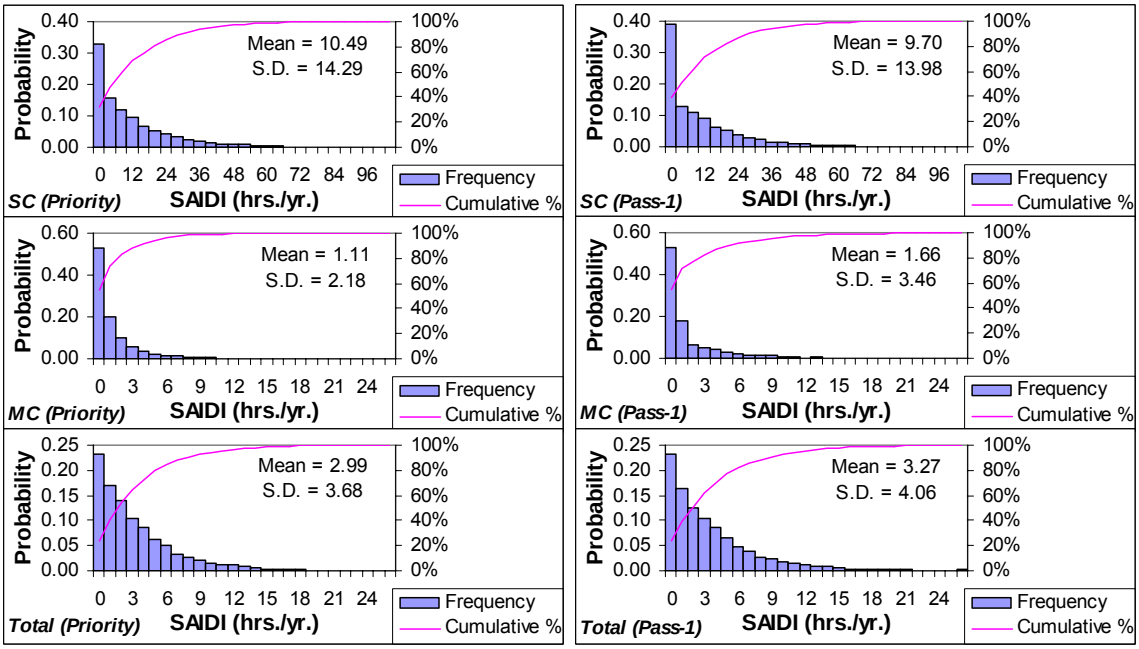

Figure 6.10: Single-circuit, multi-circuit and overall SAIDI of the RBTS using the priority order and pass-1 load curtailment policies.

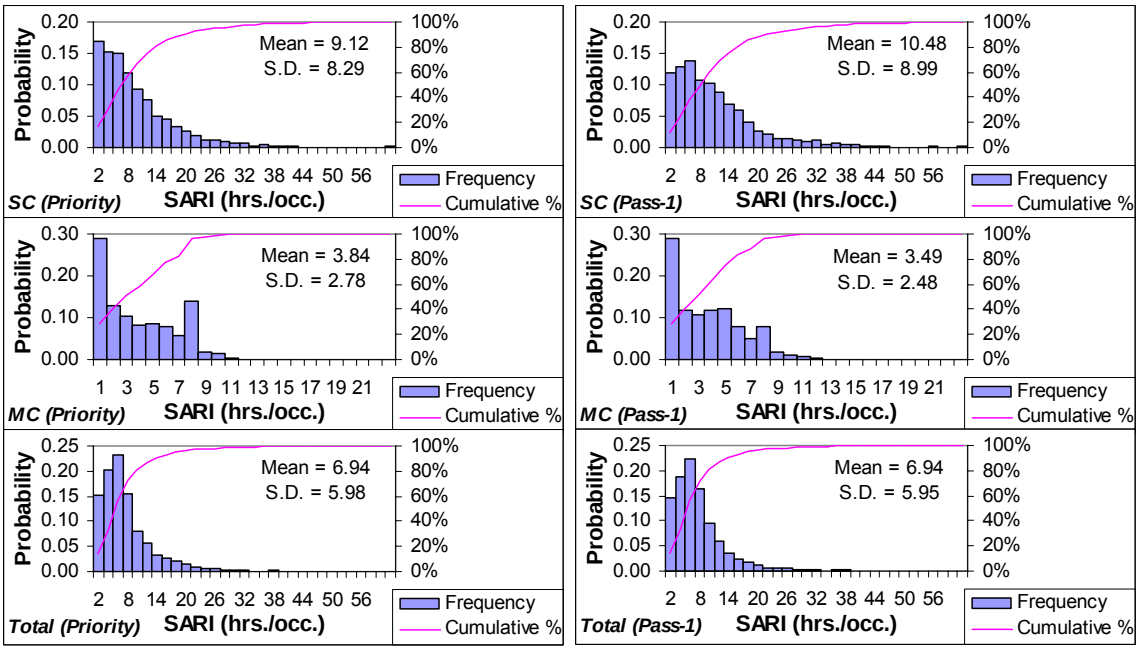

Figure 6.11: Single-circuit, multi-circuit and overall SARI of the RBTS using the priority order and pass-1 load curtailment policies.

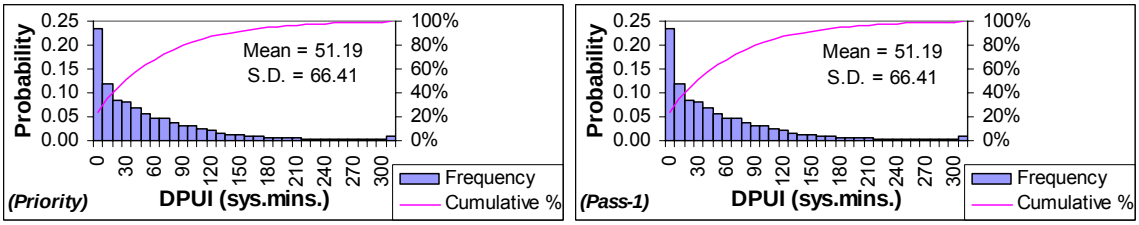

Figure 6.12: DPUI of the RBTS using the priority order and pass-1 load curtailment policies.

Figure 6.10 shows the importance of considering the distributional aspects. The SAIDI of the RBTS seems to be very reasonable but the distribution has a relatively long tail. As noted earlier, an appreciation of the distribution tail values, which although they may occur very infrequently, is important as these events can have serious system consequences. The average values, in this case, may not be valid indicators of satisfactory system performance. In such a case the performance index probability distributions provide significant additional information. Figure 6.11 shows the distributional aspects of SARI for the RBTS. The single-circuit SARI tends to be more

dispersed with a lognormal distribution form when using the pass-1 policy. The multi-circuit SARI has an exponential shape while the total SARI has more of a lognormal form. Figure 6.12 shows that the distribution shapes of the DPUI obtained using the two different load shedding policies are basically the same.

Figures 6.13 – 6.16 provide pictorial representations of the IEEE-RTS reliability performance index annual variability with the two different load curtailment policies. Figure 6.13 shows the distributions of SAIFI for the IEEE-RTS. Different load shedding policies provide relatively different distribution shapes. The mean values of SAIFI for the IEEE-RTS are further from the ordinate axis than those for the RBTS as the IEEE-RTS encounters more interruptions than the RBTS. Utilizing the pass-1 policy in the IEEE-RTS positively changes the distribution of SAIFI as the probabilities move closer to the ordinate axis, and the system performance is improved.

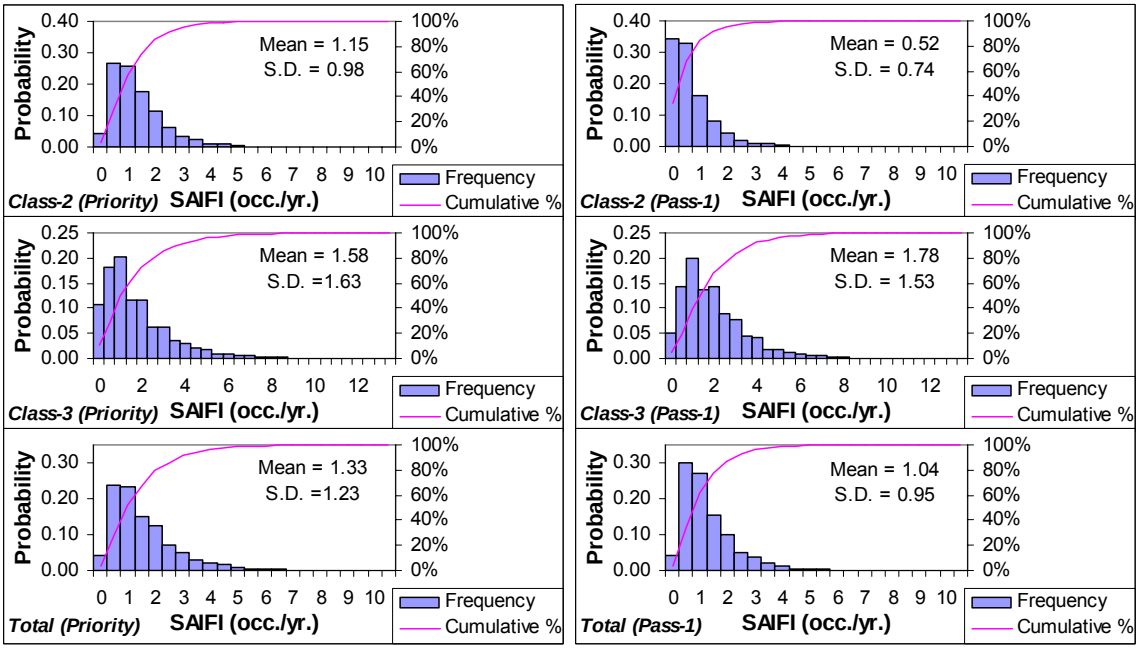

Figure 6.13: Single-circuit, multi-circuit and overall SAIFI of the IEEE-RTS using the priority order and pass-1 load curtailment policies.

Figure 6.14 shows the probability distributions of SAIDI for the IEEE-RTS. As noted earlier, the different load shedding policies have different impacts on the performance index probability distributions. This can be seen in Figure 6.14. The mean

value and the probability distributions of the total SAIDI are significantly improved by using the pass-1 policy rather than the priority order policy.

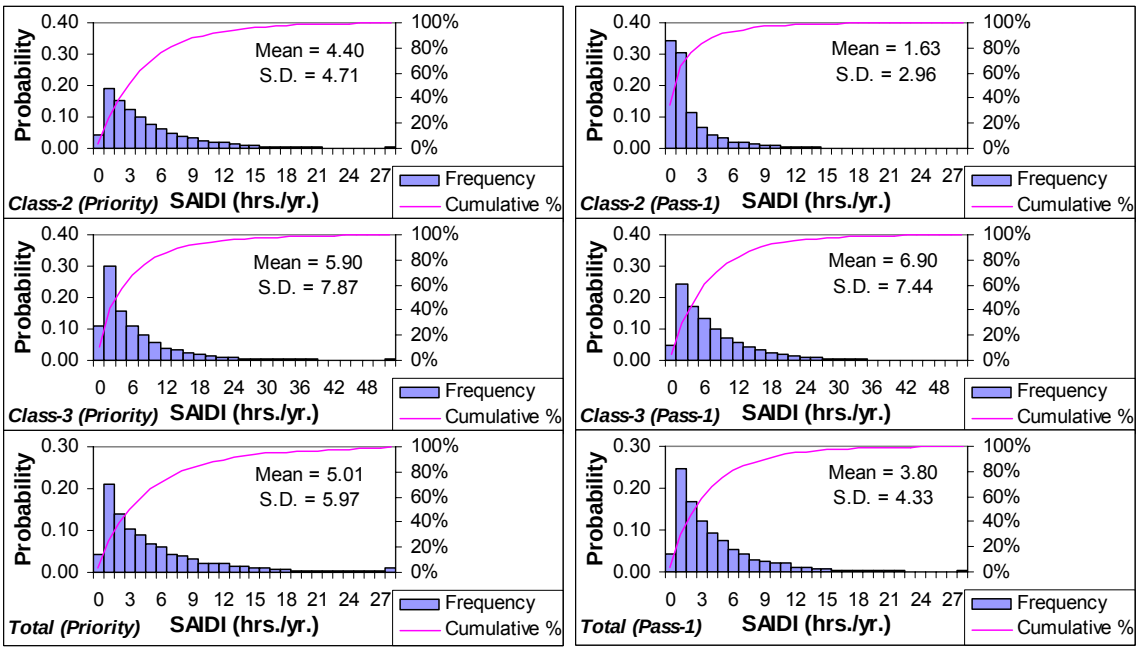

Figure 6.14: Single-circuit, multi-circuit and overall SAIDI of the IEEE-RTS using the priority order and pass-1 load curtailment policies.

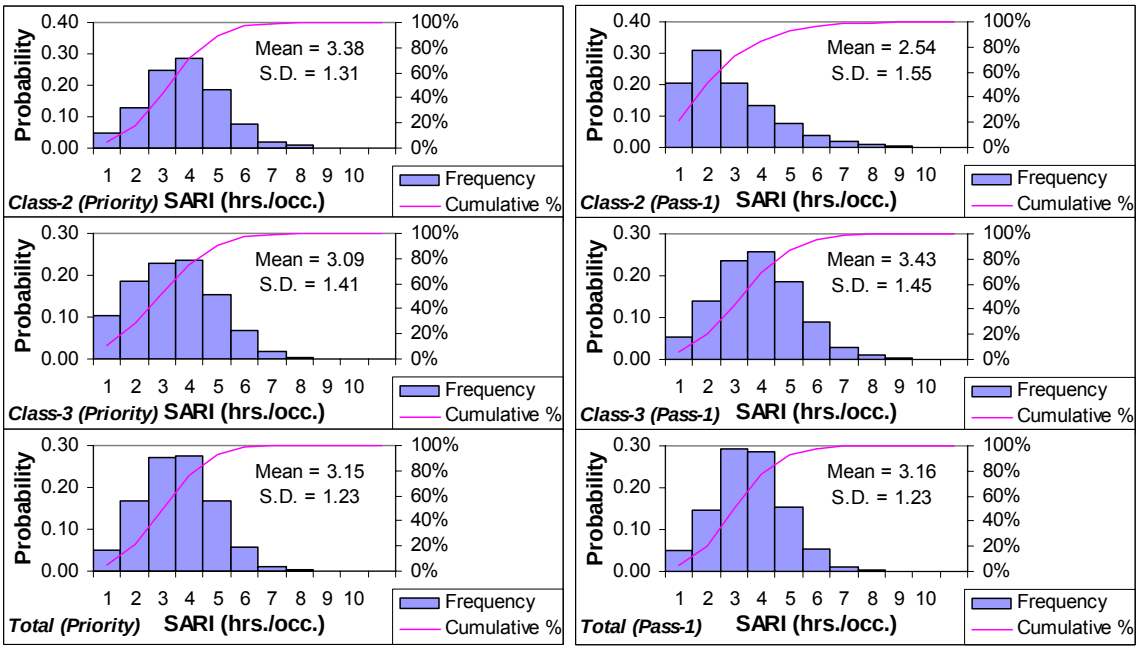

Figure 6.15: Single-circuit, multi-circuit and overall SARI of the IEEE-RTS using the priority order and pass-1 load curtailment policies.

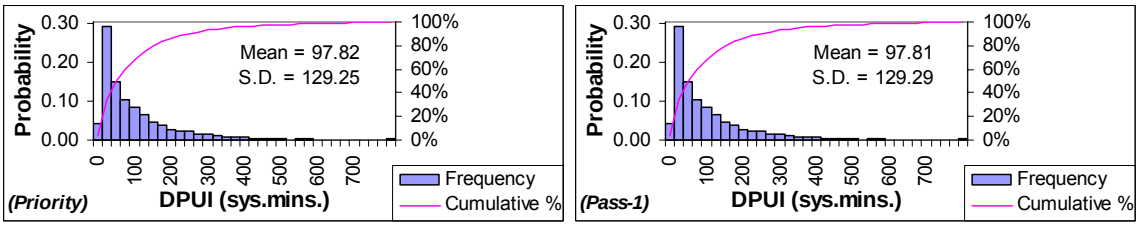

Figure 6.16: DPUI of the IEEE-RTS using the priority order and pass-1 load curtailment policies.

Figure 6.15 shows the probability distributions of SARI for the IEEE-RTS based on the two different load shedding policies. The probability distributions of the Voltage Class 2 and Class 3 DP and overall system SARI are more likely to have lognormal or normal distribution characteristics. Figure 6.16 shows that the distribution shapes of DPUI obtained using the two different load shedding policies are very similar. The probability distributions of DPUI are highly dispersed. This is also true for the RBTS. The mean DPUI of the IEEE-RTS is considerably higher than that of the RBTS.

In conclusion, the concept of predicting system reliability performance index probability distributions for composite generation and transmission systems is presented in this section. The mean index values are important indicators of system and delivery point performance but provide only single risk dimensions. The resulting appreciation of the risk may be insufficient when the index distribution is highly skewed. Performance index probability distributions can provide valuable additional insight. System performance indices have unique characteristics that are dependent on the system topology and the system operating conditions. System operating strategies, involving load curtailment procedures, have considerable impact on the system performance indices. The results indicate that the system performance indices can be improved by utilizing appropriate load shedding philosophies. A load curtailment policy that provides the best system performance for one system may not be the right choice for another. The appropriate load curtailment policy is, therefore, system dependent.

6.4 Sensitivity Analyses of Performance Index Probability Distributions

In this section, sensitivity studies have been conducted to investigate the reliability index probability distribution characteristics under different selected situations. Two factors are examined, namely the effect of repair process distributions and the effect of changing system conditions such as increased system peak loads. Performance index probability distributions are used to illustrate these effects in this section.

6.4.1 Effect of the Repair Process Distributions

Bulk electric power systems are basically repairable systems. If a component in the system such as a generating unit or a transmission link fails, it is usually repaired and put back into operation. The restoration times in this process can be considered as random variables. An integral part of the sequential simulation approach is to sample random variates from probability distributions. This section presents the effect that repair process probability distributions have on the bulk electric system reliability performance index probability distributions. The failure processes (time to failure, TTF) are assumed to follow an exponential distribution similar to that used in the previous section. The hazard rate of the failure process in this case is therefore constant. This is a reasonable assumption in normal operation. Different distributions for the repair process (time to repair, TTR) are examined in order to identify the effect of the distributions on the reliability performance indices. The mean time to failure (MTTF) and mean time to repair (MTTR) of each component are kept the same in order to maintain consistency. It is also assumed that all components have the same underlying distribution for each case study. It should be noted, however, that no added complexity is imposed on the simulation if different components have different distributions. In this study, the Weibull distribution models are used to present the probability distribution function of the repair time process. The Weibull distribution is composed of two important parameters designated as the scale factor (α) and the shape factor (β). The time-dependent Weibull probability distribution function, $f(t)$, is shown in Equation (6.5) [22]:

$$f(t) = \frac{\beta}{\alpha^{\beta}} t^{(\beta-1)} e^{-(\frac{t}{\alpha})^{\beta}} \tag{6.5}$$

The simulated duration, T, using the inverse transform of the Weibull probability distribution function is:

$$T = \alpha(-\ln U)^{\frac{1}{\beta}} \tag{6.6}$$

where: U = A uniformly distributed random number [0,1],

α = Scale factor,

β = Shape factor.

The three different shape factors (β), 1.0, 2.0 and 3.5 used in this study are illustrated in Figure 6.17. The Weibull distributions with these three shape factors have quite different and distinct distribution shapes. The exponential, Rayleigh and normal distributions are Weibull distributions with shape factors of 1, 2 and 3.5 respectively as shown in Figure 6.17. As shown in Equation (6.6), when the Weibull distribution has a shape factor of 1.0 (β = 1), this equation is equivalent to Equation (2.4) in Chapter 2, which is the inverse transform of the exponential distribution.

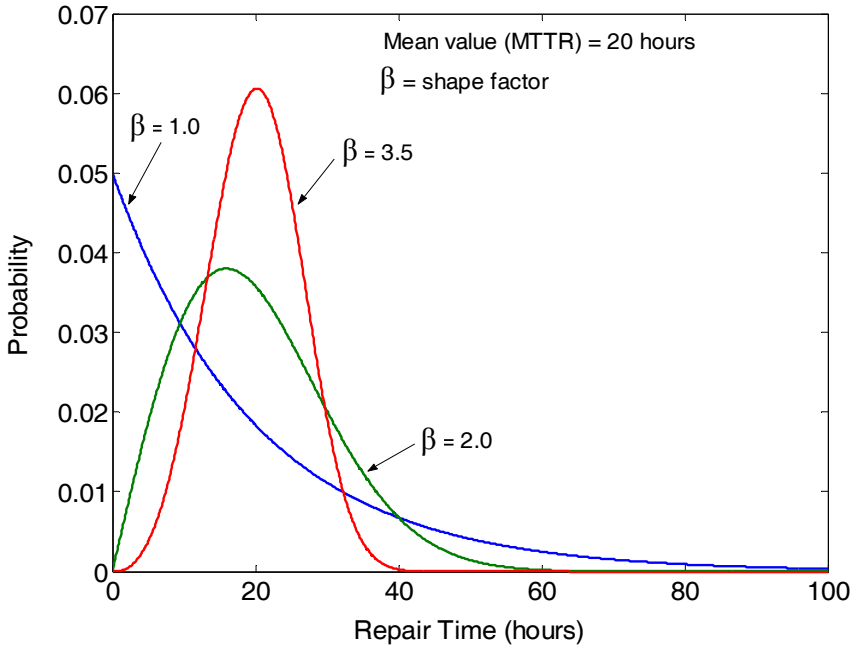

Figure 6.17: Weibull distribution characteristics with three different shape factors.

It is worth noting that the use of distribution shapes other than an exponential requires more detailed investigation to identify the shape of the repair time distribution using actual data. It may not be an easy task for most utilities to determine accurate shapes for TTF and TTR from the outage database. The MTTF and MTTR are the most available data and are generally used in conjunction with an exponential distribution. When using the Weibull distribution model, the scale factor and shape factor need to be identified, and mean value and variance can then be calculated. This is not usually the case for most utilities and they are more likely to start modeling using a knowledge of the mean values such as MTTF and MTTR. In order to use Weibull distributions to characterize the TTF and TTR, the shape factor is specified initially. When the shape factor (β) and mean value (μ) are identified, the scale factor (α) can be heuristically calculated using a gamma function as shown in the following equation.

$$\mu = \alpha.\Gamma\left(\frac{1}{\beta}+1\right) \tag{6.7}$$

where: Γ = The gamma function,

μ = Mean value, i.e. MTTF and MTTR.

Figures 6.18 – 6.20 respectively illustrate the probability distributions of the selected SAIFI, SAIDI and SARI for the RBTS obtained using the three different repair time shape factors. Figures 6.21 – 6.23 respectively show the probability distributions of the selected SAIFI, SAIDI, SARI and DPUI for the IEEE-RTS obtained using three different repair time shape factors. The pass-1 load curtailment philosophy is utilized in this study. The simulation results are based on 8,000 and 6,000 simulation years for the RBTS and the IEEE-RTS respectively. Reliability index probability distributions are normally created as frequency histograms with discrete intervals (bins) as shown in the previous sections. The probability distributions shown in this section are, however, presented using approximate continuous distributions for illustration purposes rather than histograms. The use of smooth curves in representing the probability distributions facilitates comparisons of the various scenario results on the same axis. Figure 6.18 shows that the probability distributions of the single and multi-circuit SAIFI for the

RBTS associated with the three different repair time distributions are considerably similar.

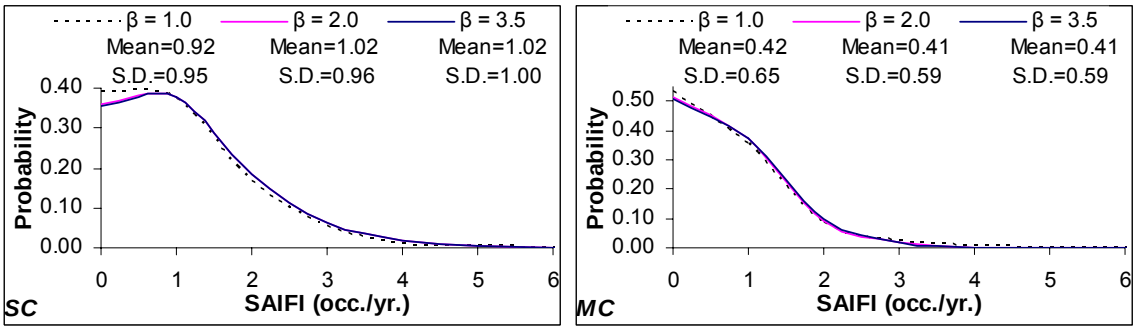

Figure 6.18: Probability distributions of single and multi-circuit SAIFI for the RBTS associated with the three different repair process distributions.

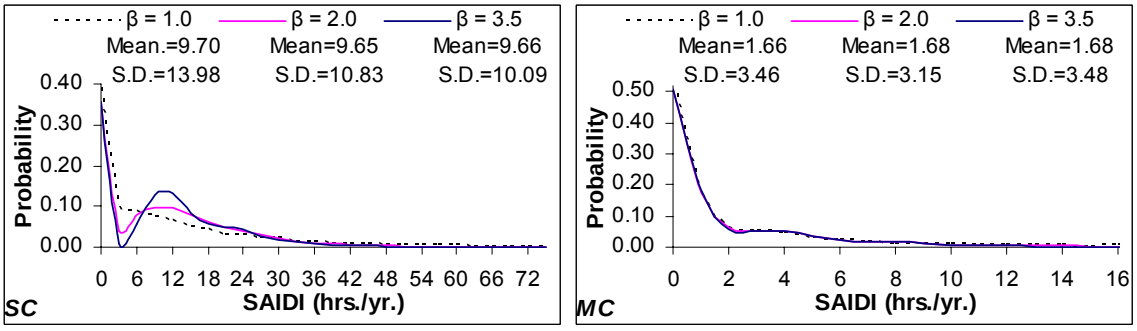

Figure 6.19: Probability distributions of single and multi-circuit SAIDI for the RBTS associated with the three different repair process distributions.

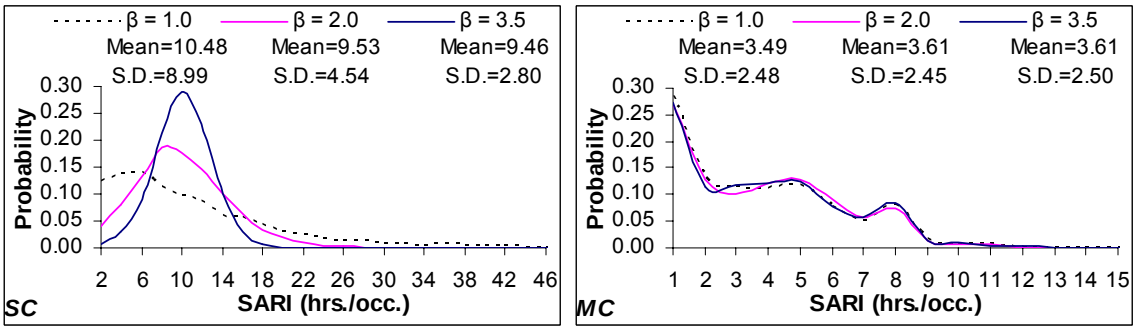

Figure 6.20: Probability distributions of single and multi-circuit SARI for the RBTS associated with the three different repair process distributions.

Figures 6.19 and 6.20 respectively show that the single circuit SAIDI and SARI is significantly affected when using different repair time distribution shapes, whereas these impacts on the probability distributions of the multi-circuit SAIDI and SARI are relatively small. This is due to the fact that the probability distributions of SAIDI and SARI are directly dependent on the component repair time model. Another reason is that a single circuit delivery point is basically dependent on a single component, the loss of which will result in load curtailment. A single circuit delivery point is therefore very sensitive to the component modeling process. The probability distributions of the single circuit SARI are therefore basically similar to the distribution shapes of the component repair time. On the other hand, the multi-circuit delivery points are considerably less affected by the component repair time distribution characteristics as such delivery points are well meshed and the loss of a single element will not cause load curtailment.

Figures 6.21 – 6.23 show that the IEEE-RTS probability distributions for SAIFI, SAIDI and SARI with the three different repair time distributions are relatively similar for both voltage classes. This is due to the fact that the IEEE-RTS has no single circuit delivery points. The impact of component repair time distributions is therefore less significant on the performance index probability distributions for the IEEE-RTS.

In conclusion, the component repair time distributions have a considerable impact on the probability distributions of the performance indices of the single circuit delivery point. The impact is however less significant for the performance index probability distributions of the multi-circuit delivery points. Many load points in practical bulk electric systems are usually highly meshed, and many bulk supply points are therefore categorized as multi-circuit delivery points. Consequently, the impact of component repair time distributions on bulk electric system reliability index probability distributions is relatively insignificant. On the other hand, reliability index probability distributions of electric distribution systems, which are basically radial systems, tend to be greatly affected by the component repair time distribution model.

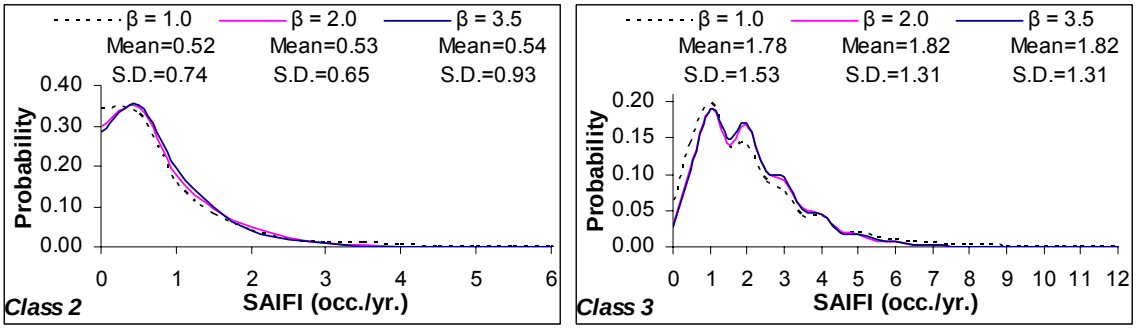

Figure 6.21: Probability distributions of Voltage Class 2 and Class 3 SAIFI for the IEEE-RTS associated with the three different repair process distributions.

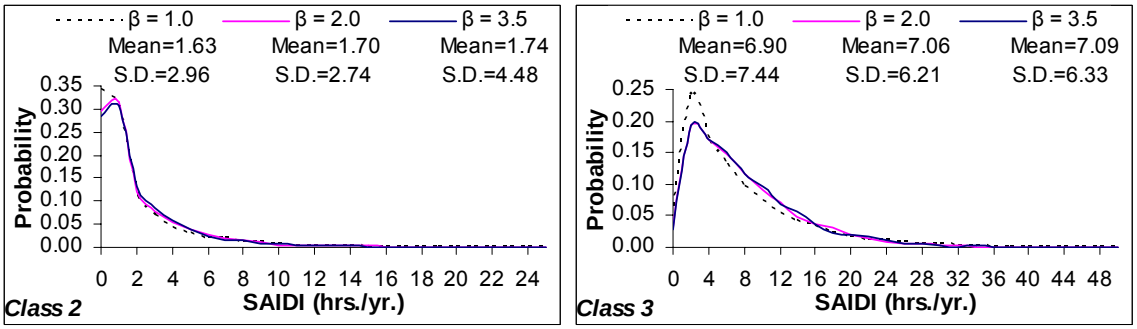

Figure 6.22: Probability distributions of Voltage Class 2 and Class 3 SAIDI for the IEEE-RTS associated with the three different repair process distributions.

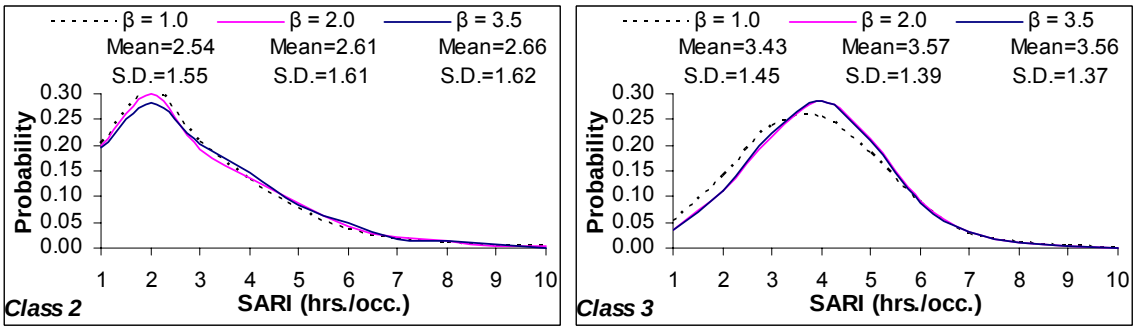

Figure 6.23: Probability distributions of Voltage Class 2 and Class 3 SARI for the IEEE-RTS associated with the three different repair process distributions.

6.4.2 Effect of Changing System Conditions

The results obtained in the previous sections indicate that performance index probability distributions have unique characteristics that are basically dependent on the system topology and operating philosophy. In this section, the impact on the performance index probability distributions of system conditions such as peak load level changes and system reinforcement options is investigated and illustrated by application to the RBTS. The probability distributions of the overall SAIFI, SAIDI and DPUI are illustrated using two study scenarios. The first scenario presents the results obtained using the original RBTS configuration shown in Figure 3.2. In the second scenario, the RBTS is reinforced by adding another transmission line between Bus 5 and Bus 6 in order to diminish the impact of a single circuit delivery point at Bus 6.

The results obtained using the first scenario with different system peak load levels are graphically presented together with the expected values in Figure 6.24. Figure 6.24 shows that load growth not only results in increased expected performance indices but also significantly impacts the associated distributions. The variation in the performance index probability distribution characteristics is dependent on the system conditions. The distributions shown in Figure 6.24 exhibit Weibull distribution characteristics with different shape factors. For example, the exponential, Rayleigh and normal distributions are Weibull distributions with shape factors of 1, 2 and 3.5 respectively. The distributions of SAIFI, SAIDI and DPUI at the individual peak loads shown in Figure 6.24 are generally similar in form, but the shape factors are not identical in each case. This implies that each reliability performance index has a unique distribution characteristic for each particular circumstance. The performance index probability distributions under lower system peak load levels, i.e. 179 and 188 MW, are less dispersed with higher predicted probability of occurrence, whereas higher system peak loads such as 206 MW create more dispersion and uncertainty in the performance indices with lower predicted probability of occurrence. Operating a system in a highly stressed environment will result in increased difficulties for system engineers to manage the system risk with a high degree of confidence.

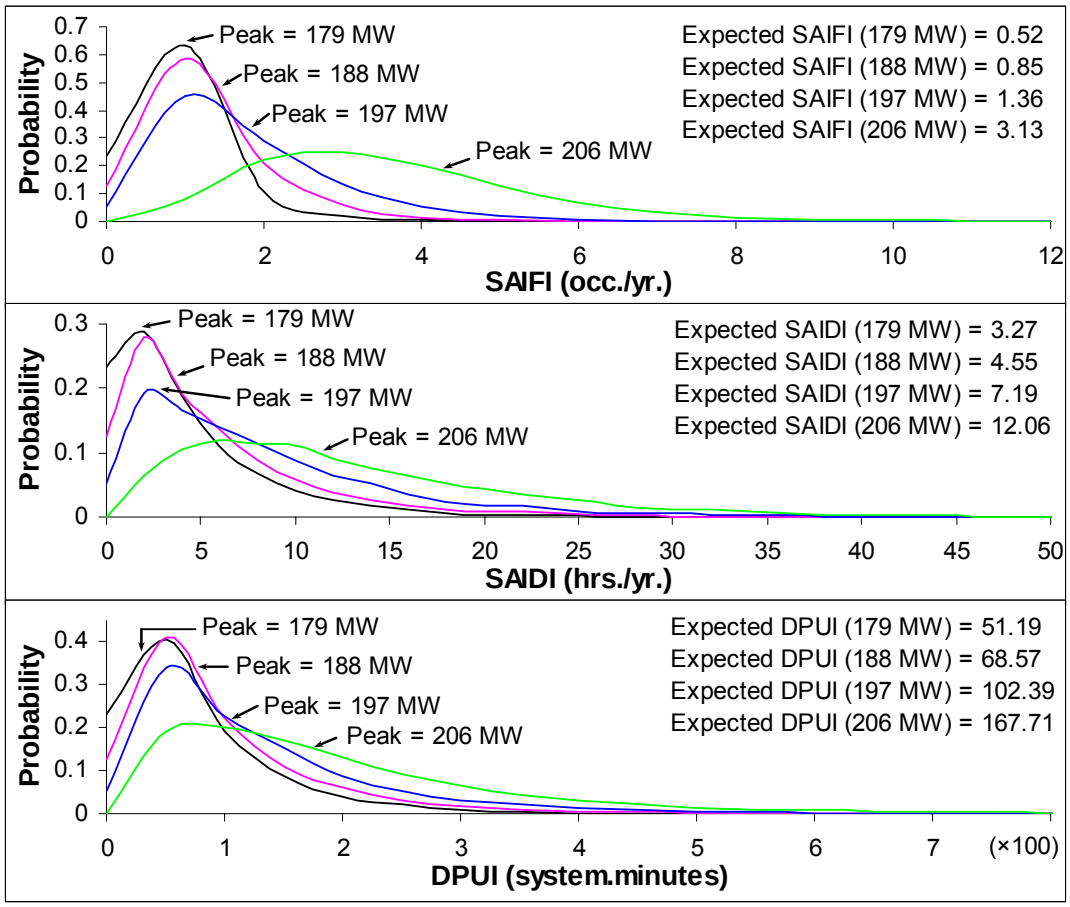

Figure 6.24: Performance index probability distributions of the original RBTS at different system peak loads.

Figure 6.25 shows the probability distributions of SAIFI, SAIDI and DPUI at the different system peak loads for the reinforced RBTS (the second scenario). The original RBTS results shown in Figure 6.24 are also compared and presented as dashed curves in Figure 6.25. Two lines (dashed and undashed) indicate the expected values of the performance indices at the different peak loads for the original and reinforced RBTS respectively. Figure 6.25 shows that there is a noticeable improvement due to the reinforcement in all the performance index probability distributions at the original system peak load (179 MW) as the distributions transform from log-normal to exponential shapes. The degree of uncertainty (dispersion) is decreased significantly by adding a transmission line between Bus 5 and Bus 6. There is still a considerable improvement due to the reinforcement in all the performance index probability

distributions when the system peak load increases to 188 MW. As the system peak load increases to 197 MW, the improvement in the SAIFI probability distribution is relatively small while the improvements in the probability distributions of SAIDI and DPUI are still quite obvious. This implies that the addition of a transmission line between Bus 5 and Bus 6 does not effectively reduce the interruption frequency at this system peak load (197 MW), but it is effective in reducing the interruption duration and unserved energy.

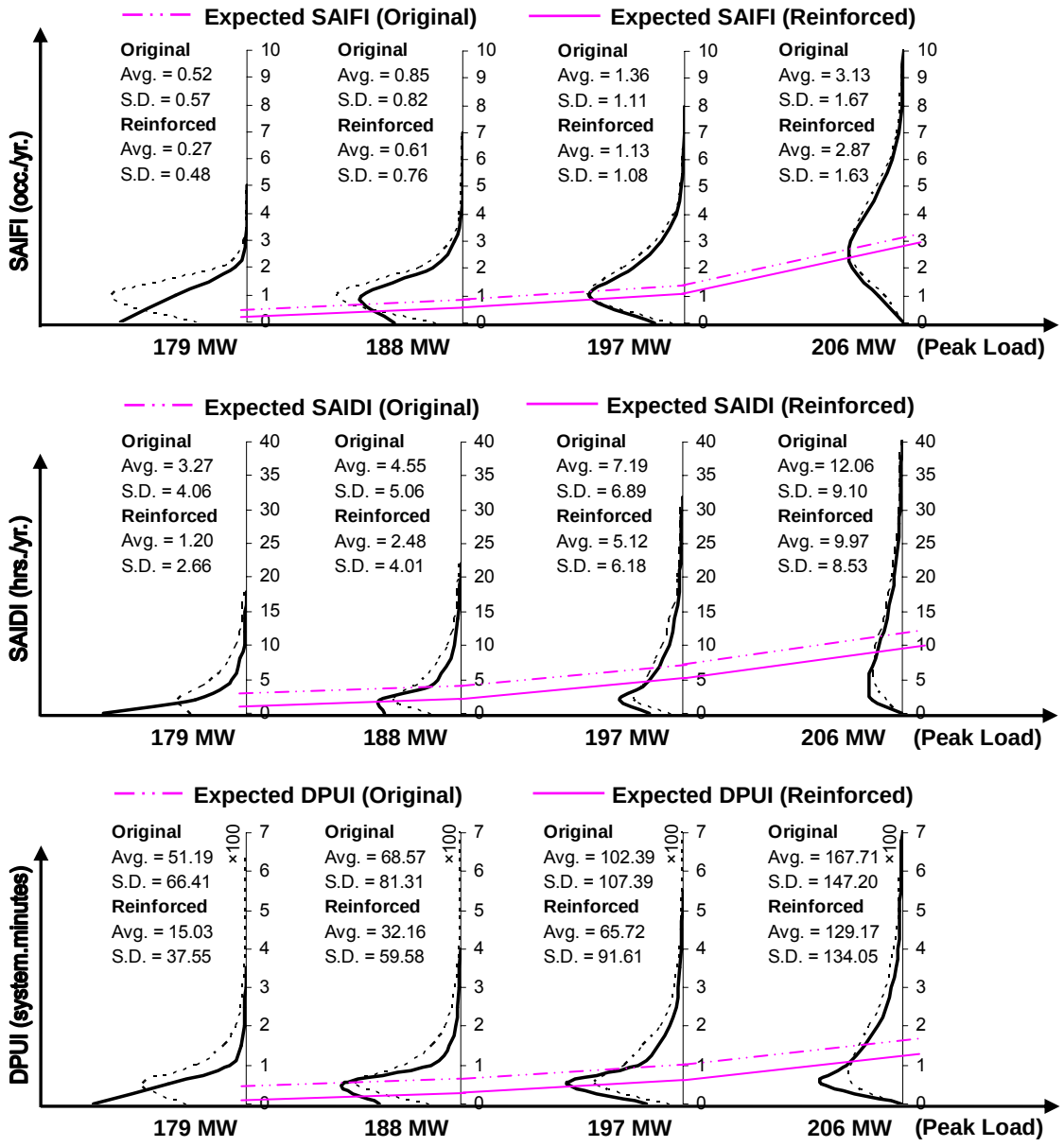

Figure 6.25: Performance index probability distributions of the original and reinforced RBTS at different peak load levels.

When the system peak load increases to 206 MW, there is relatively little improvement in the SAIFI and SAIDI probability distributions due to adding this transmission line. The main reason for this is that the system with this peak load, i.e. 206 MW, is generation deficient. Under these conditions, the system can no longer satisfy the N-1 deterministic criterion, i.e. the loss of the largest unit (40 MW). Generation reinforcement should be considered under these circumstances.

It should be noted that the above comments are focused on performance index probability distribution aspects directly related to the degree of risk uncertainty. As shown in Figure 6.25, the gap between the two lines illustrates the marginal improvement due to this transmission line addition using the expected values of SAIFI, SAIDI and DPUI. The width of the gap with increasing system peak loads is reasonably constant for each index. The expected values, therefore, provide only a single risk dimension without any knowledge of the residual uncertainty. Performance index probability distributions offer additional information insight and provide a multi-dimensional risk assessment. The concept of reliability index probability distribution analysis can be used as a supplementary tool in risk management to manage and control future potential risks arising within the system. This risk assessment tool could provide power engineers and risk managers with a more profound knowledge of their bulk electric system, and help them recognize system risk with higher confidence when making decisions. It offers additional information insight for planning engineers on when system improvement and reinforcements should be conducted to reduce future potential risk and uncertainty.

6.5 Conclusions

This chapter presents the development of reliability index probability distributions for bulk electric systems using a sequential simulation approach. Reliability index probability distributions for both delivery point and overall system are illustrated. The results show that the reliability index probability distributions at the individual delivery points have unique characteristics. These unique aspects are basically due to

system topology and system operating conditions. System operating strategies, especially those related to load curtailment policies, have important impacts on the individual delivery point characteristics. In contrast, the load curtailment policies have relatively little impact on the overall system reliability indices other than those related to reliability worth. The concept of predicting the future reliability performance indices associated with their probability distributions for bulk electric systems is also demonstrated in this chapter. The mean index values are important indicators of system and delivery point performance but provide only single risk dimensions. The resulting appreciation of the risk may be insufficient when the index distribution is highly skewed. Performance index probability distributions provide valuable additional information. The results indicate that the system performance indices can be improved by utilizing appropriate load shedding philosophies. A load curtailment policy that provides the best system performance for one system may not be the right choice for another. The appropriate load curtailment policy is, therefore, system dependent.

Sensitivity analyses have also been conducted to investigate the impacts of repair time distribution modeling and changes in the system conditions, i.e. increased peak load and system reinforcement, on performance index probability distributions. The results show that component repair time distribution characteristics can have considerably impact on the probability distributions of the duration-related indices such as SAIDI and SARI of a single circuit delivery point. The impact is, however, less significant on the probability distributions of SAIDI and SARI for multi-circuit delivery points. The impact of system peak loads and transmission reinforcement on performance index probability distribution characteristics is investigated in this chapter. The results show that changing system conditions can have a significant impact on the performance index probability distribution characteristics. Synthesizing bulk electric system reliability performance index probability distributions provides a multi-dimensional risk assessment tool that complements the single risk dimension provided by an expected or average value. This concept can prove useful in managing and controlling system risks with acceptable confidence.

CHAPTER 7
RELIABILITY INDEX PROBABILITY DISTRIBUTION UTILIZATION IN A PERFORMANCE BASED REGULATION (PBR) FRAMEWORK

7.1 Introduction

The electric power industry in North America and indeed throughout the world is undergoing deregulation in regard to its structure, operation and governance [81]. The basic intention of deregulation in the power industry is to increase competition in order to obtain better service quality and lower production costs. The demand for electricity is very sensitive to price, and therefore the lowest cost power supplier will be the most attractive to a customer. This has put great pressure on electric utilities to reduce costs, either by deferring capital projects or by increasing maintenance intervals, which can result in deterioration of the system reliability [82]. The question of achieving a balance between costs and service quality is therefore a key issue in today's power market. A mechanism known as performance based regulation (PBR) has been introduced to encourage power utilities to become more economically efficient, and at the same time to discourage utilities from sacrificing service quality in the pursuit of economic objectives [83]. The concept of PBR in the power industry was initially introduced for electric distribution systems [82 – 86]. The PBR concept is also under consideration in the field of composite generation and transmission systems and bulk electric system performance indices have the potential to be key elements in this regulated approach. The reliability performance index probability distributions described in the previous chapter are used as integral elements in the PBR mechanism described in this chapter to incorporate the risk uncertainties associated with expected financial payments in a PBR regime.

7.2 Performance Based Regulation (PBR) for Bulk Electric Systems

A regulatory approach designated as performance based regulation (PBR) has been proposed by policymakers involved in deregulating the electric power industry. The PBR approach decouples the price that a utility charges for its service from its cost, and is intended to provide an electricity utility with incentives for economic gain. This mechanism is offered as an alternative to more traditional cost-of-service regulatory practices. The PBR regime attempts to link rewards to desired results or targets. It works like a contract that rewards a power utility for providing good reliability or service quality and penalizes a utility for providing poor reliability [82, 86].

7.2.1 A Basic PBR Framework

Generally, a PBR framework is composed of three different sections designated as the reward, penalty and dead zones. In implementing PBR, a neutral zone or dead zone is introduced where neither a penalty nor a bonus is given. If the reliability performance is worse than the neutral zone boundary, a penalty is applied. Penalties are usually increased as the performance deteriorates and are frozen when a maximum penalty value is reached. Rewards for good reliability performance work in a similar way. Rewards are increased as the performance improves and are frozen when a maximum bonus value is reached, as shown in Figure 7.1 [82].

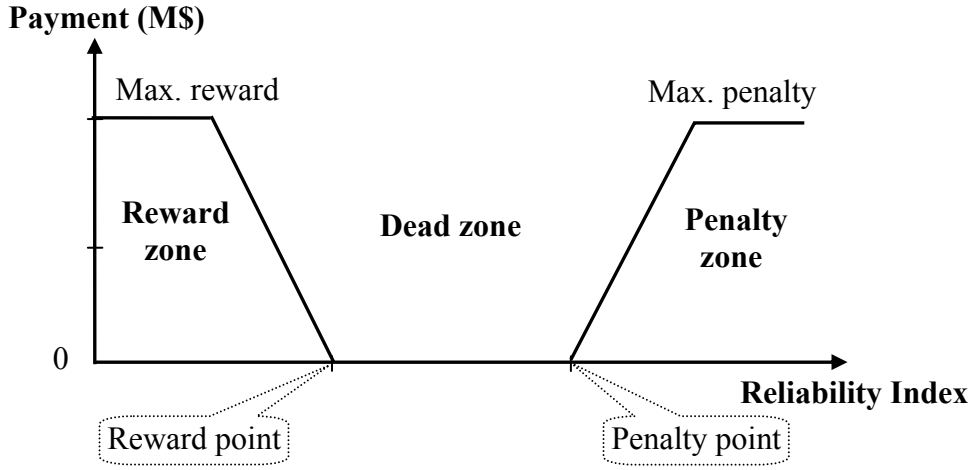

Figure 7.1: A general structure of performance based regulation (PBR).

An appropriate PBR framework has to be constructed in order to initiate a PBR mechanism. The attention is initially focused on the location and the width of the dead zone. References [84 – 87] suggest that the historical average reliability index should reside in the dead zone of the proposed PBR framework, and preferably at the dead zone center. The dead zone should not be too wide in order to create an effective and efficient PBR framework. A very wide dead zone makes it difficult for a utility to benefit from improving its reliability performance and may also lead a utility to let its system reliability performance deteriorate in the pursuit of economic objectives without encountering the penalty zone. On the other hand, the dead zone should not be too narrow as this may make it too difficulty for a power utility to maintain its reliability performance in the dead zone due to the highly random behavior of bulk systems. Such a situation will therefore create increased pressure and introduce the utility to more financial risk rather than creating economic incentives.

It appears that BES reliability index probability distributions are considerably more dispersed than those of electric distribution systems, and the standard deviations of bulk electric system performance indices are usually large or even larger than their mean values. This is due to the fact that bulk electric systems are normally much more reliable than distribution systems as bulk electric systems are usually well meshed and interconnected. The width of the dead zone was therefore arbitrarily set at one standard deviation (± S.D./2) in the PBR framework applied in this research. The basic PBR framework is shown in Figure 7.2.

Figure 7.2 shows the proposed PBR framework for bulk electric system reliability performance utilization. The width of the dead zone is set at one standard deviation with the mean value of the reliability index at the center of the dead zone. The width of the reward transition from the starting reward point to the maximum reward is one half of the standard deviation (S.D./2). The width of the penalty transition is set in a similar way. The reward and penalty payments shown on the vertical axis are represented as a per unit (p.u.) value in order to make its values adjustable to any maximum payment criterion determined by the regulator. On the horizontal axis, the

reliability performance indices used in the PBR protocol are normally SAIFI and SAIDI for distribution systems [82 – 87] as both SAIFI and SAIDI are required to provide an overall appreciation of customer service reliability reflecting different customer impacts (interrupted frequency and accumulated duration respectively). These two performance measures are also applied in the PBR applications in bulk electric systems. In this research work, the PBR procedure is applied to SAIFI and SAIDI separately. The two components are added to provide the overall reward/penalty payment. The mathematical model of the reward/penalty payment structure (RPS) based on a power utility perspective is formulated as shown in Equation (7.1) using SAIFI and the parameters shown in Figure 7.2.

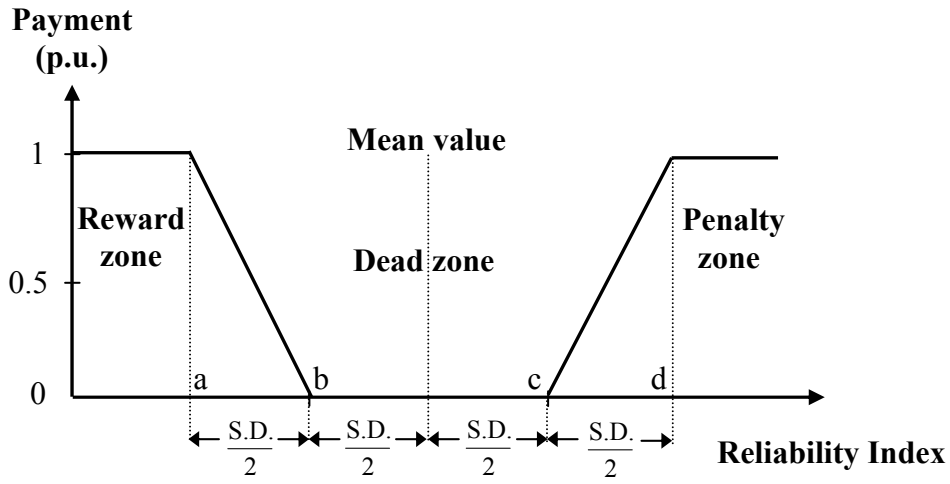

Figure 7.2: A basic PBR framework for bulk electric systems.

$$RPS = \begin{cases} 1 & SAIFI \le a \\ (SAIFI - b) \times slope_{ab} & a < SAIFI < b \\ 0 & b \le SAIFI \le c \\ -(SAIFI - c) \times slope_{cd} & c < SAIFI < d \\ -1 & SAIFI \ge d \end{cases} \quad (7.1)$$

As noted earlier, the width of the slope for the reward/penalty zones is half of the standard deviation and the maximum payment is 1.0 per unit. The slope shown in Figure 7.2 and expressed in Equation (7.1) can be therefore calculated as follows:

$$Slope = \frac{(1-0)}{\frac{S.D.}{2}} = \frac{2}{S.D.} \tag{7.2}$$

The SAIFI can be modeled by its probability distribution. The expected reward/penalty payment (ERP) is calculated using Equation (7.3). The SAIDI model can also be formulated in the same way.

$$ERP = \sum \left(RP_i \times P_i \right) \tag{7.3}$$

where: i = An individual element or a class interval in the frequency histogram,

RP_i = The reward/penalty payment (per unit) calculated using Equation (7.1) based on $SAIFI_i$ or $SAIDI_i$,

P_i = The probability of $SAIFI_i$ or $SAIDI_i$.

The maximum reward/penalty payments can be determined based on regulatory concerns or on negotiations between the regulatory agency and the power utility. For example, if regulators and power utilities adopt customer interruption cost in the planning and operation process, the IEAR or VoLL can be used in conjunction with the annual unserved energy to determine the maximum reward/penalty payments. If the regulator and the power utility do not utilize customer outage costs, then other monetary factors such as an annual price cap identified by the regulatory agency can be applied, i.e. if the annual price cap is equal to 10 cents/kWh and the annual energy consumption in the system is 1000 GWh/year, the maximum reward/penalty payment could be calculated by the multiplying these two factors to give 100 million dollars. This amount is given as a simple example, and could be scaled up or down as appropriate in a practical application. Other monetary keys such as the annual allowed revenue (revenue cap) for a power utility could also be used to identify the maximum payments. These are simply some of the possible factors that could be used to determine the maximum reward/penalty payments. The actual maximum payments for an individual power utility will depend on the policy adopted by the associated regulator. The maximum

reward/penalty payments applied in this research are therefore presented in terms of per unit (p.u.) values and are adaptable to any payment criterion adopted.

7.2.2 PBR Application Using Actual Historical Reliability Data

The service reliability indices in this section are past performance measures obtained by compiling system outage statistics. Power utilities are normally required to monitor the reliability indices and report them to a regulator on an annual basis. Virtually all the major utilities in Canada are actively engaged in reporting past performance indices, using the Canadian Electricity Association (CEA) protocols [76, 77]. There are also several online publications on bulk electric system reliability performance reporting [88, 89]. This section illustrates the potential utilization of available bulk electric system reliability data in the PBR framework described in the previous section. Table 7.1 presents actual historical bulk electric system reliability performance data from Canada [76, 77], Philippines (two separate areas) [88] and Thailand [89]. Bulk electric system reliability performance statistics in terms of the mean values and standard deviations (S.D.) of the historical data presented in Table 7.1 are shown in Table 7.2.

Table 7.1: Actual historical data on bulk electric system reliability performance.

Country	Reliability Index	Year						
		1998	1999	2000	2001	2002	2003	2004
Canada (Overall)	SAIFI (occ/yr)	1.40	1.10	1.00	0.90	0.90	1.00	--
	SAIDI (hrs/yr)	6.19	1.90	1.46	1.40	1.69	6.02	--
Philippines (Mindanao)	SAIFI (occ/yr)	2.56	2.13	5.44	1.73	1.63	--	--
	SAIDI (hrs/yr)	3.50	3.52	8.82	3.30	16.22	--	--
Philippines (Luzon)	SAIFI (occ/yr)	4.38	2.45	2.48	3.82	1.92	--	--
	SAIDI (hrs/yr)	12.87	7.34	8.07	10.02	5.48	--	--
Thailand	SAIFI (occ/yr)	--	0.91	0.92	0.74	0.45	0.36	0.42
	SAIDI (hrs/yr)	--	1.40	0.85	0.63	0.25	0.37	0.43

The results shown in Table 7.2 are calculated using the available data presented in Table 7.1. The calculated mean values and standard deviations (S.D.) shown in Table 7.2 are used to set the dead zone and other components in the PBR framework described

in the previous section. Figure 7.3 illustrates the superposition of the SAIFI and SAIDI distributions on the PBR framework for each individual system. The expected reward/penalty payments (ERP) shown in Figure 7.3 were calculated using Equations (7.1) – (7.3) and the data presented in Table 7.1.

Table 7.2: Historical data statistics of bulk electric system reliability performance.

System	SAIFI (occ/yr)		SAIDI (hrs/yr)	
	Mean	S.D.	Mean	S.D.
Canada (overall)	1.05	0.19	3.11	2.33
Philippines (Mindanao)	2.70	1.58	7.07	5.62
Philippines (Luzon)	3.01	1.04	8.76	2.82
Thailand	0.63	0.26	0.65	0.42

Figure 7.3 shows that each individual bulk system will face different reward and penalty payments for its reliability performances. A positive ERP value implies that the utility will expect a reward from the regulator while the negative ERP value indicates an expected penalty payment. The hypothetical PBR structure associated with the historic data tends to provide a reasonable reliability performance range and a target for the power utilities to compete as all the expected reward/penalty payments are relatively small (close to neutral) with exception of Canada in which the expected penalty payment based on SAIDI is quite high (-0.15 p.u.) and the dead zone width for SAIFI is quite small. This is due to the fact that the historic data for Canada are aggregated values from all the major utilities in Canada, not just from a specific utility.

The monitoring and reporting of the annual reliability indices shown in Table 7.1 is intended to encourage utilities to maintain or exceed their existing service reliability performance. The application of PBR introduces a form of financial risk to a power utility that did not previously exist. In order to manage this risk, a power utility should attempt to estimate the uncertainty associated with this aspect of system performance. The concept of reliability index probability distribution analysis can assist power utilities to deal with the financial uncertainty associated with their reliability performance.

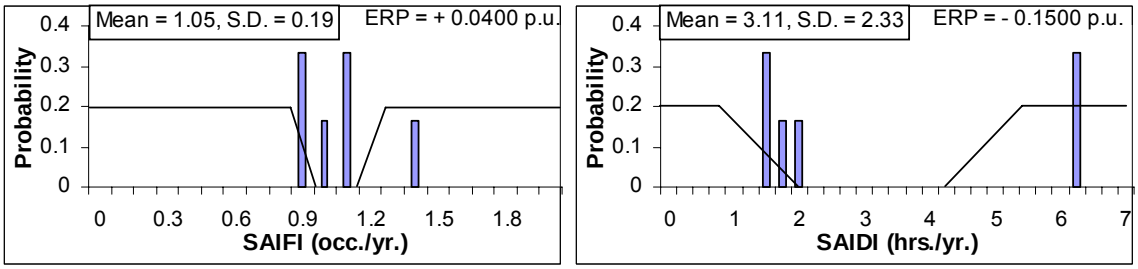

Canada (Overall)

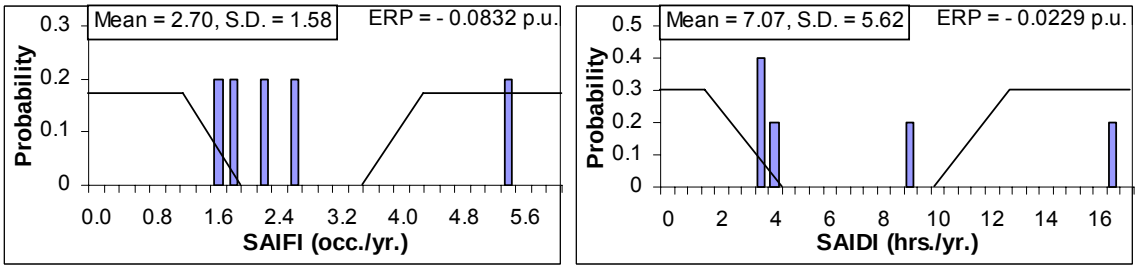

Philippines (Mindanao)

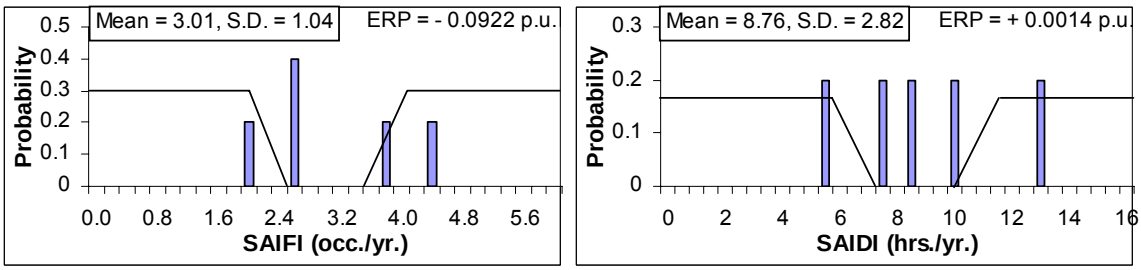

Philippines (Luzon)

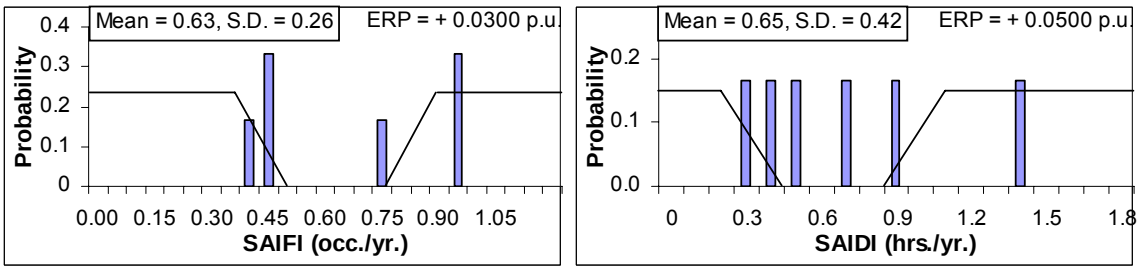

Thailand

Figure 7.3: Combination of the SAIFI and SAIDI histograms and the hypothetical PBR for individual bulk electric systems.

7.2.3 PBR Application Using Simulation Results

This section demonstrates the utilization of reliability performance index probability distributions obtained using simulation in the PBR framework. As shown in the previous chapter, reliability performance index probability distributions are usually represented by frequency histograms with discrete class intervals. The class interval selection can affect the shapes of the probability distributions and also the calculation of the expected reward/penalty payments in a PBR protocol. This effect is relatively small when an appropriate class interval is selected. A popular class interval selection criterion designated as Sturges' rule [90] is shown in Equation (7.4) and can be used in the probability distribution studies. This criterion is appropriate for moderate sample sizes less than 200, but it leads to oversmoothed histograms for large sample sizes [91, 92]. Sturges' rule is appropriate for practical PBR applications as the available historical data obtained from power utilities is usually given by a small number of years, i.e. 10 years. In this research, the simulation is done over a few thousand years. The class interval selection criterion designated as Scott's rule [93] shown in Equation (7.5) is adopted in this chapter to approximately estimate reasonable class intervals in frequency histogram construction using the simulation results.

Sturges' rule:

$$A\ class\ interval\ (bin\ width) \;=\; \frac{Range\ of\ Data}{1 + log_2 N} \tag{7.4}$$

Scott's rule:

$$A\ class\ interval\ (bin\ width) \;=\; \frac{3.49 \times S.D.}{N^{\frac{1}{3}}} \tag{7.5}$$

where: N is the number of samples, and $S.D.$ is the standard deviation.

The class intervals of the probability distributions shown in the previous chapter are designated by the upper bound values, not the mid values of the intervals. The calculation of the expected reward/penalty payments (ERP) expressed in Equation (7.3)

is, however, obtained using the mid interval values rather than the designated upper bound values shown in the frequency histograms.

Figure 7.4 presents the probability distribution of the overall SAIFI for the IEEE-RTS using the priority order policy, implanted on a designated PBR framework based on the structure noted earlier. The ERP calculation using Equation (7.3) is shown in Table 7.3.

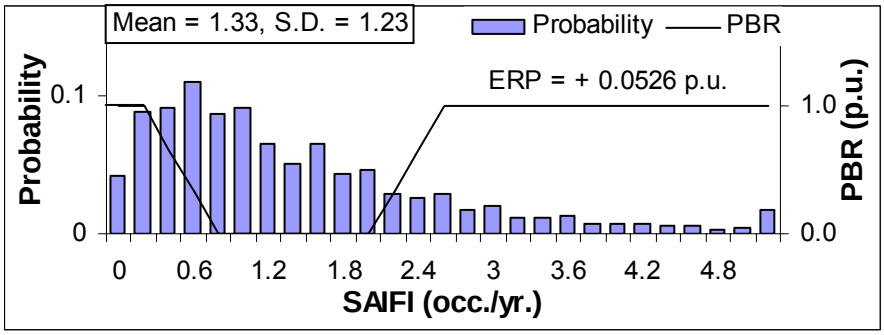

Figure 7.4: The SAIFI distribution for the IEEE-RTS obtained using the priority order policy implemented in a PBR framework.

The expected reward/penalty payment (ERP) shown in Table 7.3 and in Figure 7.4 is a positive value (+0.0526 p.u.). This indicates that the IEEE-RTS based on SAIFI in this PBR framework expects to receive a reward payment from the regulator. For example, if the maximum payment is M$ 100, the power utility can expect to receive 5.26 M$/year on average based on the SAIFI performance. In a similar manner, Figure 7.5 shows the SAIDI distribution for the IEEE-RTS using the priority order policy under the designated PBR structure. Figure 7.5 also shows that the ERP is a positive value (+0.0034 p.u.). The power utility in this case expects to receive reward payments from the regulator based on both SAIFI and SAIDI performances.

Table 7.3: The ERP calculation for the overall SAIFI distribution of the IEEE-RTS.

$SAIFI_i$ (mid value)	Probability (P_i)	RP_i (p.u.)	Payment (p.u.)
0	0.0418	1	0.0418
0.1	0.0892	1	0.0892
0.3	0.0917	0.6683	0.0613
0.5	0.1107	0.3423	0.0379
0.7	0.0873	0.0163	0.0014
0.9	0.0920	0	0
1.1	0.0658	0	0
1.3	0.0513	0	0
1.5	0.0658	0	0
1.7	0.0433	0	0
1.9	0.0472	0	0
2.1	0.0288	-0.2608	-0.0075
2.3	0.0268	-0.5868	-0.0157
2.5	0.0285	-0.9128	-0.0260
2.7	0.0172	-1	-0.0172
2.9	0.0197	-1	-0.0197
3.1	0.0120	-1	-0.0120
3.3	0.0117	-1	-0.0117
3.5	0.0127	-1	-0.0127
3.7	0.0068	-1	-0.0068
over 3.7	0.0497	-1	-0.0497
			$\sum$ = **0.0526**

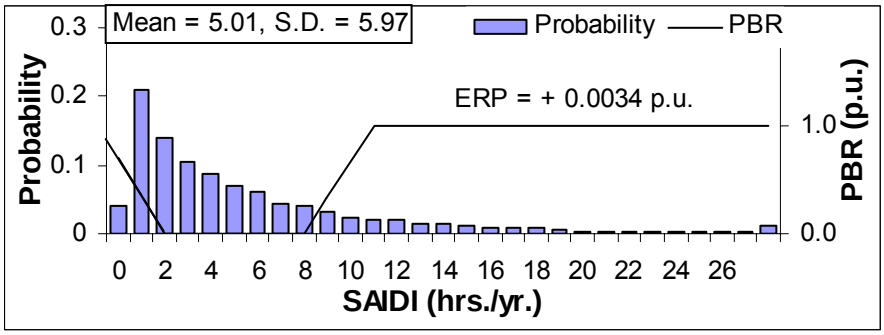

Figure 7.5: The SAIDI distribution for the IEEE-RTS obtained using the priority order policy implemented in a PBR framework.

As noted in the previous chapter, adopting an appropriate load shedding policy can improve the reliability performance of a bulk electric system. If the IEEE-RTS initially operated using the priority order philosophy, the system operator could adjust the future operating policy in order to improve overall system reliability performance

and therefore increase the potential to receive more reward payments under a specified PBR regime. Figures 7.6 and 7.7 respectively present the IEEE-RTS SAIFI and SAIDI distributions obtained using two different load shedding policies implemented in a PBR framework. In this example, it is assumed that the system is initially operated using a priority order policy before the PBR protocol is activated. The PBR structure is therefore based on the past performance utilizing the priority order policy. The system operator tries to maintain or improve the system reliability performance by changing the operating philosophy to the pass-1 policy after the PBR mechanism has been adopted. The distributions illustrated in Figures 7.6 and 7.7 are represented using approximate continuous curves for comparison purposes.

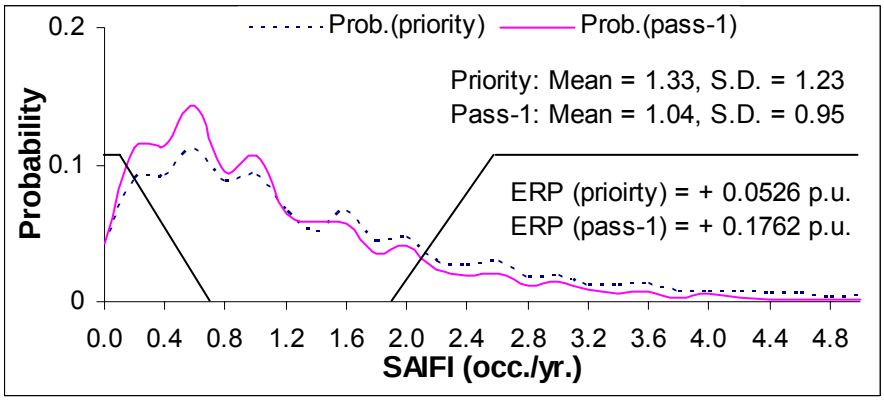

Figure 7.6: The SAIFI distributions for the IEEE-RTS obtained using two different load curtailment policies implemented in a PBR framework.

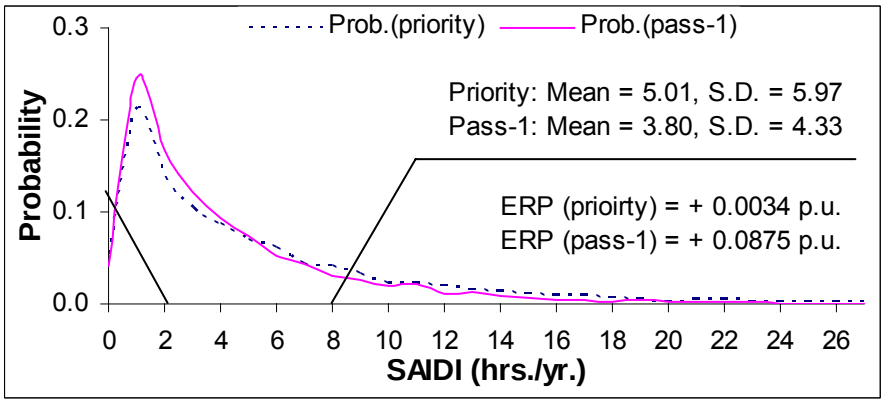

Figure 7.7: The SAIDI distributions for the IEEE-RTS obtained using two different load curtailment policies implemented in a PBR framework.

Figure 7.6 shows that by changing the load curtailment philosophy from the priority order policy to the pass-1 policy, the utility can expect to receive considerably more reward payments based on the SAIFI distribution performance. Similarly, Figure 7.7 indicates that there is also the potential to receive more reward payments based on the SAIDI distributions.

The results shown above are based on the utilization of the overall IEEE-RTS SAIFI and SAIDI distributions under the PBR protocol. In practical situations, the PBR mechanism could be applied to individual subsystems rather than the overall system as system topology can have a considerable impact on reliability performance. The reliability performance of individual subsystems may be quite different. The overall system reliability performance may seem reasonably good, but the performance for some areas (subsystems) in the system may be poor and undesirable. The following example demonstrates the application of the PBR mechanism to the two individual areas designated as Voltage Class 2 and Class 3 in the IEEE-RTS.

Figures 7.8 and 7.9 respectively show the reliability performance index distributions of the areas designated by Voltage Class 2 and Class 3 in the IEEE-RTS. The system is assumed to be initially operated using the priority order policy before the PBR protocol is activated. The PBR structure is therefore based on the past performance utilizing the priority order policy for each subsystem. Figure 7.8 indicates that there is a significant improvement in the reliability performance of the Voltage Class 2 subsystem when the utility switches the system operating philosophy from the priority order policy to the pass-1 policy. The resulting ERP for both SAIFI and SAIDI improve significantly under the PBR mechanism after changing the load curtailment philosophy. It is important to note that the maximum reward/penalty payments used in this case are not the same as the designated amounts for the overall system. The maximum payment for the subsystem should be some proportion of the maximum payment for the overall system based on the annual energy consumption or revenue allowance for the individual subsystem. The proportion of the annual energy consumption for the Voltage Class 2 subsystem is approximately 47% of the overall system energy consumption.

Consequently, if the maximum payment for the overall system is M$ 100, the maximum payment for the Voltage Class 2 subsystem is therefore M$ 47.

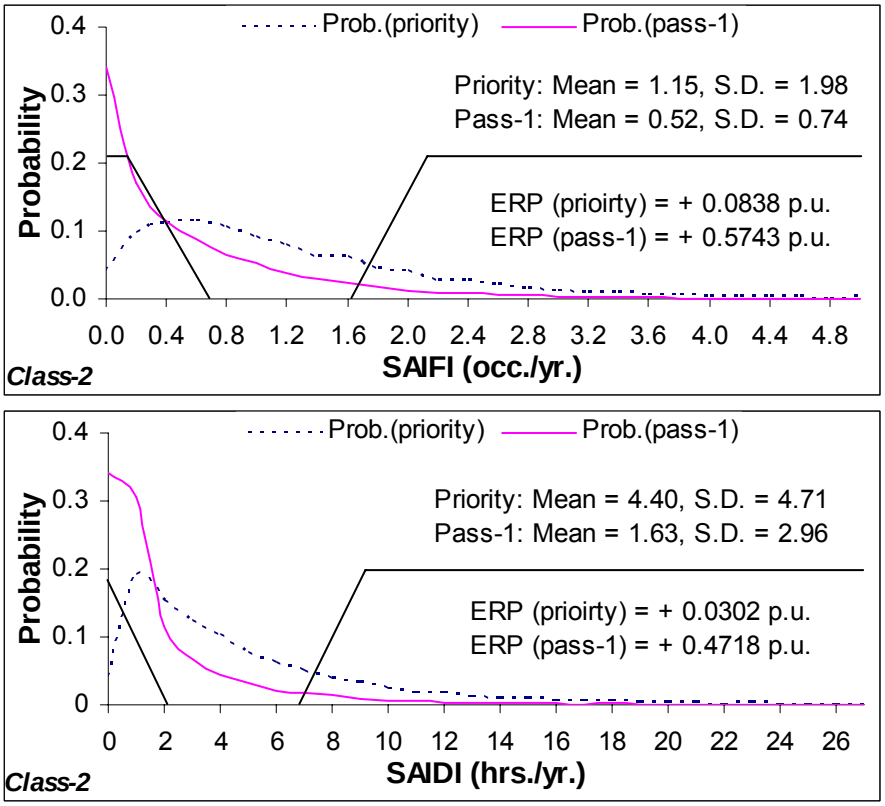

Figure 7.8: SAIFI and SAIDI distributions for the Voltage Class 2 subsystem in the IEEE-RTS obtained using two different load curtailment policies implemented in a PBR framework.

While there is a significant improvement in the reliability performance of the Voltage Class 2 subsystem and its resulting ERP, the reliability performance indices of the Voltage Class 3 subsystem as shown in Figure 7.9 deteriorate by changing the load curtailment philosophy from the priority order policy to the pass-1 policy. The reliability degradation for the Voltage Class 3 subsystem is, however, less significant than the major reliability improvement in the Voltage Class 2 subsystem. The resulting ERP for the Voltage Class 3 subsystem under the new operating policy is expected to be a penalty payment (negative value) for both SAIFI and SAIDI. These expected penalty payments due to the Voltage Class 3 subsystem are considerably less than the expected

reward payments in the Voltage Class 2 subsystem. The overall system performance shown in Figures 7.6 and 7.7 therefore yield positive values of ERP which imply expected utility rewards when combining the expected payments from both subsystems.

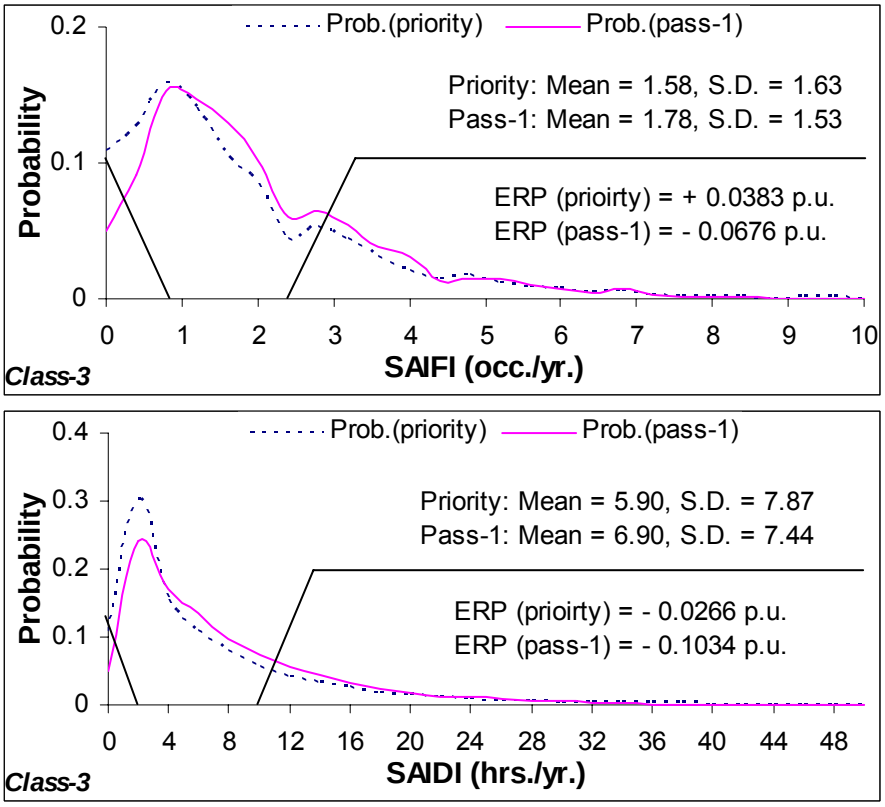

Figure 7.9: SAIFI and SAIDI distributions for the Voltage Class 3 subsystem in the IEEE-RTS obtained using two different load curtailment policies implemented in a PBR framework.

7.3 Discussion on PBR Applications for Bulk Electric Systems

The basic methodology in a PBR application to bulk electric systems is introduced in the previous section. This process will involve considerable details and negotiations between power utilities and regulators in actual situations and each situation could be quite unique. The general concepts described in the previous section are quite basic in each process. A power utility could negotiate an initial PBR which is easy for it to meet based on its operating situation. The utility could adjust its reliability

performance strategy based on its position in the PBR framework. It may want to spend less money on reliability if the operating point is less than the initial penalty point, and it may want to spend more on reliability if the operating point is a little larger than the reward commencement point [85]. A reliability assessment model is required in both cases to determine the impact of a reliability improvement and cost saving strategy. A detailed understanding of the probability distribution of the relevant reliability indices will help a power utility to effectively negotiate and manage the PBR.

It is important to note that considerable care is required to establish appropriate dead zone boundaries for both SAIFI and SAIDI. These boundaries should not unduly penalize a utility and should provide appropriate incentives for a utility to improve its reliability performance (both SAIFI and SAIDI). The imposed reward/penalty policies should therefore be carefully designed in order to encourage power utilities to maintain appropriate reliability levels. Possible PBR structure modifications can encourage utilities to move their reliability performances in the direction intended by the regulator. As noted in the previous section, the decision to use ± S.D./2 is arbitrary and the assigned dead zone width should be carefully considered by the regulator. The SAIDI reward payment for the IEEE-RTS cannot, however, reach the capped value (maximum payment) when utilizing half a standard deviation as the width of the reward transition zone, i.e. Figures 7.5, and 7.7 etc. This is due to that fact that the SAIDI distributions for bulk electric systems are considerably more dispersed than the SAIFI distributions as severe contingencies due to a single event can result in long outage durations. The regulator in this case could try to encourage the utility to improve outage durations (SAIDI) by adjusting the reward zone and making it more attractive for the utility to move in the required direction. The structure adjustments can be done in various ways. One possible approach for encouraging SAIDI improvement is illustrated in Figure 7.10.

Figure 7.10 is similar to the basic PBR framework shown in Figure 7.2. The difference is only the width of the reward transition zone. The width is reduced from S.D./2 to S.D./4, and therefore the reward slope is increased (4/S.D.). This adjusted framework will provide more incentive for the utility (IEEE-RTS in this case) to

improve its SAIDI performance. The adjusted PBR framework for the SAIDI parameter may prove to be more efficient in regard to encouraging the power utility to improve its system than the framework shown in Figure 7.2. As previously noted, establishing a PBR process will involve considerable discussion and negotiations between the utilities and regulators in actual situations. The adjustment described above is only one of many possible ways to modify the PBR framework in a particular case. The possible adjustments are system dependent, and require agreement between the regulatory agency and the power utilities concerned.

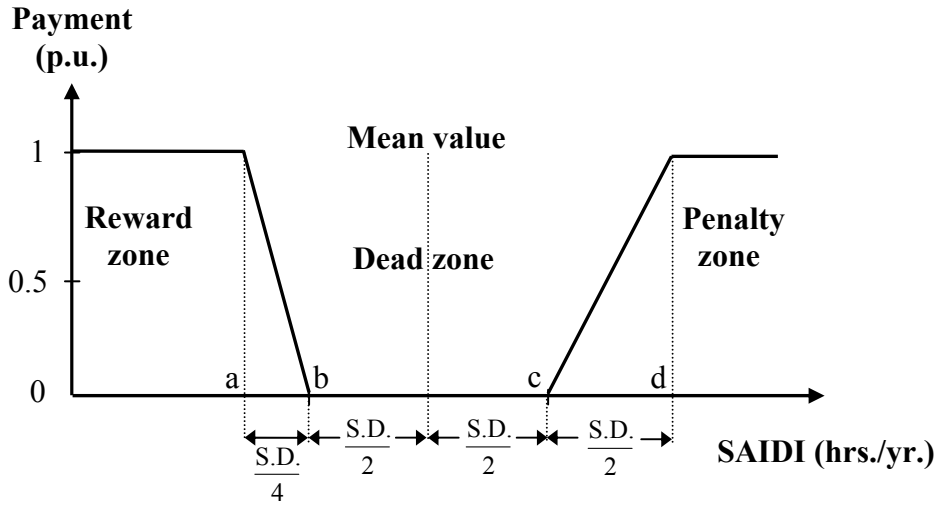

Figure 7.10: An adjusted PBR framework for SAIDI parameter.

It is worth noting that applying PBR to the reliability performance of a bulk electric system could be quite different than applying PBR to electric distribution systems. Distribution systems are basically monopoly companies, and have the responsibility to provide electric service within a designated area. This is not the case for bulk electric systems particularly in a deregulated electricity environment where conventional vertically integrated utilities are decomposed into separate commercial entities dealing with generation and transmission functions. The effect of unbundling these functions has, in some cases, made it difficult to assign specific responsibility for providing continuity of electric supply to the system customers. The question of responsibility is becoming increasingly important, as no commercial entity wants to assume responsibility or receive the blame for the actions of another. This therefore

creates a potential difficulty in directly assigning PBR frameworks for bulk electric systems.

If the bulk electric system (composite generation and transmission system) is owned by a single utility, i.e. a vertically integrated utility, the regulator can directly negotiate the PBR protocol with the utility who owns and operates all the generation and transmission facilities in the system. However, this is not likely the case in restructured electric utilities where separate generation and transmission companies own and operate their own facilities, and Independent System Operators (ISO) coordinate the activities of all these entities to ensure the reliability and security of the entire electric system. An ISO is theoretically a not-for-profit organization who does not participate in the electricity market trades nor own generation facilities for business. The ISO's activities, however, significantly impact all the power companies as well as the overall system reliability performance due to the key role it plays. Consequently, if the ISO works and operates inefficiently, the overall system reliability performance could deteriorate. On the other hand, the ISO can improve the reliability performance of the overall system if it operates efficiently. As shown in the previous section, the overall bulk electric system reliability performance can be improved by adopting appropriate operating policies such as the load curtailment philosophy. It may therefore be possible to link the ISO to the PBR framework set by the regulator. This could be quite controversial if the basic PBR protocol is applied directly to the ISO as the ISO is a not-for-profit organization and does not own generation nor transmission facilities for business, and therefore the ISO should not be penalized and faced with financial risk. In order to encourage the ISO to work efficiently, the PBR mechanism could be applied by establishing a reward zone while leaving out a penalty zone in the PBR framework or setting a penalty zone at a very low penalty payment level. In such a framework, the ISO might be motivated by the regulator to work efficiently and receive a bonus (reward payment) based on system reliability performance improvement. This could encourage the ISO to coordinate more effectively with the generation and transmission companies in the system planning, operating and design phases in order to improve the current and future system reliability performance. The above discussion presents the possibility of potential PBR mechanism

application to the ISO function. This concept will, however, require considerable study before it can be applied in practice.

Another potential utilization of a PBR protocol in bulk electric system reliability performance is to apply it directly to transmission companies (Transcos) who own and operate the regional wires. A potential PBR application to encourage the reliability performance of a transmission company has been recently proposed [88]. Reference [88] demonstrates the five year historical reliability performance indices of three transmission companies. These reliability data show the variation in the reliability performance indices from year to year, and also the variation in the reliability performance indices from one transmission company to another. The bulk electric system reliability performance indices are monitored under the Grid Code in order to develop future performance reward/penalty mechanisms for the transmission companies (Transcos). The performance index probability distribution analysis described in this thesis could prove useful in such an application. The following example is focused on the reliability performance index probability distributions of a transmission company (Transco) in a PBR framework by application to the RBTS.

Electric power systems are moving towards restructured electricity regimes by creating competition and commercialization of electric power supply among relevant participants under the transmission open access paradigm. This restructured environment results in an increased utilization of transmission networks which were not originally designed for competition and the extremely heavy utilization purposes. The trend to increased transmission network utilization continues to grow. In order to illustrate this, the original RBTS described in Section 3.6.1 has been modified in order to create a scenario where there is an increased utilization of the transmission network. The system modification is as follows:

- Add 3×20MW generating units at Bus 1.
- Add a transmission line between Buses 5 and 6 to support the single circuit at Bus 6.
- The system peak load is increased by 20%.

This modified system is designated as the modified RBTS and used as the base case. Under this system condition, the total generation is 300 MW and the system peak demand is 215.14 MW (39.4% reserve margin). The utilization of lines # 1 and 6 (L1 and L6) shown in Figure 3.2 is approximately 85% of the line rating under the modified system peak condition. Losing one of these parallel lines will create an overload on the remaining line during high load periods and could result in load curtailments. The system under this condition has an abundance of generation, but the system tends to have a transmission deficiency. The results obtained using the above modified condition are designated as the base case results.

It is assumed in this example that all the transmission facilities of the modified RBTS are owned by one transmission company (Transco), and all the generation facilities are owned by other utilities. Since the focus of this example is specifically on the transmission network, all the generating units are assumed to be 100% reliability which means that the loss of supply due to generation is excluded from the resulting reliability performance measures, and therefore only the impact of transmission contingencies is considered. Figures 7.11 and 7.12 respectively show the SAIFI and SAIDI distributions due to transmission contingencies in the modified RBTS implemented in a PBR framework. The PBR framework in this case follows the structure shown in Figure 7.2.

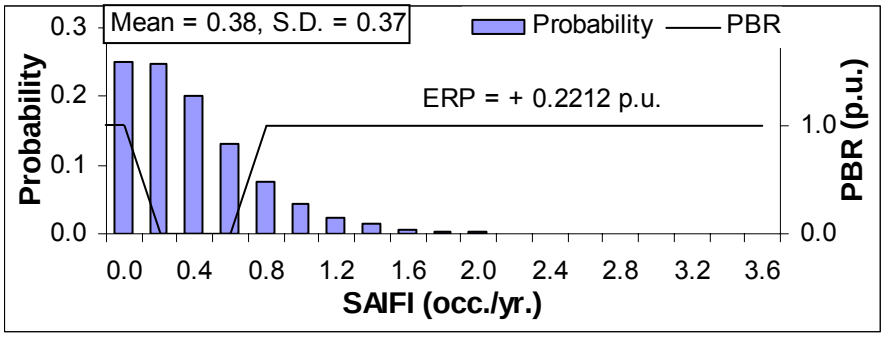

Figure 7.11: SAIFI distribution due to transmission contingencies in the modified RBTS obtained using the pass-1 policy implemented in a PBR framework.

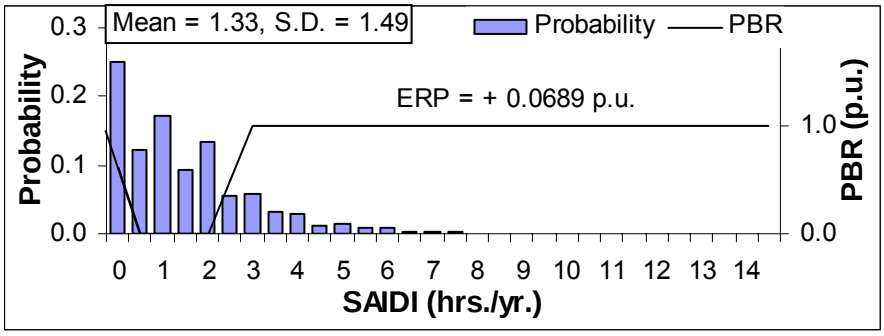

Figure 7.12: SAIDI distribution due to transmission contingencies in the modified RBTS obtained using the pass-1 policy implemented in a PBR framework.

Figures 7.11 and 7.12 indicate that the transmission company expects to receive reward payments from the regulator based on both SAIFI and SAIDI performances under the base case condition. Figures 7.13 and 7.14 respectively show the SAIFI and SAIDI distributions implemented in the PBR mechanism when the peak load increases by 5%. Figures 7.13 and 7.14 show that when the system peak load is increased by 5%, the SAIFI and SAIDI distributions change considerably. The expected SAIFI and SAIDI approximately increase by a factor of two over the base case. The resulting ERP for both SAIFI and SAIDI switch from positive values to negative values. This implies that the transmission company under this circumstance should expect penalty payments for both SAIFI and SAIDI performances. As noted earlier, the modified RBTS is transmission deficit due to the significant utilization of lines # 1 and 6. The loss of either line on this parallel circuit will lead to an overload on the remaining line and load curtailment may be required. The transmission company in this case should pursue transmission reinforcement in order to support the future load growth. Without any transmission improvement, the transmission company should expect significant penalty payments in future operation under this PBR mechanism.

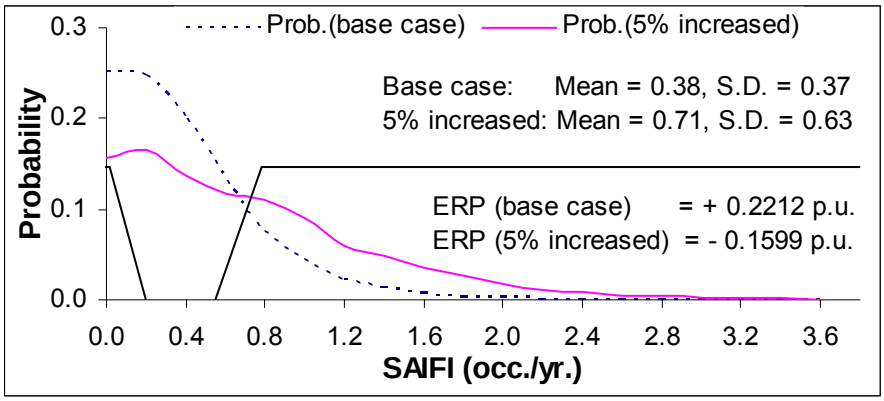

Figure 7.13: SAIFI distributions due to transmission contingencies for the two scenarios in the modified RBTS obtained using the pass-1 policy implemented in a PBR framework.

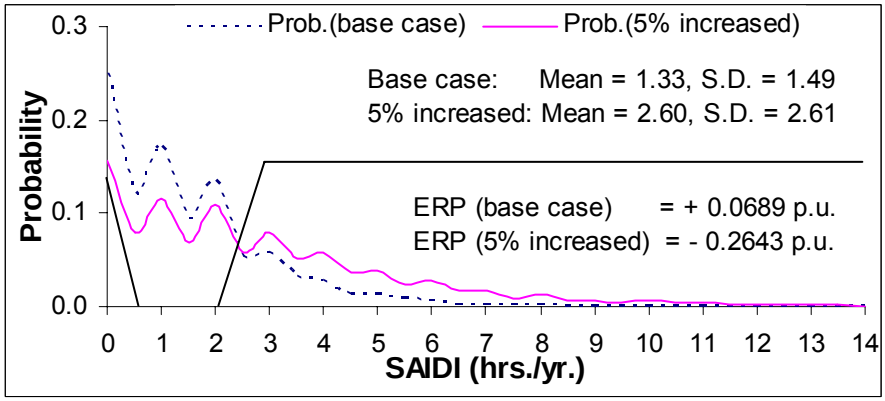

Figure 7.14: SAIDI distributions due to transmission contingencies for the two scenarios in the modified RBTS obtained using the pass-1 policy implemented in a PBR framework.

7.4 Conclusions

This chapter presents the potential utilization of bulk electric system reliability performance index probability distributions in a performance based regulation (PBR) mechanism. The concept of applying a PBR structure in a bulk electric system is discussed. The SAIFI and SAIDI for a bulk electric system are individually utilized in the PBR protocol. Reliability performance index probability distributions of bulk electric

systems tend to be more dispersed than those of electric distribution systems. The determined dead zone width in the PBR framework could therefore be quite different than that proposed for electric distribution systems. Both historical and simulated bulk electric system reliability performance indices are applied to hypothetical PBR frameworks in this chapter. The results show that power utilities may be able to adopt appropriate operating policies such as those related to load curtailment in order to improve system reliability performance and therefore receiving increased reward payments from the regulator. The potential utilization of a PBR protocol for overall bulk electric systems is presented and an example of the utilization of reliability performance index probability distributions in a PBR mechanism applied to a transmission company is demonstrated. The concept of using bulk electric system reliability performance index probability distributions in PBR applications as presented in this chapter could prove useful to power utilities in managing and controlling financial risk in the new restructured power industry.

CHAPTER 8
BULK ELECTRIC SYSTEM WELL-BEING ANALYSIS

8.1 Introduction

Bulk electric system (BES) reliability assessment can be divided into two basic aspects designated as system adequacy and system security. Bulk electric system adequacy assessment is focused on the existence of sufficient facilities within the system to satisfy the consumer load demand within the basic system operational constraints. A BES includes the facilities necessary to generate sufficient energy and the associated transmission required to transport the energy to the actual bulk supply points (distribution delivery points). Adequacy assessment of BES has been generally conducted using probabilistic techniques [2, 13, 94, 95]. Security considerations in BES are generally considered by focusing on the operation of the system in different operating conditions designated as normal, alert, emergency and extreme emergency states [44, 96, 97] as shown in Figure 8.1. A BES security assessment normally utilizes the traditional deterministic criterion known as the N-1 security criterion [6, 7] in which the loss of any BES component (a contingency) will not result in system failure. In this approach, a system is able to withstand disturbances, i.e. due to BES equipment failures, without violating any system constraints when the system is initially operating in its normal state. There are two types of security analysis: transient (dynamic) and steady-state (static). Transient stability assessment consists of determining if the system oscillations following an outage or a fault will cause loss of synchronism between generators. The objective of static security analysis as focused in this chapter is to determine whether, following the occurrence of a contingency, there exists a new steady-state secure operating point where the perturbed power system will settle after the dynamic oscillations have damped out.

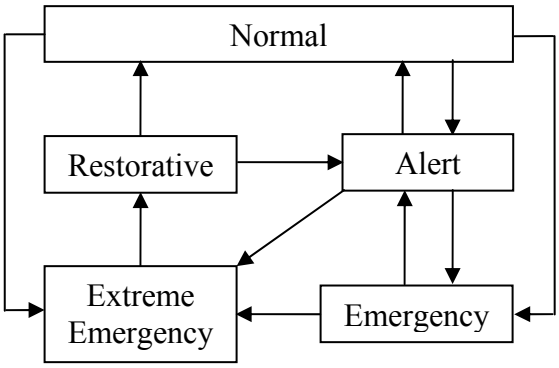

Figure 8.1: System operating states (security considerations).

Figure 8.1 shows that the overall power system can be divided into several states in terms of the degree to which the adequacy and security constraints are satisfied. The state definitions of these operating states are as follows [97].

The normal state is defined as "*In the normal state, all equipment and operation constraints are within limits, including that the generation is adequate to supply the load (total demand), with no equipment overloaded. In the normal state, there is sufficient margin such that the loss of any elements, specified by some criteria, will not result in a limit being violated. The particular criteria, such as all single elements, will depend on the planning and operating philosophy of a particular utility*". From the definition it is clear that the system is both adequate and secure in the normal state.

The alert state is defined as "*If a system enters a condition where the loss of some element covered by the operating criteria will result in a current or voltage violation, then the system is in the alert state. The alert state is similar to the normal state in that all constraints are satisfied, but there is no longer sufficient margin to withstand an outage (disturbance). The system can enter the alert state by the outage of equipment, by a change in generation schedule, or a growth in the system load*". In the alert state, the system is therefore adequate, but not secure.

The emergency state is defined as "*If a contingency occurs or the generation and load changes before corrective action can be (or is) taken, the system will enter the*

emergency state. No load is curtailed in the emergency state, but equipment or operating constraints have been violated. If control measures are not taken in time to restore the system to the alert state, the system will transfer from the emergency state to the extreme emergency state". In this state both adequacy and security constraints are violated. This is a temporary state which requires operator action because equipment operating constraints have been violated. The first objective will be to remove the equipment operating constraints without load curtailment, by such means as redispatch or startup of additional generation, voltage sources adjustment, etc. If successful, this could bring the system back to the alert state, where further actions would still be necessary to achieve the normal state.

The extreme emergency state is defined as "*In the extreme emergency state, the equipment and operating constraints are violated and load is not supplied*". In this state, load has to be curtailed in a specific manner in order to return from this state to another state.

The restorative state is defined as "*To transfer out of the extreme emergency state, the system must enter the restorative state to reconnect load and resynchronize the network. The loop can then be close by either entering the alert state or the normal state*".

The system can be returned to the normal state from the alert state by taking preventive action. Restoration from the emergency state to the alert state can be achieved by taking corrective action. The system can be returned to the restorative state from the extreme emergency state by means of emergency action. The system can return to the alert state or to the normal state from the restorative state by taking the restorative action.

The inclusion of the security considerations described above in an adequacy evaluation can overcome some of the difficulties associated with the more traditional methods. This chapter extends the concept of the BES adequacy assessment described in

Chapter 3 by incorporating steady-state security considerations. This extended adequacy assessment is designated as "security constrained adequacy analysis". This analysis is directly linked to the operation of a power system by the classification into different operating states that are dependent on the degree of adequacy and security. The system well-being approach [9, 10] is therefore based on security constrained adequacy evaluation and provides the ability to incorporate the deterministic criteria used in static security assessment into the probabilistic framework utilized in conventional adequacy evaluation.

8.2 System Well-Being Analysis Concepts

Most electric power utilities use deterministic techniques such as the traditional N-1 security criterion to assess system reliability in transmission system planning. These deterministic techniques do not provide an assessment of the actual system reliability as they do not incorporate the probabilistic or stochastic nature of the system behavior and component failures. These approaches, therefore, are not consistent [98] and do not provide an accurate basis for comparing alternative equipment configurations and performing economic analyses. In contrast, probabilistic methods can respond to the significant factors that affect the reliability of a system. These techniques provide quantitative indices, which can be used to decide if the system performance is acceptable or if changes need to be made. Most of the published papers on reliability assessment of bulk electric systems are based on probabilistic approaches [2, 13, 94, 95]. There is, however, considerable reluctance to use probabilistic techniques in many areas due to the difficulty in interpreting the resulting numerical indices. Although deterministic criteria do not consider the stochastic behavior of system components, they are easier for regulators, managers, system planners and operators to appreciate than numerical risk indices determined using probabilistic techniques. This difficulty can be alleviated by incorporating the accepted deterministic criteria in a probabilistic framework to assess the well-being of the BES. The concept of quantifying the different operating states of a power system described in [96, 97] was introduced in [44] using an analytical approach. This was extended in [99] using a Monte Carlo state sampling technique. The concepts

were further extended to large system analysis in [100] based on a non-sequential Monte Carlo simulation approach. The well-being structure shown in Figure 8.2 is a simplification of the operating state framework [44, 96, 97] previously presented in Figure 8.1 and was proposed in [9]. System well-being can be categorized into the three states of healthy, marginal and at risk as shown in Figure 8.2. In the healthy state, all equipment and operating constraints are within limits and there is sufficient margin to serve the total load demand even with the loss of any element, i.e. generator or transmission line. In the marginal state, the system is still operating within limits, but there is no longer sufficient margin to satisfy the acceptable deterministic criterion. In the at risk state, equipment or system constraints are violated and load may be curtailed.

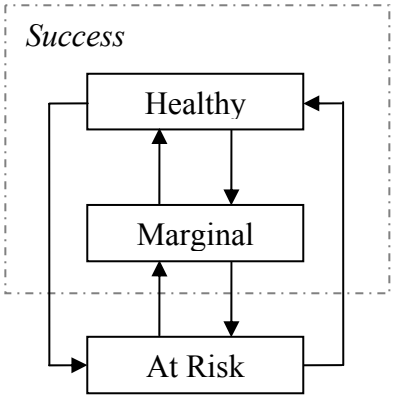

Figure 8.2: System well-being framework.

The system well-being concept shown in Figure 8.2 is a probabilistic framework incorporating the simplified operating states associated with the accepted deterministic N-1 security criterion [6, 7]. System well-being analysis, therefore, provides a combined framework that incorporates both the deterministic and probabilistic perspectives. It provides system engineers and risk managers with a quantitative interpretation of the degree of system security (N-1, healthy) and insecurity (marginal) in a bulk electric power system. Reliability indices calculated with the inclusion of appropriate deterministic criteria provide power system planners, designers, engineers and operators with additional system information. The degree of system well-being can be quantified in terms of the probabilities and frequencies of the healthy and marginal states in

addition to the traditional risk indices. This chapter is focused on system well-being analysis using sequential Monte Carlo simulation. The advantage when utilizing a sequential simulation technique, besides providing more accurate frequency and duration assessments, is the ability to create well-being index probability distributions. It is important to appreciate the inherent variability in the reliability indices and the likelihood of specific values being exceeded. This knowledge can be assessed from the probability distributions associated with the expected values.

8.3 Overall Sequential Simulation Process for System Well-Being Analysis

8.3.1 Basic Procedure of Bulk Electric System Reliability Evaluation

The procedure for well-being analysis of a composite power system is similar to the basic process used in bulk electric system reliability evaluation described in Section 3.5 and is briefly illustrated as follows:

Step 1: Specify the initial state of each component. Normally, it is assumed that all components are initially in the normal state (up state).

Step 2: Simulate the duration of each component residing in its present state using the inverse transform method and the distribution functions of the component failure and repair rates.

Step 3: Repeat step 2 in a given time span, normally a year. A chronological transition process (up and down state) for each component is then constructed in a given time span. Chronological hourly load models for individual delivery points are constructed and incorporated in the analysis.

Step 4: The simulated operation (fast decoupled AC load flow analysis) is assessed for each hour during a given time span. If operating constraints occur, corrective actions are required to alleviate the constraints and load curtailed if necessary.

Step 5: At the end of each simulated year, the delivery point and system adequacy indices are calculated and updated. Steps 2-4 are repeated until the coefficient of variation is less than the specified tolerance error.

8.3.2 System Well-Being Analysis Considerations

The procedure described in the previous section is basically the overall process for bulk electric system reliability evaluation using sequential simulation. The well-being analysis process can be implemented and extended as a sub-procedure in Step 4. The following procedures are an extension of Step 4 to include system well-being considerations.

Step 4.a: In each simulation hour, the simulation results can be categorized in the following three categories:

Category: 1. There is no system contingency, go to Step 4.b.

Category: 2. There exists system contingency(s) but no load curtailed, go to Step 4.c.

Category: 3. There exists system contingency(s) and load curtailed. If the system is in this category (Category 3), this implies that the system is in a risk state. The risk indices are update and then directly proceed to the next simulated hour.

Step 4.b: If there is no system contingency, the critical generating unit such as a largest unit is assumed to be out of service. The system is then assessed whether there is a generation constraint at that simulated hour or not. If there exists a generation constraint, update the marginal indices since this simulated hour does not meet the N-1 criterion. Otherwise, update the healthy indices and then proceed to the next simulated hour. If the system tends to be a transmission deficient system, the most critical transmission facility should be also considered in a similar process as described above for a generation constraint. (If the system contains single circuit delivery points, i.e. radial

load buses, these delivery points should be excluded in the system well-being analysis as single circuit delivery points are normally categorized as "N-1 acceptable" in an actual system. Components, i.e. radial lines, connected to these delivery points should therefore not be included in the contingency selection process of system well-being analysis when determining the marginal and healthy states. The at risk state indices for these delivery points can, however, still be quantified under Category 3 in Step 4.a.)

Step 4.c: If there is a system contingency(s) but no load curtailment, contingency selection is investigated and a contingency list is built (contingency selection is addressed in the next section.). Components in the contingency list are tested one at the time. If any selected component leads to system violations, corrective actions are required to alleviate the constraints and load is curtailed if necessary. If load is curtailed, update the marginal indices and then skip the rest of components in the contingency list and proceed to the next simulated hour. If all the components in the contingency list do not cause any load curtailment, update the healthy state and proceed to the next simulated hour.

8.3.3 Contingency Selection

The deterministic N-1 criterion is utilized for security assessment in the well-being framework analysis. The purpose of a contingency selection process is to reduce and limit the set of outaged components (contingencies) to be considered. This dramatically speeds up the simulation process of security assessment. For generation facilities, the largest generating units at different locations in the system are considered, i.e. at two or more different generator buses. For transmission facilities, the process for transmission contingency selection is as follows:

Step 1: Transmission contingency ranking is used to evaluate a scalar performance index (PI) that measures how much a particular component outage might affect

the system [42]. The PI can be measured in terms of line flows or bus voltage changes or a combination of both. This step (transmission contingency ranking) is calculated only once before starting the simulation process and the ranking results are stored for the future use.

Step 2: In each simulation hour, when there is transmission contingency(s) but no load curtailment (Step 4.c), the concept of a bounding technique [42, 101] is used in order to select the critical components to add to the contingency list. The basic concept of a bounded network is that a transmission outage tends to have a localized effect. The loss of a next transmission facility (N-1) which is located far away from the original outaged transmission facility tends to have less effect than the loss of one that is close to the original outage. Only transmission facilities that are closest to the original outaged one are added into a contingency list. An example of the bounded network technique is illustrated in Figure 8.3.

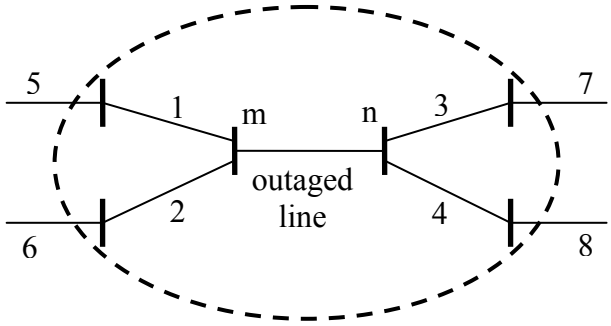

Figure 8.3: Bounded network.

In Figure 8.3, if a line outage occurs between buses *m* and *n*. Lines # 1, 2, 3 and 4 are added into the contingency list. Lines # 5, 6, 7 and 8 which are two lines away from the original outaged line are not considered. After that, transmission lines that are in a contingency list (lines # 1-4) will be ranked using the performance index (PI) obtained from Step 1. The reason in ranking these selected lines is that the computational time can be reduced when the top ranked components in the list tend to cause system problems more than the

bottom ranked components in the list. The mis-ranking of PI will not affect the result accuracy, but will only relatively affect the computation time of the simulation.

Step 3: The next step is to add the most critical transmission line based on the performance index (PI) into the list (if this critical component is not yet included in Step 2). Finally, the generation contingencies (the largest generating units at different locations selected prior) are added to the list to obtain the complete contingency selection list for a particular simulation hour.

8.4 Simulation Results

This section demonstrates system well-being results based on the reinforced RBTS and the original IEEE-RTS case studies. The load shedding philosophy used in system well-being analysis is the pass-2 policy described in Section 3.4.5, as its philosophy has an impact on delivery points in proximities of elements on outage, which are random in nature. The pass-2 policy is, therefore, to share well-being and risk among all the delivery points within the system rather than heavily curtailing loads at one particular bus while leaving some buses relatively untouched. This load curtailment policy is used throughout the research related to system well-being studies. The well-being indices are the probabilities, frequencies and durations of the healthy, marginal and risk states, and are as follows:

Prob{H} = Probability of the healthy state (/year)
Prob{M} = Probability of the marginal state (/year)
Prob{R} = Probability of the at risk state (/year)
Freq{H} = Frequency of the healthy state (occurrences/year)
Freq{M} = Frequency of the marginal state (occurrences/year)
Freq{R} = Frequency of the at risk state (occurrences/year)
Dur{H} = Average residence duration in the healthy state (hours/occurrence)
Dur{M} = Average residence duration in the marginal state (hours/occurrence)
Dur{R} = Average residence duration in the at risk state (hours/occurrence)

The residence duration of each state can be roughly calculated using the ratio of the state probability to the state frequency based on the overall simulation years. The accurate residence duration, however, should be calculated by considering it on an individual simulation year basis. The average residence duration of each state shown in this chapter is based on the individual simulation year approach.

8.4.1 Case Studies on the Reinforced RBTS

In this section, the original RBTS described in Section 3.6.1 has been reinforced by adding a transmission line (Line # 10) between Bus 5 and Bus 6 in order to support the original single circuit delivery point at Bus 6. The reinforced RBTS is designated as the R-RBTS and is shown in Figure 8.4.

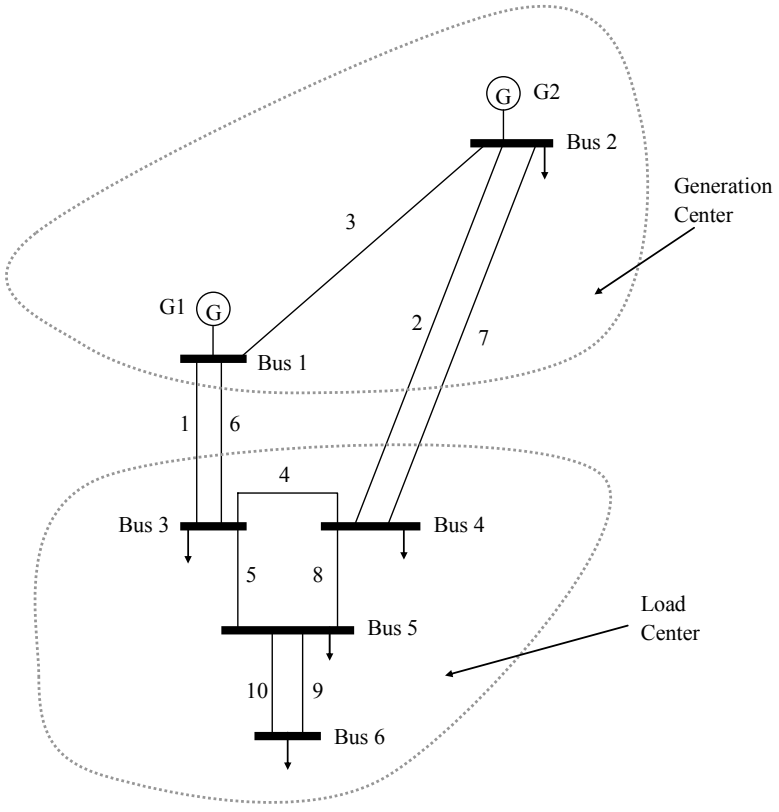

Figure 8.4: A single line diagram of the reinforced RBTS (R-RBTS).

System well-being results obtained using the R-RBTS shown in this section are based on two study scenarios. The first scenario is designated as the base case and

presents the results obtained using the reinforced RBTS configuration and the conditions described in Section 3.6.1. In the second scenario, the reinforced RBTS described in Section 3.6.1 is modified to simulate a future system condition in which 2×20MW generating units are added to Bus 1 and the load growth is 13%. A simulation period of 4,000 years was used in these studies instead of 8,000 years utilized in earlier chapters. The reason for this is that system well-being analysis using sequential simulation requires considerably more computation effort. The simulation year used in the system well-being analysis is therefore reduced to a half of the number of the simulation years used in earlier chapters. The coefficient of variation of the expected energy not supplied (EENS) based on 4,000 simulated years is less than 2.5%. The computation time used in this case for the R-RBTS is approximately 27 minutes.

A. System Base Case

Table 8.1 presents the base case well-being indices for the delivery points and for the overall R-RBTS. It is important to note that the delivery point indices are directly affected by the load curtailment philosophy used in the analysis. This effect is however relatively minor for the overall system indices [102]. The contingency selection process also directly affects the delivery point well-being indices. The main focus in system well-being analysis is on the security of the system as a whole rather than on individual delivery points as violations of a delivery point are considered to be a system security operation problem. The delivery point well-being indices, however, provide supplementary information to the overall system well-being indices.

The Prob{R} and Freq(R} respectively shown in Table 8.1 are identical to the Probability of Load Curtailment (PLC) and Expected Frequency of Load Curtailment (EFLC) used in conventional bulk electric system reliability evaluation [2, 13]. The system reliability in the base case shown in Table 8.1 is relatively high (low system risk, Prob{R}=0.000434). The degree of system well-being can be appreciated using Prob{H}. In this scenario, the degree of system well-being is relatively high (Prob{H}=0.931260). This indicates that the probability of the system residing in a state

in which the loss of any single component following random system contingencies will not result in a load curtailment condition is 93.1%. Freq{H} indicates that there are 91.59 times on average when the system leaves the healthy state and Dur{H} indicates that the system resides in the healthy state for 92.01 hours on average before departure to another state.

Table 8.1: Delivery point and overall system well-being indices for the R-RBTS (base case).

Indices	Delivery Point					Overall System
	Bus 2	Bus 3	Bus 4	Bus 5	Bus 6	
Prob{H}	0.999031	0.968715	0.938950	0.936986	0.995899	**0.931260**
Prob{M}	0.000909	0.030924	0.060758	0.063006	0.004097	**0.068307**
Prob{R}	0.000060	0.000361	0.000293	0.000008	0.000003	**0.000434**
Freq{H}	3.95	63.27	89.17	89.81	5.33	**91.59**
Freq{M}	3.98	63.77	89.65	89.83	5.34	**92.37**
Freq{R}	0.15	0.71	0.53	0.02	0.01	**0.83**
Dur{H}	3383.58	140.47	95.61	94.63	2160.93	**92.01**
Dur{M}	1.91	4.23	5.90	6.11	6.84	**6.44**
Dur{R}	3.20	4.31	4.57	3.09	3.57	**4.37**

B. System Future Case

In this scenario, the R-RBTS environment described in Section 3.6.1 in Chapter 3 has been modified to consider a situation in which 2×20MW generating units are added to Bus 1 and the load has grown by 13%. This scenario creates an increased utilization of the existing transmission network, which is a common situation under the transmission open access paradigm. Table 8.2 shows the future case well-being indices for the delivery points and for the overall R-RBTS.

Table 8.2 shows the system well-being indices for the future case where the system conditions have created increased transmission utilization compared to the base case. The R-RBTS shown in Figure 8.4 has a generation center located in the northern part of the system while the most of the system loads are located in the southern area. There are, therefore, significant power transfers from the north to the south through the

two double circuits (Lines # 1 and 6, and Lines # 2 and 7). The transmission utilization on Lines # 1 and 6 in this scenario is approximately 80% of the line ratings while that of Lines # 2 and 7 experiences approximately 50% of the line ratings during the system peak demand. The power flow on Lines # 2 and 7 is less than those on Lines # 1 and 6 as they are long transmission circuits with relatively high impedances. The loss of any one transmission line in the critical path (Lines # 1 and 6) during a high demand period could result in an overload on the remaining line.

Table 8.2: Delivery point and overall system well-being indices for the R-RBTS (future case).

Indices	**Delivery Point**					**Overall System**
	Bus 2	**Bus 3**	**Bus 4**	**Bus 5**	**Bus 6**	
Prob{H}	0.999815	0.914914	0.908233	0.900544	0.995425	**0.882243**
Prob{M}	0.000178	0.084730	0.091696	0.099427	0.004572	**0.117378**
Prob{R}	0.000007	0.000356	0.000071	0.000028	0.000002	**0.000380**
Freq{H}	1.06	137.79	152.32	156.37	7.31	**146.18**
Freq{M}	1.07	137.67	152.42	156.42	7.31	**147.09**
Freq{R}	0.02	1.02	0.17	0.08	0.01	**1.08**
Dur{H}	6182.71	59.84	53.73	51.90	1541.53	**54.29**
Dur{M}	1.36	5.38	5.26	5.56	5.60	**6.98**
Dur{R}	2.61	3.06	3.44	3.11	3.80	**3.07**

Table 8.2 indicates that even though the system risk under the future scenario (Prob{R} = 0.000380) is lower than that of the base case shown in Table 1 (Prob{R} = 0.000434), the Prob{M} for the future scenario is considerably higher, which indicates the potential of the system moving from the marginal state to the at risk state in the near future. The Prob{H} is, therefore, relatively low under the future system condition. The acceptable healthy state probability level is dependent on the management philosophy, which can vary from one system to another. The results shown in Table 8.2 illustrate an example of a system with a future scenario in which the system reliability is maintained (even lower risk compared to the base case), but with an increased system stress level (high marginal probability) as more of the contingencies that resided in the healthy state for the base case move to the marginal state for the future scenario. A knowledge of contingency movements, particularly when they move from healthy to marginal, is very

important and are not identified using traditional probabilistic reliability assessment (risk indices) until they actually move into the at-risk region when they suddenly have a severe effect. The outcome is not easily identified if only at-risk states are considered since the at-risk probabilities do not change to any significant degree [10]. The well-being approach, therefore, attempts to bridge the gap between the deterministic and probabilistic approaches by addressing the need to determine the likelihood of encountering marginal system states as well as that of encountering system at-risk states. The system well-being concept provides a comprehensive knowledge of specific system conditions, and additional information on what the degree of the system vulnerability might be under a particular system condition.

C. System Well-Being Index Probability Distributions

The results shown in the previous sections are based on the average or expected values of the well-being indices. One advantage when utilizing sequential Monte Carlo simulation in system well-being analysis is the ability to provide system well-being index probability distributions associated with their expected values. The system well-being index probability distributions, which provide a pictorial representation of the annual variability of the indices, are illustrated in this section. The overall system well-being indices obtained using the two scenarios presented in Tables 8.1 and 8.2 are graphically presented in Figure 8.5 accompanied by the expected or average (avg.) values and the standard deviations (S.D.). Reliability index probability distributions are normally created as frequency histograms using discrete intervals (bins). The probability distributions shown in this chapter are, however, presented using approximate continuous distributions for illustration purposes rather than histograms. The use of smooth curves in representing the probability distributions facilitates comparisons of the various scenario results on the same axis.

Figure 8.5 shows that the distributions of the healthy and marginal state indices (probability, frequency and duration) tend to have normal distribution characteristics for both the base case and future scenarios. The distributions of the at risk indices, however,

have exponential trends due to the fact that the system reliability under these two scenarios is relatively high (low system risk). Figure 8.5 also shows that the well-being index probability distributions (probability and frequency) of the less healthy system condition (future scenario) have more dispersion and therefore more uncertainty with lower predicted probability of occurrence compared to those of the base case. The probability distribution of the residence duration in the healthy state for the less healthy system (future scenario) is, however, less dispersed with shorter residence times than that for the base case. Operating a system in such an environment (less healthy) will, therefore, make it more difficult for system engineers to manage the potential system risk with a high degree of confidence.

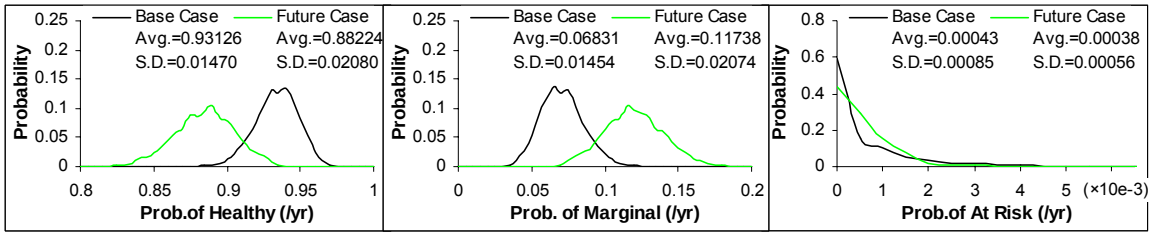

Probabilities of healthy, marginal and at risk states

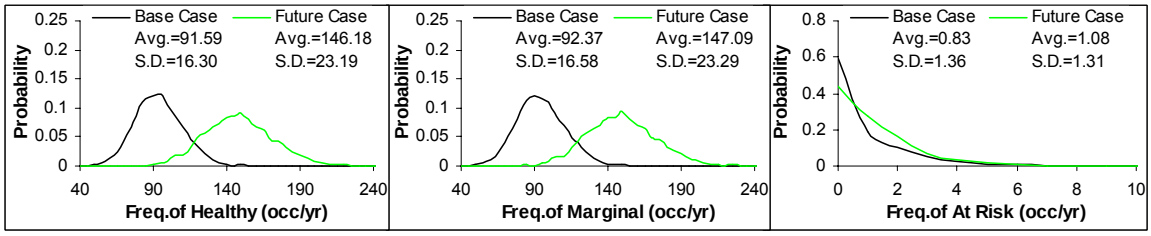

Frequencies of healthy, marginal and at risk states

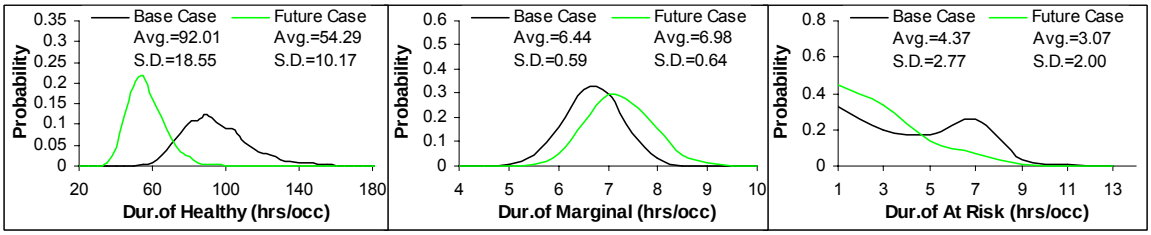

Residence durations in healthy, marginal and at risk states

Figure 8.5: System well-being index probability distributions of the R-RBTS for the base case and future scenarios.

8.4.2 Case Studies on the IEEE-RTS

In this section, the original IEEE-RTS described in Section 3.6.2 is used in the system well-being studies. System well-being results obtained using the IEEE-RTS shown in this section are also based on two study scenarios. The first scenario is designated as the base case and presents the results obtained using the original IEEE-RTS described in Section 3.6.2. In the second scenario, the original IEEE-RTS described in Section 3.6.2 is modified to simulate a future system condition with a 4% load growth compared to the original peak load condition. A simulation period of 3,000 years was used in these studies instead of 6,000 years utilized for the IEEE-RTS in earlier chapters due to the considerable computation expensive associated with well-being analysis. The coefficient of variation of the expected energy not supplied (EENS) based on 3,000 simulated years is less than 2.5%. The computation time used in this case for the IEEE-RTS is approximately 1315 minutes. Tables 8.3 – 8.5 respectively show the delivery point and overall system well-being probabilities, frequencies and residence durations of the two scenarios for the IEEE-RTS.

Table 8.3: Delivery point and system well-being probabilities for the IEEE-RTS.

Delivery Point	Base Case (1.00 p.u. load)			Future Case (1.04 p.u. load)		
	Prob{H} (/yr)	Prob{M} (/yr)	Prob{R} (/yr)	Prob{H} (/yr)	Prob{M} (/yr)	Prob{R} (/yr)
1	0.99872	0.00118	0.00011	0.99827	0.00146	0.00027
2	0.99762	0.00215	0.00023	0.99596	0.00345	0.00060
3	0.99636	0.00343	0.00021	0.99447	0.00499	0.00054
4	0.99622	0.00356	0.00022	0.99446	0.00501	0.00053
5	0.99568	0.00403	0.00029	0.99305	0.00625	0.00069
6	0.99483	0.00482	0.00035	0.99187	0.00731	0.00082
7	0.99431	0.00546	0.00023	0.99299	0.00651	0.00050
8	0.99656	0.00308	0.00035	0.99439	0.00487	0.00074
9	0.99743	0.00246	0.00011	0.99693	0.00280	0.00026
10	0.99634	0.00345	0.00020	0.99485	0.00465	0.00050
13	0.99294	0.00613	0.00093	0.98965	0.00849	0.00186
14	0.99882	0.00113	0.00004	0.99867	0.00123	0.00010
15	0.99700	0.00263	0.00037	0.99495	0.00423	0.00083
16	0.99515	0.00425	0.00061	0.99208	0.00663	0.00130
18	0.95423	0.04274	0.00303	0.92805	0.06633	0.00562
19	0.99529	0.00417	0.00055	0.99307	0.00575	0.00118
20	0.99838	0.00141	0.00021	0.99757	0.00181	0.00062
System	**0.94784**	**0.04804**	**0.00412**	**0.91970**	**0.07212**	**0.00818**

Table 8.3 shows that some of the Prob{H} in the base case transfers to Prob{M} or even Prob{R}, and some of the Prob{M} in the base case transfers to the Prob{R} when the peak load increases by 4% in the future scenario. Table 8.3 indicates that most of the delivery points in the base case are very healthy as the Prob{H}of all the delivery points with the exception of DP18 are considerably higher than 0.99. The Prob{H} of DP18 is, however, only 0.95423 which drives the Prob{H} of the overall system to 0.94784. As noted earlier, DP18 is attached to many elements including a 400 MW generating unit at the bus and another 400 MW generating unit at a neighboring bus. There are also no other load buses in close proximity of DP18. System constraints that occur in this area and result in load curtailments will therefore create interruptions at this load bus. The basic focus in system well-being analysis is on the security of the system as a whole rather than on individual delivery points, as violations of a delivery point are considered to be a system security operating problem. The delivery point well-being indices, in this case, provide supplementary information to the overall system well-being indices under a particular operating strategy and the location of critical components. It is interesting to note that although the Prob{R} for the R-RBTS base case shown in Table 8.1 is approximately 10 times smaller (higher reliability) than that of the IEEE-RTS base case shown in Table 8.3, the Prob{M} of the R-RBTS base case is larger than that of the IEEE-RTS base case. This implies that the R-RBTS base case has a higher degree of system stress (marginal state) compared to the IEEE-RTS base case even though it has a lower degree of system risk.

Table 8.4 shows the well-being frequencies for the IEEE-RTS under the two scenarios. The results indicate that when the peak load increases by 4% (future case), there are considerably more movements from one state to another than occur under the base case condition. Table 8.5 shows the well-being residence durations for the IEEE-RTS with the two scenarios. The results indicate that when the peak load increases by 4% (future case), the system resides in the healthy state for shorter periods while spending more time in the marginal and risk states.

Table 8.4: Delivery point and system well-being frequencies for the IEEE-RTS.

Delivery Point	Base Case (1.00 p.u. load)			Future Case (1.04 p.u. load)		
	Freq{H} (occ/yr)	Freq{M} (occ/yr)	Freq{R} (occ/yr)	Freq{H} (occ/yr)	Freq{M} (occ/yr)	Freq{R} (occ/yr)
1	4.02	3.90	0.29	5.99	5.70	0.73
2	7.42	7.23	0.62	13.83	13.53	1.63
3	7.13	7.02	0.61	12.77	12.63	1.37
4	7.38	7.27	0.60	13.02	12.83	1.36
5	9.24	9.16	0.80	15.55	15.53	1.69
6	10.89	10.84	0.95	17.40	17.47	1.93
7	13.70	13.81	0.62	16.34	16.59	1.15
8	8.29	8.32	0.86	11.22	11.43	1.64
9	4.66	4.47	0.29	6.22	5.95	0.68
10	8.17	8.15	0.53	13.31	13.02	1.32
13	14.48	15.00	2.03	20.77	21.37	4.27
14	2.01	2.05	0.11	2.51	2.53	0.27
15	7.52	7.57	0.94	12.05	11.99	1.99
16	11.27	11.48	1.51	17.08	17.33	3.01
18	90.27	92.97	6.37	120.07	125.32	10.10
19	9.24	9.57	1.33	13.54	13.70	2.76
20	4.75	4.73	0.75	6.90	6.54	1.49
System	**89.67**	**93.99**	**9.24**	**120.18**	**129.03**	**15.99**

Table 8.5: Delivery point and system well-being residence durations for the IEEE-RTS.

Delivery Point	Base Case (1.00 p.u. load)			Future Case (1.04 p.u. load)		
	Dur{H} (hrs/occ)	Dur{M} (hrs/occ)	Dur{R} (hrs/occ)	Dur{H} (hrs/occ)	Dur{M} (hrs/occ)	Dur{R} (hrs/occ)
1	3897.19	2.34	3.00	2846.30	2.06	3.01
2	2230.01	2.60	3.00	988.58	2.22	2.96
3	2217.30	3.53	2.97	1046.57	3.06	3.28
4	1973.66	3.87	2.98	999.74	3.19	3.12
5	1544.26	3.50	3.03	780.78	3.34	3.43
6	1266.43	3.73	3.03	688.75	3.55	3.44
7	1043.63	3.44	3.01	803.94	3.40	3.60
8	1671.97	3.27	3.49	1190.86	3.75	3.73
9	3112.65	4.17	3.16	2323.99	3.60	3.07
10	1721.78	3.74	3.09	929.64	3.10	3.07
13	871.73	3.61	3.74	534.60	3.48	3.55
14	4931.50	4.99	2.82	4539.09	4.36	2.71
15	1918.60	3.00	3.19	1081.18	3.05	3.45
16	1170.54	3.25	3.31	669.70	3.34	3.54
18	101.71	4.02	3.93	71.96	4.64	4.55
19	1441.26	3.80	3.38	872.22	3.66	3.52
20	3065.74	2.84	2.41	2122.98	2.48	3.52
System	**99.97**	**4.42**	**3.66**	**70.35**	**4.86**	**4.25**

The results shown in Tables 8.3 – 8.5 are the average or expected values of the well-being indices. The overall system well-being index probability distributions for the two scenarios are graphically presented in Figure 8.6 together with the expected or average (avg.) values and the standard deviations (S.D.). Figure 8.6 shows that the distributions of the healthy and marginal state indices (probability, frequency and duration) tend to have normal distribution characteristics for both the base case and future scenarios. The distributions of the at risk indices are, however, different from the general exponential forms shown in Figure 8.5 for the R-RBTS. The reason for this is that the IEEE-RTS is basically less reliability than the R-RBTS and the resulting distributions move further away from the ordinate axis. In general, the system well-being index probability distribution characteristics for the healthy and marginal states

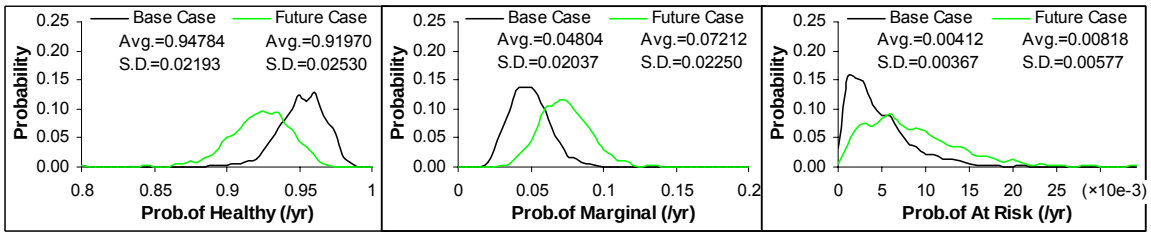

Probabilities of healthy, marginal and at risk states

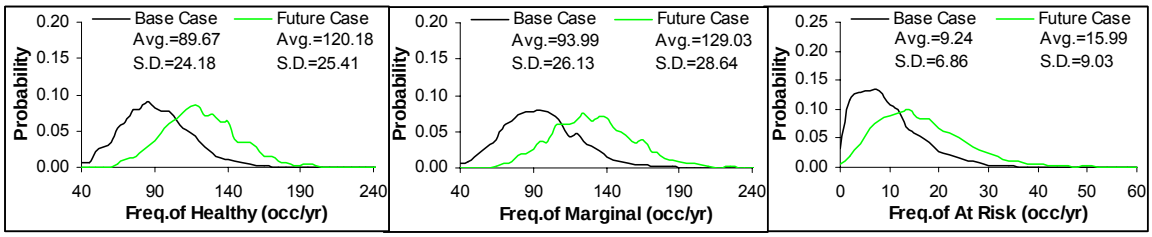

Frequencies of healthy, marginal and at risk states

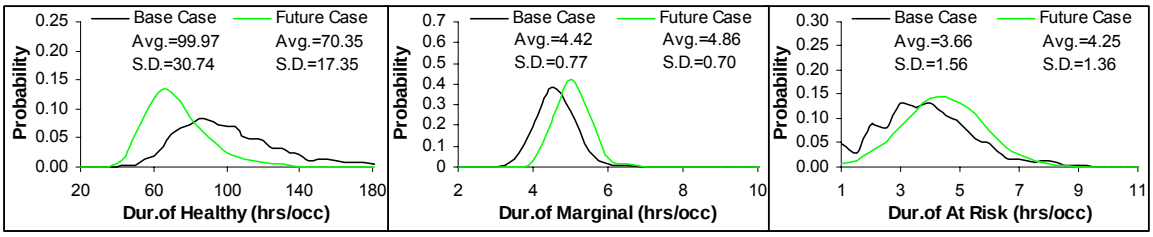

Residence durations in healthy, marginal and at risk states

Figure 8.6: System well-being index probability distributions of the IEEE-RTS for the base case and future scenarios.

shown in Figures 8.5 and 8.6 are quite similar in form. The distributions (probability and frequency) of the less healthy system condition (future scenario) have more dispersion and therefore more uncertainty with lower predicted probability of occurrence than those of the base case. The probability distribution of the residence duration in the healthy state for the less healthy system (future scenario) is, however, less dispersed with shorter residence times than that of the base case.

8.5 Conclusions

There is growing interest in combining deterministic considerations with probabilistic assessment in order to evaluate the "system well-being" of a composite generation and transmission system and to evaluate the likelihood, not only of entering a complete failure state, but also the likelihood of being very close to trouble. Bulk electric system well-being analysis using sequential Monte Carlo simulation is presented in this chapter. The overall simulation procedure incorporating system well-being considerations and the associated contingency selection process is described. The system well-being concept provides a probabilistic framework that incorporates a practical simplification of the traditional operating states associated with the accepted deterministic N-1 security criterion. Well-being analysis, therefore, provides a combined framework that incorporates both deterministic and probabilistic perspectives by determining the likelihood of encountering marginal system states as well as encountering system at risk states. One advantage when utilizing a sequential simulation technique, besides providing accurate frequency and duration assessments, is the ability to create well-being index probability distributions. The well-being concept is illustrated in this chapter by application to the reinforced RBTS and the IEEE-RTS. The analyses indicate that different system conditions that result in a similar degree of system risk may not necessarily have the same degree of system stress (marginal state). The system well-being concept provides system engineers and risk managers with comprehensive information on the degree of system vulnerability under a particular system scenario.

CHAPTER 9
COMBINED BULK ELECTRIC SYSTEM RELIABILITY FRAMEWORK USING ADEQUACY AND STATIC SECURITY INDICES

9.1 Introduction

As previously noted in Chapter 1, bulk electric system (BES) reliability assessment can be divided into the two basic aspects of system adequacy and system security. The basic concepts and some results on bulk electric system adequacy assessment are presented in Chapters 3 – 6. The inclusion of static security aspects in traditional adequacy evaluation is presented in the previous chapter in the form of system well-being analysis that incorporates the deterministic N-1 security criterion. This analysis offers a quantitative interpretation of the degree of system security (N-1, healthy) and insecurity (marginal) in a bulk electric power system in terms of probabilities, frequencies and state residence durations. The degree of severity due to system failure is not determined by the basic probability and frequency indices obtained using system well-being analysis. In contrast, traditional system adequacy assessment does not include a quantitative evaluation of the degree of system security, but estimates the system severity in physical and monetary terms. A combined reliability framework considering both adequacy and static security perspectives is presented in this chapter. This is achieved using a combination of reliability indices obtained using both conventional adequacy assessment and system well-being analysis.

9.2 Selected Indices for the Overall BES Reliability Framework

There is a wide range of bulk electric system reliability indices. Although all the reliability indices have their own purpose and usefulness, presenting them all in an overall framework involves a voluminous set, particularly when considering both adequacy and static security aspects. A compact or focused combined framework can be created by selecting distinctive reliability indices. The selected reliability indices should collectively provide an effective overall assessment of the system reliability. It is important to emphasize that bulk electric system reliability indices associated with the at risk state in system well-being analysis (static security assessment) are identical to the predictive reliability indices related to load curtailment in adequacy assessment. These relationships are as follows:

- The probability of the at risk state is equivalent to the Probability of Load Curtailment (Prob{R} = PLC).
- The frequency of the at risk state is equivalent to the Expected Frequency of Load Curtailment (Freq{R} = EFLC).

In system well-being analysis, the probabilities and frequencies of healthy and marginal states are distinctive and provide additional information from a security perspective that complements the predictive indices obtained in an adequacy assessment. The probability and frequency of the at risk state are also adequacy indices as noted above. The probabilities and frequencies of the healthy, marginal and at risk states provide a security perspective in the overall framework. The notations of these indices are as follows:

Prob{H} = Probability of the healthy state (/year)
Prob{M} = Probability of the marginal state (/year)
Prob{R} = Probability of the at risk state (/year)
Freq{H} = Frequency of the healthy state (occurrences/year)
Freq{M} = Frequency of the marginal state (occurrences/year)
Freq{R} = Frequency of the at risk state (occurrences/year)

The security indices shown above indicate the system reliability in the form of probabilities and frequencies. The magnitude or severity associated with the system at risk state is not recognized. This information can be provided by conventional adequacy assessment indices such as the delivery point unavailability index (DPUI), the expected energy not supplied (EENS) and the expected customer interruption cost (ECOST). The DPUI is a severity index that can be used to compare systems of different sizes. The EENS estimates the supply unreliability in terms of energy curtailments and the ECOST indicates the expected customer monetary losses due to electric supply interruptions. These three reliability indices complement the security indices noted earlier. There is a direct relationship between the DPUI and the EENS, as the DPUI is the ratio of the EENS to the system peak load. The utilization of DPUI associated with the system peak load therefore includes an appreciation of the EENS. The DPUI can also be used to compare the system severity with that of other bulk electric systems. The reliability indices selected to estimate the severity of system failure based on an adequacy perspective are as follows:

DPUI = Delivery point unreliability index (system·minutes)
ECOST = Expected customer interruption cost (dollars/year)

These two adequacy indices together with the six security indices described earlier provide a sufficient and effective overall framework that includes both adequacy and static security considerations. Prob{R}, Freq{R}, DPUI and ECOST are designated as adequacy indices and Prob{H}, Prob{M}, Freq{H} and Freq{M} are designated as security indices in the analyses presented in this chapter.

The effectiveness of the proposed overall framework for bulk electric system reliability analysis considering both adequacy and static security are examined and illustrated by application to several practical case studies involving different systems and conditions. The case studies are presented in the following sections using two basic scenarios. The first scenario is focused on bulk electric systems with generation deficiencies. The second scenario is focused on bulk systems with transmission deficiencies. The reinforced RBTS and the IEEE-RTS are used as test systems.

9.3 Case Studies on Generation Deficient Systems

Generation deficient environments were created in both the reinforced RBTS and the original IEEE-RTS by increasing the load in each system.

9.3.1 The Reinforced RBTS (R-RBTS)

The R-RBTS is illustrated in Figure 8.4 in the previous chapter. In this system, a transmission line has been added between Bus 5 and Bus 6 in order to support the single circuit delivery point at Bus 6. This system, therefore, has a relatively strong transmission network. The total generation is 240 MW and the original system peak load is 179.28 MW. The combined system reliability indices considering both adequacy and security for the R-RBTS associated with different system peak demands are shown in Table 9.1. The results shown in Tables 9.1 are based on 4,000 simulation years and have a coefficient of variation of EENS that is less than 2.5%. The load shedding philosophy used throughout this chapter is the pass-2 policy.

Table 9.1 shows that the system reliability indices gradually degrade as the system peak load progressively increases. When the system peak load is greater than 197.21 MW, the generation is not able to meet the demand when the largest generating unit (40MW unit) is on outage. It is important to note that the system peak demand shown in Table 9.1 excludes transmission losses. The transmission loss in the R-RBTS is in the range of 3 – 4%. The total system demand (load + loss) for the 197.21 MW peak load is therefore slightly in excess of 200 MW. The DPUI increases significantly when the system load grows beyond this level. This observation is also applicable to the frequency indices such as Freq{H}, Freq{M} and Freq{R}. The Prob{H}, however, behaves in a somewhat different manner, as it gradually decreases as the load grows. The Prob{H} does not dramatically decrease under the condition when the N-1 security criterion (an outage of the largest generating unit) is violated (at the peak load). Security indices such as Prob{H} and Prob{M} are less sensitive than adequacy indices such as DPUI in a generation deficient environment. The utilization of Prob{H} as a single

security index does not provide a valid indicator of the overall system well-being and should be used in conjunction with the other indices. The results based on a combined reliability framework indicate that the adequacy indices tend to be more adversely affected in a generation deficient environment than the security indices.

Table 9.1: Overall system reliability indices (adequacy and security) of the reinforced RBTS for various system peak demands.

System Indices	System peak load demand in MW							
	179.28 MW	182.87 MW	186.45 MW	190.04 MW	193.62 MW	197.21 MW	200.79 MW	204.38 MW
Prob{H} (/yr)	0.93126	0.92369	0.91747	0.91261	0.90899	0.90579	0.89879	0.88592
Prob{M} (/yr)	0.06831	0.07574	0.08177	0.08637	0.08964	0.09239	0.09896	0.11103
Prob{R} (/yr)	0.00043	0.00057	0.00076	0.00102	0.00137	0.00182	0.00225	0.00305
Freq{H} (occ/yr)	91.59	93.89	98.69	101.43	104.98	108.74	145.55	195.54
Freq{M} (occ/yr)	92.37	94.96	100.27	103.54	107.73	111.90	149.49	202.54
Freq{R} (occ/yr)	0.83	1.15	1.68	2.24	2.91	3.37	4.23	7.44
DPUI (sys.mins)	15.61	21.25	28.80	38.75	51.91	69.12	88.92	116.32
ECOST (M$/yr)	0.195	0.263	0.358	0.484	0.651	0.872	1.120	1.454

9.3.2 The Original IEEE-RTS

The original IEEE-RTS described in Section 3.6.2 is used in this study. The total generation is 3405 MW and the system peak load is 2754.75 MW. The original IEEE-RTS has a very strong transmission network and a weak generation system. The combined system reliability indices considering both adequacy and security for the original IEEE-RTS with different system peak demands are shown in Table 9.2. The results are based on 3,000 simulation years and have a coefficient of variation of EENS that is less than 2.5%. The load shedding philosophy is based on the pass-2 policy.

Table 9.2 shows that the overall system reliability indices degrade as the system peak load progressively increases. As discussed earlier, the system peak demand levels shown exclude transmission losses. The total system consumption in each case is therefore slightly higher than that shown in Table 9.2. In a similar manner to the results shown in Table 9.1, the adequacy indices of DPUI and ECOST increase dramatically at the high peak loads while the security indices of Prob{H} and Prob{M} gradually

deteriorate. Generation deficiencies have a significant adverse effect on the system adequacy indices as the severity of supply interruptions increase rapidly as the system peak load increases. Generation deficient environments, however, tend to have relatively less effect on the system security indices than on the system adequacy indices. Case studies on transmission deficient environments are examined in the following section.

Table 9.2: Overall system reliability indices (adequacy and security) of the original IEEE-RTS for various system peak demands.

System Indices	System peak load demand in MW				
	2699.66 MW	2754.75 MW	2809.85 MW	2864.94 MW	2920.04 MW
Prob{H} (/yr)	0.95888	0.94784	0.93406	0.91970	0.90381
Prob{M} (/yr)	0.03831	0.04804	0.06002	0.07212	0.08522
Prob{R} (/yr)	0.00280	0.00412	0.00592	0.00818	0.01097
Freq{H} (occ/yr)	72.22	89.67	102.91	120.18	145.46
Freq{M} (occ/yr)	75.88	93.99	109.10	129.03	156.30
Freq{R} (occ/yr)	6.55	9.24	12.09	15.99	21.85
DPUI (sys.mins)	66.23	98.39	144.17	207.24	290.97
ECOST (M$/yr)	14.430	21.517	31.622	45.582	64.221

9.4 Case Studies on Transmission Deficient Systems

As previously noted, electric power systems are moving towards restructured regimes by creating competition and commercialization of power supply among the relevant participants under a transmission open access paradigm. This restructured environment results in an increased utilization of transmission networks which were not originally designed for competition and heavy utilization. The case studies presented in this section are focused on heavily utilized transmission conditions in order to examine these impacts on both the adequacy and security indices. The system reliability behavior in the transmission deficient cases is compared with that under the generation deficient environments described in the previous section. The R-RBTS and IEEE-RTS are modified to provide increased utilization of the system transmission facilities.

9.4.1 The Modified R-RBTS

The reinforced RBTS (R-RBTS) used in the previous section and shown in Figure 8.4 in Chapter 8 has been modified as follows:

- Add 3×20MW generating units at Bus 1.
- Increase the system peak load by 20% (from 179.28 MW to 215.14 MW).

This modified system is designated as the modified R-RBTS (MR-RBTS) in this chapter. In this system, the total generation is 300 MW and the system peak demand is 215.14 MW (39.4% reserve margin). The utilization of Lines # 1 and 6 is approximately 85% of the line rating for the system peak condition. Losing one of these parallel lines will create an overload on the remaining line during high load periods and may result in load curtailments. The system under this condition has an abundance of generation, but tends to be transmission deficient.

The combined delivery point and system reliability indices considering both adequacy and security for the MR-RBTS are shown in Table 9.3. The load shedding philosophy used is the pass-2 policy, and the coefficient of variation of EENS is less than 2.5% for 4,000 simulation years. As previously noted, the delivery point indices are influenced by the load curtailment philosophy used and the contingency selection process employed. The main focus is on the security of the system as a whole rather than on the individual delivery points, as violations of a delivery point are considered to be a system security operating problem. The delivery point indices, however, provide supplementary information to the overall system well-being indices, and are useful when selecting system reinforcements for specific areas.

Table 9.3 indicates that the system under this condition has an acceptable probability of the at risk state (Prob{R} = 0.00079) and an acceptable DPUI (19.97 sys.mins). The Prob{M} is, however, quite high, which indicates the potential for the system to encounter the at risk state. The Prob{H} is relatively low under this system

condition. The acceptable healthy probability level for a given system is one component in its reliability criteria and can vary from one system to another. The results shown in Table 9.3 illustrate an example of a system that satisfies the adequacy criteria, but has considerable potential risk (high Prob{M}) for system security problems. This illustrates that security indices are adversely affected in a transmission deficient environment more than are the adequacy indices.

Table 9.3: Overall delivery point and system reliability indices (adequacy and security) of the MR-RBTS.

Bus No.	Prob{H} (/yr)	Prob{M} (/yr)	Prob{R} (/yr)	Freq{H} (occ/yr)	Freq{M} (occ/yr)	Freq{R} (occ/yr)	DPUI (sys.mins)	ECOST (k$/yr)
2	0.99975	0.00024	0.000005	1.69	1.73	0.02	--	0.865
3	0.89733	0.10190	0.000768	158.47	158.13	1.75	--	160.912
4	0.90336	0.09656	0.000069	211.21	211.34	0.19	--	28.032
5	0.88756	0.11236	0.000080	196.96	197.08	0.30	--	11.632
6	0.99535	0.00464	0.000004	8.98	8.98	0.01	--	0.545
Sys.	**0.86200**	**0.13721**	**0.00079**	**172.01**	**173.36**	**1.80**	**19.97**	**201.986**

Table 9.4 shows the Prob{H} and DPUI for the R-RBTS at the peak load of 204.38 MW as presented in Table 9.1 and the MR-RBTS results previously illustrated in Table 9.3. The R-RBTS is in a generation deficient condition but its Prob{H} is higher than the Prob{H} of the MR-RBTS which is in a transmission deficient condition. The DPUI of the R-RBTS is, however, considerably higher than that of the MR-RBTS. This indicates that two systems with similar degrees of system security can have quite different levels of system adequacy. This situation can also occur in reverse, as two systems can have similar adequacy indices and quite different levels of security.

Table 9.4: Comparisons of the Prob{H} and DPUI for the R-RBTS at the 204.38 MW peak load and for the MR-RBTS.

System	Prob{H} (/yr)	DPUI (sys.mins)
R-RBTS	0.88592	116.32
MR-RBTS	0.86200	19.97

9.4.2 The Modified IEEE-RTS

The original IEEE-RTS described in Section 3.6.2 is modified as follows:

- The load levels of all the delivery points are increased to 1.5 p.u. of the original values. The peak load for the modified system is 1.5×2,850 = 4,275 MW. (When considering the coincidence of the chronological loads at all the buses, the actual system peak load is 4,132.13 MW.)
- The generation at the five following generator buses is doubled: Buses 16, 18, 21, 22 and 23 (12 generating unit additions). The total number of generating units in the modified system is 32+12 = 44 units with a total system capacity of 3,405+1,915 = 5,320 MW.
- The line rating of Line # 10 (an underground cable between Buses 6 and 10) is increased to 1.5 p.u. of the original rating.
- The capacities of the synchronous condenser at Bus 14 and the reactor at Bus 6 are increased to 1.5 p.u. of the original capacities.

There is significant transmission utilization in the modified IEEE-RTS as a considerable amount of power is transferred from the north to the southern system. Even though the overall system reserve margin is 24%, the southern part (138 kV) of the modified system has both generation and transmission deficiencies. Both the northern and southern areas have transmission constraints. The system under this condition is similar to many current systems in which electricity competition has resulted in increased numbers of independent power producers and heavy increases in transmission utilization.

The overall delivery point and system reliability indices considering both adequacy and security are shown in Table 9.5. The load shedding philosophy used is the pass-2 policy similar to that used for previous cases, and the coefficient of variation of EENS is less than 5% with 3,000 simulation years. The delivery point indices shown in Table 9.5 provide supplementary information to the overall system indices, and are useful in system reinforcement planning. This issue is addressed later.

Table 9.5: Overall delivery point and system reliability indices (adequacy and security) for the modified IEEE-RTS.

Bus No.	Prob{H} (/yr)	Prob{M} (/yr)	Prob{R} (/yr)	Freq{H} (occ/yr)	Freq{M} (occ/yr)	Freq{R} (occ/yr)	DPUI (sys.mins)	ECOST (M$/yr)
1	0.98795	0.01198	0.00007	65.06	65.60	0.39	--	0.020
2	0.98890	0.01102	0.00008	55.73	53.59	0.35	--	0.044
3	0.96296	0.03670	0.00034	76.13	76.30	0.90	--	0.859
4	0.95635	0.04320	0.00044	113.12	113.26	1.07	--	0.774
5	0.93537	0.06436	0.00027	171.42	171.23	0.83	--	0.428
6	0.90084	0.09876	0.00040	206.12	206.02	1.14	--	0.828
7	0.98988	0.01002	0.00010	56.25	55.85	0.55	--	0.041
8	0.94524	0.05440	0.00036	151.16	150.88	0.99	--	1.043
9	0.97941	0.02019	0.00040	58.26	57.63	0.87	--	0.621
10	0.85015	0.14957	0.00028	246.61	246.72	0.81	--	0.642
13	0.99669	0.00317	0.00014	15.72	15.86	0.45	--	0.414
14	0.99640	0.00354	0.00006	16.69	16.60	0.19	--	0.137
15	0.99817	0.00177	0.00006	10.99	10.68	0.20	--	0.155
16	0.98895	0.01092	0.00013	63.20	60.04	0.49	--	0.166
18	0.98319	0.01596	0.00085	92.45	90.08	2.48	--	2.593
19	0.80146	0.19811	0.00043	205.77	205.98	1.43	--	1.346
20	0.84962	0.15017	0.00021	153.77	153.85	1.08	--	0.793
Sys.	**0.69183**	**0.30656**	**0.00161**	**335.15**	**341.15**	**4.03**	**51.90**	**10.903**

The results show in Table 9.5 indicate that the modified IEEE-RTS has a very high marginal state probability (Prob{M}= 0.30656). The system under this condition is not healthy even though the system adequacy indices are reasonable. System security analysis provides the opportunity to appreciate future potential risks (marginal state) in situations in which the adequacy indices of a system appear acceptable. The combined reliability framework provides an overall appreciation of both system security and adequacy under a particular condition. Freq{H} indicates that the system under this condition is expected to depart from the healthy state 335.15 times in a year. The average system residence time in the healthy state before moving to the marginal or at risk states is 18.47 hours, which is less than one day. System operators may, therefore, have to be prepared to encounter an alert condition every day.

As shown in Tables 9.3 and 9.5, the MR-RBTS and the modified IEEE-RTS under the specified conditions are vulnerable to violating the N-1 security criterion.

Transmission system reinforcements should therefore be considered and are illustrated in the following section. It is again important to note that generation deficiencies tend to have more significant impacts on system adequacy than on system security. In contrast, transmission deficiencies have more significant impacts on system security rather than on system adequacy. The overall system reliability can be examined by utilizing a combined framework analysis that incorporates both adequacy and security perspectives.

9.5 Transmission System Reinforcements Incorporating Both Adequacy and Static Security Considerations

The fundamental task in transmission planning is to develop the system as economically as possible while maintaining an acceptable reliability level. The deterministic N-1 criterion has been widely accepted and used by system planners in transmission planning practice for many years. The deterministic N-1 criterion has two weaknesses. First, multiple component failure events are excluded from consideration. Second, only the outcomes of single component failure events are analyzed but their probabilities of occurrence are not considered. A failure event which is extremely undesirable, but has a low probability of occurrence cannot be ignored in the deterministic approach. Planning alternatives based on deterministic N-1 analysis will therefore lead to overinvestment [103]. System well-being analysis alleviates the two weaknesses noted above by incorporating the deterministic N-1 criterion in a probabilistic framework. In the system well-being framework, the marginal state is identified and classified using the deterministic N-1 criterion. The marginal state is, therefore, recognized as the N-1 insecure state. As noted above, the utilization of a deterministic approach in transmission planning can result in overinvestment. It is therefore of interest to translate or transform the N-1 insecure state (marginal) into a monetary form and use it as a security cost factor in the transmission planning process. This proposed security cost is designated as the expected potential insecurity cost (EPIC) and is obtained using the multiplication of the probability of the marginal state (Prob{M}) and the expected customer interruption cost (ECOST), as shown in Equation (9.1).

$$\textit{Expected Potential Insecurity Cost (EPIC)} = \textit{Prob\{M\}} \times \textit{ECOST} \quad (9.1)$$

The ECOST is the expected monetary impact on customers due to supply failures and is normally used in the adequacy assessment domain. The Prob{M} indicates the potential system insecurity if a specified element based on the N-1 criterion fails and results in load curtailments. There is no actual customer outage cost under the N-1 insecure state (marginal) if the specified element does not actually fail. Operating a system under insecure conditions can, however, create system stress and require preventive action by the system operators. The insecurity cost can be related to existing costs associated with implementing preventive actions under insecure situations. For example, when system operators realize that a current operating state will not satisfy the next specified N-1 contingency, they may decide to take preventive action such as starting additional generating units, redispatching etc., to improve system security or to reduce the magnitude of severity if the contingency occurs. Enhancing system security can have considerable associated cost. The repetitive cost of preventive actions may be much larger than the occasional monetary impact of consumer disconnections [104]. The expected potential insecurity cost (EPIC) expressed in Equation (9.1) is designated as the deterministic N-1 security cost, and is a surrogate for the preventive cost associated with system insecure conditions.

The deterministic N-1 security cost (EPIC) and the adequacy cost component (ECOST) can be combined to determine an overall reliability cost based on both adequacy and security concerns. The total monetary loss in the combined reliability framework is designated as the expected overall reliability cost (EORC) as shown in Equation (9.2).

$$\textit{Expected Overall Reliability Cost (EORC)} = \textit{ECOST} + \textit{EPIC} \quad (9.2)$$

The deterministic cost (EPIC) can be considered as an increment of the overall reliability cost (EORC). For example, if the potential insecurity cost based on the deterministic N-1 criterion is low (Prob{M} is low), the EPIC will be relatively small

and therefore insignificant. It therefore will not send a signal to the system planner to implement system reinforcement, which could lead to overinvestment. In contrast, if the EPIC is high (Prob{M} is high), this will add a significant increment to the overall reliability cost (EORC) and indicate that the system planner should consider system reinforcements based on the deterministic N-1 criterion.

The concept of utilizing an overall reliability cost considering both adequacy and security concerns in transmission system reinforcement analysis is demonstrated by application to the MR-RBTS and the modified IEEE-RTS.

9.5.1 Transmission Reinforcement in the MR-RBTS

The generation center of the RBTS is located in the northern part of the system while the most of the loads are located in the southern area as shown in Figure 8.4. Significant amounts of power are therefore transferred from the north to the south through two double circuits (Lines # 1 and 6, and Lines # 2 and 7). The transmission utilizations of Lines # 1 and 6 are approximately 85% of the line ratings while those of Lines # 2 and 7 are approximately 54% of the line ratings during system peak demand. The power flows on Lines # 2 and 7 are less than those on Lines # 1 and 6 because they are very long transmission circuits with much higher impedances. The loss of any one transmission line in the critical path (Lines # 1 and 6) during a high demand period can result in an overload on the remaining line.

Transmission reinforcements can be achieved by various transmission planning schemes. In this section, two reinforcement options are considered for illustration and comparison purposes. The two reinforcement schemes involve either utilizing flexible AC transmission system (FACTS) devices or constructing a new transmission line. The FACTS technology is based on the concept of using power electronic devices for power flow control at the transmission level. The transmission components become active elements by self-adjusting their related parameters, and play important roles in meeting power transfer requirements and increasing the security margins. New transmission line

construction is becoming increasingly difficult due to the lack of financial and regulatory incentives, public discouragement due to environmental concerns and physical right-of-way restrictions. There is therefore increasing utilization of FACTS technology as a means of extending the capability of existing transmission networks without adding new transmission lines [105, 106]. The addition of FACTS devices can improve the system transfer capability by alleviating the transmission loading constraints. There are various types of FACTS devices by which different transmission parameters, i.e. line impedance, phase angle etc., can be adjusted. The FACTS devices utilized in this section are assumed to be a thyristor-controlled series compensation type that can control line impedance. For example, the thyristor-controlled series capacitor can vary the impedance to levels below and up to the line's natural impedance, whereas the thyristor-controlled series reactor can add positive impedance to a value above the line's natural impedance [105]. The variable series controlled impedance used in this study is permitted to vary by ± 50% of the line impedance [106].

An assumption made regarding FACTS device additions in this study is that FACTS devices perform their function when required to alleviate overloads on the corresponding lines. The FACTS devices offer major potential advantages in both the static and dynamic operation of transmission lines. The following analyses utilize the ability of a FACTS device to increase the load carrying capability of the corresponding transmission line.

As noted earlier, the load center of the modified RBTS is located in the southern area and the generation center is in the northern area. This results in significant transmission utilization of Lines # 1 and 6 during system peak demand. System reinforcement using FACTS device additions or a new transmission line are therefore initially considered in order to alleviate the potential loading problem on Lines # 1 and 6. Three possible transmission reinforcement alternatives for the MR-RBTS are listed below.

Alternative 1: FACTS additions to Lines # 1 and 6 (between Buses 1 and 3)
Alternative 2: FACTS additions to Lines # 2 and 7 (between Buses 2 and 4)

Alternative 3: A new transmission line between Buses 1 and 3

In Alternative 1, FACTS devices are installed on both parallel lines (Lines # 1 and 6) between Bus 1 and Bus 3. Installing a FACTS device on only one of the two parallel lines will create an unsatisfactory overload on the other parallel line that does not have a FACTS device installed. This also applies to Alternative 2 where FACTS devices are installed on both Lines # 2 and 7. The new transmission line (Alternative 3) is assumed to be in parallel, and have identical line parameters and rating to those of Lines # 1 and 6. The overall system reliability indices considering both adequacy and static security concerns for the three reinforcement alternatives are shown in Table 9.6 together with the base case results (no reinforcement) given in Table 9.3.

Table 9.6 shows that adding FACTS on Lines # 1 and 6 (Alternative 1) can considerably decrease the probability and frequency of the at risk state, and the severity of supply interruption. Alternative 1, however, is not very effective from the security perspective as there is relatively little improvement in Prob{H} compared to the base case. In this alternative, FACTS devices control the transmission line overloads on Lines # 1 and 6 by increasing the line impedance by 50% (at the maximum level) in order to force some power to flow through the alternative path (from Bus 1 to Bus 2, and then Bus 2 to Bus 4 in this case). Changing the natural power flow direction in this case is, however, not very efficient as the Lines # 2 and 7 impedances are relatively large due to the long transmission lines.

Table 9.6: Overall system reliability indices (adequacy and security) of the MR- RBTS associated with the three transmission reinforcement alternatives.

System Indices	Base case	Alternative 1	Alternative 2	Alternative 3
Prob{H} (/yr)	0.86200	0.86703	0.87727	0.99343
Prob{M} (/yr)	0.13721	0.13256	0.12257	0.00653
Prob{R} (/yr)	0.00079	0.00041	0.00016	0.00004
Freq{H} (occ/yr)	172.01	134.85	116.61	10.61
Freq{M} (occ/yr)	173.36	135.73	117.16	10.68
Freq{R} (occ/yr)	1.80	1.07	0.60	0.09
DPUI (sys.mins)	19.97	10.39	3.95	1.33
ECOST (k$/yr)	201.986	121.880	48.175	16.988

Alternative 2 is more effective than Alternative 1 from an adequacy perspective and there is a slight improvement in the security indices. In Alternative 2, the FACTS devices control the transmission line overloads on Lines # 1 and 6 by decreasing the line impedance of Lines # 2 and 7 by 50% (at minimum level) and therefore increase the power flow on these two lines. The FACTS additions to Lines # 2 and 7 are more effective from a reliability point of view than adding FACTS to Lines # 1 and 6.

The overall system reliability indices are greatly improved by adding a transmission line between Bus 1 and Bus 3 (Alternative 3). The adequacy indices of DPUI and ECOST obtained for Alternative 2 are comparable to those obtained using Alternative 3, but the security indices for the two cases are considerably different. This shows that in this case, transmission reinforcement by FACTS additions is quite competitive with new transmission line construction based on adequacy assessment. The FACTS additions, however, provide only a marginal improvement in the system stress level while the line addition alternative provides a significant reduction in the system stress level.

The expected overall reliability cost (EORC) for all the reinforcement alternatives are presented in Table 9.7. These results show that the EPIC for Alternative 3 is insignificant compared to its ECOST.

Table 9.7: Associated reliability costs (adequacy and security considerations) in k$/year for the modified RBTS associated with different reinforcement alternatives.

Reinforcement Options	ECOST	EPIC = Prob{M}×ECOST	EORC
Base case (no reinforcement)	201.986	0.13721×201.986 = 27.714	229.700
Alter. 1 (FACTS at Lines # 1 and 6)	121.880	0.13256×121.880 = 16.156	138.036
Alter. 2 (FACTS at Lines # 2 and 7)	48.175	0.12257×48.175 = 5.905	54.080
Alter. 3 (a new line)	16.988	0.00653×16.988 = 0.111	17.099

The reinforcement option of adding a new transmission line to the system has the lowest EORC, and provides significant better overall reliability than the FACTS device additions (Alternatives 1 and 2). This option cannot, however, be considered to be the

optimum choice without conducting a reliability cost/worth analysis. The following presents an approach to determine the optimum reinforcement alternative.

Reliability cost/worth analysis [107, 108] as applied in power system planning is sometimes designated as value-based reliability [109], cost-benefit [110] or minimum cost planning [111] assessment. The basic concept is illustrated in Figure 5.1. In the present era of electricity competition and deregulation, customers and agencies are challenging implicit reliability criteria as the only bases for project justification, and are pressing for requirements to include customer interruption costs as a component of the total project cost [110]. As shown in Figure 5.1, the utility cost increases with increased system reliability levels. The customer interruption cost, in contrast, decreases as the system reliability increases. Utility customers receive the least cost service when the combined utility and customer outage costs are minimized. Reliability cost/worth analysis therefore establishes a balance between the costs of improving service reliability with the benefits that the improvement brings to the customer. The balance is achieved by minimizing the total cost (TOC) shown in Equation (9.3).

$$\textit{Total Cost (TOC)} = \textit{Utility Cost} + \textit{Expected Overall Reliability Cost} \quad (9.3)$$

The utility cost consists of two main components, which are the capital (investment) cost, and the operating and maintenance costs. In order to simplify the calculation, operating cost elements such as production costs are not included in the evaluation. The maintenance cost is added to the capital cost as a part of the fixed costs. The following economic terms are used to determine the utility investment cost [112]:

$$\textit{Capital Recovery Factor (CRF)} = \frac{i(1+i)^n}{(1+i)^n - 1} \quad (9.4)$$

$$\textit{Annual capital payment (ACP)} = P \times CRF \quad (9.5)$$

where: i = A discount rate or present worth rate,

n = A number of years considered,

P = Present project cost.

The capital recovery factor (CRF) indicates the equal regular payments that are equivalent to a present amount of money [112]. For example, \$1.0 today is equivalent to \$0.10185 every year for the next 20 years assuming a discount rate (present worth rate) of 8% per year. The annual capital payment (ACP) indicates the uniform series of annual payments (an annuity) from the beginning of the construction year through *n* years for the useful lifetime of the project.

Reliability cost/worth analysis is applied to the three transmission reinforcements in the following.

Alternative 1: FACTS device additions on Lines # 1 and 6

FACTS device cost = 4.0 M\$/unit

Number of FACTS devices = 2

Useful lifetime considered = 20 years

FACTS device maintenance cost (during useful lifetime) = 5% of the project cost

Discount rate (present worth rate) = 8% per year

Therefore, CRF $= \dfrac{0.08(1+0.08)^{20}}{(1+0.08)^{20}-1} = 0.10185$

Project cost (P) = investment cost + maintenance cost

$= 2\times4.0$ (M\$) $+ 0.05\times2\times4.0$ (M\$) $= 8.40$ (M\$)

Therefore, annual capital payment (ACP) = P×CRF = 8.40×0.10185 = 0.856 M\$/yr.

The total cost (TOC) expressed in Equation (9.3) is a summation of the annual capital payment (ACP) and the expected overall reliability cost (EORC). As shown in Table 9.7, the expected overall reliability cost (EORC) associated with adding FACTS devices on L1 and L6 is 138.036 k\$/yr.

Total cost (TOC) = ACP + EORC = 0.856 M\$/yr + 0.138 M\$/yr = 0.994 M\$/yr

Alternative 2: FACTS device additions on Lines # 2 and 7

The expected overall reliability cost (EORC) associated with adding FACTS devices on L2 and L7 is 54.080 k\$/yr (Table 9.7). The total cost is as follows:

Total cost (TOC) = ACP + EORC = 0.856 M$/yr + 0.054 M$/yr = 0.910 M$/yr

Alternative 3: New transmission line addition

Investment cost of a 230 kV transmission line = 0.48 M$/km

New transmission line length = 75 km

Useful lifetime considered = 40 years

Line maintenance cost (during a useful lifetime) = 5% of the project cost

Discount rate (present worth rate) = 8% per year

$$\text{CRF} = \frac{0.08(1+0.08)^{40}}{(1+0.08)^{40}-1} = 0.08386$$

Project cost (P) = investment cost + maintenance cost

= 0.48×75 (M$) + 0.05×0.48×75 (M$) = 37.80 (M$)

Therefore, annual capital payment (ACP) = P×CRF = 37.80×0.08386 = 3.169 M$/yr.

The expected overall reliability cost (EORC) associated with adding a new transmission line (Table 9.7) is 17.099 k$/yr.

Total cost (TOC) = ACP + EORC = 3.169 M$/yr + 0.017 M$/yr = 3.186 M$/yr

The reliability cost/reliability worth components due to the three reinforcement options are summarized in Table 9.8.

Table 9.8: Summary of reliability cost/reliability worth components for the three reinforcement projects in the MR-RBTS.

Reinforcement Project	ACP (M$/yr)	EORC (M$/yr)	TOC (M$/yr)
Base case (no reinforcement)	0	0.230	0.230
Alter. 1 (FACTS at Lines # 1 and 6)	0.856	0.138	0.994
Alter. 2 (FACTS at Lines # 2 and 7)	0.856	0.054	0.910
Alter. 3 (a new line)	3.169	0.017	3.186

Table 9.8 indicates that the total cost of the base case (no reinforcement) results in the least cost option. The total costs due to FACTS device additions (Alternatives 1 and 2) are approximately four times larger than that of the base case, while the total cost due to a new line addition is over thirteen times higher than that of the base case. In this

case, the test system is a small system and the EORC obtained is not very large compared to the annual investment cost of a device addition. This does not, however, mean that it is not worth conducting system reinforcement in this case. The alternative involving FACTS addition on Lines # 2 and 7 is a compromise between the system reliability and the economic concerns, and may be an attractive option for short-term system reinforcement as the total cost is less than one third of that for a new transmission line. This option provides system adequacy indices that are reasonably comparable to those provided by building a new transmission line.

It is important to note that the results shown in Table 9.8 are on a one year basis. Transmission expansion planning normally considers a longer period than one year, i.e. 5 or 10 years in the future. For example, an adopted reinforcement scheme should meet the reliability criteria over a future target period. The above example is extended to investigate a four year transmission planning period during which it is assumed that the system should have a Prob{H} at the level of 0.86 or above. An annual system load growth of 4.2% is used in the analysis. The transmission reinforcement is assumed to be completed at the beginning of the initial year or the first year of the target period, and the results for the first year are shown in Tables 9.6 and 9.8. Equations (9.6) and (9.7) are used [103] to consider the present value of the total annual capital cost (ACP) and the total expected overall reliability cost (EORC) for the four year period.

$$Total\ ACP = ACP\sum_{j=1}^{m}\frac{1}{(1+i)^{j-1}} \tag{9.6}$$

$$Total\ EORC = \sum_{j=1}^{m}\frac{EORC_j}{(1+i)^{j-1}} \tag{9.7}$$

where: m = The planning period in years (4 years in this illustration).

i = The discount rate described earlier, assumed to be 8% in this study.

The overall system reliability indices and related costs for the next three years (2^{nd}, 3^{rd}, 4^{th} years) are presented in Table 9.9. Alternative 1 is not considered further as

the results shown in Table 9.6 indicate that Alternative 2 offers a better system reliability and a lower total cost than Alternative 1.

Table 9.9: Overall system reliability indices and the related costs of the two reinforcement alternatives in the MR-RBTS for the three years.

System Indices	2nd year		3rd year		4th year	
	Alter. 2 (FACTS)	Alter. 3 (Line)	Alter. 2 (FACTS)	Alter. 3 (Line)	Alter. 2 (FACTS)	Alter. 3 (Line)
Prob{H} (/yr)	0.87032	0.99187	0.86210	0.98761	0.85518	0.98004
Prob{M} (/yr)	0.12922	0.00806	0.13706	0.01219	0.14340	0.01954
Prob{R} (/yr)	0.00046	0.00007	0.00085	0.00020	0.00141	0.00042
Freq{H} (occ/yr)	118.04	13.57	119.23	25.35	120.75	32.39
Freq{M} (occ/yr)	119.00	13.73	120.88	25.88	122.89	33.09
Freq{R} (occ/yr)	1.17	0.20	2.03	0.58	2.79	0.84
DPUI (sys.mins)	9.50	2.55	21.87	5.82	42.67	13.14
ECOST (M$/yr)	0.106	0.032	0.237	0.074	0.465	0.166
EPIC (M$/yr)	0.014	0.000	0.032	0.001	0.067	0.003
EORC (M$/yr)	0.120	0.032	0.269	0.075	0.532	0.169
ACP (M$/yr)	0.856	3.169	0.856	3.169	0.856	3.169

Equations (9.6) and (9.7) are used to calculate the present value of the total ACP and the total EORC over the four year planning period.

For Alternative 2:

$$\text{Total ACP} = 0.856\left(\frac{1}{(1+0.08)^0}+\frac{1}{(1+0.08)^1}+\frac{1}{(1+0.08)^2}+\frac{1}{(1+0.08)^3}\right) = 3.062 \text{ (M\$)}$$

$$\text{Total EORC} = \frac{0.054}{(1+0.08)^0}+\frac{0.120}{(1+0.08)^1}+\frac{0.269}{(1+0.08)^2}+\frac{0.532}{(1+0.08)^3} = 0.818 \text{ (M\$)}$$

Total cost (TOC) for the four year period = 3.062 + 0.818 = 3.880 (M$)

For Alternative 3:

$$\text{Total ACP} = 3.169\left(\frac{1}{(1+0.08)^0}+\frac{1}{(1+0.08)^1}+\frac{1}{(1+0.08)^2}+\frac{1}{(1+0.08)^3}\right) = 11.335 \text{ (M\$)}$$

$$\text{Total EORC} = \frac{0.017}{(1+0.08)^0}+\frac{0.032}{(1+0.08)^1}+\frac{0.075}{(1+0.08)^2}+\frac{0.169}{(1+0.08)^3} = 0.245 \text{ (M\$)}$$

Total cost (TOC) for the four year period = 11.335 + 0.245 = 11.580 (M$)

The total costs calculated above indicate that the ratio of the total costs for the two alternatives during the four year period is 2.98 (11.580/3.880), whereas the ratio of the total costs based on one year shown in Table 9.8 is 3.50 (3.186/0.910). This implies that the benefit of the FACTS addition in Alternative 2 decreases when a longer period is considered (long term planning). The Prob{H} in the fourth year for the FACTS addition alternative is lower than the pre-specified reliability criterion of 0.86 and therefore Alternative 2 does not meet the reliability criterion. Additional reinforcement would, therefore, be required to achieve the reliability goal over this period. This will require additional investment, and a higher total investment over the planning period. In contrast, Alternative 3 provides acceptable adequacy and security over the entire period. In conclusion, the proposed transmission reinforcement using FACTS device additions only temporarily alleviates the transmission constraints and involves relatively high system stress and potential risk in the future. Constructing a new transmission line rather than installing FACTS devices in this case appears to be promising for long-term system planning and should be studied further.

9.5.2 Transmission Reinforcement in the Modified IEEE-RTS

As shown in Table 9.4, the modified IEEE-RTS is transmission deficient due to the transmission loads created by the significant power flows from the north to the south of the system. This section conducts transmission reinforcement planning in order to improve the system reliability. A system investigation is required in order to identify proper locations for effective transmission reinforcement, and to identify the possible transmission reinforcement schemes. Two criteria are used in order to select effective locations for transmission reinforcements. The first criterion is based on line overload analysis of the base case. The number of overload hours of all the transmission facilities are recorded in the simulation to obtain the average overload in hours/year. This criterion can help to identify the critical transmission facilities from a system adequacy perspective. The second criterion is based on Freq{H} of all the delivery points of the

base case shown in Table 9.5. Freq{H} is the number of times that each delivery point leaves the healthy state. This criterion can be used to identify critical locations from a security perspective.

As shown in Table 9.5, the delivery point at Bus 10 has the highest Freq{H}. This is 246.61 occ/yr and is following by the Bus 6 load point with 206.12 occ/yr. A transmission reinforcement plan to improve system security can be focused on these two buses. The single line diagram of the IEEE-RTS in Figure 3.3 shows that Buses 10 and 6 are connected to each other by Line # 10. This line has an average overload of less than 0.1 hr/yr. The transmission line connecting Bus 6 to Bus 2 (Line # 5) has an average overload of 1.0 hr/yr. If Line # 10 is on outage, Line # 5 will not be able to serve all the load at Bus 6 during the peak load condition. A potential reinforcement scheme could therefore be focused on this location. The transmission line that encounters the highest number of average overload hours (18 hrs/yr) is Line # 23 connecting Bus 14 and Bus 16. The second highest average overload (3 hrs/yr) is on Line # 6 connecting Bus 3 and Bus 9. The following five possible reinforcement alternatives were selected for investigation using the two selection criteria.

Alternative 1: A one line addition between Buses 2 and 6
Alternative 2: A one line addition between Buses 14 and 16
Alternative 3: A one line addition between Buses 2 and 6, and a one line addition between Buses 3 and 9
Alternative 4: A one line addition between Buses 14 and 16, and a one line addition between Buses 11 and 14
Alternative 5: Combining Alternatives 3 and 4 (four lines in total)

Each of these five alternatives will create parallel path(s) with existing transmission circuit(s). The loss of one parallel line will, therefore, not interrupt all the power flow between the corresponding buses. The overall system reliability indices for the modified IEEE-RTS with the five system reinforcement alternatives and the base case values are shown in Table 9.10.

Table 9.10: Overall system reliability indices for the modified IEEE-RTS with the five different system reinforcement alternatives.

System Indices	Base case	Alter. 1	Alter. 2	Alter. 3	Alter. 4	Alter. 5
Prob{H} (/yr)	0.69183	0.96491	0.70561	0.96755	0.70562	0.98036
Prob{M} (/yr)	0.30656	0.03352	0.29296	0.03123	0.29304	0.01868
Prob{R} (/yr)	0.00161	0.00158	0.00143	0.00122	0.00134	0.00096
Freq{H} (occ/yr)	335.15	80.57	321.80	75.05	324.12	38.60
Freq{M} (occ/yr)	341.15	82.29	327.43	76.40	329.27	39.28
Freq{R} (occ/yr)	4.03	4.13	3.50	3.58	3.47	2.65
DPUI (sys.mins)	51.90	47.35	38.50	30.48	30.06	20.74
ECOST (M$/yr)	10.903	9.913	8.073	6.267	6.343	4.341

The results shown in Table 9.10 indicate that Alternative 1 (adding a line between Bus 2 and Bus 6) effectively relieves the N-1 security problem and improves the overall system security, as Prob{H} increases from 0.69183 to 0.96491. This reinforcement option is, however, not very effective in improving the system adequacy as DPUI only reduces to 47.35 sys.mins compared to 51.90 sys.mins in the base case. Alternative 2 does not effectively improve the system security as Prob{H} only slightly increases from 0.69183 to 0.70561. This alternative, however, considerably improves the system adequacy as DPUI reduces to 38.50 sys.mins. Alternative 1 was selected based on the high value of Freq{H} which is a security based indicator and Alternative 2 was selected based on the highest average overload hour on Line # 23, which is an adequacy based indicator. As expected, Alternative 1, therefore, improves the system security while Alternative 2 improves the system adequacy.

Alternative 3 is intended to improve both system security and system adequacy. As noted earlier, Line # 6 encounters an average overload of 3 hrs/yr. This alternative, which is an extension of Alternative 1, improves both the system security and the system adequacy. The Prob{H} is slightly better than that of Alternative 1 and the DPUI reduces from 47.35 sys.mins to 30.48 sys.mins. This results in an ECOST reduction of almost 3.5 M$/yr.

Alternative 4 is considered in order to further reduce DPUI from that obtained with Alternative 2, by adding one more line between Bus 11 and Bus 14. The reason for

adding this line is that the addition of a second line between Bus 14 and Bus 16 will increase the power flow through this path creating an average overload on Line # 19 of 1.0 hr/yr. The line addition between Bus 11 and Bus 14 in Alternative 4 decreases the potential of an overload on this path. Table 9.10 shows that Alternative 4 results in a reduction of the DPUI from 38.50 sys.mins in Alternative 2 to 30.48 sys.mins. The Prob{H} for these two alternatives are basically the same and indicate that the line addition between Bus 11 and Bus 14 does not improve system security.

Alternative 5 is a combination of Alternatives 3 and 4, and involves a total of four additional lines. Alternative 5 should provide considerable improvement in both the system security and system adequacy. As shown in Table 9.10, the overall reliability indices are considerably better than those for Alternatives 3 and 4, and are a considerable improvement over those of the base case. This alternative provides the best reliability benefit of the selected transmission reinforcement schemes, but involves significant investment. The economic analyses conducted on the five transmission reinforcement options are briefly illustrated in the following.

The construction costs of 138 kV and 230 kV lines are assumed to be 0.40 M$/km and 0.48 M$/km respectively. The useful lifetime of a new transmission line is 40 years, and the discount rate is 8% per year. The line maintenance cost is 5% of the project expenses. The annual capital payments (ACP) for all the reinforcement alternatives are shown in Table 9.11.

Table 9.11: Annual capital payments (ACP) for the different reinforcement alternatives in the modified IEEE-RTS.

Reinforcement Options	Investment cost (M$)	Maintenance Cost (M$)	CRF	ACP (M$/yr)
Alternative 1	0.40×80 = 32.000	1.600	0.08386	2.818
Alternative 2	0.48×43 = 20.640	1.032	0.08386	1.817
Alternative 3	0.40×80 + 0.40×50 = 52.000	2.600	0.08386	4.579
Alternative 4	0.48×43 + 0.48×46 = 42.720	2.136	0.08386	3.762
Alternative 5	52.000 + 42.720	4.736	0.08386	8.340

Table 9.12 shows the reliability cost/reliability worth components associated with the five different reinforcement alternatives.

Table 9.12: Reliability cost/reliability worth components associated with the five different reinforcement alternatives in the modified IEEE-RTS.

Reliability cost/worth components	Base Case	Alter. 1	Alter. 2	Alter. 3	Alter. 4	Alter. 5
ECOST (M$/yr)	10.903	9.913	8.073	6.267	6.343	4.341
EPIC (M$/yr)	3.342	0.333	2.365	0.196	1.859	0.081
EORC (M$/yr)	14.245	10.246	10.438	6.463	8.202	4.422
ACP (M$/yr)	0.000	2.818	1.817	4.579	3.762	8.340
TOC (M$/yr)	**14.245**	**13.064**	**12.255**	**11.042**	**11.964**	**12.762**

Table 9.12 indicates that Alternative 3 (adding a new line between Bus 2 and Bus 6, and another line between Bus 3 and Bus 9) results in the lowest total cost (TOC) of the five alternatives, followed by Alternatives 4, 2, 5 and 1 respectively. It is interesting to note that adding four new transmission lines in Alternative 5 results in a lower total cost than by adding one new line in Alternative 1. It is important to note that the results shown in Table 9.12 are on a one year basis from which Alternative 3 is the optimum choice. Alternative 5, which offers significant adequacy and security improvements, could prove to be the most attractive when considering the future load growth. Long term planning analysis can be conducted as illustrated in the previous section to examine the potential of each alternative.

In conclusion, the overall reliability framework proposed in this thesis incorporates the deterministic N-1 criterion in a probabilistic framework, and results in the joint inclusion of both adequacy and security considerations in system planning. Recent discussions [113] indicate that there is a need to re-design and apply deterministic techniques that include probabilistic considerations in order to assess increased system stress due to the restructured electricity environment. The desired technique should be capable of maintaining an acceptable balance between system utilization and the required system reliability. The overall reliability framework

considering both adequacy and security concerns described in this chapter can fulfill the tasks noted in [113].

9.6 Conclusions

An overall reliability analysis framework considering both adequacy and security perspectives is demonstrated in this chapter using system well-being analysis and traditional adequacy assessment. System well-being (security) analysis is used to quantify the degree of N-1 security (healthy) and the N-1 insecurity (marginal) in terms of probabilities and frequencies. Traditional adequacy assessment is incorporated to quantify the magnitude of the severity and the consequences associated with system failure. Selected adequacy-based and security-based indices are used to create a combined reliability framework. Various case studies are illustrated in this chapter based on different system conditions involving generation and transmission deficient situations. The results based on overall reliability analysis indicate that adequacy indices are adversely affected by a generation deficient environment and security indices are adversely affected by a transmission deficient environment. A system planning process using combined adequacy and security considerations offers an additional reliability-based dimension. The combined adequacy and security framework presented in this chapter can assist system planners to appreciate the overall benefits of possible reinforcement options, and prove useful in the decision making process. Various possible reinforcement alternatives have been examined in this chapter using reliability cost/reliability worth considerations. The concept of a combined reliability framework should prove useful in the present electric utility environment where system stress is becoming increasingly important.

CHAPTER 10
WIND POWER INTEGRATION IN BULK ELECTRIC SYSTEM RELIABILITY ANALYSIS

10.1 Introduction

There has been considerably interest in utilizing wind for electric power generation in many systems throughout the world during the last two decades. Wind power is considered to be an encouraging and promising alternative for power generation because of its tremendous environmental, social and economic benefits, together with public support and government incentives. As reported by the Canadian Electricity Association (CEA), Canada has committed itself to a specific target of 10,000 megawatts of installed wind power capacity by 2010 [114]. There is currently 590 megawatts of wind capacity across Canada (retrieved on August 24, 2005 from the Canadian Wind Energy Association [115]). This target will therefore require an annual wind power growth rate of approximately 60%. Wind power is, however, an intermittent energy source that behaves far differently than conventional energy sources. The reliability impact of such a highly variable energy source is an important aspect that must be assessed when the wind power penetration is significant.

Relatively little work has been done on bulk electric system reliability analysis associated with wind energy due to the complexity associated with including detailed modeling of both the generation and transmission facilities in addition to the wind characteristics. An advantage of utilizing sequential Monte Carlo simulation in bulk electric system reliability evaluation is that the framework already exists to incorporate the chronological characteristics of wind (diurnal and season wind speeds), load profiles and the chronological transition states of all the components within a system. Sequential

simulation can, therefore, provide realistic and more accurate results than other traditional methods when considering wind power. Research work on the impact of wind power generation in bulk electric system reliability is investigated and illustrated in this chapter. The studies conducted in this chapter are focused on the adequacy of bulk electric systems containing wind power. The concept of incorporating security considerations described in Chapters 8 and 9 is not considered in this chapter.

10.2 Wind Energy Conversion System

The wind energy conversion system (WECS) model is basically composed of two main parts designated as the wind speed model and the wind turbine generator (WTG) model. These two segments are briefly described as follows:

10.2.1 Wind Speed Modeling

An essential prerequisite in incorporating WECS in power system reliability analysis using sequential Monte Carlo simulation is to realistically simulate the hourly wind speed. Wind speed varies with time and location and at a specific hour is related to the wind speeds of the immediate previous hours. Wind speed models, therefore, have unique characteristics that are dependent on their geographies. The two wind regimes utilized in this paper were modeled using auto-regressive moving average (ARMA) time series models [116]. The general expression of the ARMA(n,m) model is as follows:

$$y_t = \sum_{i=1}^{n} \phi_i y_{t-i} + \alpha_t - \sum_{j=1}^{m} \theta_j \alpha_{t-j} \tag{10.1}$$

where: y_t is the time series value at time t, ϕ_i ($i=1,2,\ldots,n$) and θ_j ($j=1,2,\ldots,m$) are the auto-regressive and moving average parameters respectively, $\{\alpha_t\}$ is a normal white noise process with zero mean and variance of σ_a^2, i.e. $\alpha_t \in NID(0,\sigma_a^2)$, where NID denotes Normally Independent Distributed.

The hourly simulated wind speed SW_t at time t is obtained from the mean speed μ_t, its standard deviation σ_t and the time series y_t as shown in Equation (10.2).

$$SW_t = \mu_t + \sigma_t y_t \tag{10.2}$$

Using Equation (10.1), new values of y_t can be calculated from current random white noise α_t and previous values of y_{t-i}. Equation (10.2) is used to generate the hourly wind speeds incorporating the wind speed time series.

The studies presented in this chapter utilize wind speed models and data from two different sites located in the province of Saskatchewan. This information is designated as Regina and Swift Current data. Table 10.1 shows the hourly mean wind speed and the standard deviation at the two different sites. The ARMA models for the two sites are given in Equations (10.3) and (10.4). The Regina wind model shown in Equation (10.3) was developed and published in [116]. The Swift Current wind model shown in Equation (10.4) was developed using the ARMASA Toolbox [117, 118] associated with the System Identification Toolbox [119] in the MATLAB Program. Hourly wind speed time data from 1996-2003 (8 year series) obtained from Environment Canada were used in the ARMA model development, and hourly wind speed data from 1984-2003 (20 years) at the Swift Current site were used to calculate the hourly mean wind speed and standard deviation. Wind speed data for the two locations used in the study are shown in Table 10.1.

Table 10.1: Wind speed data at the two different sites.

Sites	Regina	Swift Current
Mean wind speed (km/h), μ	19.52	19.46
Standard deviation (km/h), σ	10.99	9.70

Regina: ARMA (4,3):

$$\begin{aligned} y_t = {} & 0.9336 y_{t-1} + 0.4506 y_{t-2} - 0.5545 y_{t-3} + 0.1110 y_{t-4} \\ & + \alpha_t - 0.2033 \alpha_{t-1} - 0.4684 \alpha_{t-2} + 0.2301 \alpha_{t-3} \end{aligned} \tag{10.3}$$

$$\alpha_t \in NID(0, 0.409423^2)$$

Swift Current: ARMA (4,3):

$$y_t = 1.1772 y_{t-1} + 0.1001 y_{t-2} - 0.3572 y_{t-3} + 0.0379 y_{t-4} + \alpha_t - 0.5030 \alpha_{t-1} - 0.2924 \alpha_{t-2} + 0.1317 \alpha_{t-3} \quad (10.4)$$

$$\alpha_t \in NID(0, 0.524760^2)$$

10.2.2 Wind Turbine Generator Modeling

The power output characteristics of a wind turbine generator (WTG) are quite different from those of conventional generating units. The wind speed has a major effect on the power output. There is a non-linear relationship between the power output of the WTG and the wind speed. The relation can be described using the operational parameters of the WTG. The three commonly used parameters are the cut-in, rated and cut-out wind speeds. The hourly power output can be obtained from the simulated hourly wind speed using Equation (10.5).

$$P(SW_t) = \begin{cases} 0 & 0 \le SW_t < V_{ci} \\ (A + B \times SW_t + C \times SW_t^{\,2}) \times P_r & V_{ci} \le SW_t < V_r \\ P_r & V_r \le SW_t < V_{co} \\ 0 & SW_t \ge V_{co} \end{cases} \quad (10.5)$$

Where P_r, V_{ci}, V_r and V_{co} are the rated power output, the cut-in wind speed, the rated wind speed and the cut-out wind speed of the WTG respectively. The constants *A, B* and *C* are determined by V_{ci}, V_r and V_{co} as expressed in Equation (10.6) [120], and the wind turbine generator power curve is shown in Figure 10.1. All the WTG units used in this study are assumed to have a rated capacity of 2 MW, and cut-in, rated and cut-out speeds of 14.4, 36 and 80 km/h respectively. The failure rates and repair times of all the WTG are 2 failures/year and 44 hours respectively.

$$A = \frac{1}{(V_{ci} - V_r)^2} \left\{ V_{ci}(V_{ci} + V_r) - 4 V_{ci} V_r \left[\frac{V_{ci} + V_r}{2 V_r} \right]^3 \right\},$$

$$B = \frac{1}{(V_{ci} - V_r)^2} \left\{ 4(V_{ci} + V_r) \left[\frac{V_{ci} + V_r}{2 V_r} \right]^3 - (3 V_{ci} + V_r) \right\}, \quad (10.6)$$

$$C = \frac{1}{(V_{ci} - V_r)^2} \left\{ 2 - 4 \left[\frac{V_{ci} + V_r}{2 V_r} \right]^3 \right\}.$$

Figure 10.1 shows the relationship between the power output of the WTG and the wind speed. The relationship is commonly known as the "Power Curve". At a specific time, the output power of a WTG can be obtained from the hourly simulated wind speeds by applying the power curve.

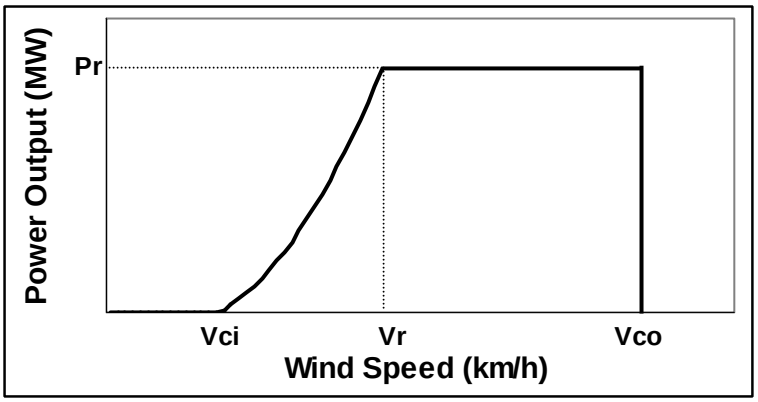

Figure 10.1: Wind turbine generator power curve.

Figure 10.2 shows the hourly simulated wind speeds for two consecutive simulation years based on the Regina model, and the resulting power output of 40 MW of WECS during a selected period in the two simulation years.

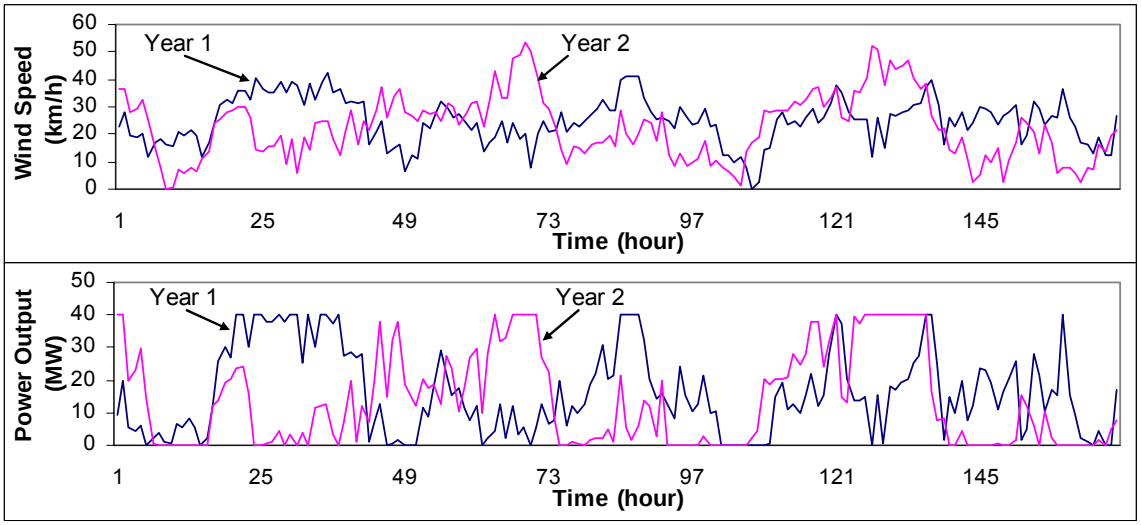

Figure 10.2: Hourly simulated wind speeds and resulting power output of 40 MW of WECS during the first week of January in two simulation years.

The simulated results shown in Figure 10.2 are for illustration purposes in order to demonstrate how simulated wind characteristics and the resulting power outputs of the WECS can vary from year to year even during the same period of the year. In a large number of simulation years, some years may have good wind and some years may have poor wind for power generation.

The chronological power output of the WECS shown in Figure 10.2 can be represented as the chronological transition process of a system generation component, and directly incorporated into Step 3 of the sequential simulation process for bulk electric system reliability analysis described in Section 3.5.

10.3 Generation Adequacy Assessment Associated with WECS

Although this thesis is focused on composite generation and transmission system reliability evaluation, it is important to investigate and appreciate some of the relevant features of wind power that impact generation adequacy and subsequently affect the reliability of composite power systems. Two important factors associated with wind power in generation adequacy assessment are considered in the following sections. These are the effect of wind speed correlations between wind farms, and the effect of wind power on load carrying capability.

10.3.1 Effect of Wind Speed Correlations between WECS

The utilization of multiple wind farms (WECS) is more advantageous than that of a single WECS from a reliability perspective. Quantitative results are illustrated in [121] assuming that the wind regimes at the various locations are totally independent (uncorrelated). This is a reasonable assumption when the distances between the various wind farms are very large. The assumption of site wind independence can be extremely optimistic if the sites are in reasonably close proximity. This section extends the concept of utilizing multiple wind sites illustrated in [121] by considering different degrees of wind speed correlation and examining these impacts on the overall system reliability. A

technique to correlate wind speed time series in wind speed simulation models is shown in the following. This technique is used later in this chapter to study this effect in bulk electric systems.

The wind speed correlation between two wind sites can be calculated using cross-correlation. The cross-correlation index (R_{xy}) is a measure of how well two time series follow each other [122, 123]. The value of R_{xy} is near the maximum value of 1.0 if the up and down movements of the two time series occur in the same direction (positively correlated). The value is close to zero if the two time series are basically uncorrelated, i.e. the two time series do not follow each other. The cross-correlation equation is shown in Equation (10.7).

$$R_{xy} = \frac{\frac{1}{n}\sum_{i=1}^{n}(x_i - \mu_x)(y_i - \mu_y)}{\sigma_x \sigma_y} \tag{10.7}$$

where: R_{xy} is the cross-correlation coefficient, x_i and y_i are elements of the 1st and 2nd time series respectively, μ_x and μ_y are the mean values of the1st and 2nd time series, σ_x *and* σ_y are the standard deviations of the 1st and 2nd time series, n is the number of points in the time series.

As previously noted, auto-regressive moving average (ARMA) time series models are used for wind speed simulation in this research. An ARMA model is composed of two sub-components, which are the auto-regressive (AR) model involving lagged terms on the time series itself (wind speeds from previous hours), and the moving average (MA) model involving lagged terms on the noise or residuals, which are random (non-autocorrelated and normally distributed). It is, therefore, possible to adjust the wind speed correlation between two or more different wind locations by selecting or determining the random number seeds (initial numbers) for the random number generator process used in the MA model. If the simulated wind speed time series for two different locations are generated at the same time using a single random number seed for the random number generator process, the time series of the wind speeds for these two

locations will, therefore, be highly correlated ($R_{xy} \geq 0.94$, for example). On the other hand, if a random number seed is assigned for each wind location and is used in its own random number generator process, the simulated wind speed time series obtained will become fully independent (uncorrelated, i.e. $R_{xy} \leq 0.05$).

This procedure can be used to generate the two extreme scenarios of highly dependent wind speeds and highly independent wind speeds at different locations. Based on the approach presented, the level of correlation between two or more wind speed time series can be adjusted by selecting appropriate random number seeds. For example, consider the wind regimes at Regina and Swift Current and assume that the cross-correlation coefficient between the two locations is 0.48. Further assume that Regina is used as the base location and that the assigned random number seed for this location is "*X"*. The task is to determine a seed for the Swift Current data which will result in a correlation coefficient of 0.48 with respect to the wind regime at Regina. Assume that this seed is a proportional value of *"X"*, for example *"mX"*, where *"m"* is real number. The next step is to pick some value (*m*) and test it in the wind speed simulation process to determine the best *"m"* that results in a correlation of 0.48. This step is a trial and error process but is relatively straightforward.

The concept described above is illustrated using wind speed simulations based on the Regina and Swift Current ARMA time series models. Figure 10.3 shows the simulated wind speed time series during a selected period for Regina and Swift Current with cross-correlation coefficients of 0.94, 0.48 and 0.05. Figure 10.3 shows that when R_{xy} is equal to 0.94, the wind speed time series between the two sites are highly correlated. An R_{xy} of 0.48 illustrates that the two wind regimes are partially correlated. In the final case, an R_{xy} of 0.05 illustrates that the two wind speed time series are fully independent.

Figure 10.4 shows the probability distributions of the annual power outputs from the combined 40 MW installed capacity from two wind farms (20 MW Regina and 20 MW Swift Current) at different correlation levels between the two sites.

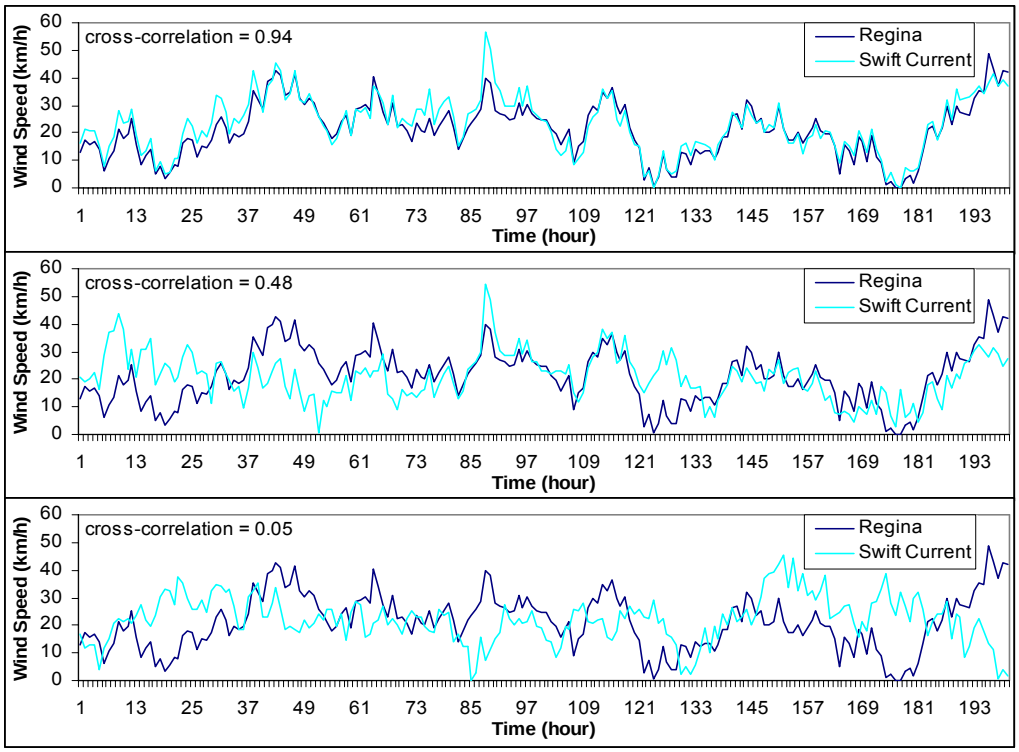

Figure 10.3: Different simulated wind speed correlations between Regina and Swift Current.

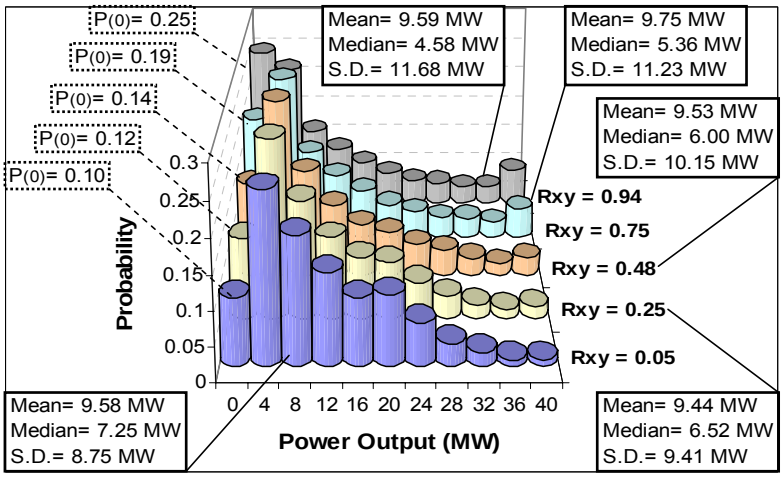

Figure 10.4: Probability distributions of the annual power output at different correlation levels for the Regina and Swift Current wind regimes.

Figure 10.4 clearly shows that when the cross-correlation coefficient between the two wind regimes decreases, the probability of having zero power output ($P_{(0)}$), the

probability of having maximum power output ($P_{(40)}$) and the standard deviation (S.D.) decrease while the median value increases. This figure illustrates the impact of correlation on the expected annual power output from two wind farms.

The generation adequacy assessment results shown in this section were obtained using a composite generation and transmission system reliability program (RapHL-II). The focus of this study is on generation adequacy. Transmission elements are assigned zero failure rates and therefore their contingencies are not considered. It should however be appreciated that in this case, transmission constraints such as line capacity limits and transmission power loss are still included in the analysis framework. The most common reliability indices used in HL-I analysis are the loss of load expectation (LOLE), the loss of load frequency (LOLF) and the loss of energy expectation (LOEE). These three reliability indices respectively are comparable to the expected duration of load curtailment (EDLC), the expected frequency of load curtailment (EFLC) and the expected energy not supplied (EENS) used in HL-II analysis.

Table 10.2 shows the impact on the RBTS reliability indices of wind speed correlation at the two wind farms (Regina and Swift Current data). The results shown in Table 10.2 are based on two WECS penetration levels; 40MW in total (20MW at each site) and 80MW in total (40MW at each site). The LOLF and LOLE shown in Table 10.2 are graphically portrayed in Figure 10.5. Figure 10.5 shows the positive impact on system reliability when the wind regimes at the two locations are less correlated (more independent). The reliability indices based on the 2×40MW WECS case tend to decline slightly faster than those based on the 2×20MW WECS case when the cross-correlation decreases. The reliability indices, which tend to saturate at a higher penetration due to a single wind farm, i.e. 80MW, if a single wind farm is used, can be further improved when multiple wind farms with lower wind speed correlations are installed instead of a single wind farm with the same total installed capacity. Another interesting point is that the system reliability based on the 2×20MW WECS case with fully independent wind regimes (R_{xy} = 0.05) is similar to that for the 2×40MW WECS case with fully dependent

wind regimes (R_{xy} = 0.94) even though the total installed capacities differ by a factor of two.

Table 10.2: Reliability indices of the RBTS including the two wind farms (Regina and Swift Current data) with different wind speed correlations.

WECS Capacity	Correlation (R_{xy})	LOLF (occ/yr)	LOLE (hrs/yr)	LOEE (MWh/yr)
40 MW	R_{xy} = 0.94	0.60	1.92	17.05
	R_{xy} = 0.75	0.59	1.85	16.10
	R_{xy} = 0.48	0.57	1.76	15.14
	R_{xy} = 0.25	0.53	1.61	13.82
	R_{xy} = 0.05	0.51	1.57	13.49
80 MW	R_{xy} = 0.94	0.53	1.51	13.54
	R_{xy} = 0.75	0.51	1.37	11.99
	R_{xy} = 0.48	0.47	1.23	10.59
	R_{xy} = 0.25	0.41	1.04	8.97
	R_{xy} = 0.05	0.39	0.98	8.46

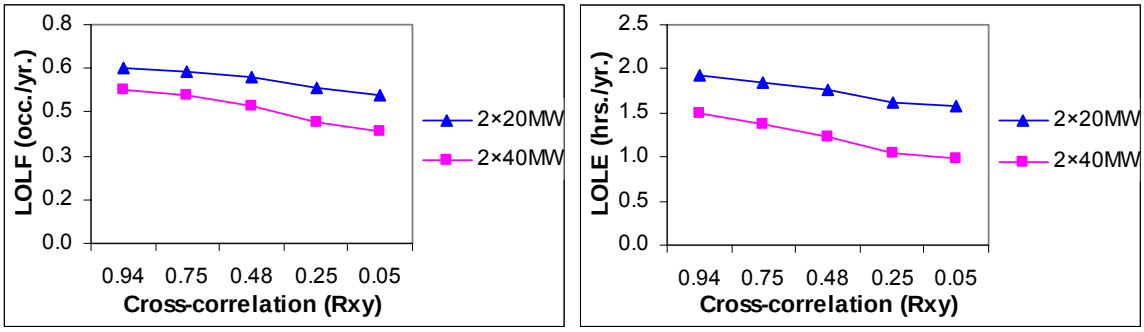

Figure 10.5: RBTS reliability indices including two wind farms (Regina and Swift Current regimes) with different wind speed correlations.

The correlation levels between two wind regimes are related to the distance between the two wind farms. A lower correlation in the two wind regimes implies that they are physically far from each other. There is a higher system reliability improvement when the two wind farms are further apart as the wind power at the two sites can support or assist each other and variations in the total wind power are, therefore, smoothed out. The maximum correlation of the two wind regimes used in this chapter is not equal to 1.0 due to the uniqueness of the ARMA time series model for each wind regime.

The concept of selecting initial seeds that relate to a particular cross-correlation coefficient between different wind locations is also applicable to a single wind farm, for example, a large-scale wind farm covering a widespread area. Wind regimes within this large-scale wind farm could be relatively variable, geographically dependent, and highly correlated. In order to obtain more accuracy in wind speed simulation associated with WECS, this single (large-scale) wind farm can be modeled with several ARMA time series sets in which each ARMA model represents an individual sub-location within the large-scale wind farm area. The concept of selecting seeds based on the cross-correlation coefficient can be applied when the correlation level between these sub-locations are known.

10.3.2 Effects of WECS on Load Carrying Capability

The capacity benefit associated with a generating capacity addition can be evaluated by determining the increase in the system load carrying capability due to the addition of the generating facility. A WECS has a capacity value and can contribute to long-term reserve when it can replace conventional generation while maintaining the same level of system reliability. One reliability-based technique used to measure the benefit associated with a capacity addition is to determine the effective load carrying capability (ELCC) [2, 124 – 126]. The basic concept in this approach is to gradually increase the system peak load until the level of system reliability associated with a facility addition is the same as that of the base case (the original system without WECS).

Studies of a system containing WECS indicates that the generating capacity adequacy index LOLF is affected quite differently than the LOLE and LOEE indices due to the inherent variability of the wind. It is, therefore, of interest to investigate how the selected LOLF and LOLE criterion responds to perceived system load carrying capability. The most commonly used reliability index in the ELCC approach is the LOLE which indicates how many hours in a given period (normally a year) a generating system cannot satisfy the overall system demand. The LOLF index of a system including WECS is quite unique and is affected quite differently than the LOLE indices due to the

hour-to-hour variations in wind speed. The unique aspect of LOLF is examined in this section by utilizing this index to calculate the ELCC for a system including WECS. The ELCC obtained using the LOLE and LOLF based indices are designated as $ELCC_{(LOLE)}$ and $ELCC_{(LOLF)}$ respectively and are illustrated in Figure 10.6.

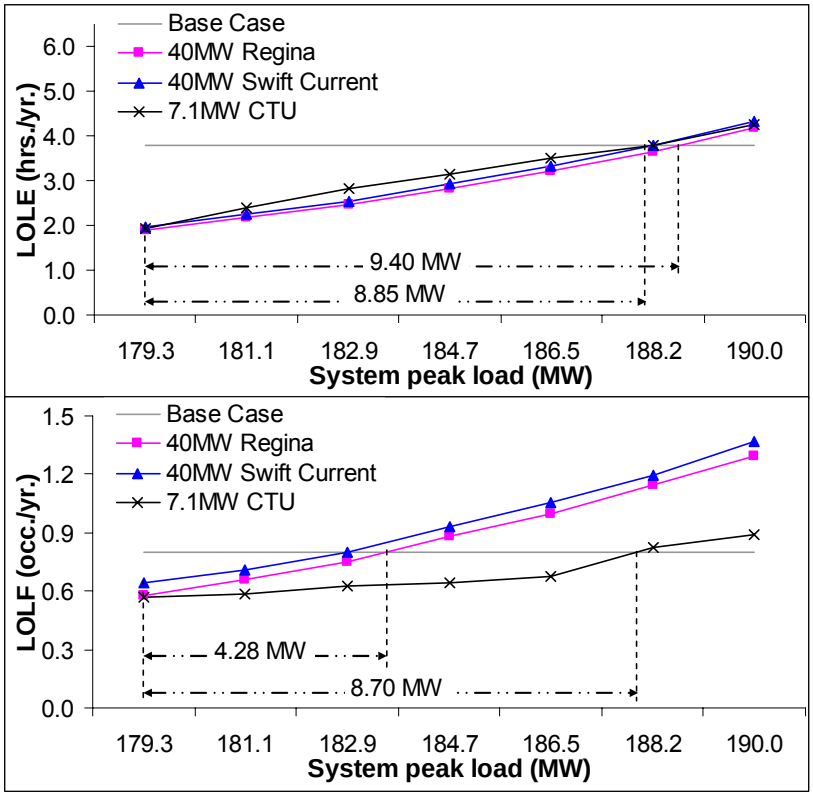

Figure 10.6: ELCC obtained using LOLE and LOLF indices ($ELCC_{(LOLE)}$ and $ELCC_{(LOLF)}$).

Figure 10.6 shows the load carrying capabilities obtained using LOLE and LOLF based indices for three study scenarios on the RBTS. Two scenarios demonstrate the peak load carrying capability based on 40 MW of WECS installed capacity using Regina and Swift Current data. The third scenario used for comparison purposes is based on the load carrying capability obtained from a 7.1 MW combustion turbine unit (CTU) that provides a comparative reliability level (LOLE) under the original peak load condition to that obtained with 40 MW of WECS installed capacity with Regina data. The base case indicates the original system reliability when there is no other generation added to the system. The results illustrated in Figure 10.6 show that load carrying capabilities

obtained using the LOLE index for the three cases have relatively similar profiles whereas those obtained using the LOLF index are distinctly different for the WECS cases and the CTU case. The load carrying capabilities obtained using the LOLE and LOLF for the 7.1 MW CTU case are very similar (8.85 MW and 8.70 MW respectively) while the $ELCC_{(LOLE)}$ and $ELCC_{(LOLF)}$ for the 40 MW WECS installed capacity with Regina data are significantly different (9.40 MW and 4.28 MW respectively). The utilization of a LOEE index in load carrying capability assessment has also been examined and it appears that the utilization of LOEE provides similar results to those obtained using the LOLE based index. The focus, therefore, in the following is on comparisons of LOLE and LOLF in load carrying capability analysis.

The utilization of a LOLF index when dealing with wind power provides an appreciation of the intrinsic behavior of this highly variable source in regard to the overall system reliability. It is obvious in this example that additional generation in the form of WECS provides a system reliability benefit that is quite different from that of a conventional generator. This is shown in Figure 10.6 where the $ELCC_{(LOLE)}$ and $ELCC_{(LOLF)}$ for WECS are quite different, while they are very similar for the conventional generating unit. The capacity value obtained using the $ELCC_{(LOLF)}$ includes the frequency of supply interruptions due to wind power variability, and therefore has both adequacy and security connotations. Figure 10.6 shows that the ELCC determined using the LOLF and the LOLE are different for the two wind sites. The wind farm with Swift Current data has a lower $ELCC_{(LOLF)}$ than that obtained using Regina data due to the higher hourly wind speed variations, which can be investigated using the auto-correlation test. Figure 10.7 shows the $ELCC_{(LOLE)}$ and $ELCC_{(LOLF)}$ obtained using Regina and Swift Current data at different wind power penetration levels. Wind penetration level percentages are calculated using the total WECS installed capacity divided by the total system generation capacity which includes both conventional generating units and WECS.

Figure 10.7 shows that the $ELCC_{(LOLE)}$ and $ELCC_{(LOLF)}$ percentages decline when the WECS installed capacity increases. The differences in $ELCC_{(LOLE)}$ and

$ELCC_{(LOLF)}$ at very low wind power penetrations are not significant, but the difference increases sharply and then gradually declines. Although the $ELCC_{(LOLE)}$ obtained using the Regina and Swift Current data are quite similar, the $ELCC_{(LOLF)}$ obtained using these two sites are relatively different. The $ELCC_{(LOLF)}$ based on Swift Current data is considerably lower than that based on Regina data. The difference between the two ELCC profiles indicates the potential difference in capacity benefits based on adequacy and security considerations. The difference for the Swift Current data is considerably larger than that for the Regina data. This implies that even though the long-term planning capacity values for both locations are quite competitive, the operational benefits at Swift Current are potentially lower than those for Regina due to Swift Current's higher hourly wind variation.

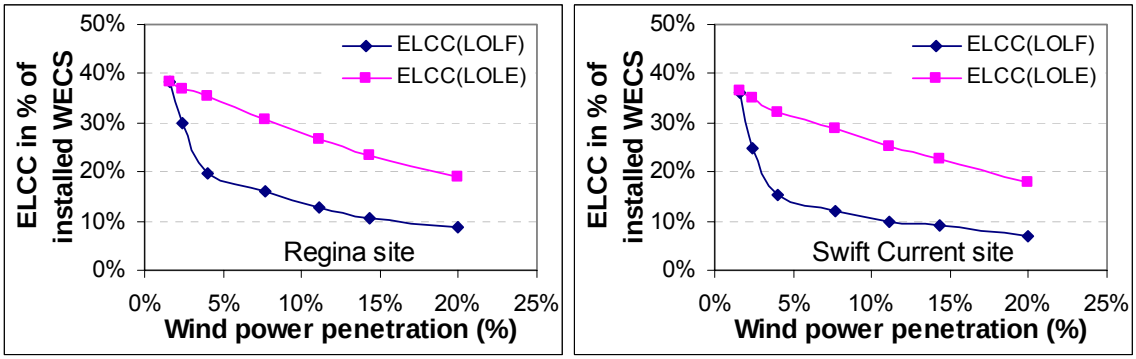

Figure 10.7: $ELCC_{(LOLE)}$ and $ELCC_{(LOLF)}$ for the RBTS at different penetration levels.

Some studies suggest that the capacity benefit of a WECS obtained using the LOLE is relatively close to the WECS capacity factor. This depends on wind conditions and wind power penetration. Power utilities who utilize frequency-related reliability criteria could suffer from overestimating the potential of WECS capacity benefits in their systems based on LOLE. The ELCC is a function of the system capability composition, the equipment parameters, desired system reliability, the system size, and the wind conditions at the site. The profile differences shown in Figure 10.7 could be different for other systems even though the same wind regimes are utilized. This is further illustrated as shown in Figure 10.8 using the IEEE-RTS. A similar conclusion to that drawn for Figure 10.7 can be applied to Figure 10.8. The differences between the $ELCC_{(LOLE)}$ and $ELCC_{(LOLF)}$ profiles shown in Figure 10.7 for the smaller system

(RBTS) case are more significant than those shown in Figure 10.8 for the larger system (IEEE-RTS). The utilization of both LOLE and LOLF indices provides a more comprehensive assessment of the risk of system interruptions for a power system with significant wind energy.

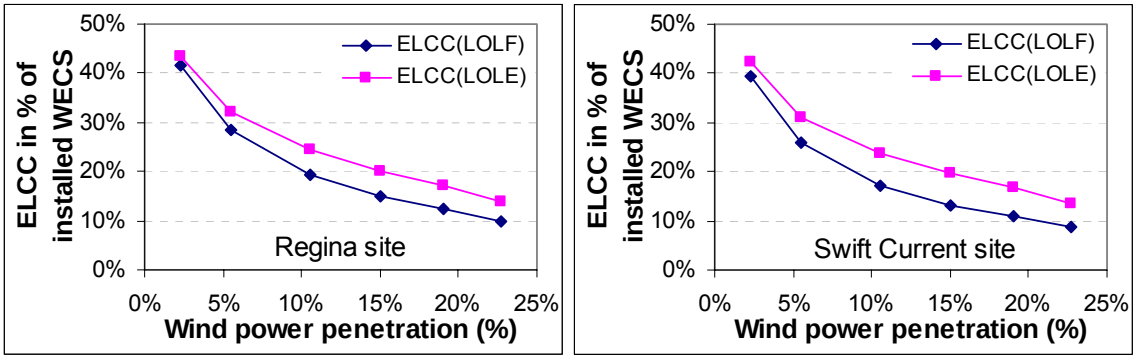

Figure 10.8: $ELCC_{(LOLE)}$ and $ELCC_{(LOLF)}$ for the IEEE-RTS at different penetration levels.

10.4 Transmission Constraints and Reinforcements Associated with WECS

The previous section is focused on generating adequacy (HL-I) analysis in which transmission contingencies are not incorporated. In this section, both generation and transmission contingencies (HL-II analysis) are considered. Connecting the WECS to different locations in a bulk system can have different impacts on the overall system reliability depending on the system topology and conditions. Connecting a large-scale WECS to an area which has weak transmission could create system operating constraints and provide less system benefit than connecting it to an area with stronger transmission. This section investigates bulk electric system transmission constraints associated with a large-scale wind farm. Transmission reinforcement in a weak transmission area in order to absorb more wind power in a system is also illustrated in this section.

10.4.1 Effect of Connecting a Large-Scale WECS at Different Locations

This section investigates the reliability impact of connecting a WECS at different locations in a bulk electric system. Two study scenarios are used in this section. The first scenario is based on the original IEEE-RTS described in Section 3.6.2. This system has a

strong transmission network (high transfer capability margin), but is generation deficient. The second scenario is based on the modified IEEE-RTS described in Section 9.4.2. There is significant transmission utilization in this system as the bulk of the generating capacity is located in the northern area. Considerable power is therefore transferred from the northern to the southern portion. This creates transmission congestion in the northern part (230 kV). The southern area (138 kV) can be considered to have both generation and transmission deficiencies.

Selected reliability indices obtained using the original and modified IEEE-RTS without WECS additions are shown in Table 10.3. These results are designated as the base case values and are compared with the results obtained in a series of studies involving different WECS connections. The load shedding philosophy used in this analysis is the pass-1 policy, and the number of simulation years is 6,000 years.

Table 10.3: Base case system reliability indices of the original and modified IEEE-RTS (No WECS addition).

Overall System Reliability Indices	Original IEEE-RTS	Modified IEEE-RTS
EFLC (occ/yr)	9.02	3.78
EDLC (hrs/yr)	35.26	13.55
ECOST (M$/yr)	18.962	10.094
DPUI (sys.mins)	97.81	47.65

Buses 1, 8, 13 and 18 were selected for connection to a WECS in order to examine the reliability impact associated with system location. Two different WECS installations with 120 MW and 480 MW of installed capacity were considered. In the 120 MW WECS case, a single transmission line with a line rating of 308 MVA is used to connect the WECS to the bulk system. In the 480 MW WECS case, two transmission lines with individual line ratings of 308 MVA are used to connect the WECS to the bulk system. The failure rate and average repair time of the transmission lines are 1 failure/year and 10 hours respectively. All the wind turbine generators (WTG) are assumed to be identical with the reliability parameters and power curve characteristics

described in Section 10.2.2. The Regina wind regime is utilized in this study and it is assumed that wind power is dispatched whenever it is available.

Tables 10.4 and 10.5 respectively show the system reliability indices for the original IEEE-RTS with the 120 MW and 480 MW WECS connected at the selected locations in the system.

Table 10.4: System reliability indices for the original IEEE-RTS when 120 MW of WECS is connected at the four different locations using a single line.

Overall System Reliability Indices	Location to Connect the WECS			
	at Bus 1	at Bus 8	at Bus 13	at Bus 18
EFLC (occ/yr)	7.95	7.80	8.18	7.85
EDLC (hrs/yr)	29.00	28.83	32.02	28.98
ECOST (M$/yr)	15.172	15.179	15.882	15.254
DPUI (sys.mins)	78.49	78.54	82.05	78.92

Table 10.5: System reliability indices for the original IEEE-RTS when 480 MW of WECS is connected at the four different locations using two lines.

Overall System Reliability Indices	Location to Connect the WECS			
	at Bus 1	at Bus 8	at Bus 13	at Bus 18
EFLC (occ/yr)	8.22	8.97	6.37	6.47
EDLC (hrs/yr)	24.59	24.53	19.86	20.25
ECOST (M$/yr)	11.057	10.955	10.391	10.589
DPUI (sys.mins)	57.09	56.70	53.78	54.78

All the reliability indices shown in Tables 10.4 and 10.5 can be used for comparison purposes. The frequency-related index EFLC and the severity index DPUI are focused on due to their relationships with the variability of wind power and with the size of the WECS installed capacity. Table 10.4 shows that the system reliability indices when connecting the 120 MW WECS at the four different locations are relatively similar. There are reasonable improvements in system reliability compared to the original IEEE-RTS base case shown in Table 10.3. Connecting the 120 MW WECS to Bus 13 provides the lowest reliability improvement for the four locations. This is not the case in the 480 MW WECS study as shown in Table 10.5. The results in this study show

that connecting the 480 MW WECS at Bus 13 results in the highest reliability improvement for the four buses. The reason for this is that there is a considerable change in the network power flows when significant wind power is injected at Bus 13. Bus 13 is in a central location and supports both the central and southern areas. Power flow in the western side will subsequently reduce. Table 10.5 also indicates that connecting the 480 MW WECS to Bus 1 or Bus 8 leads to lower reliability improvements than when connecting the WECS to Bus 13 or Bus 18. The reason for this is that the 480 MW WECS results in transmission congestion (overload on Line # 1 when connecting the WECS to Bus 1, and overloads on Lines # 12 and 13 when connecting the WECS to Bus 8). This is due to the fact that most of the transmission line ratings in the southern part (138 kV) of the IEEE-RTS are limited to 208 MVA. A significant amount of wind power will cause system congestion if all the available wind power is dispatched prior to conventional generation and there is no wind power curtailment policy. Connecting a 480 MW WECS to Bus 13 or Bus 18 is more advantageous as the transmission network in the north (230 kV) is much stronger than that in the south. The differences in reliability improvement shown in Table 10.5 when connecting the 480 MW WECS at the four different locations are, however, not very significant for the original IEEE-RTS.

The second scenario is based on the modified IEEE-RTS. This system is considered to be under stress due to the considerable utilization of the transmission network. A significant amount of power flows from the north to the south due to the abundance of generation in the north and the southern area has both generation and transmission constraint problems. Similar studies to those conducted on the original IEEE-RTS were conducted on the modified IEEE-RTS. Tables 10.6 and 10.7 respectively show the system reliability indices for the modified IEEE-RTS when 120 MW and 480 MW of WECS capacities are added to the system.

Tables 10.6 and 10.7 indicate that connecting the 120 MW or 480 MW WECS to the southern part of the modified IEEE-RTS (Bus 1 or Bus 8) significantly improves the overall system reliability. The improvement is more than that obtained by connecting the WECS in the northern area (Bus 13 or Bus 18). The severity indices are considerably

different for the cases when the WECS are connecting in the northern and southern areas. The DPUI for the Bus 1 and Bus 8 cases (southern) are very similar, and the DPUI for the Bus 13 and Bus 18 cases (northern) are similar. This is basically due to the fact that the heavy power flows from the north to the south are reduced when the WECS are installed in the southern region which increases the available transfer capability margins of the northern transmission facilities.

Table 10.6: System reliability indices for the modified IEEE-RTS when 120 MW of WECS is connected at the four different locations using a single line.

Overall System Reliability Indices	Location to Connect the WECS			
	at Bus 1	at Bus 8	at Bus 13	at Bus 18
EFLC (occ/yr)	3.66	3.56	3.71	3.77
EDLC (hrs/yr)	11.54	11.80	13.25	13.13
ECOST (M$/yr)	8.154	8.186	9.977	9.732
DPUI (sys.mins)	38.34	38.35	46.34	45.66

Table 10.7: System reliability indices for the modified IEEE-RTS when 480 MW of WECS is connected at the four different locations using two lines.

Overall System Reliability Indices	Location to Connect the WECS			
	at Bus 1	at Bus 8	at Bus 13	at Bus 18
EFLC (occ/yr)	4.84	3.11	3.13	5.06
EDLC (hrs/yr)	11.53	9.02	10.07	15.11
ECOST (M$/yr)	5.701	6.068	8.917	9.638
DPUI (sys.mins)	26.21	28.23	42.84	45.35

As shown in Table 10.6 for the 120 MW WECS scenario, all the EFLC for the four cases decrease compared with the base case values shown in Table 10.3. This is not the case for the 480 MW WECS study shown in Table 10.7 where the EFLC is higher than that of the base case shown in Table 10.3 when the WECS is connected to Bus 1 or to Bus 18. The EFLC when the WECS is connected to Bus 8 or to Bus 13 decreases compared to that for the base case. Connecting the 480 MW WECS to Bus 1 creates considerable transmission congestion (overload) on Line # 1 (underground cable between Bus 1 and Bus 2). Similarly, Line # 23 (between Bus 14 and Bus 16) is heavily congested when the 480 MW WECS is connected to Bus 18 due to heavier power flow

from the north to the south. It is interesting to note that the DPUI as shown in Table 10.7 for the cases when the 480 MW WECS is connected to Bus 13 or Bus 18 only slightly decrease compared to the DPUI when the 120 MW WECS is connected to Bus 13 or Bus 18 as shown in Table 10.6. This implies that adding additional wind power at these buses is not very effectively in improving the system reliability. The reliability improvement percentages in the DPUI due to the WECS over the base case DPUI presented in Table 10.3 are shown in Figure 10.9.

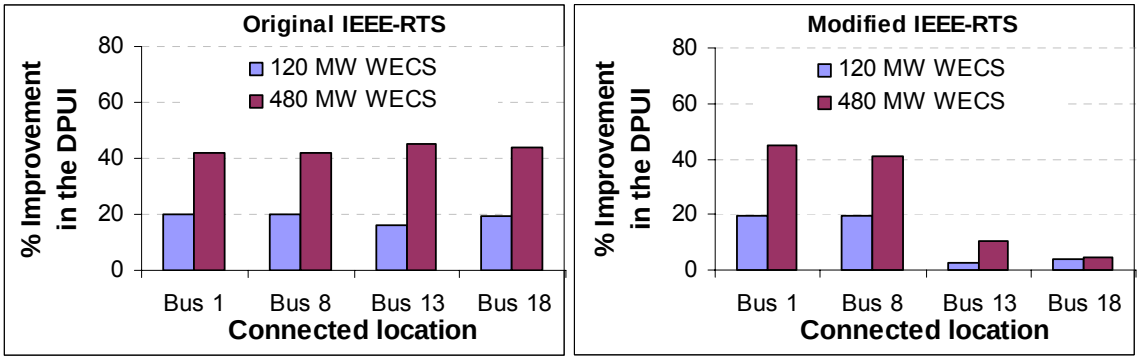

Figure 10.9: DPUI improvement over the base case by adding 120 MW and 480 MW of WECS capacity to the original and the modified IEEE-RTS.

In conclusion, the impact of wind power on system reliability is not only dependent on the wind regime, but is also related to the connection point in the bulk system. This impact is also dependent on the overall system topology and the operating conditions particularly those associated with transmission limitations. For example, the locations used to connect the WECS in the modified IEEE-RTS play more important roles in reliability improvement than those used when connecting the WECS to the original IEEE-RTS. This is due to the fact that there is significant transmission utilization in the modified IEEE-RTS, and therefore more transmission constraints compared to the original IEEE-RTS. Transmission capacities play an important role in restricting the maximum amount of wind power that a system can absorb without creating deterioration in the overall system reliability. The following section investigates the maximum amount of wind power that a system can absorb without deteriorating the overall system reliability when connecting the WECS at specific locations.

10.4.2 Transmission Capacity Limitations Associated with WECS

A bulk electric system can encounter transmission capacity limitation problems when a large-scale WECS is connected to a weak transmission area. The maximum amount of wind power that a system can absorb without violating the system constraints is dependent on the connection point in the system. This section examines the reliability impacts when various amounts of wind power are injected into a bulk electric system at specified locations. The modified IEEE-RTS is used in this study. Buses 1 and 8 were selected as the specific connection points. WECS installed capacities of 120, 240, 360 and 480 MW are used. Two transmission lines with individual line ratings of 308 MVA, similar to those described in the previous section, are used in this study to connect the WECS to the system for all the WECS installed capacities. Case studies based on the utilization of single and multiple wind farms are also considered in this section.

A. Single Wind Farm

The Regina wind regime is used to model the WECS in this section. Tables 10.8 and 10.9 respectively show the system reliability indices for the modified IEEE-RTS when the WECS is connected to Bus 1 and Bus 8. Table 10.8 indicates that the EFLC decreases when the WECS capacity increases from 120 MW to 240 MW. The EFLC for the case of 360 MW capacity, however, increases compared to the 240 MW value. A higher EFLC can be expected when the WECS capacity increases beyond 360 MW due to the fact that there is an average overload duration of 2 hrs/yr on Line # 1 (between Buses 1 and 2) when 360 MW of WECS is added at Bus 1. An average overload duration of 16 hrs/yr on Line # 1 occurs when the 480 MW of WECS is added at Bus 1. It should be noted that in these studies, there is no wind power curtailment policy applied and all the available wind power is used prior to dispatching conventional generation. It is also important to note that even though the EFLC increases when the WECS addition at Bus 1 exceeds 240 MW, the DPUI gradually decreases when larger WECS are utilized. These studies indicate that based on the EFLC, the maximum WECS

capacity that should be connected at Bus 1 is around 240 MW. Additional studies using different WECS capacities should be conducted to determine the specific value.

Table 10.8: System reliability indices for the modified IEEE-RTS when different WECS capacities are connected at Bus 1.

Overall System Reliability Indices	WECS Installed Capacity			
	120 MW	240 MW	360 MW	480 MW
EFLC (occ/yr)	3.36	3.19	3.28	4.84
EDLC (hrs/yr)	11.20	10.02	9.51	11.53
ECOST (M$/yr)	7.822	6.816	6.118	5.701
DPUI (sys.mins)	36.52	31.70	28.23	26.21

Table 10.9: System reliability indices for the modified IEEE-RTS when different WECS capacities are connected at Bus 8.

Overall System Reliability Indices	WECS Installed Capacity			
	120 MW	240 MW	360 MW	480 MW
EFLC (occ/yr)	3.32	3.02	2.88	3.11
EDLC (hrs/yr)	11.23	10.00	9.26	9.02
ECOST (M$/yr)	8.237	7.246	6.550	6.068
DPUI (sys.mins)	38.54	33.74	30.38	28.23

In a similar manner, Table 10.9 indicates that the maximum WECS capacity that should be connected at Bus 8 is around 360 MW. This is due to the average overload durations on Lines # 12 and 13 respectively of 0.5 and 1 hr/yr. Tables 10.8 and 10.9 show that the WECS capacities that the bulk system can absorb at the two different connection points are considerably different. In practice, the location of a large-scale wind farm is dependent on the existence of a suitable wind regime. The studies shown in this section can be used to investigate the reliability benefit of all the potential BES connection points in close proximity to the wind power development area. The studies can also be used to assist in system reinforcement planning to assess the system capability to absorb more wind power at specified locations.

B. Multiple Wind Farms

A single wind farm is used in the previous section to examine the maximum WECS capacity that a system can absorb, without violating the system constraints. In the case of a single wind farm, the maximum wind power at a specific point of time could be very close or equal to the total WECS installed capacity as all the WTG are subject to the same wind regime. This is not the case for multiple large-scale wind farms where the WTG at different locations may not be subjected to the same wind speed. Consequently, the total maximum wind power produced will not often be equal to the sum of the individual wind farm capacities. The transmission network may in fact be able to absorb more WECS capacity when multiple wind farms are used. This section examines the impact of multiple wind farms on system reliability improvement. Two wind regimes designated as Regina and Swift Current are used in this study. The wind speeds for the two wind farms are assumed to have a cross-correlation factor (R_{xy}) of 0.75. The installed capacity of each wind farm is assumed to be equal, and therefore the total installed capacity is twice the individual wind farm capacity. The two wind farms are assumed to be in reasonably close proximity and connected to the modified IEEE-RTS at Bus 1 through two transmission lines as illustrated in Figure 10.10. A similar arrangement is used to add WECS capacity at Bus 8 in the following analyses.

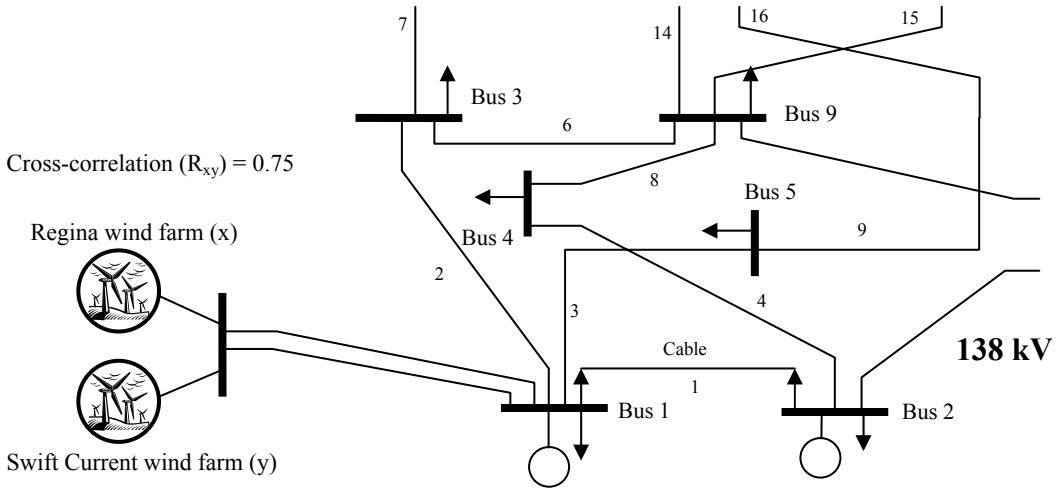

Figure 10.10: Multiple wind farms connected to Bus 1 of the modified IEEE-RTS.

Tables 10.10 and 10.11 respectively show the system reliability indices when two identical capacity WECS and different total installed capacities are connected at Bus 1 and Bus 8.

Table 10.10: System reliability indices for the modified IEEE-RTS when two identical capacity WECS and different total capacities are connected at Bus 1.

Overall System Reliability Indices	WECS Installed Capacity			
	120 MW	240 MW	360 MW	480 MW
EFLC (occ/yr)	3.38	3.16	3.19	4.43
EDLC (hrs/yr)	11.26	10.00	9.37	10.69
ECOST (M$/yr)	7.918	6.777	6.101	5.670
DPUI (sys.mins)	37.07	31.55	28.28	26.13

Table 10.11: System reliability indices for the modified IEEE-RTS when two identical capacity WECS and different total capacities are connected at Bus 8.

Overall System Reliability Indices	WECS Installed Capacity			
	120 MW	240 MW	360 MW	480 MW
EFLC (occ/yr)	3.32	3.00	2.86	2.92
EDLC (hrs/yr)	11.24	10.02	9.22	8.74
ECOST (M$/yr)	8.281	7.324	6.602	5.974
DPUI (sys.mins)	38.81	34.28	30.70	27.71

The results shown in Tables 10.10 and 10.11 for the multiple WECS cases can be compared with those shown in Tables 10.8 and 10.9 for the single WECS cases. In general, there is more reliability benefit when two wind farms, which are reasonably close to each other (R_{xy} = 0.75) are utilized rather than using a single wind farm. The frequency and duration related indices (EFLC and EDLC) basically improve by using two wind farms. The severity index DPUI for each WECS addition is basically similar to that obtained using a single wind farm.

Table 10.10 indicates that the EFLC for the 360 MW WECS case is very close to the 240 MW case when connecting two WECS to Bus 1. This implies that the maximum WECS capacity that the system can absorb, can be increased compared to the single wind farm case. The average overload duration on Line # 1 in the 360 MW two wind

farm case is reduced to 1 hr/yr from 2 hrs/yr for the single wind farm. The EFLC increases due to transmission congestion on Line # 1 for the 480 MW two wind farm case. The average overload duration on Line # 1 for the 480 MW two wind farm case reduces to 12 hrs/yr compared to the 16 hrs/yr for the 480 MW single wind farm. This suggests that transmission reinforcement is required in order to add more WECS capacity at Bus 1.

Table 10.11 shows the results when the two wind farms are connected at Bus 8. The results indicate that the EFLC for the 480 MW WECS case is very close to the 360 MW value when the two WECS are connected at Bus 8. The maximum WECS capacity that the system can absorb through Bus 8, can be increased to 480 MW compared to 360 MW under a single farm situation. This indicates that the bulk system can absorb the total 480 MW installed capacity from two wind farms through Bus 8 without requiring major system reinforcement.

The results show that Bus 8 can absorb up to 480 MW of WECS and that Bus 1 cannot absorb 480 MW of WECS without severely violating the transmission constraints. Transmission system reinforcement is considered in the following section for the case in which 480 MW of WECS in two wind farms is added at Bus 1 in the modified IEEE-RTS.

10.4.3 Transmission Reinforcement Planning Associated with WECS

Two wind farms with a total of 480 MW installed capacity are assumed to be located in the south-western region of the modified IEEE-RTS shown in Figure 10.10. The shortest path to connect the wind farm to the bulk system is through Bus 1 and is 80 km in length. The distances from the wind farms to Bus 3 and Bus 4 are approximately 100 km in each case. As noted earlier, there is a transmission limitation when connecting 480 MW of WECS to Bus 1. This section examines possible transmission reinforcement alternatives in order to absorb this amount of wind capacity without severely violating the transmission constraints. This section describes three studies. The first study

considers the case where the wind farm owner pays for the connection path to the bulk system. The wind farm owner will attempt to minimize the overall connection costs by building two transmission lines to the closest bus. In the second study, the system planner negotiates with the wind farm owner to reroute the connection path to benefit the overall system reliability. In this case, the system planner should subsidize some part of the connection cost incurred by the wind farm owner. Reliability cost/reliability worth analyses are conducted on the selected transmission reinforcement alternatives to determine the optimum planning option in the third study.

A. Wind Farm Owner Pays the Overall Connection Costs

In this section, it is assumed that the wind farm owner chooses to build two parallel lines to Bus 1. This is the shortest path to the bulk system (80 km in length). This would be the economically preferable option from a wind farm owner's perspective and does not consider any possible bulk system constraints that might arise from injecting a significant amount of wind power at this location. The bulk system planner is considered to be responsible for any system reinforcements required in order to absorb the 480 MW of WECS into the system. Five selected reinforcement alternatives are shown in Figure 10.11. These alternatives are designated as follows:

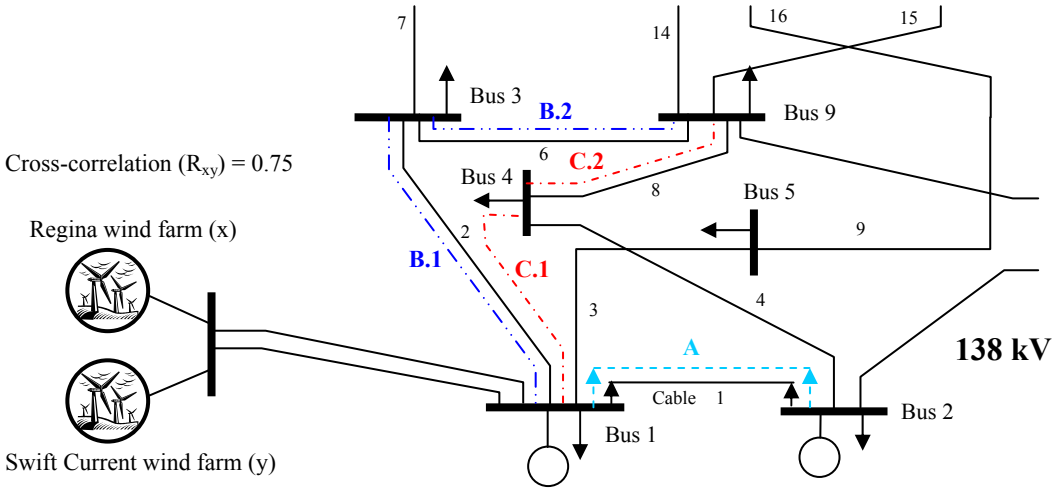

Figure 10.11: Transmission reinforcement alternatives (Alternatives 1 – 5) for the modified IEEE-RTS with the 480 MW WECS addition.

Alternative 1: Constructing Line A

Alternative 2: Constructing Line B.1

Alternative 3: Constructing Line C.1

Alternative 4: Constructing Lines B.1 and B.2

Alternative 5: Constructing Lines C.1 and C.2

The system reliability indices for the five transmission reinforcement cases (Alternatives 1 – 5) for the modified IEEE-RTS with the 480 MW WECS addition are shown in Table 10.12.

Table 10.12: System reliability indices for the modified IEEE-RTS with the five transmission reinforcement alternatives when the 480 MW WECS addition is connected to Bus 1.

Overall System Reliability Indices	Transmission Reinforcement Alternative				
	Alter. 1	Alter. 2	Alter. 3	Alter. 4	Alter. 5
EFLC (occ/yr)	2.77	4.01	3.05	3.53	2.88
EDLC (hrs/yr)	8.18	9.45	8.45	8.47	7.75
ECOST (M$/yr)	5.123	4.729	5.740	4.339	4.609
DPUI (sys.mins)	24.27	21.59	26.50	19.86	21.19

Table 10.12 shows that Alternative 1 (constructing line A) provides the lowest EFLC and a low EDLC. This is due to the fact that transmission congestion on Line # 1 is alleviated by constructing a parallel path. Alternative 2 (constructing line B.1) provides the least reliability improvement. The reason for this is that constructing line B.1 does not effectively alleviate the overload on Line # 1. The average overload duration on Line # 1 in this case decreases slightly from 12 hrs/yr, before reinforcement to 10 hrs/yr. Alternative 3 (constructing line C.1) reduces the average overload duration on Line # 1 to 2 hrs/yr. The average overload duration on Line # 1 decreases slightly to 9 hrs/yr by constructing lines B.1 and B.2 (Alternative 4). The severity index DPUI in this case is the lowest of the five alternatives. Alternative 4 strengthens the transmission around Bus 3 which results in a considerable reduction in the unserved energy at this bus. Alternative 5 (constructing lines C.1 and C.2) results in the lowest EDLC and the

second lowest EFLC. An overload on Line # 1, however, still exists for an average of 2 hrs/yr. Reliability cost/worth analyses of these five reinforcement alternatives are addressed later in this chapter.

B. Wind Farm Connection Costs Partially Subsidized by the System Planner

In the previous section, the wind farm owner is assumed to construct the required connection at the minimum cost. This involves the shortest path with parallel circuits on the same structure. This process does not involve transmission network limitation considerations, and any positive or negative impacts on the overall system reliability. In this study, the system planner is assumed to be involved in deciding which connection path should be utilized. Negotiations between the system planner and the wind farm owner to consider alternative connection paths and the resulting additional connection costs incurred are required in this case. The system planner should pay for any increase in the connection costs incurred due to rerouting the connection paths to benefit the overall system reliability. Six selected transmission reinforcement alternatives are considered in this section, and are designated as Alternatives 6 – 11. These alternatives are shown in Figures 10.12 – 10.14 and are described as follows:

Alternative 6: Constructing Line D
Alternative 7: Constructing Lines D and B.2
Alternative 8: Constructing Line E
Alternative 9: Constructing Lines E and C.2
Alternative 10: Constructing Lines D and E
Alternative 11: Constructing Lines D, E and C.2

The system reliability indices for Alternatives 6 – 11 for the modified IEEE-RTS with the 480 MW WECS addition are shown in Table 10.13.

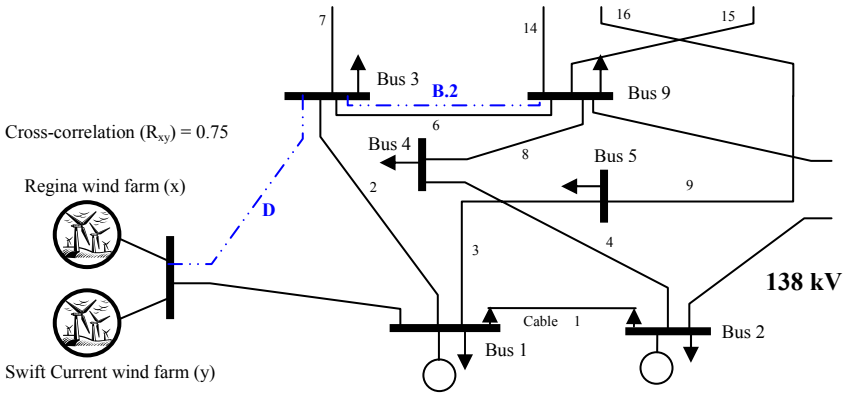

Figure 10.12: Transmission reinforcement alternatives (Alternatives 6 and 7) for the modified IEEE-RTS with the 480 MW WECS addition.

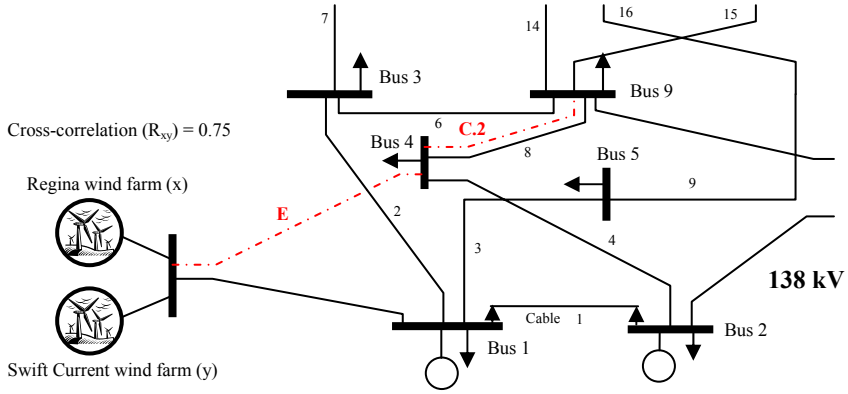

Figure 10.13: Transmission reinforcement alternatives (Alternatives 8 and 9) for the modified IEEE-RTS with the 480 MW WECS addition.

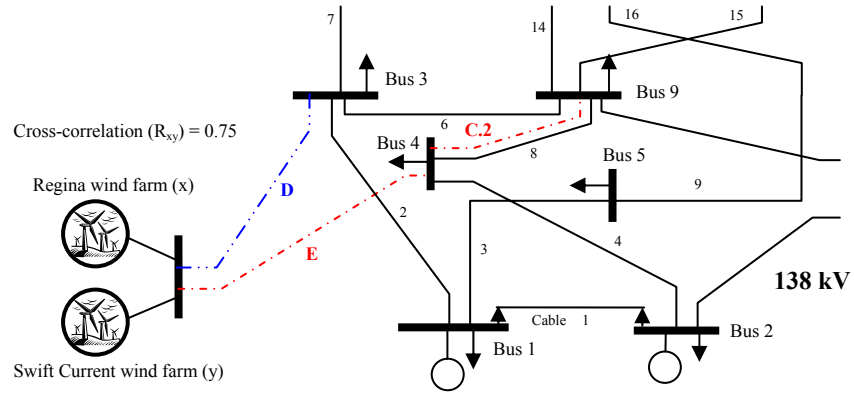

Figure 10.14: Transmission reinforcement alternatives (Alternatives 10 and 11) for the modified IEEE-RTS with the 480 MW WECS addition.

Table 10.13: System reliability indices for the modified IEEE-RTS with the six transmission reinforcement alternatives when 480 MW of WECS is connected to the system.

Overall System Reliability Indices	Transmission Reinforcement Alternative					
	Alter. 6	Alter. 7	Alter. 8	Alter. 9	Alter. 10	Alter. 11
EFLC (occ/yr)	2.71	2.49	2.63	2.39	2.53	2.31
EDLC (hrs/yr)	7.26	6.85	7.51	6.80	6.49	6.10
ECOST (M$/yr)	4.174	3.664	4.883	4.216	3.394	3.146
DPUI (sys.mins)	19.33	17.13	22.83	19.81	16.13	14.99

Table 10.13 indicates that Alternative 11 provides the highest overall system reliability improvement followed by Alternative 10. Overload on Line # 1 is eliminated in the case of Alternatives 8 – 11 due to rerouting the connection paths. An average overload duration of 1 hr/yr on Line # 1 still exists in Alternatives 6 and 7. The severity index DPUI for Alternatives 6 and 7 are, however, lower than those for Alternatives 8 and 9. As noted earlier, transmission reinforcement at Bus 3 results in a significant decrease in unserved energy at this bus.

An economic analysis of the eleven transmission reinforcement alternatives are examined using reliability cost/reliability worth considerations in the next section. An optimum solution may not come from the alternative that provides the highest reliability, and the alternative with the lowest investment cost may not be utilized if it does not provide suitable reliability improvement.

C. Transmission Reinforcement Selection Using Reliability Cost/Worth Analysis

The concept and application of reliability cost/reliability worth analysis are illustrated in Chapter 9 considering both adequacy and security perspectives. A similar cost/worth analysis process is applied in this chapter. The studies conducted in this chapter are, however, focused on adequacy assessment and security-related costs are not considered in this analysis. The customer interruption cost (ECOST) is used together with the investment cost incurred in order to determine the minimum cost option.

In this economic study, the focus is on the utility costs that are incurred due to transmission reinforcements. If the system planner negotiates with the wind farm owner to reroute the connection path in order to improve the overall system reliability, part of the connection costs should be paid by the system planner. This additional cost is taken into account in the following economic analysis. Reliability cost/worth analyses for all the eleven transmission reinforcement alternatives described earlier were conducted using the following assumptions.

Investment cost of a 138 kV overhead transmission line = 0.4 M$/km
Investment cost of a 138 kV underground transmission line = 2.4 M$/km
Transmission line length: Line A = 5 km (underground cable)
Line B.1 = 88 km, Line B.2 = 50 km
Line C.1 = 36 km, Line C.2 = 44 km
Line D = 100 km, Line E = 100 km
Useful lifetime considered = 40 years
Line maintenance cost (during a useful lifetime) = 5% of the project cost
Discount rate (present worth rate) = 8% per year

Therefore, CRF $= \dfrac{0.08(1+0.08)^{40}}{(1+0.08)^{40}-1} = 0.08386$

The wind farm owner pays the transmission connection costs for Alternatives 1 to 5.

For Alternative 1: Constructing Line A (underground cable)
Project cost (P_1) = investment cost + maintenance cost
= 2.4×5 (M$) + 0.05×2.4×5 (M$) = 12.60 (M$)
The annual capital payment (ACP_1) = P_1×CRF = 12.60×0.08386 = 1.057 M$/yr.

For Alternative 2: Constructing Line B.1
Project cost (P_2) = 1.05×(0.4×88) = 36.96 (M$)
The annual capital payment (ACP_2) = P_2×CRF = 36.96×0.08386 = 3.099 M$/yr.

For Alternative 3: Constructing Line C.1

Project cost (P_3) = 1.05×(0.4×36) = 15.12 (M$)

The annual capital payment (ACP_3) = P_3×CRF = 15.12×0.08386 = 1.268 M$/yr.

For Alternative 4: Constructing Lines B.1 and B.2

Project cost (P_4) = 1.05×(0.4×88 + 0.4×50) = 57.96 (M$)

The annual capital payment (ACP_4) = P_4×CRF = 57.96×0.08386 = 4.861 M$/yr.

For Alternative 5: Constructing Lines C.1 and C.2

Project cost (P_5) = 1.05×(0.4×36 + 0.4×44) = 33.60 (M$)

The annual capital payment (ACP_5) = P_5×CRF = 33.60×0.08386 = 2.818 M$/yr.

In Alternatives 6 – 11, the system planner negotiates with the wind farm owner to reroute the connection points to provide an overall system reliability benefit. This introduces a possible additional investment cost to the wind farm owner as this requires the construction of longer lines rather than utilizing the shortest path to the bulk system. The investment cost associated with constructing two different paths will be higher than that required to build parallel circuits on the same structure. In this case, the system planner will have to provide funding in order to convince the wind farm owner to reroute the required transmission. In this study, the additional investment and maintenance costs of any rerouted transmission path is paid by the system planner.

The length of the original shortest parallel path from the wind farms to Bus 1 is 80 km. The investment cost of a second line is assumed to be 50% of the cost of the first line when a double circuit structure is used. The wind farm owner's connection cost is as follows:

Project cost (P) = investment cost + maintenance cost

$$= (0.4\times 80 + \frac{1}{2}\times 0.4\times 80) + 0.05\times(0.4\times 80 + \frac{1}{2}\times 0.4\times 80)$$

$$= 50.40 \text{ (M\$)}$$

The original connection cost for the wind farm owner is M$ 50.40. Any additional investment costs due to a rerouted path that exceeds the original connection cost of M$ 50.40 is subsidized by the system planner.

Annual capital payments due to transmission reinforcement planning conducted by the system planner for Alternatives 6 to 11 are as follows:

For Alternative 6: Alternative 6: Constructing Line D (rerouted)

P_6 = (cost of line D + cost of a line to Bus 1) – original connection cost

= 1.05×(0.4×100 + 0.4×80) – 50.40 = 25.20 (M$) (rerouted cost)

The annual capital payment (ACP_6) = P_6×CRF = 25.20×0.08386 = 2.113 M$/yr.

For Alternative 7: Constructing Lines D (rerouted) and B.2

P_7 = 25.20 + 1.05×(0.4×50) = 46.20 (M$)

The annual capital payment (ACP_7) = P_7×CRF = 46.20×0.08386 = 3.874 M$/yr.

For Alternative 8: Constructing Line E (rerouted)

P_8 = (cost of line E + cost of a line to Bus 1) – original connection cost

= 1.05×(0.4×100 + 0.4×80) – 50.40 = 25.20 (M$) (rerouted cost)

The annual capital payment (ACP_8) = P_8×CRF = 25.20×0.08386 = 2.113 M$/yr.

For Alternative 9: Constructing Lines E (rerouted) and C.2

P_9 = 25.20 + 1.05×(0.4×44) = 43.68 (M$)

The annual capital payment (ACP_9) = P_9×CRF = 43.68×0.08386 = 3.663 M$/yr.

For Alternative 10: Constructing Lines D (rerouted) and E (rerouted)

P_{10} = 1.05×(0.4×100 + 0.4×100) – 50.40 = 33.60 (M$)

The annual capital payment (ACP_{10}) = P_{10}×CRF = 33.60×0.08386 = 2.818 M$/yr.

For Alternative 11: Constructing Lines D (rerouted), E (rerouted) and C.2

P_{11} = 33.60 + 1.05×(0.4×44) = 52.08 (M$)

The annual capital payment (ACP_{11}) = $P_{11} \times CRF = 52.08 \times 0.08386 = 4.367$ M$/yr.

The total cost (TOC) of each reinforcement alternative is obtained by summing the expected customer interruption cost (ECOST) and the annual capital payment (ACP). The total costs for all the alternatives are on a one year basis and are shown in Table 10.14. The lowest TOC indicates the optimum alternative based on reliability cost and reliability worth.

Table 10.14: Reliability cost/worth components for the transmission reinforcement alternatives in the modified IEEE-RTS with a 480 MW WECS addition.

Reinforcement Alternative	ACP (M$/yr)	ECOST (M$/yr)	TOC (M$/yr)
Alternative 1	1.057	5.123	6.180
Alternative 2	3.099	4.729	7.828
Alternative 3	1.268	5.740	7.008
Alternative 4	4.861	4.339	9.200
Alternative 5	2.818	4.609	7.427
Alternative 6	2.113	4.174	6.287
Alternative 7	3.874	3.664	7.538
Alternative 8	2.113	4.883	6.996
Alternative 9	3.663	4.216	7.879
Alternative 10	2.818	3.394	6.212
Alternative 11	4.367	3.146	7.513

Table 10.14 indicates that Alternative 1 provides the lowest TOC of 6.180 M$/yr following by Alternatives 10 (6.212 M$/yr) and 6 (6.287 M$/yr). Alternative 1 involves only a short length of underground cable. Alternative 10 is very competitive with Alternative 1 as the TOC of Alternative 10 is only 0.032 M$/yr higher than that of Alternative 1. When considering the components in the total cost, the ECOST due to Alternative 10 is 1.729 M$/yr lower than that of Alternative 1. As shown in Tables 10.12 and 10.13, Alternative 10 provides the second best reliability improvement while Alternative 1 is second last in reliability improvement for the eleven reinforcement alternatives. Alternative 1 with the lowest investment cost does not provide a comparable reliability improvement to that of Alternative 10. The system planner is not involved in the selection of the system connection point for Alternative 1. Alternative 10

involves agreement between the system planner and the wind farm owner to reroute the system connections to provide overall system reliability benefits. Alternative 10 is more advantageous than Alternative 1 and is the best option of the proposed transmission reinforcement planning schemes. This option will facilitate the addition of 480 MW of WECS to the bulk system and provide overall system reliability improvement. Alternative 10 should also prove to be the most attractive when considering future load growth. Long term planning analysis should be conducted as illustrated in Chapter 9 to examine the potential of each alternative.

10.5 Conclusions

Wind power integration in bulk electric system reliability evaluation is presented in this chapter. One advantage of utilizing sequential Monte Carlo simulation in bulk electric system reliability evaluation is that the framework already exists to incorporate the chronological characteristics of wind (diurnal and season wind speeds). Sequential simulation is therefore ideally suited to the analysis of intermittent generating resources such as wind energy conversion systems (WECS). The WECS models involving wind turbine generator power curve characteristics and hourly simulated wind speed using the auto-regressive moving average (ARMA) time series model are illustrated in this chapter. A wind speed simulation model and a correlation adjustment technique to incorporate multiple wind regimes are also presented in this chapter. The correlation adjustment technique provides realistic wind speed simulations for wind regimes that are related to each other. Analyses at both HL-I and HL-II to investigate the reliability impacts associated with wind power are presented. The impact of different degrees of wind speed correlation on the overall system reliability is examined using HL-I analysis. The results show that there is a higher system reliability improvement when wind speeds between wind farms are less correlated, as the wind power at the two sites can support or assist each other and variations in the total wind power are smoothed out. The capacity value of WECS based on the effective load carrying capability (ELCC) technique is investigated using the LOLE and LOLF as the criterion reliability indices. The results

show that the $ELCC_{(LOLE)}$ and $ELCC_{(LOLF)}$ are similar for a conventional generating unit, but can be considerably different for WECS.

The effect of connecting a large-scale WECS at different locations in a bulk electric system is investigated. The results show that the impact on the system reliability of a WECS addition is dependent on the location used to connect the WECS to the bulk system. This is related to the system topology and conditions, particularly when there are transmission system limitations. This chapter also investigates the maximum amount of wind power that can be absorbed by a system without severely violating the system constraints. The maximum amount can vary when connecting the WECS at different locations. The analyses presented in this chapter can be used to determine the maximum WECS installed capacity that can be injected at specified locations in a bulk electric system, and assist system planners to create potential transmission reinforcement schemes to facilitate large-scale WECS additions to the bulk system. Transmission reinforcement planning associated with large-scale WECS, and the utilization of reliability cost/worth analysis in the examination of reinforcement alternatives are also illustrated in this chapter.

CHAPTER 11
SUMMARY AND CONCLUSIONS

Electric power utilities are facing increasing uncertainty regarding the political, economic, societal and environmental constraints under which they have to operate existing systems and plan future systems, and methods capable of analyzing the reliability of bulk electricity systems much larger than in those the past are needed. Modern developments in high speed computation facilities now permit the realistic utilization of sequential Monte Carlo simulation in practical bulk electric system reliability assessment resulting in a more complete understanding of bulk electric system risks and associated uncertainties. This research work is focused on composite generation and transmission system reliability evaluation using sequential Monte Carlo simulation. Sequential simulation can be used to reasonably represent most contingencies and the complex operating characteristics inherent in a bulk electric system and also provide a comprehensive range of reliability indices in both adequacy and steady-state security analyses. Two significant advantages when utilizing sequential simulation are the ability to obtain accurate frequency and duration indices, and the opportunity to synthesize the reliability index probability distributions associated with the mean values.

Non-sequential Monte Carlo simulation techniques are briefly introduced in Chapter 2 together with the basic concepts and methodology of the sequential Monte Carlo simulation approach. The advantages and disadvantages of utilizing the sequential Monte Carlo simulation technique are also discussed in this chapter.

Chapter 3 presents the basic elements in bulk electric system reliability analysis using sequential Monte Carlo simulation. A general review of the basic delivery point

and system indices is presented. Network solution techniques and corrective action methods involving system operating constraints violations are described. Approximate methods for split network and ill-conditioned network solutions are also addressed. The concept of applying different load curtailment philosophies and their implementation in a linear programming technique is discussed in this chapter. The overall sequential simulation procedure for bulk electric system reliability analysis is demonstrated. A computer software using AC based load flow has been developed in this research work and is designated as RapHL-II (Reliability analysis program for HL-II). The two test systems known as the RBTS and IEEE-RTS used throughout the research work are briefly illustrated.

Chapter 4 examines the utilization of sequential and non-sequential Monte Carlo simulation to calculate the interruption frequency indices of a bulk electric power system. Available DC based load flow software known as SECOREL and MECORE respectively are used to investigate the inherent differences in the calculated interruption frequency index by using sequential and non-sequential Monte Carlo simulation. Two factors that influence the frequency index calculation are the system failure state transitions and the demand chronology. These factors are examined and illustrated in this chapter. The results show that the impact of chronology is highly significant, and can exceed the impact of failure state transitions [127]. The sequential simulation approach is the most comprehensive technique available and can be used to provide frequency index estimates that can serve as benchmarks against which other approximate techniques such as the non-sequential method can be compared.

Reliability worth assessment methodologies for bulk electric systems are presented in Chapter 5. The event-based customer interruption cost evaluation (EBCost) technique described in References [68, 69] was implemented in the simulation software (RapHL-II) to provide realistic and accurate incorporation of the temporal variations in customer outage costs in reliability worth analysis. The results obtained using this method therefore can also serve as benchmarks in the development of more approximate methods required due to the absence of detailed information in many real life situations.

Three approximate methods designated as the average demand interrupted, the average delivery point restoration duration and the average system restoration duration approaches are developed and compared in this chapter. These approximate methods can be practically applied in the absence of detailed system information.

Chapter 6 presents the development of delivery point and system reliability index probability distributions in bulk electric systems using the sequential simulation approach. The results show that the reliability index probability distributions for the individual delivery points have unique characteristics. These unique aspects are due to system topology, operating policies and conditions [128]. System operating strategies, particularly those related to load curtailment policies, have important impacts on the individual delivery point characteristics. The load curtailment policies, however, have relatively little impact on the overall system reliability indices other than those related to reliability worth [102]. The concept of predicting bulk electric system reliability performance indices and their probability distributions [129, 130] is demonstrated in this chapter and sensitivity analyses are conducted to investigate the impacts of repair time distribution modeling. The results show that component repair time distribution characteristics have a considerable effect on the probability distributions of duration-related indices such as the SAIDI and SARI of a single circuit delivery point. The impact is, however, less significant on the probability distributions of SAIDI and SARI for multi-circuit delivery points.

The utilization of bulk electric system reliability performance index probability distributions in a performance based regulation (PBR) mechanism is introduced in Chapter 7. The SAIFI and SAIDI for bulk electric systems are utilized in separate reward/penalty PBR frameworks. Actual historical data and simulated bulk electric system reliability performance indices are applied to hypothetical PBR frameworks in this chapter. A discussion of the potential utilization of the PBR protocol for overall bulk electric systems is presented. This discussion is extended to include the utilization of reliability performance index probability distributions in a PBR mechanism applied to a transmission company.

Bulk electric system well-being analysis using sequential Monte Carlo simulation is presented in Chapter 8. The system well-being concept provides a probabilistic framework that incorporates a practical simplification of the traditional operating states associated with the accepted deterministic N-1 security criterion, and therefore steady-state security considerations are recognized in system well-being analysis. The results indicate that different system conditions that result in a similar degree of system risk may not necessarily result in the same degree of system stress [131]. The reverse is also true. The utilization of sequential simulation in bulk electric system well-being analysis provides accurate frequency and duration assessments and the associated well-being index probability distributions.

Chapter 9 introduces a combined reliability analysis framework for bulk electric systems that includes both security and adequacy perspectives. The combined framework is achieved using system well-being analysis and traditional adequacy assessment. System well-being analysis is used to quantify the degree of N-1 security and N-1 insecurity in terms of probabilities and frequencies. Traditional adequacy assessment is incorporated to quantify the magnitude of the severity and consequences associated with system failure. Selected adequacy-based and security-based indices are used to create a comprehensive combined reliability framework. The results based on the combined reliability framework indicate that system adequacy is adversely affected by a generation deficient environment and system security is adversely affected by a transmission deficient environment. A system planning process using combined adequacy and security considerations offers an additional reliability-based dimension. The proposed process is illustrated by considering a series of possible reinforcement alternatives in the two test systems using reliability cost/reliability worth considerations.

Wind power integration in bulk electric system reliability evaluation is presented in Chapter 10. Reliability analyses at both HL-I and HL-II involving WECS are illustrated in this chapter. The impact of different degrees of wind speed correlation on the overall system reliability is examined using HL-I analysis. The capacity value of WECS using the effective load carrying capability (ELCC) technique is investigated

using the LOLE and LOLF as criterion reliability indices. The results show that the $ELCC_{(LOLE)}$ and $ELCC_{(LOLF)}$ are similar for a conventional generating unit, but can be quite different for WECS. The effect of connecting a large-scale WECS at different locations in a bulk electric system is investigated. The results show that the impact of wind power on system reliability is affected by the connection location particularly when there are transmission system limitations. The maximum amount of wind power that can be absorbed by a system at specific locations without creating severe system constraints is also investigated. Transmission reinforcement planning associated with large-scale WECS, and reliability cost/worth analysis associated with reinforcement alternatives are also illustrated in this chapter.

A comprehensive technique utilizing sequential simulation for composite system reliability evaluation has been implemented in a developed software designated as RapHL-II and used in this thesis. The computer software utilizes an AC-based power flow technique which provides an opportunity to incorporate reactive power and voltage considerations in the reliability simulation framework. Reactive power and voltage constraints are becoming serious concerns due to increased utilization of transmission networks created by the current transmission open access paradigm. The RapHL-II software can be used to obtain predictive reliability indices for individual delivery points and for the overall system together with their probability distributions. Reliability worth considerations are playing an increasing role in power system planning and operation. A comprehensive technique for reliability worth assessment is therefore essential, and implemented in the RapHL-II software.

Non-sequential simulation requires considerably less computation time than sequential simulation, particularly in large bulk system reliability studies. The sequential technique can, however, provide more accurate reliability indices, particularly in regard to the frequency of load point and system failures, but also requires considerable additional data in the form of individual bus chronological load profiles. Both techniques therefore have advantages and disadvantages in the reliability evaluation of large practical bulk electric power systems. Both techniques can, however, be used to provide

reasonable estimates of system adequacy given that the underlying differences and approximations are understood.

The concept of applying reliability index probability distributions to manage bulk electricity system risk is introduced in this thesis. Synthesizing bulk electric system reliability performance index probability distributions provides a multi-dimensional risk assessment tool that can complement the single risk dimension provided by an expected or average value. Reliability index probability distribution analysis can be used as a supplementary tool to manage and control future potential risks arising within a bulk electric system. This risk assessment tool can provide power engineers and risk managers with a more profound knowledge of their bulk electric system. It offers additional information insight for planning engineers on when system improvements and reinforcements should be conducted to reduce future potential risk and uncertainty.

Most electric power utilities use deterministic techniques such as the traditional N-1 security criterion to assess system reliability in transmission system planning. These deterministic approaches are not consistent and do not provide an accurate basis for comparing alternate equipment configurations and performing economic analyses as they do not incorporate the probabilistic or stochastic nature of the system behavior and component failures. There is therefore growing interest in combining deterministic considerations with probabilistic assessment in order to evaluate the "system well-being" of a composite generation and transmission system and to evaluate the likelihood, not only of entering a complete failure state, but also the likelihood of being very close to trouble. The system well-being concept presented in this thesis provides system engineers and risk managers with a comprehensive appreciation of specific system conditions, and additional information on the degree of system vulnerability under a particular system condition using a quantitative interpretation of the degree of system security and insecurity.

The combined bulk electric system reliability framework created in this thesis can provide system planners with an appreciation of the degrees of system adequacy and

security under particular system conditions. The developed combined adequacy and security framework can assist system planners to realize the overall benefits associated with a system reinforcement option based on the degree of adequacy and security, and therefore facilitate the decision making process. The combined reliability framework should prove particularly useful in restructured electricity environments where system stress is becoming increasingly important.

Wind power is an intermittent energy source that behaves quite differently than conventional energy sources. The reliability impact of this highly variable energy source is an important aspect that must be assessed as wind power penetration increases. Sequential simulation is ideally suited to the analysis of such an intermittent generating source. Bulk electric system reliability analysis associated with wind power as demonstrated in this thesis provides an opportunity to investigate the reliability benefits when wind power is injected at specified locations in a bulk electric system, and can facilitate system reinforcement planning.

The required computation effort is a major challenge when utilizing sequential Monte Carlo simulation in bulk electric system reliability analysis. This is particularly true when conducting system well-being analysis. An actual bulk electric system may contain over one thousand buses. Using a normal personal computer (a single processor) may be computational expensive or infeasible. The utilization of multi-processors such as parallel and distributed processing environments for sequential simulation is proposed in Reference [132] by application to the Brazilian 1,389 bus system. The resulting computational time is reasonable for system planning applications. This is one possible effective solution to the computation effort dilemma. Alternatively, in order to obtain realistic delivery point reliability indices in large-scale bulk electric systems, the overall system can be divided into subsystems and reliability analyses conducted separately in each subsystem. Attention can be focused on the area in which the reinforcement is applied rather than on the entire bulk electric system. This is an exciting area for future research.

REFERENCES

1. R. Billinton, L. Salvaderi, J. D. McCalley, H. Chao, Th. Seitz, R. N. Allan, J. Odom and C. Fallon, "Reliability Issues in Today's Electric Power Utility Environment", *IEEE Transactions on Power Systems*, Vol. 12, No. 4, November 1997, pp. 1708-1714.

2. R. Billinton and R. N. Allan, *Reliability Evaluation of Power Systems*, 2nd Edition, Plenum Press, New York, 1996.

3. L. Philipson and H. L. Willis, *Understanding Electric Utilities and Deregulation*, Marcel Dekker, New York, 1999.

4. K. Bhattacharya, M. H. J. Bollen and J. E. Daalder, *Operation of Restructured Power Systems*, Kluwer Academic Publishers, Boston, 2001.

5. R. Billinton and R. N. Allan, "Power System Reliability in Perspective", *IEE Electronics and Power*, Vol. 30, No. 3, March 1984, pp. 231-236.

6. North American Electric Reliability Council Planning Standards. Available at: http://www.nerc.com.

7. Union for the Co-ordination of Transmission of Electricity (UCTE), Policy 3: Operational Security (final policy 1.3 E, 20.07.2004), Association of Transmission System Operators in Continental Europe. Available at: http://www.ucte.org.

8. K. A. Pullen, "Deterministic Reliability", *IEEE Transactions on Reliability*, Vol. 38, No. 3, August 1989, pp. 354.

9. R. Billinton and G. Lian, "Composite Power System Health Analysis Using a Security Constrained Adequacy Evaluation Procedure", *IEEE Transactions on Power Systems*, Vol. 9, No. 2, May 1994, pp. 936-941.

10. R. N. Allan and R. Billinton, "Probabilistic Assessment of Power Systems", *Proceedings of the IEEE*, Vol. 88, No. 2, February 2000, pp. 140-162.

11. R. Billinton, "Composite System Reliability Evaluation", *IEEE Transactions on Power Apparatus and Systems*, Vol. PAS-88, April 1969, pp. 276-280.

12. R. Billinton, "Composite System Adequacy Assessment – the Contingency Enumeration Approach", *IEEE Tutorial Course 90EHO311-1-PWR*, 1990.

13. R. Billinton and W. Li, *Reliability Assessment of Electrical Power Systems Using Monte Carlo Methods*, Plenum Publishing, New York, 1994.

14. R. N. Allan, R. Billinton, S. M. Shahidehpour and C. Singh, "Bibliography on the Application of Probability Methods in Reliability Evaluation 1982-1987", *IEEE Transactions on Power Systems*, Vol. 3, No. 4, November 1988, pp. 1555-1564.

15. R. N. Allan, R. Billinton, A. M. Briepohl and C. H. Grigg, "Bibliography on the Application of Probability Methods in Reliability Evaluation 1987-1991", *IEEE Transactions on Power Systems*, Vol. 9, No. 1, February 1994, pp. 41-49.

16. R. N. Allan, R. Billinton, A. M. Briepohl and C. H. Grigg, "Bibliography on the Application of Probability Methods in Reliability Evaluation 1992-1996", *IEEE Transactions on Power Systems*, Vol. 14, No. 1, February 1999, pp. 51-57.

17. R. Billinton, M. Fotuhi-Firuzabad and L. Bertling, "Bibliography on the Application of Probability Methods in Reliability Evaluation 1996-1999", *IEEE Transactions on Power Systems*, Vol. 16, No. 4, November 2001, pp. 595-602.

18. R. Billinton and W. Li, "Hybrid Approach For Reliability Evaluation of Composite Generation and Transmission Systems Using Monte Carlo Simulation and Enumeration Technique", *IEE Proceedings-C*, Vol. 138, No. 3, May 1991, pp. 233-241.

19. M. V. F. Pereira, M. E. P. Maceira, G. C. Oliveira and L. M. V. G. Pinto, "Combining Analytical Models and Monte Carlo Techniques in Probabilistic Power System Analysis", *IEEE Transactions on Power Systems*, Vol. 7, No. 1, February 1992, pp. 265-272.

20. R. Billinton and W. Li, "A System State Transition Sampling Method for Composite System Reliability Evaluation", *IEEE Transactions on Power Systems*, Vol. 8, No. 3, August 1993, pp. 761-771.

21. R. Billinton and A. Sankarakrishnan, "A System State Transition Sampling Technique for Reliability Evaluation", *Reliability Engineering and System Safety*, Vol. 44, 1994, pp. 131-134.

22. R. Y. Rubinstein, *Simulation and the Monte Carlo Methods*, Wiley, New York, 1981.

23. R. Ubeda and R. N. Allan, "Sequential Simulation Applied to Composite System Reliability Evaluation", *IEE Proceeding-C*, Vol. 139, No. 2, March 1992.

24. R. N. Allan and J. Roman, "Reliability Assessment of Generation Systems Containing Multiple Hydro Plant Using Simulation Techniques", *IEEE Transactions on Power Systems*, Vol. 4, No. 3, August 1989, pp. 1074-1080.

25. M. V. F. Pereira and L. M. V. G. Pinto, "A New Computational Tool for Composite Reliability Evaluation", *IEEE Transactions on Power Systems*, Vol. 7, No. 1, February 1992, pp. 258-264.

26. MD. E. Khan, *A Security Based Approach to Composite Power System Reliability Evaluation*, Ph. D. Thesis, University of Saskatchewan, 1991.

27. L. R. Ford and D. R. Fulkerson, *Flow in Networks*, Princeton University Press, Princeton, New Jersey, 1962.

28. R. L. Sullivan, *Power System Planning*, Mcgraw-Hill Book Company, New York, 1977.

29. EPRI Report, *Transmission System Reliability Methods – Mathematical Models, Computing Methods and Results*, Technical Report EPRI EL-2126, Power Technologies Inc., Schenectady, New York, July 1982.

30. B. Stott, "Review of Load Flow Calculation Methods", *Proceedings of the IEEE*, Vol. 62, July 1974, pp. 916-929.

31. B. Stott and O. Alsac, "Fast Decoupled Load Flow", *IEEE Transactions on Power Apparatus and Systems*, Vol. PAS-93, May/June 1974, pp. 859-869.

32. G. W. Stagg and A. H. El-Abiad, *Computer Methods in Power System Analysis*, Mcgraw-Hill Book Company, New York, 1968.

33. R. Billinton and R. N. Allan, *Reliability Assessment of Large Electric Power Systems*, Kluwer Academic Publishers, Boston, 1988.

34. A. Jonnavithula, *Composite System Reliability Evaluation Using Sequential Monte Carlo Simulation*, Ph. D. Thesis, University of Saskatchewan, 1997.

35. U.S.-Canada Power System Outage Task Force, *Final Report on August 14, 2003 Blackout in the United States and Canada: Causes and Recommendations*, April 2004. Available at: http://www.nerc.com/~filez/blackout.html.

36. D. William and Jr. Stevenson, *Elements of Power System Analysis*, Mcgraw-Hill Book Company, New York, 1982.

37. J. Sherman and W. J. Morrison, "Adjustment of an Inverse Matrix Corresponding to a Change in One Element of a Given Matrix", *Annals of Mathematical Statistics*, Vol. 21, 1950, pp.124-126.

38. R. Billinton and S. Kumar, "Adequacy Evaluation of a Composite Power System – A Comparative Study for Existing Programs", *CEA Transactions*, *Engineering and Operating Division*, Vol. 24, Part 3, Paper No. 85-SP-141, March 1985, pp. 1-14.

39. S. Kumar, *Adequacy Evaluation of Composite Power Systems*, Master's Thesis, University of Saskatchewan, July 1984.

40. T. K. P. Medicherla, *Reliability Evaluation of Composite Generation and Transmission Systems*, Ph.D. Thesis, University of Saskatchewan, December 1978.

41. D. G. Luenberger, *Linear and Nonlinear Programming*, 2nd Edition, Addison-Wesley, Reading, Massachusetts, 1984.

42. A. J. Wood and B. F. Wollenberg, *Power System Generation, operation and control*, 2nd Edition, Wiley, New York, 1996.

43. V. A. Sposito, *Linear and Nonlinear Programming*, The Iowa State University Press, Ames, Iowa, 1975.

44. R. Billinton and E. Khan, "A Security Based Approach to Composite Power System Reliability Evaluation", *IEEE Transactions on Power Systems*, Vol. 7, No.1, February 1992, pp.65-72.

45. H. P. William, P. F. Brian, A. T. Saul and T. V. William, *Numerical Recipes in C: The Art of Scientific Computing*, Cambridge University Press, New York, 1988.

46. S. Kumar and R. Billinton, "Low Bus Voltage and Ill-Conditioned Network Situations in a Composite System Adequacy Evaluation", *IEEE Transactions on Power Systems*, Vol. PWRS-2, No. 3, August 1987, pp. 652-659.

47. M. J. D. Powel, *Problems to Unconstrained Optimization*, New York Academic Press, 1972.

48. R. Billinton, G. Wacker and G. Tollefson, *Assessment of Reliability Worth in Electric Power Systems in Canada*, NSERC Strategic Grant STR0045005, June 1993.

49. R. Billinton, G. Wacker and J. Gates, *Electric Service Reliability Worth Evaluation for Government, Institutions and Office Buildings*, NSERC Industrially Oriented Research Grant IOR 1500347, June 1996.

50. K. K. Kariuki and R. N. Allan, "Evaluation of reliability worth and value of lost load", *IEE Proceedings-Generation, Transmission and Distribution*, Vol. 143, No. 2, March 1996, pp. 171-180.

51. R. Billinton and et al, "A Reliability Test System for Educational Purposes- Basic Data", *IEEE Transactions on Power Systems*, Vol. PWRS-3, No. 4, August 1989, pp. 1238-1244.

52. IEEE Task Force, "IEEE Reliability Test System", *IEEE Transactions on Power Apparatus and Systems*, Vol. PAS-98, Nov/Dec 1979, pp. 2047-2054.

53. L. Salvaderi, "Monte Carlo Simulation Techniques in Reliability Assessment of Composite Generation and Transmission Systems, *IEEE Tutorial Course 90EHO311-1-PWR*, 1990.

54. A. Sankarakrishnan and R. Billinton, "Sequential Monte Carlo simulation for composite power system reliability analysis with time varying loads", *IEEE Transactions on Power Systems*, Vol. 10, No. 3, August 1995, pp. 1540-1545.

55. W. Li, *Installation Guide and User's Manual for the MECORE program*, July 1998.

56. A. C. G. Melo, M. V. F. Pereira and A. M. Leite da Silva, "Frequency and Duration Calculations in Composite Generation and Transmission Reliability Evaluation", *IEEE Transactions on Power Systems*, Vol. 7, No. 2, May 1992, pp. 469-476.

57. R. Billinton, G. Wacker, E. Wojczynski, "Comprehensive Bibliography of Electrical Service Interruption Costs", *IEEE Transactions on Power Apparatus and Systems*, PAS-102, 1983, pp. 1831-1837.

58. G. Wacker, R. Billinton, "Customer Cost of Electric Service Interruptions", *Proceedings of the IEEE*, Vol. 77, No. 6, June 1983, pp. 919-930.

59. R. Billinton, G. Wacker, E. Wojczynski, *Customer Damage Resulting from Electric Service Interruptions*, R & D Project, Canadian Electrical Association, Volume One – Report, 1982.

60. R. Billinton, R. N. Allan and L. Salvaderi, *Applied Reliability Assessment in Electric Power Systems*, The Institute of Electrical and Electronics Engineering, Inc., New York, 1989.

61. G. Wacker, E. Wojczynski and R. Billinton, "Cost/Benefit Considerations in Providing an Adequate Electric Energy Supply", *Third International Symposium on Large Engineering Systems*, July 10-11, 1980, St. John's, Newfoundland, pp. 3-8.

62. CIGRE, TF 38.06.01, *Methods to Consider Customer Interruption Costs in Power System Analysis*, CIGRE Report No.191, August 2001, pp.100.

63. A. A. Chowdhury, T. C. Mielnik, L. E. Lawton, J. J. Sullivan and A. Katz, "Reliability Worth Assessment in Electric Power Delivery Systems", *Proceedings of the 2004 IEEE/PES-GM*, Denver, June, 2004.

64. G. Kjolle, K. Samdal, J. Heggset, A.T. Holen, "Application of General Interruption Cost Data in the Framework of Quality Supply Regulations and Financial Compensation for Energy not Supplied", *IEEE/PES WM 2000*, Singapore, Paper No. 542.

65. "*Standard Industrial Classification 1980*", Statistics Canada, Standard Division, Published under the authority of the Minister of Supply and Service Canada, Ottawa, December 1980.

66. R. Billinton, "Evaluation of Reliability Worth in an Electric Power System", *Reliability Engineering and System Safety*, Vol. 46, 1994, pp. 15-23.

67. W. Wangdee, *Event-Based Customer Interruption Cost Evaluation*, M.Sc. Thesis, University of Saskatchewan, Spring 2003.

68. R. Billinton and W. Wangdee, "Estimating Customer Outage Costs due to a Specific Failure Event", *IEE Proceedings-Generation, Transmission and Distribution*, Vol. 150, No. 6, November 2003, pp. 668-672.

69. R. Billinton and W. Wangdee, "Approximate Methods for Event-Based Customer Interruption Cost Evaluation", *IEEE Transactions on Power Systems*, Vol. 20, No. 2, May 2005, pp.1103-1110.

70. W. Wangdee and R. Billinton, "Utilization of Time Varying Event-Based Customer Interruption Cost Load Shedding Schemes", *8th International Conference on Probability Methods Applied to Power Systems (PMAPS)*, September 2004, Iowa, USA (Selected for publication in the International Journal of Electrical Power & Energy Systems).

71. A. Sankarakrishnan and R. Billinton, "Effective Techniques for Reliability Worth Assessment in Composite Power System Networks Using Monte Carlo Simulation", *IEEE Transactions on Power Systems*, Vol. 11, No. 3, August 1996, pp.1255-1261.

72. R. Billinton and A. Jonnavithula, "Application of Sequential Monte Carlo Simulation to Evaluation of Distributions of Composite System Indices", *IEE Proceedings-Generation, Transmission and Distribution*, Vol. 144, No. 2, March 1997, pp. 87-90.

73. IEEE Task Force, "Bulk System Reliability – Predictive Indices", *IEEE Transactions on Power Systems*, Vol. 5, No. 4, November 1990, pp. 1204-1213.

74. IEEE Task Force, "Bulk System Reliability – Measurement and Indices", *IEEE Transactions on Power Systems*, Vol. 4, No. 3, August 1989, pp. 829-835.

75. IEEE Task Force, "Reporting Bulk Power System Delivery Point Reliability", *IEEE Transactions on Power Systems*, Vol. 11, No. 3, August 1996, pp.1262-1268.

76. "*Bulk Electricity System: Delivery Point Interruptions and Significant Power Interruptions 1998-2002 Report*", Canadian Electricity Association, August 2003.

77. "*Bulk Electricity System: Delivery Point Interruptions and Significant Power Interruptions 1999-2003 Report*", Canadian Electricity Association, December 2004.

78. R. Billinton and W. Wangdee, "Bulk Electricity System Reliability Performance Assessment", *IX Symposium of Specialists in Electric Operational and Expansion Planning (SEPOPE)*, May 23-27, 2004, Rio de Janeiro, Brazil.

79. R. Billinton and J. Satish, "Predicting Assessment of Bulk System Reliability Performance Indices", *IEE Proceedings-Generation, Transmission and Distribution*, Vol. 14, No. 5, September 1994, pp. 466-472.

80. R. Billinton and X. Tang, "Predicting Bulk Electricity System Performance Indices", *Proceedings of IEEE Canadian Conference on Electrical and Computer Engineering (CCECE2000)*, Vol. 2, March 2000, pp. 750-754.

81. R. Billinton, "Reliability Considerations in the New Electric Power Utility Industry", Canadian Electricity Association, *Electricity 97' Conference and Exposition*, April 1997.

82. R. E. Brown and J. J. Burke, "Managing the Risk of Performance Based Rates", *IEEE Transactions on Power Systems*, Vol. 15, No. 2, May 2000, pp. 893-898.

83. Ontario Energy Board, *Electric Distribution Rate Handbook*, 2000.

84. Z. Pan, *Electric Distribution System Risk Assessment Using Reliability Index Probability Distributions*, M. Sc. Thesis, University of Saskatchewan, Spring 2003.

85. R. Billinton and Z. Pan, "Incorporating Reliability Index Probability Distributions in Performance Based Regulation", *Proceedings of IEEE Canadian Conference on Electrical and Computer Engineering (CCECE02)*, Vol. 1, May 2002, pp. 12-17.

86. R. Billinton, L. Cui and Z. Pan, "Quantitative Reliability Considerations in Determination of Performance Based Rates and Customer Service Disruption Payments", *IEE Proceedings-Generation, Transmission and Distribution*, Vol. 149, No. 6, November 2002, pp. 640-644.

87. R. Billinton and Z. Pan, "Historic Performance-Based Distribution System Risk Assessment", *IEEE Transactions on Power Delivery*, Vol. 19, No. 4, October 2004, pp. 1759-1765.

88. Energy Regulatory Commission, "*Regulatory Reset for the National Transmission Corporation (TRANSCO) for 2006 to 2010*", September 2004. Available at: http://www.erc.gov.ph/2-transmission.htm.

89. Electricity Generating Authority of Thailand, *Annual Reports (1999-2004)*. Available at: http://www.egat.co.th/english/annual_reports/.

90. H. A. Sturges, "The Choice of a Class Interval", *Journal of the American Statistical Association*, Vol. 21, 1926, pp. 65-66.

91. D.W. Scott, *Multivariate density estimation: theory, practice, and visualization*, John Wiley & Sons: New York, 1992.

92. M.P. Wand, "Data-Based Choice of Histogram Bin Width", *The American Statistician*, Vol. 51, No. 1, February 1997.

93. D.W. Scott, "On optimal and data-based histograms", *Biometrika*, Vol. 66, 1979, pp. 605-610.

94. IEEE Task Force, "Reliability Assessment of Composite Generation and Transmission Systems", *IEEE Tutorial Course 90EHO311-1-PWR*, February 1990.

95. M. V. F. Pereira and N. J. Balu, "Composite Generation/Transmission Reliability Evaluation", *Proceedings of the IEEE*, Vol. 80, No. 4, April 1992, pp. 470-490.

96. L. H. Fink and K. Carlsen, "Operating Under Stress and Strain", *IEEE Spectrum*, Vol. 15, No. 3, March 1978, pp. 48-53.

97. EPRI Final Report, *Composite-System reliability Evaluation: Phase 1 – Scoping Study*, Tech. report EPRI EL-5290, Dec 1987.

98. R. Billinton and R. Mo, "Deterministic/Probabilistic Contingency Evaluation in Composite Generation and Transmission Systems", *IEEE/PES General Meeting*, Vol. 2, June 2004, pp. 2232-2237.

99. E. Khan and R. Billinton, "A Hybrid Model for Quantifying Different Operating States of Composite Systems", *IEEE Transactions on Power Systems*, Vol. 7, No. 1, February 1992, pp. 187-193.

100. A. M. Leite da Silva, L. C. de Resende, L. A. F. Manso and R. Billinton, "Well-Being Analysis for Composite Generation and Transmission Systems", *IEEE Transactions on Power Systems*, Vol. 19, No. 4, November 2004, pp. 1763-1770.

101. V. Brandwajn, "Efficient Bounding Method for Linear Contingency Analysis", *IEEE Transactions on Power Systems*, Vol. 3, February 1988, pp. 38-43.

102. W. Wangdee and R. Billinton, "Impact of Load Shedding Philosophies on Bulk Electric System Reliability Analysis Using Sequential Monte Carlo Simulation", *Electric Power Components and Systems*, Vol. 34, No. 3, March 2006.

103. W. Li, *Risk Assessment of Power Systems: Models, Methods, and Applications*, John Wiley & Sons, Hoboken, NJ, 2005.

104. D. S. Kirschen, D. Jayaweera, D. P. Nedic and R. N. Allan, "A Probabilistic Indicator of System Stress", *IEEE Transactions on Power Systems*, Vol. 19, No. 3, August 2004, pp.1650-1656.

105. N. G. Hingorani, "Flexible AC Transmission", *IEEE Spectrum*, Vol. 30, No. 4, April 1993, pp.40-45.

106. F. D. Galiana, K. Almeida, M. Toussaint, J. Griffin, D. Atanackovic, B. T. Ooi and D. T. McGillis, "Assessment and Control of the Impact of FACTS Devices on Power System Performance", *IEEE Transactions on Power Systems*, Vol. 11, No. 4, November 1996, pp.1931-1936.

107. G. Tollefson, R. Billinton and G. Wacker, "Comprehensive Bibliography on Reliability Worth and Electrical Service Interruption Costs", *IEEE Transactions on Power Systems*, Vol. 6, No. 4, November 1991, pp. 1980-1990.

108. R. Billinton and J. Oteng-Adjei, "Utilization of Interrupted Energy Assessment Rates in Generation and Transmission System Planning", *IEEE Transaction on Power Systems*, Vol. 6, No. 3, August 1991, pp. 1245-1253.

109. J. G. Dalton, D. L. Garrison and C. M. Fallon, "Value-Based Reliability Transmission Planning", *IEEE Transaction on Power Systems*, Vol. 11, No. 3, August 1996, pp. 1400-1408.

110. A. A. Chowdhury and D. O. Koval, "Application of Customer Interruption Costs in Transmission Network Reliability Planning", *IEEE Transaction on Industry Applications*, Vol. 37, No. 6, November/December 2001.

111. W. Li and R. Billinton, "A Minimum Cost Assessment Method For Composite Generation and Transmission System Expansion Planning", *IEEE Transaction on Power Systems*, Vol. 8, No. 2, May 1993, pp. 628-635.

112. H. G. Stoll, *Least-Cost Electric Utility Planning*, John Wiley & Sons, New York, 1989.

113. N. D. Reppen, "Increasing Utilization of the Transmission Grid Requires New Reliability Criteria and Comprehensive Reliability Assessment", *the 8th International Conference on Probability Methods Applied to Power Systems (PMAPS)*, September 2004, Iowa, U.S.A.

114. Canadian Electricity Association, *An Assessment of the Prospects for Wind Power Development in Canada*, December 2004. Available at: http://www.canelect.ca.

115. Canadian Wind Energy Association (CWEA), *Canada's Installed Capacity*. Available at: http://www.canwea.ca/en/CanadianWindFarms.html.

116. R. Billinton, H. Chen and R. Ghajar, "Time-Series Models for Reliability Evaluation of Power Systems Including Wind Energy", *Microelectronics and Reliability*, Vol. 36, No. 9, 1996, pp. 1253-1261.

117. P. M. T. Broersen, *ARMASA Matlab Toolbox* [online]. Available at: http://www.tn.tudelft.nl/mmr/downloads.

118. P. M. T. Broersen and S. de Waele, "Finite Sample Properties of ARMA Order Selection", *IEEE Transactions on Instrumentation and Measurement*, Vol. 53, No. 3, June 2004, pp.645-651.

119. L. Ljung, *System Identification Toolbox for Use with MATLAB*, User's Guide Version 5.0.2, The MathWorks Inc., July 2002.

120. P. Giorsetto and K. F. Utsurogi, "Development of a New Procedure for Reliability Modeling of Wind Turbine Generators", *IEEE Transactions on Power Apparatus and Systems*, Vol. PAS-102, No. 1, 1983, pp.134-143.

121. R. Billinton and Guang Bai, "Generating Capacity Adequacy Associated with Wind Energy", *IEEE Transactions on Energy Conversion*, Vol. 19, No. 3, September 2004, pp. 641-646.

122. B. Ernst, *Analysis of Wind Power Ancillary Service Characteristics with German 250 MW Wind Data*, NREL Report No. TP-500-26969, 1999.

123. H. Holttinen, "Hourly Wind Speed Variations in the Nordic Countries", *Wind Energy*, Vol. 8, No. 2, April/June 2005, pp. 173-195.

124. R. Billinton, Hua Chen and R. Ghajar, "A Sequential Simulation Technique for Adequacy Evaluation of Generating Systems Including Wind Energy", *IEEE Transactions on Energy Conversion*, Vol. 11, No. 4, December 1996, pp. 728-734.

125. R. Billinton, Hua Chen and R. Ghajar, "Assessment of Risk-Based Capacity Benefit Factors Associated with Wind Energy Conversion Systems", *IEEE Transactions on Power Systems*, Vol. 13, No. 3, August 1998, pp.1191-1196.

126. M. R. Milligan, *Modeling Utility-Scale Wind Power Plants, Part 2: Capacity Credit*, NREL Report No. TP-500-29701, March 2002.

127. R. Billinton and W. Wangdee, "Impact of Utilizing Sequential and Non-Sequential Simulation Techniques in Bulk Electric System Reliability Assessment", *IEE Proceedings-Generation, Transmission and Distribution*, Vol. 152, No. 5, September 2005, pp. 623-628.

128. R. Billinton and W. Wangdee, "Delivery Point Reliability Indices of a Bulk Electric System Using Sequential Monte Carlo Simulation", *IEEE Transactions on Power Delivery*, 2006 (accepted for publication).

129. R. Billinton and W. Wangdee, "Predicting Bulk Electricity System Performance Indices Using Sequential Monte Carlo Simulation", *IEEE Transactions on Power Delivery*, 2006 (accepted for publication).

130. W. Wangdee and R. Billinton, "Reliability Performance Index Probability Distribution Analysis of Bulk Electricity Systems", *Proceedings of IEEE Canadian Conference on Electrical and Computer Engineering (CCECE05)*, May 2005 (Selected for publication in the Canadian Journal on Electrical and Computer Engineering, Vol. 30, No. 4, Fall 2005).

131. W. Wangdee and R. Billinton, "Bulk Electric System Well-Being Analysis Using Sequential Monte Carlo Simulation", *IEEE Transactions on Power Systems*, 2006 (accepted for publication).

132. C. L. T. Borges, D. M. Falcao, J. C. O. Mello and A. C. G. Melo, "Composite Reliability Evaluation by Sequential Monte Carlo Simulation on Parallel and Distributed Processing Environments**",** *IEEE Transactions on Power Systems*, Vol. 16, No. 2, May 2001, pp.203-209.

APPENDIX A: RANDOM NUMBER GENERATION

Random numbers are a key ingredient in a Monte Carlo simulation process. A random number generated by a mathematical model is theoretically not truly random, and it is, therefore, designated as a pseudo-random number. Pseudo-random numbers used in the simulation process should, however, closely approximate the ideal properties of uniformity and independence in order to assure the randomness. There are many methods available for generating random numbers. The technique used in this thesis is designated as a multiplicative congruential pseudo-random generator. The general form of congruential methods based on a fundamental congruence relationship can be expressed as follows [13, 103]:

$$x_{i+1} = (ax_i + c)(\text{mod } m) \tag{A.1}$$

where a is the multiplier, c is the increment and m is the modulus; a, c and m are nonnegative integers. Equation (A.1) can be more specifically called a mixed congruential pseudo-random generator. As noted earlier, the pseudo-random generation method used in this research is the multiplicative congruential pseudo-random generator which is a particular case of the mixed congruential generator described in Equation (A.1) with $c = 0$. The multiplicative congruential pseudo-random generator can, therefore, be expressed as:

$$x_{i+1} = ax_i(\text{mod } m) \tag{A.2}$$

The module notation (mod m) for the multiplicative congruential generator means that

$$x_{i+1} = ax_i - mk_i \tag{A.3}$$

where $k_i = (ax_i/m)$ denotes the largest positive integer in ax_i/m.

Given an initial starting value, x_0, that is called a seed, Equation (A.1) generates a random number sequence which lies between [0, m]. A random number sequence uniformly distributed is the interval [0, 1] can be obtained by

$$U_i = \frac{x_i}{m} \tag{A.3}$$

Clearly, such a sequence will repeat itself in at most m steps, and will therefore be periodic. If the repeat period equals m, it is called a full period. Different choices of the parameters a and m produce large impacts on the statistical features of random numbers. Based on many statistical tests, the following parameters provide satisfactory statistical features in generated random numbers:

$m = 2^{31} - 1,$

$a = 16807$ or 630360016

The initial starting value (a seed), x_0, can be any odd number.

APPENDIX B: LINEAR PROGRAMMING TECHNIQUES

B.1 Simplex Methods for Linear Programming [13, 36, 103]

The linear programming problem is to minimize or maximize a linear objective function while satisfying a set of linear equality and inequality constraints. It has the following standard form:

$$\begin{aligned} &\text{minimize} && \boldsymbol{c}^T\boldsymbol{x} \\ &\text{subject to} && \boldsymbol{A}\boldsymbol{x} = \boldsymbol{b} \\ & && \boldsymbol{0} \le \boldsymbol{x} \le \boldsymbol{h} \end{aligned} \tag{B.1}$$

where: $\boldsymbol{c}$, $\boldsymbol{h}$ and $\boldsymbol{x}$ are the n-dimensional column vectors, $\boldsymbol{b}$ is an m-dimensional column vector, and $\boldsymbol{A}$ is $m \times n$ dimensional matrix. This is a generalized simplex form to include both lower and upper bounds constraints of variable $\boldsymbol{x}$.

B.1.1 Primal Simplex Method

The primal simplex method for a linear programming problem includes the following steps:

Step 1: Determine an initial basic feasible solution using the artificial variable technique and create an initial simplex tableau:

In tableau, y_{ij} and y_{i0} are the coefficients corresponding to matrix $\boldsymbol{A}$ and vector $\boldsymbol{b}$, respectively, following each Gaussian elimination step; $r_j = c_j - z_j$ ($j = m+1,..., n$), where c_j are the coefficients in the objective function of the original problem, which are known as direct cost coefficients; $z_j = \sum c_j y_{ij}$ are known as composite cost coefficients and r_j are know as relative cost coefficients; $z_0 =$

$\sum c_i y_{i0}$ is the value of the objective function at the present step; e_j = + or – (j = *1,..., n*), which is called the sign row. For the initial basic feasible solution,

$$x_i = \begin{cases} y_{i0} & \text{if } x_i \text{ is a basic variable} \\ 0 & \text{if } x_i \text{ is a nonbasic variable} \end{cases} \tag{B.2}$$

and all the e_j take + signs.

$\boldsymbol{x}$	x_1	.	.	.	.	x_m	x_{m+1}	.	.	.	x_n	$\boldsymbol{b}$
	c_1		.	.	.	c_m	c_{m+1}	.	.	.	c_n	
x_1	1	0	.	.	.	0	$y_{1,m+1}$	.	.	.	y_{1n}	y_{10}
x_2	0	1	.	.	.	0	$y_{2,m+1}$	.	.	.	y_{2n}	y_{20}
.	.	.	.	.	.	.	.	.	.	.	.	.
.	.	.	.	.	.	.	.	.	.	.	.	.
.	.	.	.	.	.	.	.	.	.	.	.	.
x_i	0	0		1		0	$y_{i,m+1}$	.	.	.	y_{in}	y_{i0}
.	.	.	.	.	.	.	.	.	.	.	.	.
.	.	.	.	.	.	.	.	.	.	.	.	.
.	.	.	.	.	.	.	.	.	.	.	.	.
x_m	0	0	.	0	.	1	$y_{m,m+1}$	.	.	.	y_{mn}	y_{m0}
	0	0	.	0	.	0	r_{m+1}	.	.	.	r_n	$-z_0$
	e_1	e_2	.	0	.	e_m	e_{m+1}	.	.	.	e_n	

Step 2: Select $r_k = min\{r_j < 0, (j = m+1,..., n)\}$. The k^{th} column is called the pivotal column. If there is no negative r_j, the present solution is already an optimal and feasible solution and the simplex process ends. The values of the variables are determined according to the signs of e_j. If e_j = +, $x_j = x_j$ and if e_j = –, $x_j = h_j - x_j$. If there still exists negative r_j, go to Step 3.

Step 3: Calculate the following three values for the elements in the selected pivotal column:

- h_k
- $\theta_1 = min\{y_{i0}/y_{ik}\}$ for all $y_{ik} > 0$ (if there is no positive y_{ik}, $\theta_1 = \infty$)
- $\theta_2 = min\{(y_{i0} - h_i)/y_{ik}\}$ for all $y_{ik} < 0$ (if there is no negative y_{ik}, $\theta_2 = \infty$)

Step 4: Modify the simplex table according to the magnitude of the three values in Step 3:

- If h_k is the minimum, the last column is subtracted by the column that is the product of the k^{th} column and h_k and then the k^{th} column is multiplied by -1 (including the change of the sign for e_k). The base remains unchanged.
- If θ_1 is the minimum and θ_1 appears in the q^{th} row, then y_{qk} is selected as the pivot.
- If θ_2 is the minimum and θ_2 appears in the q^{th} row, then $y_{q0(new)} = y_{q0(old)} - h_q$, y_{qq} is multiplied by -1 and the sign of e_q is changed; y_{qk} is selected as the pivot.

Step 5: With the selected pivot element y_{qk}, conduct the Gaussian elimination in the simplex table so that the pivot becomes 1 and the other elements in the pivotal column become 0. The updated simplex table is obtained; go to Step 2.

B.1.2 Dual Simplex Method

In the previous section, the primal simplex method starts from an initial feasible solution and then an optimal solution is gradually obtained while retaining feasibility in its algorithm. On the other hand, the dual simplex method starts with an initial basic solution satisfying optimality of the objective function but not satisfying feasibility. Feasibility is gradually obtained under the condition that optimality is retained. Which method is utilized depends upon the features of the problems to be solved. If an initial feasible solution can be easily obtained, the primal simplex algorithm is used. If an initial optimal but nonfeasible solution can be obtained, the dual simplex algorithm is used. The basic steps of the dual simplex method can be summarized as follows:

Step 1: Create the initial simplex tableau of the primal problem corresponding to a dual basic feasible solution $\boldsymbol{x_B}$, that is $r_j \geq 0$ for $j = m+1,..., n$, in the simplex tableau.

Step 2: If $\boldsymbol{x_B} \geq 0$, that is, there is no negative element in the column $\boldsymbol{b}$ of the simplex tableau, then an optimal and feasible solution is already reached. If there are any negative elements in the column of $\boldsymbol{b}$, go to Step 3.

Step 3: Select the smallest value in the negative elements of x_B:

$$min\{(x_B)_i | (x_B)_i < 0\} = x_q \tag{B.3}$$

The x_q is leaving base variable. This means that the q^{th} row is the pivotal row.

Step 4: Check all elements of the pivotal row y_{qj} ($j = 1,..., n$). If all the elements $y_{qj} \geq 0$, there is no feasible solution. If there are negative elements in the pivotal row, then

$$\theta = min\{(z_j - c_j)/y_{qj} | y_{qj} < 0\} = (z_k - c_k)/y_{qk} \tag{B.4}$$

where c_j, z_j and y_{qj} are the same as defined in the primal simplex method, and x_k is the entering base variable, which means that the k^{th} column is the pivotal column.

Step 5: With the pivot element y_{qk}, conduct the Gaussian elimination to update the simplex tableau. An updated optimal base $\boldsymbol{B}$ in obtained and then a new dual basic feasible solution is calculated: $\boldsymbol{x_B = B^{-1}b}$. Go to Step 2.

APPENDIX C: BASIC SYSTEM DATA FOR THE RBTS AND IEEE-RTS

Tables C.1 – C.3 and C.4 – C.6 shown the bus data, line data and generator data from the RBTS and for the IEEE-RTS respectively. (Base MVA = 100)

Table C.1: Bus data for the RBTS.

Bus No.	Load (p.u.)		P_g	Q_{min}	Q_{max}	V_0	V_{min}	V_{max}
	Active	Reactive						
1	0.00	0	1.0	0.50	-0.4	1.05	0.97	1.05
2	0.20	0.07	1.2	0.75	-0.4	1.05	0.97	1.05
3	0.85	0.28	0.0	0.00	0.0	1.00	0.97	1.05
4	0.40	0.13	0.0	0.00	0.0	1.00	0.97	1.05
5	0.20	0.07	0.0	0.00	0.0	1.00	0.97	1.05
6	0.20	0.07	0.0	0.00	0.0	1.00	0.97	1.05

Table C.2: Line data for the RBTS.

Line No.	Bus		R	X	B/2	Tap	Current Rating (p.u.)	Failure rate (occ/yr)	Repair rate (hrs)
	I	J							
1	1	3	0.0342	0.1800	0.0106	1.00	0.85	1.50	10.00
2	2	4	0.1140	0.6000	0.0352	1.00	0.71	5.00	10.00
3	1	2	0.0912	0.4800	0.0282	1.00	0.71	4.00	10.00
4	3	4	0.0228	0.1200	0.0071	1.00	0.71	1.00	10.00
5	3	5	0.0228	0.1200	0.0071	1.00	0.71	1.00	10.00
6	1	3	0.0342	0.1800	0.0106	1.00	0.85	1.50	10.00
7	2	4	0.1140	0.6000	0.0352	1.00	0.71	5.00	10.00
8	4	5	0.0228	0.1200	0.0071	1.00	0.71	1.00	10.00
9	5	6	0.0228	0.1200	0.0071	1.00	0.71	1.00	10.00

Table C.3: Generator data for the RBTS.

Unit No.	Bus No.	Rating (MW)	Failure rate (occ/yr)	Repair rate (hrs)
1	1	40.0	6.0	45.0
2	1	40.0	6.0	45.0
3	1	10.0	4.0	45.0
4	1	20.0	5.0	45.0
5	2	5.0	2.0	45.0
6	2	5.0	2.0	45.0
7	2	40.0	3.0	60.0
8	2	20.0	2.4	55.0
9	2	20.0	2.4	55.0
10	2	20.0	2.4	55.0
11	2	20.0	2.4	55.0

Table C.4: Bus data for the IEEE-RTS.

Bus No.	Load (p.u.)		P_g	Q_{min}	Q_{max}	V_0	V_{min}	V_{max}
	Active	Reactive						
1	1.08	0.22	1.92	1.20	-0.75	1.00	0.95	1.05
2	0.97	0.20	1.92	1.20	-0.75	1.00	0.95	1.05
3	1.80	0.37	0.00	0.00	0.00	1.00	0.95	1.05
4	0.74	0.15	0.00	0.00	0.00	1.00	0.95	1.05
5	0.71	0.14	0.00	0.00	0.00	1.00	0.95	1.05
6	1.36	0.28	0.00	0.00	0.00	1.00	0.95	1.05
7	1.25	0.25	3.00	2.70	0.00	1.00	0.95	1.05
8	1.71	0.35	0.00	0.00	0.00	1.00	0.95	1.05
9	1.75	0.36	0.00	0.00	0.00	1.00	0.95	1.05
10	1.95	0.40	0.00	0.00	0.00	1.00	0.95	1.05
11	0.00	0.00	0.00	0.00	0.00	1.00	0.95	1.05
12	0.00	0.00	0.00	0.00	0.00	1.00	0.95	1.05
13	2.65	0.54	5.91	3.60	0.00	1.00	0.95	1.05
14	1.94	0.39	0.00	3.00	-0.75	1.00	0.95	1.05
15	3.17	0.64	2.15	1.65	-0.75	1.00	0.95	1.05
16	1.00	0.20	1.55	1.20	-0.75	1.00	0.95	1.05
17	0.00	0.00	0.00	0.00	0.00	1.00	0.95	1.05
18	3.33	0.68	4.00	3.00	-0.75	1.00	0.95	1.05
19	1.81	0.37	0.00	0.00	0.00	1.00	0.95	1.05
20	1.28	0.26	0.00	0.00	0.00	1.00	0.95	1.05
21	0.00	0.00	4.00	3.00	-0.75	1.00	0.95	1.05
22	0.00	0.00	3.00	1.45	-0.90	1.00	0.95	1.05
23	0.00	0.00	6.60	4.50	-0.75	1.00	0.95	1.05
24	0.00	0.00	0.00	0.00	0.00	1.00	0.95	1.05

Table C.5: Line data for the IEEE-RTS.

Line No.	Bus		R	X	B/2	Tap	Current Rating (p.u.)	Failure rate (occ/yr)	Repair rate (hrs)
	I	J							
1	1	2	0.0260	0.0139	0.2306	1.00	1.93	0.24	16.00
2	1	3	0.0546	0.2112	0.0286	1.00	2.08	0.51	10.00
3	1	5	0.0218	0.0845	0.0115	1.00	2.08	0.33	10.00
4	2	4	0.0328	0.1267	0.0172	1.00	2.08	0.39	10.00
5	2	6	0.0497	0.1920	0.0260	1.00	2.08	0.39	10.00
6	3	9	0.0308	0.1190	0.0161	1.00	2.08	0.48	10.00
7	3	24	0.0023	0.0839	0.0000	1.00	5.10	0.02	768.00
8	4	9	0.0268	0.1037	0.0141	1.00	2.08	0.36	10.00
9	5	10	0.0228	0.0883	0.0120	1.00	2.08	0.34	10.00
10	6	10	0.0139	0.0605	1.2295	1.00	1.93	0.33	35.00
11	7	8	0.0159	0.0614	0.0166	1.00	2.08	0.30	10.00
12	8	9	0.0427	0.1651	0.0224	1.00	2.08	0.44	10.00
13	8	10	0.0427	0.1651	0.0224	1.00	2.08	0.44	10.00
14	9	11	0.0023	0.0839	0.0000	1.00	6.00	0.02	768.00
15	9	12	0.0023	0.0839	0.0000	1.00	6.00	0.02	768.00
16	10	11	0.0023	0.0839	0.0000	1.00	6.00	0.02	768.00
17	10	12	0.0023	0.0839	0.0000	1.00	6.00	0.02	768.00
18	11	13	0.0061	0.0476	0.0500	1.00	6.00	0.02	768.00
19	11	14	0.0054	0.0418	0.0440	1.00	6.00	0.39	11.00
20	12	13	0.0061	0.0476	0.0500	1.00	6.00	0.40	11.00
21	12	23	0.0124	0.0966	0.1015	1.00	6.00	0.52	11.00
22	13	23	0.0111	0.0865	0.0909	1.00	6.00	0.49	11.00
23	14	16	0.0050	0.0389	0.0409	1.00	6.00	0.38	11.00
24	15	16	0.0022	0.0173	0.0364	1.00	6.00	0.33	11.00
25	15	21	0.0063	0.0490	0.0515	1.00	6.00	0.41	11.00
26	15	21	0.0063	0.0490	0.0515	1.00	6.00	0.41	11.00
27	15	24	0.0067	0.0519	0.0546	1.00	6.00	0.41	11.00
28	16	17	0.0033	0.0259	0.0273	1.00	6.00	0.35	11.00
29	16	19	0.0030	0.0231	0.0243	1.00	6.00	0.34	11.00
30	17	18	0.0018	0.0144	0.0152	1.00	6.00	0.32	11.00
31	17	22	0.0135	0.1053	0.1106	1.00	6.00	0.54	11.00
32	18	21	0.0033	0.0259	0.0273	1.00	6.00	0.35	11.00
33	18	21	0.0033	0.0259	0.0273	1.00	6.00	0.35	11.00
34	19	20	0.0051	0.0396	0.0417	1.00	6.00	0.38	11.00
35	19	20	0.0051	0.0396	0.0417	1.00	6.00	0.38	11.00
36	20	23	0.0028	0.0216	0.0228	1.00	6.00	0.34	11.00
37	20	23	0.0028	0.0216	0.0228	1.00	6.00	0.34	11.00
38	21	22	0.0087	0.0678	0.0712	1.00	6.00	0.45	11.00

Table C.6: Generator data for the IEEE-RTS.

Unit No.	Bus No.	Rating (MW)	Failure rate (occ/yr)	Repair rate (hrs)
1	22	50.0	4.42	20.00
2	22	50.0	4.42	20.00
3	22	50.0	4.42	20.00
4	22	50.0	4.42	20.00
5	22	50.0	4.42	20.00
6	22	50.0	4.42	20.00
7	15	12.0	2.98	60.00
8	15	12.0	2.98	60.00
9	15	12.0	2.98	60.00
10	15	12.0	2.98	60.00
11	15	12.0	2.98	60.00
12	15	155.0	9.13	40.00
13	7	100.0	7.30	50.00
14	7	100.0	7.30	50.00
15	7	100.0	7.30	50.00
16	13	197.0	9.22	50.00
17	13	197.0	9.22	50.00
18	13	197.0	9.22	50.00
19	1	20.0	19.47	50.00
20	1	20.0	19.47	50.00
21	1	76.0	4.47	40.00
22	1	76.0	4.47	40.00
23	2	20.0	9.13	50.00
24	2	20.0	9.13	50.00
25	2	76.0	4.47	40.00
26	2	76.0	4.47	40.00
27	23	155.0	9.13	40.00
28	23	155.0	9.13	40.00
29	23	350.0	7.62	100.00
30	18	400.0	7.96	150.00
31	21	400.0	7.96	150.00
32	16	155.0	9.13	40.00

APPENDIX D: CHRONOLOGICAL LOAD DATA

D.1 Time Variation of Load

Table D.1 gives the percentage allocation of the sector peak for all the 52 weeks (1-52) of the residential sector.

Table D.1: Weekly residential sector allocation.

Week No:	Percentage Allocation	Week No:	Percentage Allocation
1	0.922	27	0.815
2	0.960	28	0.876
3	0.938	29	0.861
4	0.894	30	0.940
5	0.940	31	0.782
6	0.901	32	0.836
7	0.892	33	0.860
8	0.866	34	0.789
9	0.800	35	0.786
10	0.797	36	0.765
11	0.775	37	0.840
12	0.787	38	0.755
13	0.764	39	0.784
14	0.810	40	0.784
15	0.781	41	0.803
16	0.860	42	0.804
17	0.814	43	0.860
18	0.897	44	0.941
19	0.930	45	0.945
20	0.940	46	0.969
21	0.916	47	1.000
22	0.871	48	0.950
23	0.960	49	0.975
24	0.947	50	0.970
25	0.956	51	0.980
26	0.921	52	0.990

Table D.2: Hourly percentage of the sector peak load for all sectors.

Hour No:	Res. Average Day	Res. Peak Winter	Res. Peak Summer	Average Com.	Peak Com.	Industrial
1	0.550	0.600	0.700	0.010	0.010	0.337
2	0.500	0.550	0.650	0.010	0.010	0.337
3	0.430	0.455	0.600	0.010	0.010	0.337
4	0.370	0.400	0.550	0.010	0.010	0.337
5	0.360	0.400	0.550	0.010	0.010	0.337
6	0.380	0.395	0.510	0.030	0.030	0.337
7	0.385	0.400	0.500	0.040	0.040	1.000
8	0.425	0.450	0.540	0.250	0.350	1.000
9	0.450	0.550	0.600	0.850	0.850	1.000
10	0.550	0.650	0.650	0.900	0.900	1.000
11	0.600	0.700	0.700	0.910	0.900	1.000
12	0.700	0.800	0.800	0.920	1.000	1.000
13	0.700	0.800	0.800	0.985	0.985	1.000
14	0.750	0.850	0.850	0.975	0.975	1.000
15	0.750	0.850	0.850	0.880	0.850	1.000
16	0.750	0.850	0.850	0.865	0.865	1.000
17	0.800	0.900	0.900	0.890	0.850	1.000
18	0.850	0.950	0.950	0.900	1.000	1.000
19	0.850	0.950	0.950	0.900	1.000	1.000
20	0.860	1.000	1.000	0.640	0.950	1.000
21	0.860	1.000	1.000	0.600	0.850	1.000
22	0.800	0.900	0.900	0.420	0.750	1.000
23	0.750	0.850	0.850	0.400	0.300	1.000
24	0.650	0.750	0.750	0.025	0.020	1.000

Res. Average Day = Average (Fall/Spring season) day for the residential sector

Res. Peak Winter = Peak Winter day for the residential sector

Res. Peak Summer= Peak Summer day for the residential sector

Average Com. = Average (Fall/Spring) day for the residential sector

Peak Com. = Peak (Summer/Winter) day for the commercial sector

Table D.2: Hourly percentage of the sector peak load for all sectors (continued).

Hour No:	Govt. & Inst.	Peak Office & Building	Average Office & Building	Large Users	Peak Agri.	Average Agri.
1	0.400	0.590	0.270	0.1037	0.010	0.001
2	0.400	0.590	0.410	0.1037	0.010	0.001
3	0.400	0.450	0.350	0.1037	0.010	0.001
4	0.400	0.420	0.400	0.1037	0.010	0.001
5	0.400	0.390	0.400	0.1037	0.010	0.001
6	0.600	0.410	0.300	0.1037	0.010	0.001
7	0.700	0.750	0.550	0.1037	0.100	0.020
8	0.750	0.770	0.650	1.0000	0.200	0.100
9	0.800	0.850	0.850	1.0000	0.600	0.400
10	0.850	0.840	0.800	1.0000	0.700	0.600
11	0.900	1.000	1.000	1.0000	0.750	0.650
12	0.920	1.000	1.000	1.0000	0.800	0.670
13	0.930	1.000	0.985	1.0000	0.770	0.650
14	0.960	1.000	0.975	1.0000	0.850	0.680
15	0.970	0.985	0.850	1.0000	1.000	0.690
16	0.970	0.975	0.865	1.0000	0.970	0.760
17	1.000	0.970	0.850	1.0000	0.950	0.810
18	0.980	0.965	0.900	1.0000	0.920	0.700
19	0.800	0.950	0.900	1.0000	0.900	0.500
20	0.750	0.950	0.680	0.5000	0.750	0.350
21	0.650	0.940	0.640	0.5000	0.550	0.300
22	0.500	0.920	0.420	0.5000	0.100	0.005
23	0.430	0.720	0.400	0.5000	0.020	0.004
24	0.120	0.520	0.025	0.5000	0.010	0.003

Govt. & Inst. = Government & Institutions for all seasons

Peak Office & Building = Peak (Summer/Winter) day for the Office Building sector

Average Office & Building = Peak (Fall/Spring) day for the Office Building sector

Peak Agri. = Peak (Fall/Spring) day for the Agricultural sector

Average Agri. = Average (Summer/Winter) day for the Agricultural sector

Table D.3: Daily percentage of the sector peak load.

Day	Res.	Com.	Ind.	Govt. & Inst.	Office & Building	Large Users	Agri.
Monday	0.96	1.00	1.00	1.00	1.00	1.00	1.00
Tuesday	1.00	1.00	1.00	1.00	1.00	1.00	1.00
Wednesday	0.98	1.00	1.00	1.00	1.00	1.00	1.00
Thursday	0.96	1.00	1.00	1.00	1.00	1.00	1.00
Friday	0.97	1.00	1.00	1.00	1.00	1.00	1.00
Saturday	0.83	1.00	1.00	0.40	0.50	1.00	1.00
Sunday	0.81	1.00	1.00	0.30	0.40	1.00	1.00

D.2 Calculation of Sector Load Factors

$$\text{Sector load factor} = \frac{\sum_{k=1}^{3}\left\{\left(\sum_{i=1}^{24} x_i\right)\times\left(\sum_{i=1}^{n} w_i\right)\times\left(\sum_{i=1}^{7} d_i\right)\right\}}{364\times 24} \qquad \text{(D.1)}$$

where: k = Season type (k=1 refers to fall/spring, k=2 refers to winter and k=3 refers to summer),

n = a number of weeks in k,

$\sum_{i=1}^{24} x_i$ = summation of hourly per unit values from Tables D.2,

w_i = weekly allocation from Table D.1 for residential sector,

d_i = daily allocation from Table D.3.

1. Residential sector load factor =

$$\frac{\{(15.07\times 17.636\times 6.51)+(17\times 16.033\times 6.51)+(18\times 11.83\times 6.51)\}}{364\times 24} = 0.5598$$

2. Commercial sector load factor =

$$\frac{\{(12.43\times 22\times 7)+(13.515\times 17\times 7)+(13.515\times 13\times 7)\}}{364\times 24} = 0.5440$$

3. Large Users sector load factor =

$$\frac{\{(15.2259\times 22\times 7)+(15.2259\times 17\times 7)+(15.259\times 13\times 7)\}}{364\times 24}=0.6344$$

4. Government & Institution sector load factor =

$$\frac{\{(16.58\times 22\times 5.7)+(16.58\times 17\times 5.7)+(16.58\times 13\times 5.7)\}}{364\times 24}=0.5625$$

5. Office & Building sector load factor =

$$\frac{\{(15.47\times 22\times 5.9)+(18.955\times 17\times 5.9)+(18.955\times 13\times 5.9)\}}{364\times 24}=0.6140$$

6. Agricultural sector load factor =

$$\frac{\{(11\times 22\times 7)+(7.898\times 17\times 7)+(7.898\times 13\times 7)\}}{364\times 24}=0.3838$$

7. Industrial sector load factor =

$$\frac{\{(20.022\times 22\times 7)+(20.022\times 17\times 7)+(20.022\times 13\times 7)\}}{364\times 24}=0.8340$$

D.3 Customer Sector Allocations

Tables D.4 and D.5 show customer sector allocations at different load buses for the RBTS and IEEE-RTS respectively.

Table D.4: Customer sector allocations at different load buses for the RBTS.

Bus No.	Load Percentage of Customer Sector (%)						
	Agri.	Lrg U.	Resid.	Govern.	Indus.	Comm.	Offic.
2	0.00	0.00	36.25	27.50	17.50	18.75	0.00
3	0.00	65.29	23.41	0.00	4.68	5.53	1.09
4	0.00	0.00	47.50	0.00	40.75	11.75	0.00
5	0.00	0.00	44.50	27.75	0.00	18.50	9.25
6	37.00	0.00	39.25	0.00	15.25	8.50	0.00

Table D.5: Customer sector allocations at different load buses for the IEEE-RTS.

Bus No.	Load Percentage of Customer Sector (%)						
	Agri.	Lrg U.	Resid.	Govern.	Indus.	Comm.	Offic.
1	0.00	0.00	34.03	15.83	36.94	13.20	0.00
2	0.00	0.00	50.05	35.26	0.00	14.69	0.00
3	6.33	0.00	52.50	0.00	33.25	7.92	0.00
4	0.00	0.00	34.52	46.22	0.00	19.26	0.00
5	0.00	0.00	51.38	0.00	28.10	20.07	0.00
6	8.38	0.00	49.70	0.00	29.34	10.48	2.10
7	18.24	0.00	38.44	0.00	31.92	11.40	0.00
8	0.00	0.00	55.00	15.00	11.67	16.66	1.67
9	19.54	48.86	23.46	0.00	0.00	40.87	3.27
10	8.77	21.92	41.54	0.00	20.46	7.31	0.00
13	6.45	16.13	30.09	9.69	22.59	10.75	4.30
14	0.00	44.07	32.42	0.00	20.57	2.94	0.00
15	0.00	67.43	17.29	0.00	0.00	10.78	4.50
16	0.00	42.75	25.90	17.10	0.00	14.25	0.00
18	0.00	56.49	18.69	0.00	11.98	6.85	5.99
19	0.00	61.41	30.72	0.00	0.00	7.87	0.00
20	0.00	33.40	42.11	13.36	0.00	11.13	0.00

where: Agri. = Agricultural, Lrg U. = Large Users, Resid. = Residential,
Gover. = Government and Institution, Indus. = Industrial,
Comm. = Commercial, Offic. = Office and Building.